Use of S-sulfocysteine (SSC) as a L-cysteine source in Chinese hamster ovary (CHO) suspension batch and fed-batch cultures

TECHNISCHE UNIVERSITÄT DARMSTADT

Vom Fachbereich Chemie
der Technischen Universität Darmstadt

zur Erlangung des akademischen Grades eines
Doctor rerum naturalium (Dr. rer. nat.)
genehmigte
Dissertation

vorgelegt von
Caroline Hecklau, M.Sc.
aus Halle (Saale)

Referent: Prof. Dr. Harald Kolmar
Korreferent: Prof. Dr. Dipl.-Ing. Jörg von Hagen
Tag der Einreichung: 08.07.2016
Tag der mündlichen Prüfung: 17.10.2016

Darmstadt 2016
D17

Die vorliegende Arbeit wurde unter der Leitung von Herrn Prof. Dr. Harald Kolmar am Clemens-Schöpf-Institut für Organische Chemie und Biochemie der Technischen Universität Darmstadt sowie bei Merck KGaA in Darmstadt von Januar 2013 bis Januar 2016 angefertigt.

Publication derived from this work

Parts of this work have been published:

Hecklau, Pering, Seibel, Schnellbächer, Wehsling, Eichhorn, von Hagen, Zimmer: S-Sulfocysteine simplifies fed-batch processes and increases the CHO specific productivity via anti-oxidant activity, 2016, Journal of Biotechnology, Vol. 218, pp. 53-60.

Contribution to conferences

Hecklau, Müller, Wehsling, Kuschelewski, Zimmer: Chemically modified cysteine in CHO fed-batch processes and impact on the specific productivity, European Society for Animal Cell Technology (ESACT): C2P2: Cells, Culture, Patients, Products, Barcelona (Spain), 31.05. - 03.06.2015, poster

Table of contents

1. Abstract 1

1.1. Zusammenfassung 1

1.2. Abstract 3

2. Introduction 5

2.1. Biopharmaceutical production of therapeutic proteins 5

2.1.1. General information 5

2.1.2. Titers in mammalian mAb production 5

2.1.3. CHO cell lines 5

2.1.4. Transfection of mammalian cells 7

2.1.5. Cultivation modes for mAb production 9

2.1.6. Cell culture media 13

2.2. Antibodies 19

2.2.1. General information 19

2.2.2. Structure of an IgG1 20

2.2.3. Effector functions of the fragment crystallisable (Fc) part 22

2.2.4. Fc receptors 24

2.2.5. Relevant PTMs of therapeutic proteins 25

2.3. L-cysteine 33

2.3.1. The production of cysteine 33

2.3.2. The physicochemical properties of L-cysteine 35

2.3.3. Reaction behavior of L-cysteine in complex formulations of CDM 37

2.3.4. Reactive species (RS) - ROS, reactive nitrogen species and reactive sulfur species 38

2.3.5. Effects of L-cysteine on cell cultivation 40

2.3.6. L-cysteine stabilization in CDM 40

2.3.7. Cellular L-cysteine and L-cystine uptake 41

2.3.8. Intracellular metabolism of L-cysteine 48

2.3.9. L-cysteine based PTMs 53

2.3.10. L-cysteine and its derivatives in cell culture 55

3. Motivation 64

4. Material and Methods 65
4.1. Chemicals and reagents 65
4.2. Characterization of different SSC 66
4.3. Physicochemical tests 66
4.3.1. Solubility tests 66
4.3.2. Stability tests 67
4.4. Cell culture 67
4.4.1. Thawing 67
4.4.2. Passaging and cell expansion 67
4.4.3. Batch experiments 68
4.4.4. Small scale fed-batch experiments 68
4.4.5. Bioreactor fed-batch experiments 68
4.4.6. Specific productivity 69
4.5. mAb characterization 70
4.5.1. N-glycosylation 70
4.5.2. Charge variant 71
4.5.3. Peptide mapping 71
4.6. Mechanistic studies 72
4.6.1. Cell-free interactions of SSC with GSH 72
4.6.2. Cell spiking experiments 73
4.6.3. Inhibition experiments of selected L-glutamate transporter 73
4.6.4. Intracellular ROS measurements 74
4.6.5. RNA isolation and quantification 74
4.6.6. Quantitative Real-Time polymerase chain reaction (RT-PCR) 75
4.6.7. Western Blot 77
4.7. Offline analytics 78
4.7.1. Characterization of SSC batches 78
4.7.2. Measurement of cell concentration and viability 79
4.7.3. Measurement of metabolites 79
4.7.4. Measurement of online pH 80
4.7.5. Measurement of sulfate and thiosulfate 80
4.7.6. Protein quantification via Bradford Assay 80
4.7.7. Amino acid quantification 81

4.7.8. Intracellular total glutathione quantification 82
4.7.9. Vitamin quantification 82
4.7.10. LC-HRMS for analyte identification generated by interaction studies 82
4.7.11. Statistics 83
5. Results 84
5.1. L-cysteine derivative screening 84
5.2. Maximum solubility of SSC*Na in two different matrices 92
5.3. Stability study of SSC*Na in concentrated, chemically defined neutral pH feed 92
5.3.1. Amino acid and SSC*Na quantification 93
5.3.2. Sulfate quantification 93
5.3.3. NH_3 release 93
5.3.4. Iron concentration 94
5.3.5. Vitamin quantification 94
5.4. Characterization of SSC*Na batches produced from different synthesis routes 98
5.4.1. Purchased SSC*Na batches 98
5.4.2. Internally synthesized SSC*Na research batches 99
5.5. Replacement strategy 102
5.5.1. L-cysteine replacement by SSC*Na-A in batch mode 102
5.6. Application of single feed strategy in spin tube fed-batch processes using SSC*Na-A and PTyr2Na$^+$ with clone 2 105
5.6.1. VCD 105
5.6.2. Viabilities 105
5.6.3. Spent media analysis - IgG concentration 106
5.6.4. Spent media analysis - NH_3 concentration 106
5.6.5. Spent media analysis - Vitamin B12 concentration 106
5.6.6. Spent media analysis - SSC*Na quantification 106
5.6.7. Spent media analysis - L-cysteine quantification 107
5.6.8. Spent media analysis - L-cystine concentration 107
5.6.9. Spent media analysis - L-alanine quantification 107
5.6.10. Spent media analysis - Sulfate quantification 108
5.6.11. Spent media analysis - Thiosulfate quantification 108
5.7. Application of single feed strategy in bioreactor fed-batch processes using SSC*Na-A and PTyr2Na$^+$ with clone 2 111

5.7.1. VCD, viabilities and IgG concentration 111
5.7.2. Spent media analysis - NH_3 quantification 112
5.7.3. Spent media analysis - SSC*Na, L-cystine and vitamin B12 quantification 113
5.8. Characterization of antibodies produced from bioreactor fed-batch processes using the single feed strategy with clone 2 115
5.8.1. Charge variant distribution 115
5.8.2. N-glycosylation pattern 115
5.8.3. SSC integration in the mAb sequence 117
5.9. Determination of mechanisms being responsible for positive effects of SSC*Na-A on cell culture performance 118
5.9.1. Spiking of SSC*Na-A to cell lysates 118
5.9.2. Mechanism of SSC*Na function 119
5.10. Determination of mechanisms being responsible for toxic effects of SSC*Na on cell culture performance 130
5.10.1. Application of single feed strategy in spin tube fed-batch processes using 20 mM of SSC*Na-A together with PTyr2Na^+ using clone 3 130
5.10.2. Application of single feed strategy in spin tube fed-batch processes using different SSC batches together with PTyr2Na^+ using clone 2 131
5.10.3. Toxic effects in batch mode with two different clones 143
5.10.4. L-glutamate transporter studies 145
5.10.5. Evaluation of extracellular pH in batch and fed-batch experiments using 15 and 20 mM SSC*Na 148
5.10.6. Rescue options of toxic SSC*Na conditions in fed-batch mode 151
6. Discussion and Perspectives 154
6.1. Use of SSC*Na as a replacement for L-cysteine 154
6.1.1. Stabilization of feed formulations 154
6.2. Simplification of fed-batch processes 156
6.3. L-cysteine production from SSC 158
6.4. Positive effects of SSC on culture performance 159
6.4.1. Anti-oxidant related mechanisms with SSC*Na use 159
6.5. Toxic effects of SSC on culture performance 162
6.5.1. Relation of SSC*Na application and increased extracellular NH_3 and sulfate levels 162

6.5.2. Types of acidosis 163
6.5.3. Relation of extracellular pH drop to L-cysteine, sulfate, NH_3 and urea cycle in the application of toxic SSC*Na concentration 164
6.5.4. Rescue options 167
7. Conclusion 171
8. References 173
9. Appendix 204
9.1. Abbreviations and chemical formulas 204
9.2. List of figures 210
9.3. List of tables 213
9.4. Curriculum vitae 214
9.5. Acknowledgement 215
10. Affirmations 216

1. Abstract

1.1. Zusammenfassung

Zahlreiche Proteine, die als therapeutische Wirkstoffe zum Einsatz kommen, wie z.B. therapeutische Antikörper, werden aus Zellkulturen gewonnen. Diese Arbeit beschäftigt sich mit der Entwicklung einer komplexen, chemisch definierten, hoch konzentrierten pH neutralen Nährlösung (Feed) für die Zellkultur, die alle Nährstoffe für Fed-Batch Prozesse beinhaltet (Ein-Feed-Strategie). Dabei sollen das Zellwachstum, die Antikörperproduktion und die Charakteristika des produzierten monoklonalen Antikörpers im Vergleich zum Standard Fed-Batch Prozess nicht verändert oder sogar verbessert werden.

Es ist bekannt, dass die Aminosäure L-Cystein schnell zu schwer löslichem L-Cystin durch Oxidationsvorgänge dimerisiert. Die Zugabe von L-Cystein zu einer komplexen, chemisch definierten, hoch konzentrierten pH neutralen Nährlösung (Feed) führt zur schnellen Bildung von L-Cystin. Dies zeigt die geringe Stabilität von L-Cystein im pH neutralen Feed. L-Cystein wird daher in einem separaten, alkalischen Feed im Standard Fed-Batch Prozess der Firma Merck stabil gehalten (Zwei-Feed-Strategie). Durch die Zugabe des alkalischen L-Cystein-Feeds während der Fütterungen ergaben sich pH Spitzen in den Fed-Batch Kulturen.

Um das Ziel der Etablierung einer Ein-Feed-Strategie zu realisieren, wurden zunächst verschiedene L-Cysteinderivate getestet wie in Teil 5.1 dieser Arbeit beschrieben. Aus den getesteten L-Cysteinderivaten wurde S-Sulfocystein für weitere Tests ausgewählt, da dieses Molekül die gewünschten physikochemischen Eigenschaften besitzt. In Teil 5.3 dieser Arbeit wird gezeigt, dass S-Sulfocystein über drei Monate bei 4°C in der komplexen, chemisch definierten, hoch konzentrierten pH neutralen Nährlösung stabil ist.

In Teil 5.5 dieser Arbeit wird L-Cystein durch S-Sulfocystein in Batch Kulturen mit dem CHO Suspensionsklon 1 ersetzt. In diesen Experimenten zeigte sich, dass S-Sulfocystein L-Cystein ersetzen konnte. Dies deutet darauf hin, dass S-Sulfocystein als Cysteinquelle von diesem Klon genutzt werden konnte. Der Einsatz von S-Sulfocystein in Fed-Batch Experimenten (spin tubes, Bioreaktoren) mit CHO Suspensionsklon 2 wurde in den Teilen 5.6 und 5.7 dieser Arbeit untersucht. Bei Verwendung von 15 mM S-Sulfocystein (Ein-Feed-Strategie) zeigte sich verlängertes Zellwachstum und erhöhter Titer im Vergleich zu dem Standard Fed-Batch Prozess (Zwei-Feed-Strategie).

Der in dieser S-Sulfocystein-Kondition produzierte monoklonale Antikörper zeigte keine Unterschiede hinsichtlich N-Glykosylierung, charge variant und Sequenz im Vergleich zum Antikörper aus dem Standard Fed-Batch Prozess wie in Teil 5.8 dieser Arbeit gezeigt.

Der Mechanismus zur Wirkung von S-Sulfocystein als L-Cysteinquelle wurde in Teil 5.9 dieser Arbeit untersucht. Durch die Interaktion von S-Sulfocystein mit Glutathion bildeten sich gemischte Disulfide,

die S-Sulfocystein als Cysteinquelle nach ihrer enzymatischen Reduktion bereitstellen. Weiterhin wurden im Vergleich zu dem Standard Fed-Batch Prozess (Zwei-Feed-Strategie) erhöhte intrazelluläre Glutathionpools, erhöhte Superoxid Dismutase 1 und 2 Levels und verminderte, intrazelluläre, reaktive Sauerstoffspezies in der Ein-Feed-Kondition mit 15 mM S-Sulfocystein beobachtet. Dies deutet darauf hin, dass Mechanismen, ähnlich zur Antioxidanz, in der Kondition mit 15 mM S-Sulfocystein bestehen.

Toxische Effekte auf das Zellwachstum von CHO Suspensionsklon 2 wurden im Fed-Batch Prozess mit 20 mM S-Sulfocystein und im Batch Modus mit 1.5 mM S-Sulfocystein beobachtet. Die beobachtete Toxizität in beiden Konditionen wird einem extrazellulären pH Abfall zugeschrieben wie in Teil 5.10 dieser Arbeit gezeigt. Es wird vermutet, dass die beobachteten pH Abfälle in toxischen S-Sulfocysteinkonzentrationen für den beobachteten schnellen Zelltod in beiden Prozessformen im Vergleich zu den Standardprozessen verantwortlich sind. Weiterhin wurde in dieser Arbeit gezeigt, dass verschiedene CHO Suspensionsklone unterschiedlich auf das Cysteinderivat reagieren. Dies deutet darauf hin, dass klonabhängige Effekte bei S-Sulfocystein Verwendung auftreten.

Die Ergbenisse dieser Arbeit bestätigen das Konzept der Ein-Feed-Strategie in Fed-Batch Prozessen mit CHO Suspensionszellen. Zum ersten Mal wurde S-Sulfocystein erfolgreich als Cysteinquelle in der Zellkultur eingesetzt. Der Erfolg der S-Sulfocysteinanwendung hängt maßgeblich von der eingesetzten S-Sulfocysteinkonzentration, vom Prozesss und von dem verwendeten CHO Suspensionsklon ab.

1.2. Abstract

Numerous proteins being used as therapeutic agents such as therapeutic antibodies are produced within cell cultures. This work sought to develop a single nutrient solution (single feed) for fed-batch processes comprising all nutrients in one complex feed at neutral pH without impacting or improving cell culture performance, titer and monoclonal antibody (mAb) characteristics. The amino acid L-cysteine was shown to rapidly dimerise into poorly soluble L-cystine via oxidation mechanisms. Addition of L-cysteine to a complex, chemically defined, highly concentrated neutral pH nutrient solution (feed) resulted in rapid production of L-cystine from L-cysteine indicating poor stability of L-cysteine in the feed. To keep L-cysteine stable in the standard fed-batch process at Merck, the amino acid was maintained in an alkaline pH environment separated from the other feed nutrients (two feed strategy). The addition of the alkaline L-cysteine nutrient solution to fed-batch cultures resulted in pH peaks while feedings.

To achieve the aim of establishing the single feed strategy, screening of several L-cysteine derivatives was carried out in the part 5.1 of this work. Out of several L-cysteine derivatives, the derivative S-sulfocysteine (SSC) was chosen since it showed the desired physico-chemical properties. In part 5.3 of this work, SSC was shown to be stable over three months at 4°C in chemically defined, complex, highly concentrated neutral pH feed.

In part 5.5 of this work, L-cysteine was replaced by SSC in batch cultures with Chinese hamster ovary (CHO) suspension clone 1. It was shown that SSC was able to replace L-cysteine in batch mode indicating that SSC was used as a L-cysteine source. The use of SSC in fed-batch experiments (spin tubes, bioreactors) with CHO suspension clone 2 was examined in parts 5.6 and 5.7. Application of 15 mM SSC (single feed strategy) revealed prolonged growth and increased titer compared with the standard process (two feed strategy).

The antibody produced with 15 mM SSC showed no differences in N-glycosylation, charge variant and mAb sequence compared with antibody produced from the standard process as shown in part 5.8.

The mechanism of SSC use as a L-cysteine source was described in part 5.9. Due to its interaction with glutathione (GSH), mixed disulfides were generated. After their enzymatic reduction, L-cysteine was released and ready for metabolization. Further, increased intracellular total GSH pools, superoxide dismutase 1 and 2 (SOD-1, SOD-2) levels and decreased intracellular reactive oxygen species (ROS) concentrations were observed in the single-feed containing 15 mM SSC compared with the standard process indicating anti-oxidant related mechanisms of SSC.

Toxic effects of 20 mM SSC in fed-batch and 1.5 mM SSC in batch mode on cell growth were correlated to the external pH in part 5.10. The observed drops in pH with toxic SSC concentrations were assumed to be responsible for the monitored reproducible, rapid cell death in batch and fed-batch

cultures compared with the standard processes. Further, it was shown that different CHO suspension clones reacted differently to the derivative indicating clone dependent effects of SSC.

Overall, the results of this work confirmed the concept of the single-feed strategy in CHO suspension fed-batch culture. For the first time, SSC was successfully used as a L-cysteine source in cell culture. The successful application of SSC in cell culture was shown to be dependent on its applied concentration, the used cultivation mode and clone.

2. Introduction

2.1. Biopharmaceutical production of therapeutic proteins

2.1.1. General information

Biopharmaceutical therapeutic proteins such as mAb have become in focus on treating e.g. inflammatory diseases, cancer, neurologic disorders and infections. Over the last 30 years, 30 mAb products have been approved pointing out the importance of these therapeutic proteins (Jones et al. 2007).

Immortalized CHO cells, murine myeloma cells (e.g. NS0), baby hamster kidney cells and human embryonic kidney (HEK) 293 cells grown in suspension are widely used in mAb production as reviewed (Wurm 2004). One of the early approved antibody products was a murine mAb but the risk of immunogenicity in patients led finally to the production of humanized and fully human antibodies as reviewed (Jones et al. 2007).

Proteins produced in mammalian host systems show similar posttranslational modifications (PTMs) compared with those produced in humans. But also differences in PTMs of CHO produced proteins compared with proteins produced in HEK cells were reported such as sialic acid content (Croset et al. 2012). Although differences in PTMs arise between human and rodent cell lines, the glycosylation in rodent cell lines is more related to humans compared with the one in plants (Raju 2003). With regard to mAb production in mammalian host systems, production cells need to show prolonged viabilities, product expression and scalability (Costa et al. 2010).

2.1.2. Titers in mammalian mAb production

Historically, mAb production in mammalian cells started with a final titer of < 0.5 g/L. Improvements in cell culture media and cell line development gave rise to increased titers (Rader and Langer, 2014). Nowadays, 5-6 g/L in mammalian fed-batch processes may be routinely achieved and optimization strategies may result in titers of ~ 9 g/L to ~ 10 g/L (Lu et al. 2013; Huang et al. 2010).

2.1.3. CHO cell lines

For the most pharmaceutical-biotechnological therapeutic protein production processes, CHO cells are used.

CHO cells were isolated from an ovary of a Chinese hamster (*Cricetulus griseus*) in 1957 from T. Puck. Out of these cells, an adherent tissue culture in plates was established. These mammalian cells show a diploid karyotype and possess a chromosome number of 22 as reviewed (Wurm 2013).

With regard to therapeutic protein expression such as mAb, CHO host cells are able to be easily genetically manipulated by the introduction of the gene of interest. The expression of the desired gene

leads to large protein amounts. These rodent cells are able to be adapted from adherent to suspension culture and grow in high cell densities. Moreover, CHO cells show a relative fast generation time. For large scale therapeutic mAb production processes in bioreactors, CHO suspension cells are an ideal tool. Further, CHO cells allow safe protein production since several viruses such as human immunodeficiency virus, influenza and herpes do not replicate in these cells as reviewed (Jayapal et al. 2007).

All derived CHO cell lines are members of a family of related but highly different cell lines as their individual behavior differs in cell culture (Wurm 2013) which will be discussed in the next sections.

2.1.3.1. CHO DG44

As mentioned above, T. Puck isolated in 1957 cells by trypsination from ovary tissues of an outbred Chinese hamster. The isolated adherent cells showed a fibroblast like phenotype being characterized by irregular cytoplasmic spikes of the cells. After 10 months of culture and subsequent re-cloning, the original CHO cell line, then called CHO-ori, was created. CHO-ori cells showed an epitheloid phenotype being characterized by elongated shape and fine granularity. CHO-ori cells were not able to synthesize proline indicating loss or inactivation of proline synthesis. For cultivation of CHO-ori cells, proline needed to be added to the medium. In the lab of Chasin and Urlaub, CHO-ori cells from Siminovitch´s lab were treated with γ-rays to induce mutations. Thereby, Chasin and Urlaub fully deleted two dihydrofolate reductase (DHFR) loci on chromosome 2 leading to the nowadays widely used DHFR-negative based CHO-DG44 (*dhfr* $^{-/-}$) cells as reviewed (Wurm 2013).

2.1.3.2. CHO-K1

From the CHO-ori cells, a subline was sent to Kao and Puck in 1968. They treated the cells with ethyl methanesulfonate and N-methyl-N'-nitro-N-nitrosoguanidine and induced thereby mutations. The mutants were deficient to synthesize glycine indicating glycine supplementation of the medium (Kao and Puck 1968). This developed CHO-K1 original was maintained in the lab of Kao and Puck (Wurm 2013). A subline of a serum-free suspension CHO-K1 culture banked in the year 2002 was the base for the introduction of the glutamine synthetase (GS) system by one manufacturer giving rise to the licensed CHO K1 SV clone (Wurm 2013; Lewis et al. 2013).

2.1.3.3. CHO-S

In 1973, Thompson adapted a sister cell line of CHO-K1 to grow in suspension. These suspension cells were termed to be CHO-S original cells (CHO-So). The CHO-So cells were sent to a manufacturer

who cultivated them further. These cells were termed CHO-S commercial (CHO-Sc) as reviewed (Wurm 2013).

As shown above, the different CHO cell lines are related to each other due to the genetic background of one original isolated cell line. But the generated CHO cell lines have individual properties making every cell line unique.

2.1.4. Transfection of mammalian cells

Transfection of the chosen mammalian cell line allows their genetic modification relying on the insertion of vectors (plasmids). The plasmid carrying the gene of interest and a selection maker gene is introduced into the host cell. After cell entry, the plasmid is integrated into the host genome (stable transfection). By replication of the host genome, the integrated plasmid is going to be replicated, too, and daughter cells will contain the genetic modification as reviewed (Kim and Eberwine 2010). In case of transient transfection, plasmids undergo autonomous replication being independent of the host genome due to the existence of an origin of replication. The gene is expressed only for a finite period of time and daughter cells may not possess the transfected genetic material (Kim and Eberwine 2010).

For high level expression of the desired gene, strong promoters such as cytomegalovirus or simian virus 40 (SV40) are used as reviewed (Costa et al. 2010). For increased transcription, enhancers such as SV40 polyadenylation signals for prolonged half-life messenger ribonucleic acid (mRNA) stability are used. Moreover, insertion of the Kozak sequence for improved translational initiation is applied as reviewed (Costa et al. 2010).

2.1.4.1. Selection systems

Usually, the introduction of the gene of interest is linked to an insertion of a selection gene enabling a selective advantage. Two common selection systems are used: DHFR based systems using methotrexate (MTX) or GS based systems relying on methionine sulfoximine (MSX).

The enzyme DHFR catalyzes the conversion of folate into tetrahydrofolate (THF). THF is involved as a precursor in the synthesis of purines, pyrimidines and glycine (Camire 2000). MTX is an analogue to folate and binds to DHFR. Cells showing no DHFR expression (e.g. CHO DUXB11 ($dhfr^{+/-}$), CHO-DG44 ($dhfr^{-/-}$)) are transfected with a plasmid containing the DHFR gene and the gene of interest. After amplification of both genes, the cells are exposed to increasing MTX concentrations in a multiple step selection process in the absence of hypoxanthine and thymidine. Cells with increased copies of the DHFR will survive when being exposed to increased MTX concentrations. This process favors the selection of cells with increased copies of the DHFR gene (and the gene of interest) aiming

to select clones with increased production levels (Camire 2000). Host DHFR-negative cells need to be cultivated in presence of glycine, hypoxanthine and thymidine.

Further, cells may be selected after transfection with a puromycine resistance gene. After treatment with puromycine, only the transfected cells will survive.

The enzyme GS catalyzes the adenosine triphosphate (ATP) dependent transfer of ammonia (NH_3) on glutamate leading to the formation of glutamine. Cells which are transfected with the gene coding for GS (e.g. CHO K1) will grow in the absence of extracellular glutamine. When GS expressing cells are exposed to the glutamate analogue MSX, the molecule binds to GS thereby inhibiting the enzyme. The synthesis of glutamine is stopped and cells die. This strategy is used for the selection of clones. The transfected cells containing the gene for GS and the gene of interest are exposed to one fixed MSX concentration allowing the inhibition of the endogenous GS activity. In this process, cells with higher gene copy numbers possess higher GS levels and cell death is prevented. This process favors the selection of cells with increased copies of the GS gene (and gene of interest) aiming to select increased production levels in clones (Camire 2000).

Further, the developed proprietary cell line of a life science manufacturer is a new CHO suspension cell line which shows deletion of both alleles encoding for endogenous GS. For cultivation of the host cell line, exogenous glutamine is required. After transfection of the GS deficient CHO host cell line with the vector containing the genes for GS and the gene of interest, the transfected cells grow in the absence of glutamine without the need of MSX for selection.

2.1.4.2. Transfection methods

To ensure cell entry of the plasmid carrying the gene of interest, several transfection methods from biological, physical and chemical background are established. As a biological method, viral transfection is known. Micro-injection, electroporation, laser-based transfection represent physical transfection techniques. As chemical procedures, calcium phosphate and cation lipid transfection are accepted as reviewed (Kim and Eberwine 2010; Wurm 2004; Costa et al. 2010).

The procedures are simple but not targeted pointing out the importance of the site of integration. The latter impacts the transcription rate of the desired gene based on the surrounding chromatin environment at the integration site (position effect).

Targeted transfection methods comprise clustered regularly interspaced short palindromic repeats/Cas 9, zinc finger nucleases and transcription activator-like effector nuclease and belong to genome editing methods.

2.1.4.3. Improved gene expression

Additional elements may be included into the plasmid. On the one hand, these elements enhance transcriptional activity of the random integration site. On the other hand, they make the random integration site become available for the transcribing enzymes. One option for enhancing gene expression is the introduction of matrix attachment regions elements. The introduction of ubiquitous chromatin opening elements relies on a similar principle as reviewed (Jones et al. 2007).

2.1.5. Cultivation modes for mAb production

2.1.5.1. General procedure from thawing to production start

As shown in figure 1, banked suspension cells are first thawed when starting the mAb production process. Next, suspension cells are pre-passaged in small scale spin tubes to adjust cells to cultivation conditions. Afterwards, the seed train is cultivated either in spin tubes, Erlenmeyer flasks or wave bioreactors to expand the cells. Cells need to be expanded for cell cultivation ensuring to generate sufficient biological material for further production processes. Finally, production processes are able to be carried out in spin tubes (small scale) or in bioreactors (lab scale or production scale).

With regard to production processes, different process modes are available. The choice of mode is dependent on cell line, product quality and stability, manufacturing capacity, process scalability and volumetric productivity. Each process mode possesses characteristic features which will be presented in the next section.

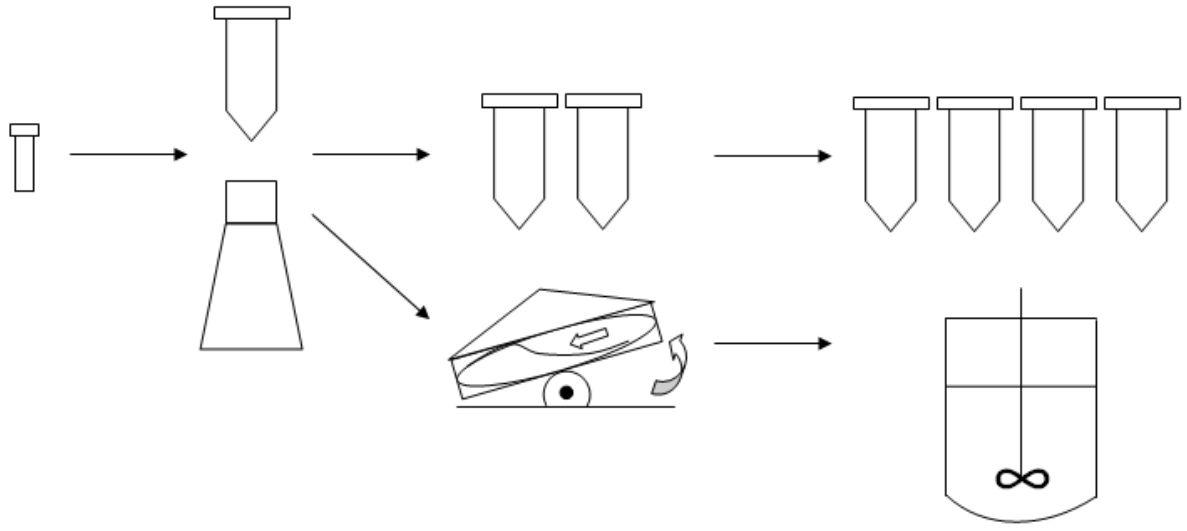

Figure 1: Cell culture workflow for protein production.

Scheme represents procedures from thawing, pre-passaging in spin tubes or Erlenmeyer tubes with subsequent expansion in spin tubes or wave bioreactors for small scale-cultivation in spin tubes or large scale cultivation in bioreactors.

2.1.5.2. Batch cultivation for therapeutic protein production

Batch cultures are defined as cultivation modes without addition of supplements as shown in figure 2. This mode is characterized by early nutrient limitations, accumulation of inhibitory or toxic components and a constant culture volume. The features of this process mode lead to temporally restricted cell growth and therefore to limited titer. Production of mAb in batch mode for research purposes was exemplary applied for hybridoma cell lines in serum-free medium. Studies of mAb production in T-flasks revealed titers of ~110 µg/mL after 150 hours due to reduced antibody secretion rates in later cultivation phase (McKinney et al. 1995). This example points out the ineffectiveness of this cultivation mode for satisfying the intense needs of therapeutic proteins.

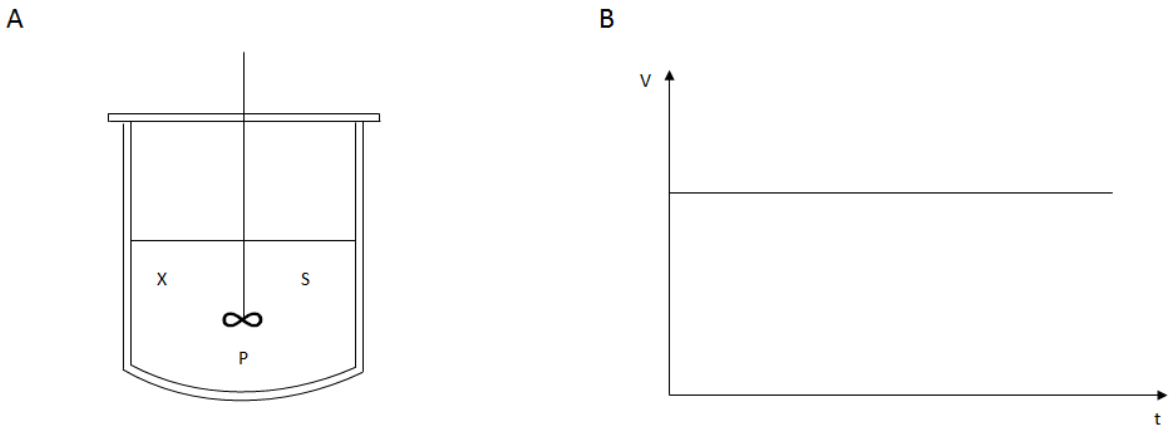

Figure 2: Cell culture and protein production in batch (discontinuous) process mode.

(A) Scheme represents process mode as batch mode wherein biomass (X) produces the product (P) by the use of substrates (S). (B) Constant culture volume is observed over the whole culture time.

2.1.5.3. Continuous cultivation for therapeutic protein production with perfusion as a special case

Continuous cell cultivation is characterized by continuous addition of fresh medium and simultaneous withdrawal of cell culture broth containing biomass, substrates, waste and product. Continuous cell cultivation is started after switching from initial batch to continuous mode as shown in figure 3. Fresh substrates are added to the culture. Simultaneously, culture broth containing biomass, substrates, waste and product is withdrawn. Inlet and outlet flow rates are equal.

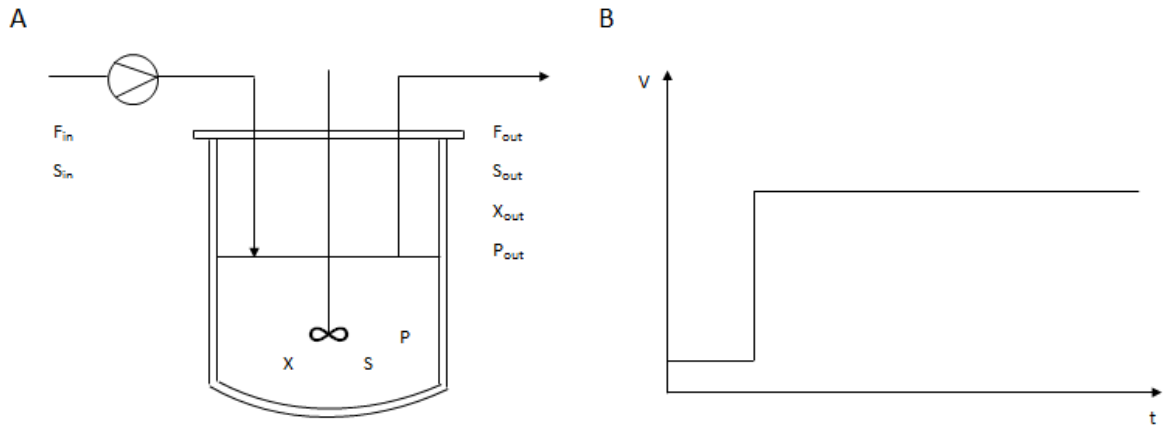

Figure 3: Cell culture and protein production in continuous process mode.

(A) Scheme represents continuous process mode with feedings and culture broth withdrawal. Via inlet, fresh substrates (S_{in}) are added with a constant inlet flow (F_{in}) to culture broth. Biomass (X) produces the product (P) by the use of substrates(S). Simultaneously, culture broth is withdrawn including biomass (X_{out}), substrate (S_{out}), product (P_{out}) and waste with a constant outlet flow rate (F_{out}). F_{in} and F_{out} are equal. (B) Due to equal inlet and outlet flow rates, culture volume is constant after switching from batch to perfusion mode.

A special case in continuous cell cultivation is the perfusion mode. Perfusion systems integrate cell retention systems aiming at the accumulation of cells in the reactor for increased titer generation while the product is going to be harvested repeatedly through the run (Wurm 2004). Schematic presentation of perfusion is shown in figure 4.

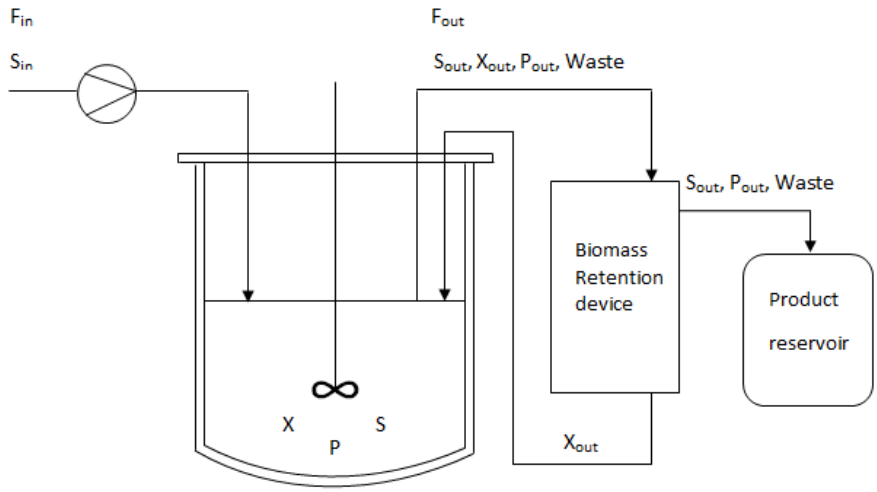

Figure 4: Cell culture and protein production in perfusion mode as a special case of continuous culture.

Scheme represents perfusion process mode with feedings and culture broth withdrawal. Biomass (X) produces the product (P) by the use of substrates (S). Via inlet, fresh substrates (S_{in}) are added with a constant inlet flow rate (F_{in}) to culture broth. Simultaneously, culture broth is withdrawn including biomass (X_{out}), substrates (S_{out}), product (P_{out}) and waste with a constant outlet flow rate (F_{out}). F_{in} and F_{out} are equal. Separation of withdrawn culture broth is carried out in biomass retention device wherein S_{out}. P_{out} and waste are separately collected and X_{out} is recycled and inserted into the bioreactor.

Perfusion processes using a CHO-K1 cell line were documented to be used for generating high viable cell concentrations (VCDs) after six days of culture as a starting material for subsequent fed-batch cultivation (Padawer et al. 2013). This points out that perfusion is able to be applied in efficient seed train cultivation for subsequent large scale cell culture production processes.

CHO cell perfusion cultures in wave bioreactors revealed cell densities of $1.3*10^8$ cells/ milliliter (C/mL) using alternating tangential flow systems and $2.14*10^8$ C/mL using tangential flow filtration. These systems show limitations due to high viscosities in high cell density cultures (Clincke et al. 2013).

2.1.5.4. Fed-batch cultivation for therapeutic protein production

Fed-batch processes are characterized by strategic and balanced feeding of highly concentrated feed solutions to the culture. This strategy delivers nutrients over the cultivation time leading to prolonged growth while the product is harvested at the end of the culture. As shown in figure 5, a fed-batch procedure is characterized by feeding nutrient cocktail(s) several times which is reflected in stepwise increased culture volume. The application of concentrated feeds ensures little changes in culture volume and nutritional environment therefore improving culture longevity and mAb production. With regard to prolonged culture time, accumulation of metabolic by-products such as lactate and NH_3 is observed.

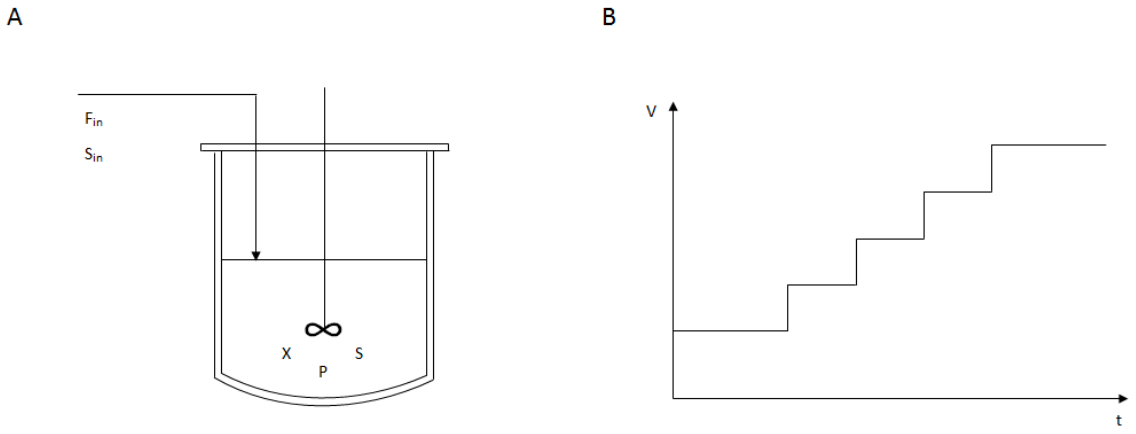

Figure 5: Cell culture and protein production in fed-batch mode.

(A) Scheme represents fed-batch process mode with feeding of nutrient cocktail(s). Biomass (X) produces the product (P) by the use of substrates (S). Via inlet, fresh substrates (S_{in}) are added with an inlet flow rate (F_{in}) to the culture broth. No culture broth is withdrawn. (B) Due to strategic feedings, culture volume increases over culture time.

Fed-batch cultures of antibody producing Sp2/0 NS0 cell lines revealed on average 7.6 fold and 3.2 fold increased final titers and volumetric productivity compared with data obtained in batch cultures, respectively, due to increased integral viable cell density (Sauer et al. 2000).

Studies with a recombinant CHO cell line expressing a nonglycosylated human mAb in fed-batch mode revealed final antibody concentrations of ~10 g/L and volumetric productivities of ~500 mg/L/day in chemically defined platforms (Huang et al. 2010). These data indicate that cells cultured in fed-batch mode did not suffer from nutrient limitation thereby increasing therapeutic product concentration compared with batch cultures.

2.1.6. Cell culture media

2.1.6.1. Media development: From serum containing to chemically defined media (CDM)

Historically, first media formulations contained serum from e.g. calf, sheep, horse or bovine. Serum was used as a rich cocktail delivering proteins, growth factors (e.g. insulin-like growth factor 1, interleukins, hormones (e.g. insulin), attachment factors (e.g. gelatins, collagens, fibronectin), lipids (e.g. sterols, phospholipids), vitamins, and trace metals to cultured cells (Whitford 2005) ensuring a broad, rich nutrient offer. Although serum contains many different essential nutrient classes, its use was associated with disadvantages such as lot-to-lot inconsistencies of individual serum batches, contamination risks via prions, mycoplasma, viruses and endotoxins (Brunner et al. 2010) making cell culture media composition not standardizable, potentially infectious and risky.

Subsequently, serum replacement as a first step in media formulation improvement was carried out using animal-origin e.g. insulin, transferrin and albumin (Jayme and Smith 2000) to mimic serum composition in a more controllable way. But the use of animal-origin proteins showed issues regarding reproducibility, qualification of raw materials and regulatory concerns.

Further research was carried out in the development of non-animal origin media components leading to CDM (Whitford 2006; Brunner et al. 2010). CDM are media wherein all components and their concentrations are known. They can either be free of peptides and proteins or may comprise supplemented proteins such as e.g. recombinant insulin to stimulate proliferation (Jayme and Smith 2000). In any case, these chemically defined formulations make the media highly reproducible, standardizable, batch consistent and free of regulatory concerns without losing their broad nutrient offer.

2.1.6.2. Components in CDM

CDM formulations are complex and rich to fulfill the nutrient supply for cultured cells. They comprise various components of different substance classes such as monosaccharides, amino acids, vitamins, trace elements, inorganic salts and buffers.

2.1.6.2.1. Carbon sources

As one carbon source used in CDM, glucose is the main energy source in aerobically cultivated cells. CHO cells were shown to take up glucose via a membrane located glucose transporter and stimulated glucose uptake was achieved in the presence of insulin (Hara et al. 1994). Glucose is transformed in glycolysis to generate pyruvate and lactic acid. By this process, the energy is stored in the form of generated metabolic ATP, other nucleotide triphosphates such as cytidine triphosphate, guanosine triphosphate and uridine triphosphate or in the coenzymes nicotinamide adenine dinucleotide phosphate (NADP) and nicotinamide adenine dinucleotide (NAD). Besides its role in energy supply, glucose is also involved in the generation of pentose sugars for nucleic acid synthesis.

As a second common carbon source, pyruvate is added to CDM formulations. With regard to pyruvate uptake by mammalian cells, it was shown that human cells possess the monocarboxylate transporter (MCT) 2 which shows high affinity for pyruvate (Lin et al. 1998). The transporter MCT2 has also been detected in the Syrian hamster whereas the MCT1 transporter has been found in CHO cells as reviewed (Halestrap and Price 1999; Garcia et al. 1994). After cell entry, pyruvate may then undergo oxidative decarboxylation in mitochondria to produce acetyl coenzyme A (CoA) entering the tricarboxylic acid cycle (TCA). L-alanine may also be produced from pyruvate by transamination. Further, pyruvate may also serve as an antioxidant.

2.1.6.2.2. Amino acids

Amino acids deliver nitrogen and sulfur which in turn are used for the build-up of proteins, nucleic acids, purine and pyrimidines, other amino acids, NADPH and NADH. L-cysteine and L-methionine serve as a source for sulfur which is used to create inter- and intra-protein disulfide bonds determining the secondary and tertiary protein structure. Further, L-cysteine is used in the build-up of GSH, an intracellular antioxidant protecting the cells from stress. Other antioxidants such as taurine and hypotaurine may be produced from L-cysteine, too.

Glutamine is the major nitrogen source and is a precursor for glutamate which is a key amino acid for transamination reactions generating other α-amino acids. When glucose levels are low, glutamine may be also used as an energy source (van der Valk et al. 2010).

2.1.6.2.3. Vitamins

Vitamins act as coenzymes or prosthetic groups (Yang and Xiong 2012) to support the function of intracellular enzymes. Most utilized vitamins in basal media formulations are biotine, choline, folic acid, inositol, nicotinamide, pantothenic acid, pyridoxine, riboflavin and thiamine, with all of these mentioned being water soluble.

Water-insoluble vitamins are vitamin A (retinol), D (calcitriol), E (tocopherol) and K. Vitamins of the e.g. vitamin E family show protection from lipid peroxidation (Wagner et al. 1996) pointing out their antioxidant behavior. Moreover, vitamins may be sensitive to air, light, oxygen or pH.

As an example of specific activity of defined vitamins, vitamin B12 is a cofactor for two enzymes, namely cytosolic methionine synthase and mitochondrial methylmalonyl CoA mutase. Methionine synthase is involved in methionine build-up. Methylmalonyl CoA mutase participates in succinyl-CoA formation for its entry in the TCA cycle (Shane 2008). Additionally, folate is involved in the build-up of deoxythymidinetriphosphate from deoxyuridinemonophosphate therefore playing an important role in deoxyribonucleic acid (DNA) metabolism as reviewed (Fenech et al. 2012). Pyridoxal phosphate (PLP) and vitamin B6 (pyridoxine) are involved in e.g. transamination, decarboxylation and racemization reactions and are participating in fatty acid metabolism as reviewed (Mooney et al. 2009). Deficiencies in vitamin supplementation may result in impacted viabilities, proliferation, differentiation and alteration of DNA methylation pointing out the linkage of nutrient levels and gene expression as reviewed (Arigony et al. 2013).

2.1.6.2.4. Trace metals

Trace metals act as cofactors of enzymes. Copper, zinc and manganese ions are incorporated in SODs (Cu-SOD/Zn-SOD, Mn-SOD). SODs play a role in the intracellular antioxidant machinery. Moreover, copper (Cu) is involved in the function of metalloproteins such as cytochrome C. As a central protein in mitochondrial respiratory chain, functional cytochrome c is essential for energy metabolism. In a CHO fed-batch process producing an immunoglobulin G (IgG), increased copper sulfate concentrations revealed increased maximum VCD and lower lactate production compared with control. The IgG aggregation level was shown to be dependent on the applied copper concentration (Qian et al. 2011). Iron is involved in the mitochondrial respiratory complexes I – III and in ferredoxins. Moreover, it participates in the catalysis of enzymatic reactions e.g. aconitase being responsible for the conversion of citrate into isocitrate. Iron is involved in electron transfer in various biochemical reactions since it is able to switch oxidative states as reviewed (Lill 2009).

2.1.6.2.5. Inorganic salts

To create an isotonic environment, the optimal osmolality of CDM is between 260- 320 mOsm/kg. Supplementation of inorganic salts is essential to avoid cell shrinkage or burst therefore preventing cell death (Yang and Xiong 2012). Moreover, delivery of sodium, potassium and calcium ions help to regulate cellular membrane potentials.

2.1.6.2.6. The bicarbonate buffer system

Media acidification through metabolic processes e.g. by lactate production needs to be prevented due to the pH sensitivity of cultured cells. The commonly used bicarbonate (HCO_3^-)/carbon dioxide (CO_2) buffer system shown in figure 6 is based on the presence of a weak base (HCO_3^-). HCO_3^- ions buffer the protons generated from lactic acid dissociation. Due to the reaction of protons and HCO_3^- ions, CO_2 is generated. The gaseous CO_2 leaves the broth and thereby stabilizes the pH of the solution.

$$\mathbf{HCO_3^- + H^+ \rightleftarrows H_2CO_3 \rightleftarrows CO_2 + H_2O}$$

Figure 6: The bicarbonate (HCO_3^-) /carbon dioxide (CO_2) buffer system.

With increasing culture time, NH_3 is produced by the cells and released into the culture broth. The produced NH_3 dissociates in water into ammonium ions (NH_4^+) and hydroxyl ions (OH^-) following the equilibrium $NH_3 + H_2O \leftrightarrow NH_4^+ + OH^-$. The OH^- ions increase the pH (lowering the proton concentration). CO_2 is added to the broth via the incubator atmosphere thereby prompting proton production to neutralize OH^- and stabilize the pH.

2.1.6.2.7. Surfactants

Additionally, surfactants such as poloxamer 188 or polysorbate 80 are added to shear sensitive cell cultures. The surfactants minimize stress resulting from shear forces or bursting gas bubbles. Addition of a surfactant to recombinant interferon gamma producing CHO cultures resulted in prolonged cell growth, increased therapeutic protein production and reduced cell lysis compared to control (Clincke et al. 2011). It was shown that the surfactant Pluronic F-68 was taken up by mammalian cells and accumulated in late endosomes and lysosomes (Gigout et al. 2008). From a physicochemical point of view surfactants in concentrated feeds were shown to keep feed media components in solution for a longer time frame (Hossler et al. 2013).

2.1.6.3. Classic CDM examples

Historically, media development started with the formulation of few first common culture media for mammalian cells. The first basal media containing serum were Eagle`s minimal essential medium (MEM), Roswell Park Memorial Institute (RPMI) medium and media based on Ham formulation.

MEM contains 12 non-essential amino acids, glutamine, eight vitamins and basic inorganic salts making this medium suitable for maintenance of cells grown in tissue culture (Yang and Xiong 2012). An enriched version of MEM was developed by Dulbecco leading to a medium containing four times

higher nutrient concentrations known as Dulbeccos minimal essential medium (DMEM) (Jayme et al. 1997).

RPMI medium is rich in phosphate and formulated for use under 5 % CO_2 atmosphere for the cultivation of suspension cells like lymphoid cells, tumor cells or primary cells (Yang and Xiong 2012).

For the cultivation of rodent cells from mouse and rat, media based on Ham formulation (Hams`F-10 and Ham`s F-12) are characterized by a rich amino acid concentration composition (Yang and Xiong 2012).

2.1.6.4. CDM development

Various cell lines show differences in cellular needs of nutrients. With the help of media optimization procedures, it is aimed to find the optimal medium for cell cultivation with regard to growth and protein production.

To start with the design of serum-free new media formulations, one option might be the mixture of 50:50 (v/v) DMEM and Ham`s F-12 further being supplemented with insulin, transferrin, selenium as a base for further optimization as reviewed (van der Valk et al. 2010).

As one optimization approach, media blending might be a technique for the improvement of cell culture media based on known mother media recipes. Such mixing approaches allow e.g. the mix of ten mother media with variable amino acid concentrations resulting in finally 192 different mixtures. The generated media may then be evaluated in cell culture concerning therapeutic protein production (Jordan et al. 2013).

With efficiency and multiple criteria analysis in mind, media mixing may be done with design of experiment (DoE) approaches. For example, screening of different media formulations is carried out with a specific mammalian cell line to identify several top media formulations based on e.g. growth and therapeutic protein production. These identified top formulations are then further mixed using DoE analysis to identify synergies to create optimal formulation mixtures. As a bottom up approach, the evaluation of spent media may help to get insight in the consumption of various media components e.g. vitamins or amino acids to optimize media formulations efficiently.

Rational culture design relies on the application of several complementary methods representing a multidimensional approach. Component titration and spent media analysis may accompany the media development in phases from screening through optimization to verification as reviewed (Jerums and Yang 2005; Gronemeyer et al. 2014).

2.1.6.5. Concentrated feeds

Feeds are highly concentrated nutrient solutions applied in fed-batch cultures for culture longevity and enhanced mAb production.

While basal media support low density cultures for initial culture progression, feed media are used for the control of different pathways in later phase of culture. As the mAb producing culture proceeds, optimized feeds are used for the prolonged growth, production and the control of product glycosylation pattern (Whitford 2006). Feed optimization is based on the evaluation of nutrient consumption rates in batch mode (Xie and Wang 1997).

Although feed media comprise fewer components, they are highly concentrated. With regard to culture volume, the addition of highly concentrated feeds in low feed volumes is beneficial since intense culture volume changes are avoided. But due to their abundance, solubility problems and interactions of feed components with each other, precipitations and color change may occur. Studies of concentrated media showed that pyruvate, bicarbonate and glutamine are factors influencing feed stability. Observed color changes may be related to Maillard reactions in bicarbonate containing media (McCoy et al. 2015).

2.2. Antibodies

2.2.1. General information

Antibodies, so-called immunoglobulins (Ig), are glycoproteins with globular structure being involved in the immune system. They are produced and secreted from B-lymphocytes in the human body (Behrsing and Micheel 2008).

As Y-shaped proteins, antibodies consist of two main structural regions namely the variable region at the top of the Y and the constant region at the stem of the Y. Two essential roles are performed by antibodies: the variable regions are necessary for antigen binding via epitope recognition while the constant region is responsible for effector functions such as natural killer cell activation, phagocytosis and activation of classical complement pathway as reviewed (Lipman et al. 2005).

MAb show monospecifity in the antigen binding site which means that they recognize one limited part of the antigen surface, called the epitope. This property makes them homogeneous and consistent. Their production began in hybridoma cells, but today they are produced from recombinant techniques relying on the genetic manipulation of host cells as described previously (Behrsing and Micheel, 2008). Polyclonal antibodies (pAbs) are antibodies which recognize several epitopes of an antigen. In an immune reaction, several antibodies specific for different epitopes of the antigen are produced. pAbs were usually produced from serum of artificially hyperimmunization donors or in egg yolk (Behrsing and Micheel 2008). As a new recombinant technique, pAbs may be produced using the Sympress™ technology. This recombinant method relies on the cultivation of different cell lines in one biorecator each expressing one distinct antibody using site-specific integration technology (Nielsen et al. 2010).

Mammalian Igs are clustered in five classes based on their constant regions, namely IgG, IgA, IgM, IgD and IgE. They differ in their physicochemical properties such as size, charge, solubility and their serologic features (*in vitro* reaction with antigens). Moreover, IgA and IgM exist as dimers and pentamers, respectively, while IgGs are mostly found in monomeric form (Wang et al. 2006). Four IgG subclasses named IgG1, IgG2, IgG3 and IgG4 are identified (Liu and May 2012) with high sequence homology. IgGs are further subgrouped into isotypes reflecting polymorphisms in the constant region of the heavy chain (Lipman et al. 2005). IgG subclasses differ in effector functions and structure with regard to inter-chain disulfide bonds and the length of the hinge region as reviewed (Walsh and Jefferis 2006; Wang et al. 2007).

2.2.2. Structure of an IgG1

An IgG1 consists of two identical heavy chains (HC) and two identical light chains (LC). One HC has a molecular mass of approximately 50 kDa while one LC has a molecular mass of approximately 25 kDa. In sum, an intact antibody has a total mass of approximately 150 kDa (Wang et al. 2007).

Each LC consists of a variable (v_L) domain and a constant (c_L) domain. One variable (v_H) and three constant (c_H) domains are found in each HC. Characteristics of an IgG1 are shown in figure 7. One LC is linked with one HC via one inter-chain disulfide bridge. Pairing of one LC with one HC is carried out between the last L-cysteine residue of the LC and the fifth L-cysteine residue of the HC. The two HCs are also paired via inter-chain disulfide bridges. In the case of an IgG1, two inter-chain disulfide bridges located in the hinge region are responsible for the pairing of the two HCs. The flexible hinge region allows lateral and rotational actions in the process of antigen binding (Adlersberg 1976). In sum, an IgG1 molecule has four inter-chain disulfide bridges.

Intra-chain disulfide bridging is associated with domain formation; in the case of an IgG1, 12 intra-chain disulfide bonds are present leading to 12 domains (Liu and May 2012). The occurrence of intra- and inter- chain disulfide bridges allows the tertiary structure of the antibody (Behrsing and Micheel 2008). Usually, the IgG1 molecule is supposed to contain 16 disulfide bridges (12 intra-chain disulfide bonds, 2 inter-chain disulfide links in the hinge region and 2 inter-chain disulfide bridges connecting HCs with LCs) (Padlan 1994).

Besides L-cysteine residues bound in disulfide bridges, free sulfhydryls may be detected in several IgG subclasses. Although the majority of L-cysteine residues are bound in disulfide bonds, four free L-cysteine residues were found in human IgG1 molecules pointing out co-existence of bound and unbound L-cysteine residues (Gevondyan et al. 2006). With regard to the LCs of recombinant IgG1, more free L-cysteine residues were found in the variable region compared with the constant region. With regard to HCs, domains were ordered from higher to lower free L-cysteine residue levels as follows: $C_{H3} > C_{H1} > C_{H2}$ > variable domains. It is suggested that low levels of free L-cysteine residues are due to incomplete disulfide bond formation formed under denaturing conditions as reviewed (Liu and May 2012).

Comparable antigen binding of the intact humanized IgG1 and the antibody containing two buried unpaired L-cysteine residues in the variable domain in the HC was found (Zhang et al. 2012). The level of free L-cysteine residues within the culture may be influenced by the amount of the oxidant Cu (II) sulfate in the culture (Chaderjian et al. 2005).

In the fragment antigen binding (Fab) fragment, the antigen binding site is located in the amino terminus and is associated with the variable regions of LC and HC. In this region, three hypervariable loops called complementary determining regions (CDR) namely CDR1, CDR2 and CDR3 are positioned. The CDRs are sequences of greatest amino acid variation. CDRs are therefore responsible for antigen recognition.

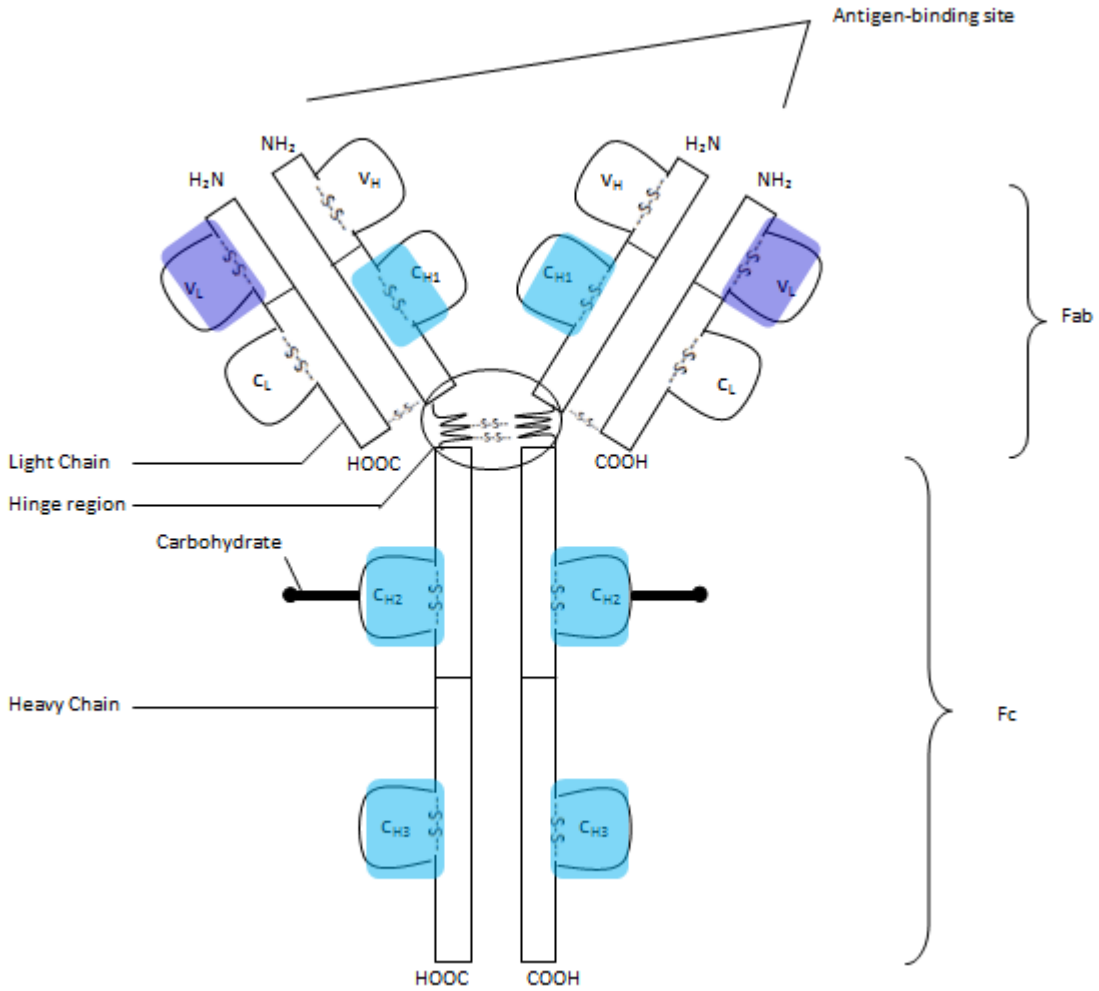

Figure 7: Structure of an IgG1 molecule.

Scheme represents heavy and light chains with domains, hinge region, glycosylation site, antigen binding site, Fab and Fc fragments and locations of possible free L-cysteine residues. Dark blue boxes mark regions in light chains as locations of possible free L-cysteine residues. Light blue boxes mark regions in heavy chains as locations of possible free L-cysteine residues. v: variable region, c: constant region, H: heavy chain, L: light chain based on reviewed data (modified from Liu and May 2012; Gevondyan et al. 2006)

Summarized, the primary antibody structure is determined via its amino acid structure and is responsible for the build-up of variable and constant regions of the HCs and LCs. Anti-parallel β sheets account for the secondary structure while these chains are then packed into globular domains being linked to neighboring domains making up the tertiary structure. Interaction of globular domains

of HCs and LCs represents the quaternary structure being functional in antigen binding and effector functions.

2.2.3. Effector functions of the fragment crystallisable (Fc) part

The Fc binds to complement proteins or to special cell receptors (Fc receptors) to initiate several immune response actions. Antibody-dependent cellular cytotoxicity (ADCC), antibody-dependent cellular phagocytosis (ADCP) and complement-dependent cytotoxicity (CDC) are effector functions being mediated by the Fc region (Moore et al. 2010) and are schematically presented in figure 8.

In ADCC (see figure 8 A), the antibodies interact via their Fab fragment with the antigens presented on pathogenic cells. Next, the Fc parts of the pathogen carrying antibodies interact with special receptors (Fcγ receptors) on effector cells of the immune system such as natural killer (NK) cells, macrophages, dendritic cells or granulocytes (neutrophils and eosinophils). After binding, some immune cells like NK cells are able to release cytotoxic compounds such as perforin and granzymes destroying the pathogenic cell via cell lysis.

In CDC (see figure 8 B), the antigen-carrying antibody interacts via its Fc part with the complement system. This process initiates the membrane attack complex making the cell membrane porous. Finally, death of pathogenic cells is carried out via cell lysis.

In contrast, ADCP relies on the interaction of the Fc part of the antigen-carrying antibody with Fcγ receptors presented on the macrophages` surface (see figure 8 C). Binding of Fc to macrophage Fcγ receptors allows transmembrane signaling. The signaling initiates pathogen internalization independent actions e.g. structural changes like microfilament reorganization for pathogen internalization. Subsequently, the macrophage surrounds the pathogen and internalizes it. The pathogen is further packed in vesicles (phagosome formation). The vesicles interact with the lysosomes of the macrophage (phagolysosome) (Hajela 1991). Synthesis and release of toxins against the pathogen e.g. oxidants (hydrogen peroxide) or degradation enzymes (proteases) are started helping the macrophage to destroy the pathogen.

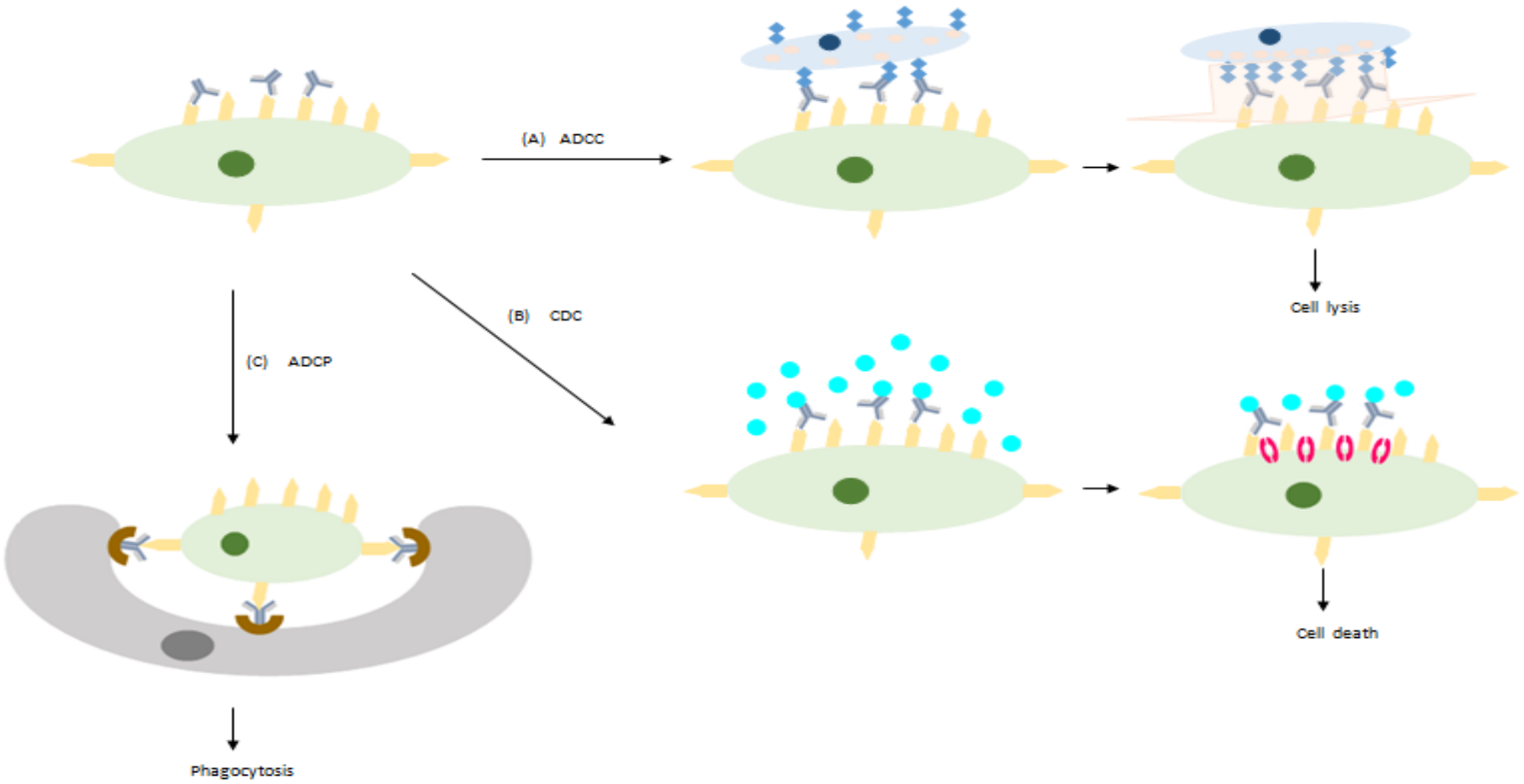

Figure 8: Schematic representation of three main effector functions mediated by Fc part of antibodies

(A) Antibody-dependent cellular cytotoxicity (ADCC). Binding of variable antibody region to antigen (yellow). Fc binding of antibodies (dark grey) to surface expressed immune cell (light blue) Fc receptors (dark blue rectangles). Release of cytotoxic compounds (pink) from immune cells leading to pathogen inactivation via cell lysis. (B) Complement-dependent cytotoxicity (CDC). Fc binding of antibodies to complement (turquoise). Pathogen inactivation by initiation of membrane attack complex (red). (C) Antibody-dependent cellular phagocytosis (ADCP). Fc binding of antibodies to surface expressed macrophage (light grey) Fc receptors (brown) and initiation of phagocytosis for pathogen inactivation.

2.2.4. Fc receptors

As previously shown, the Fc part is able to undergo interactions with special receptors so called Fcγ receptors (FcγRs) mediating thereby ADCC and ADCP (Chan and Carter 2010). With regard to effector functions, the involved FcγR receptors are located on the plasma membrane of innate immune cells. FcγR receptors belong to the immunoglobulin-like superfamily and contain three glycosylated receptor groups: FcγRI (cluster of differentiation (CD) 64), FcγRII (CD32) and FcγRIII (CD16). These receptors are typically single pass transmembrane glycoproteins (Raghavan and Bjorkman 1996). FcγRI is highly affine for the Fc part of an IgG and shows isotype specificity and is expressed on macrophages, dendritic cells, neutrophils and eosinophils.

FcγRII and FcγRIII possess lower Fc affinity but broader isotype specificity compared with FcγRI as reviewed (Nimmerjahn and Ravetch 2006). FcγRIIa is the main Fc macrophage receptor for IgG mediated ADCP. FcγRIIIa is involved in ADCC mediated by NK cells. Expression of FcγRIIIa is found on the surface of NK cells, dendritic cells and mast cells (Nimmerjahn and Ravetch 2006).

The Fc receptors may be classified into activation and inhibition receptors. Activation receptors transmit signals for activation via immunoreceptor tyrosine-based activation motifs. FcγRI, FcγRIIa, FcγRIII belong to the class of activation receptors. Activating signals are responsible for the induction of ADCC, endocytosis of immune complexes, antigen presentation, phagocytosis, cytokine or pro-inflammatory release as reviewed (Jiang et al. 2011). Inhibitory receptors use immunoreceptor tyrosine-based inhibitory motifs with FcγRIIb belonging to this receptor group as reviewed (Raghavan and Bjorkman 1996; Nimmerjahn and Ravetch 2006). Inhibitory signals are involved in the suppression of B lymphocyte, mast cell, monocyte and basophile activation. Activation and inhibition signals are involved in the regulation of immune responses as reviewed (Jiang et al. 2011).

The neonatal Fc receptor (FcRn) is located on the cell surfaces of monocytes, macrophages and dendritic cells with a transfer function of IgG from mother to fetus. Further functions are regulation of IgG serum half-life, maintenance of its serum concentration and regulation of IgG homeostasis as reviewed (Hayes et al. 2014).

Summarized, the antigen carrying IgG molecule is able to undergo effector functions with its Fc part. Next, relevant posttranslational modifications impacting Fc effector functions will be presented.

2.2.5. Relevant PTMs of therapeutic proteins

2.2.5.1. N-glycosylation

The asparagine (Asn) 297 at each C_{H2} antibody domain of the IgG1 Fc part is N-glycosylated. Besides this N-glycosylation site, Fab fragments are glycosylated in 20 % of IgG1 molecules. The hypervariable regions of an IgG may be glycosylated at position Asn58 in the second CDR in the variable region of the heavy chain (Wright et al. 1991). The glycans linked to the Fab fragments may be hyper-galactosylated, fucosylated and sialylated as reviewed (Hayes et al. 2014). Changes of N-linked CDR glycosylation may impact antigen binding (Wright et al. 1991). Severe effects on effector function are reported when C_{H2} N-glycosylation is changed since this glycosylation site is responsible for the recognition by FcγR and for the antibodies` quartenary structure as reviewed (Hayes et al. 2014).

2.2.5.1.1. Structure of N-glycans found in mammals

Figure 9 represents the scheme of the biantennary N-glycan structure linked to the C_{H2} domain of the Fc part. The core structure of this N-glycan consists of five saccharides. Precisely, the core structure consists of two β(1,4) linked N-acetylglucosamines (GlcNAc) coupled to three mannose (Man) as reviewed (Shade et al. 2013). Different monosaccharides are added to the basal N-glycan structure leading to variable carbohydrate structures representing glycan microheterogeneity.

The cellular processing machinery adds fucose (Fuc) in α(1,6) to core GlcNAc. GlcNAc is added to core Man via β(1,4) linkage. In the branches, GlcNAc is added to core Man via β(1,2) links. Galactose (Gal) is added to GlcNAc via β(1,4) linkages. Terminal sialic acid is added α(2,6) or α(2,3) to Gal leading to the mature form of an N-glycosylated Fc linked group as reviewed (Shade and Anthony 2013).

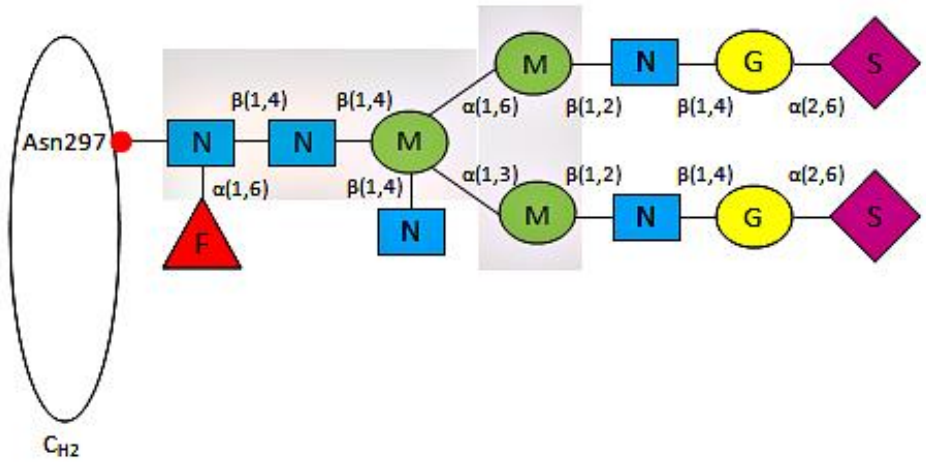

Figure 9: Schematic representation of N-glycan positioned at Asn297 in the C_{H2} domain (Fc part) of an IgG.

The biantennary structure of the N-glycan representing the core pentasaccharide is marked in grey. F: fucose, N: N-acetylglucosamine, M: Mannose, G: Galactose, S: sialic acid (modified from Shade et al. 2013).

2.2.5.1.2. Intracellular N-glycosylation

N-glycosylation of the protein is carried out in the endoplasmatic reticulum (ER) and in the Golgi apparatus. First, the oligosaccharide precursor $Glc_3Man_9GlcNAc_2$ is transferred from initially dolichol phosphate to the Asn residues of the protein consensus sequence.

In case of N-glycosylation of Asn297, the protein consensus sequence Asn-Xaa-Ser/Thr is used with Xaa being any amino acid. This process is carried out in the ER via an oligosaccharyltransferase. Then, ER-α-glucosidases I and II remove the glucose residues. The ER-α-mannosidase removes one Man rest leading to a final structure of $Man_8GlcNAc_2$ which finally enters the Golgi apparatus.

In this compartment, further reactions by glycosyltransferases and glucosidases lead to the addition or removal of sugar residues in complex series. Addition of Fuc to core GlcNAc via α(1,6) linkage is carried out via fucosyltransferase 8 (FUT8). Addition of GlcNAc to the core pentasaccharide is carried out via β(1,4)-N-acetylglucosaminyltransferases. Galactosyl transferase adds Gal to GlcNAc (Walsh and Jefferis 2006). The terminal Gal content classifies the Fc glycans into G0 (no terminal Gal), G1 (one terminal Gal) and G2 (two terminal Gal) (Raju and Jordan 2012). The sialic acids N-glycolylneuraminic acid (NGNA) and N-acetylneuraminic acid (NANA) are added to Gal residues via α(2,3) or α(2,6) sialic acid transferase dependent on the species as reviewed (Hossler et al. 2009).

2.2.5.1.3. Impact of N-glycosylation on therapeutic protein quality

The variation in terminal carbohydrates such as fucose, GlcNAc, sialic acids and Gal is described by the term glycan microheterogeneity. Glycan microheterogeneity impacts ADCC and CDC by changing

the binding behavior to Fc receptors or complement (C1q protein). As an example, the terminal Gal content may vary leading to G0, G1 and G2 glycan forms impacting product quality and bioactivity.

Human and CHO N-glycan structures show the described bianntenary structure and contain fucose. However, glycans produced in mouse cell lines show lower Fuc levels compared with those produced in CHO (Raju 2003) due to lower fucosyltransferase activities.

When comparing human and rodent Fc glycan structures, only few variations occur. Human glycan structures do not comprise terminal α Gal modification nor terminal NGNA but CHO glycans do as reviewed (Ghaderi et al. 2012). Sialic acid linkage in CHO cells is carried out via α(2,3) instead of α(2,6) linkages found in humans. Like CHO cells, mouse cell lines synthesize NGNA, too. NGNA is shown to be immunogenic to humans. This indicates the importance of the host cell line choice for therapeutic protein production.

The degree of sialylation, galactosylation, mannosylation and fucosylation impacts the effector functions as reviewed (Shade and Anthony 2013).

ADCC is impacted by the degree of glycan fucosylation. Presence of glycan Fuc reduced FcγIIIa binding as reviewed (Liu 2015). Consequently, lower Fuc levels led to increased ADCC. Studies with fucose-free glycans showed increased FcγRIIIa binding of the antibody Fc part compared with fucosylated Fc parts (Shields et al. 2002; Zauner et al. 2013).

CDC is impacted by the degree of glycan galactosylation. Terminal Gal levels may impact complement 1 (C1q) binding in CDC. Lower Gal levels were reported to reduce CDC activity as reviewed (Liu 2015). G2 glycans showed a higher complement binding activity and CDC compared with G0 glycoforms (Raju 2008).

Pharmacokinetics (PK) of a therapeutic protein may be impacted by the degree of mannosylation. Highly mannosylated recombinant IgGs showed decreased half-life and possible lower efficacy as reviewed (Liu 2015). Trimming of Man in both glycan structure arms resulted in decreased FcγRIIb binding (Mimura et al. 2001).

The sialic acid NGNA may elicit an immune response when being present in therapeutic proteins as reviewed (Hossler et al. 2009) and may impact mAb safety as reviewed (Liu 2015).

2.2.5.1.4. Altering N-glycan structures

In case of glycan optimization of the final product, glycans may be changed by genetic host cell line manipulation in upstream processes. Additionally, a change in production process parameters or media and feed formulation may impact glycan microheterogeneity as reviewed (Walsh and Jefferis 2006; Wang et al. 2007).

2.2.5.1.4.1. Genetic manipulation of the product cell line

To switch from fucosylated to non-fucosylated state of the therapeutic Ig glycans, gene deletion of necessary enzymes in the host cell may be carried out. The double knockout of the gene encoding for FUT8 and guanosine diphosphate-mannose 4,6-dehydratase (GMD) was shown to be effective in decreasing glycan fucose levels and increasing ADCC. FUT8 is responsible for the transfer of Fuc from guanosine diphosphate (GDP)-Fuc to the core GlcNAc. GMD is involved in the GDP-Fuc production as a substrate for FUT8. Double knockdown of both genes in CHO cells led to non-fucosylated IgG (Imai-Nishiya et al. 2007).

Overexpression of β-(1,4)-N-acetylglucosaminyltransferase III (GnTIII) may be also carried out to impact Fuc levels. Increased amounts of GnTIII led to an increased amount of GlcNAc glycan structures. The bisected glycan structures did not serve as a substrate for FUT8 since the intersecting GlcNAc may inhibit fucosyltransferase (Longmore and Schachter 1982).

As a way to manipulate glycan composition, nucleotide sugar transporter expression may be increased. Impacts on sialic acid content of glycans were made by increasing the endogenous sialic acid transporter expression to increase the transport into the Golgi apparatus as reviewed (McAtee et al. 2014).

2.2.5.1.4.2. Adaption of production media and feeds

Exemplary, two media and feed components are presented as options to impact glycosylation.

Uridine diphosphate N-acetylglucosamine (UDP-GlcNAc) is a precursor for cytidine 5´-monophospho-N-acetylneuraminic acid (CMP-NeuAc). CMP-NeuAc in turn is necessary for sialic acid attachment on glycans. Feeding UDP-GlcNAc may increase CMP-NeuAc concentrations and consequently influence sialylation. But UDP-GlcNAc feeding does not seem to be an option to achieve increased CMP-NeuAc levels since CMP-NeuAc feedback inhibits UDP-GlcNAc 2-epimerase (GNE). This enzyme is essential in the reaction of UDP-GlcNAc into N-acetylmannosamine (ManNAc), the first reaction in CMP-NeuAc synthesis as reviewed (Hinderlich et al. 2015). Increasing the CMP-NeuAc levels by UDP-GlcNAc feeding would result in GNE inhibition thereby limiting sialic acid production.

Since ManNAc is a direct precursor for sialic acid, increasing ManNAc media concentrations showed increased glycan sialylation as reviewed (McAtee et al. 2014). Besides the presented components impacting glycosylation of the therapeutic protein, other factors such as manganese, Gal or sodium butyrate may also help to alter glycosylation (Hossler et al. 2009).

2.2.5.1.4.3. Cell culture metabolites

As a cell culture by-product, NH_3 impacts the function of glycosylation enzymes when being present in concentrations of 2 mM due to increased pH in the Golgi. One pH sensitive enzyme in the Golgi is e.g. α(2,3)sialyltransferase indicating the impact of NH_3 on sialylation. At higher NH_3 concentrations around 20 mmol/L (mM), impaired sialylation and glycan antennary may be observed.
Lactate was not reported to impact glycosylation directly but impacts cell growth and protein productivity. Feeding of low glucose concentrations is strategical and reduces lactate concentrations. But low glucose levels impact glycosylation due to low availability of glycosylation precursors as reviewed (McAtee et al. 2014).

2.2.5.1.4.4. Process parameters

Further, differences in glycan composition were reported to be observed in different process modes. Proteins produced in perfusion mode showed higher glycan sialylation compared with proteins produced from fed-batch processes. This is possibly related to lower cell growth rate in favor of full glycosylation as reviewed (Hossler et al. 2009). Besides process mode, the process parameters pH, temperature and dissolved oxygen (DO) may impact glycosylation. Sialylation degree was dependent on culture pH showing highest Epo-Fc glycoprotein sialylation at neutral pH. Galactosylation and sialylation were found to be impacted with pH changes as reviewed (Hossler et al. 2009).
Effects of DO were shown to be product dependent. No significant changes were seen in tissue-type plasminogen activator glycosylation under hypoxic conditions while decreasing terminal galactosylation levels were reported in a recombinantly produced IgG1 when DO decreased as reviewed (Hossler et al. 2009).
Decreased culture temperature prolonged cell viability and increased protein production and therefore beneficially impacted overall glycosylation as reviewed (Hossler et al. 2009).

2.2.5.1.4.5. Glycan trimming with extracellular enzymes

With increasing culture time, the portion of damaged and dead cells increases. Due to cell damage, intracellular enzymes are released amongst other glucosidases. These enzymes trim and degrade the produced glycan structures and may impact protein function. This emphasizes the importance of product harvest time.

Summarized, glycans are involved in different functions. The quarternary structure of the antibody is determined by the N-glycan linked to the C_{H2} domain of the Fc part. Due to spatial structure determined by the Fc glycan, the antigen-carrying antibody is able to function via its Fc part.

Consequently, the Fc part of an antibody is able to interact with FcγRs or complement. This emphasizes the involvement of the glycans in biological activity. Moreover, the glycans are involved in stability and immunogenicity as reviewed (Walsh and Jefferis 2006). The glycosylation pattern may be influenced by the chosen host cell line itself, genetic host cell manipulations process conditions and media and feed formulation. These parameters need to be qualified for a certain mAb ensuring consistency in product quality.

2.2.5.2. Other PTMs

With regard to impacts on patient safety and product efficacy of therapeutic proteins *in vivo*, critical quality attributes (cQAs) need to be identified on risk-based analysis. In case of mAb, cQAs may impact biological activity, PK, pharmacodynamics, immunogenicity, and overall safety/toxicity.

2.2.5.2.1. Aggregation

Aggregation is initiated by physical or chemical interactions. Aggregates may show differences in size. Due to size differences, non visible aggregates may be termed to be "soluble" since filtration procedures using 0.22 µm pore size filters may not retain them. Aggregates being visible are designated to be "insoluble" as reviewed (Cromwell et al. 2006).

Exposed unpaired L-cysteine residues may build up disulfide bonds between antibody monomers leading to covalent bound antibody monomers. Besides covalent interplay, electrostatic and dipole-dipole interactions have been observed leading to self-association of mAb and fibrillogenic β-sheet association as reviewed (Cromwell et al. 2006).

Different types of stress in production and downstream processes have been reported to impact aggregation behavior of antibodies such as temperature, pH, buffer type, ionic strength, protein concentration and storage processes including e.g. shaking and stirring (agitation), freezing, thawing and handling as reviewed (Eon-Duval et al. 2012). Different stresses such as low pH and ultraviolet (UV) light were reported to impact aggregation behavior differently. While low pH stress generated non-covalently linked antibody dimers, UV light incubation led to chemically modified dimers showing various dimer conformations. Different stresses were shown to impact differently the biological activity of the product (Paul et al. 2012).

2.2.5.2.2. Peptide bond breakage

Chemical or enzymatic peptide bond breakage led to fragmentation of mAbs in the hinge region under pH and temperature influence. In the mAb producing cell culture, release of intracellular proteolytic

enzymes occurred which may have contaminated the final product leading to stability concerns, loss of biological activity and effector functions as reviewed (Eon-Duval et al. 2012).

2.2.5.2.3. Oxidation

ROS were shown to oxidize predominantly L-methionine into methionine sulfoxide in the Fc part due to the solvent exposure of the C_{H2}-C_{H3} region. The presence of high levels of oxidized methionine (Met) residues (Met252 and Met428) at the Fc part of an IgG revealed reduced FcRn affinity *in vitro* (Stracke et al. 2014). Lower levels of tryptophan oxidation were reported to occur in the CDR regions as reviewed (Eon-Duval et al. 2012).

2.2.5.2.4. γ-carboxylation and β-hydroxylation

Conversion of L-glutamate into γ-carboxyglutamate in the protein backbone is carried out by carboxylases. Specific hydroxylases are responsible for the conversion of L-aspartate to β-hydroxyaspartate via β-hydroxylation. Both types of amino acid modification are important for facilitated calcium binding therefore being important only in a small group of proteins such as blood coagulation proteins, namely factors VII, IX, X or the antithrombotic molecule protein C. The latter protein needed full γ-carboxylation and β-hydroxylation to display biological activity as reviewed (Walsh 2010).

2.2.5.2.5. Amidation and sulfation

In the process of amidation, the carboxy terminus end of the protein is replaced with an amide functional group ($CONH_2$). Proline amidation and cyclization of L-glutamine leads to the formation of pyroglutamate residues contributing to the basic variants. As an example, the hormone calcitonin needed the amidation for its biological activity in treating hypercalcaemia. Recombinant calcitonin production in prokaryotes showed no amidation which had to be carried out in downstream processes using a recombinant α-amidating enzyme as reviewed (Walsh 2010).

Sulfation is a post-translational modification carried out by tyrosylprotein sulfotransferase. The enzyme catalyzes the transfer of an activated sulfate from 3´-phosphoadenosine-5´-phosphosulfate (PAPS) to tyrosine residues in proteins. With regard to glycoproteins such as antibodies, carbohydrate sulfurtransferases catalyze the sulfation reaction. The sulfation of the leukocyte glycoprotein P-selectin glycoprotein ligand-1 was reported to decrease interaction with its binding partner P-selectin as reviewed (Yang et al. 2015). But recombinant non-sulfated hirudine was effective as an anticoagulant although it is normally sulfated as reviewed (Walsh 2010). This points out that no clear statement on the biological activity of a therapeutic protein in presence or absence of sulfation may be postulated.

The impact of sulfation/non-sulfation on biological activity of the therapeutics must be evaluated case by case.

2.2.5.2.6. Sequence variants

Variations in the amino acid sequence of antibodies were reported. In case of extracellular tyrosine depletion, cells starved and misincorporated preferentially phenylalanine (Phe) in recombinant mAbs instead of tyrosine (Tyr). The effect of misincorporation was connected to mistranslation and $tRNA_{Tyr}$ mischarging with Phe instead of Tyr due to structural similarities of these amino acids (Feeney et al. 2013).

Misincorporation of serine instead of Asn was reported to occur via mistranslation provoked by extracellular Asn starvation (Khetan et al. 2010). This misincorporation in the antibodys´ CDR showed only slight decrease in binding affinity (Wen et al. 2009). These examples of sequence variation point out that media formulation, process surveillance and spent media analysis are necessary to guarantee protein quality.

As shown in the previous sections, the amino acid L-cysteine plays an important role in mAb producing processes and is an important amino acid being responsible for antibody structure. In the next sections of this chapter, we will focus on the thiol group-containing amino acid L-cysteine with regard to its production, properties and its derived biological meaning. The cellular uptake will be presented as well as its role in intracellular metabolism. Due to the mentioned PTMs occurring in mAb, we will focus on aberrations in L-cysteine dependent PTMs. Due to the complex reactions of L-cysteine in medium, opportunities of L-cysteine replacement by the use of L-cysteine derivatives in different cellular cultivation applications will be discussed pointing out the aim of this work in chapter 3.

2.3. L-cysteine

2.3.1. The production of cysteine

2.3.1.1. Chemical reactions

Historically, L-cysteine was isolated from keratins extracted from e.g. hair, wool, feathers, horns, hooves and nails (Ralph et al. 1994 (b)) and may also be chemically synthesized as reviewed (Ralph et al. 1994 (b)). This points out that production of L-cystine is essential for further synthesis of L-cysteine.

As shown in figure 10, synthesis of DL-cysteine hydrochloride monohydrate was based on the reaction of chloroacetaldehyde, sodium hydrogen sulfide, NH_3 and acetone leading to the formation of the intermediate 2,2,-dimethyl-3-thiazoline. The latter compound was the base for further reactions with first hydrocyanic acid and second aqueous hydrochloride acid leading to the formation of final product with a yield of 70% (Martens et al. 1981).

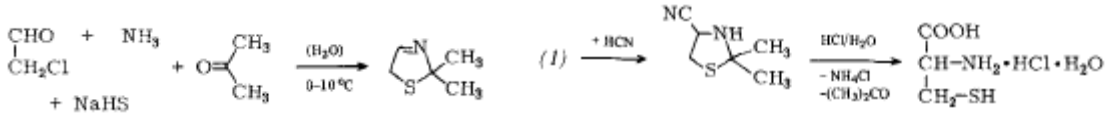

Figure 10: Chemical reaction mechanism of DL-cysteine hydrochloride monohydrate.

Conversion of chloroacetaldehyde with sodium hydrogen sulfide and NH_3 into 2,2-dimethyl-3-thiazoline with subsequent transformation into DL-cysteine hydrochloride monohydrate using hydrocyanic acid and aqueous hydrochloride acid (modified from Martens et al. 1981).

2.3.1.2. Microbial reactions

2.3.1.2.1. L-cysteine production using the genus *Bacillus sphaericus*

An established enzymatic production method of L-cysteine was based on the conversion of 3-chloro-L-alanine and hydrogen sulfide (H_2S) into L-cysteine via β-replacement reaction catalyzed by cysteine desulfhydrase (EC 4.4.1.1). This enzyme is also able to produce L-cysteine from pyruvate as reviewed (Hsiao et al. 1988). Since this enzyme found in *Enterobacter cloaceae* not only generates (see figure 11) but also degrades the desired product L-cysteine, enzyme alternatives for this reaction needed to be found. The bacterium strain *Bacillus sphaericus* L-118 was shown to possess the enzyme O-acetylserine sulfhydrylase being capable to carry out the presented reaction without degrading the desired product L-cysteine.

$$\mathbf{L-ClCH_2CH(NH_2)COOH + NaHS \rightarrow L-HSCH_2CH(NH_2)COOH + NaCl}$$

Figure 11: Enzymatic L-cysteine production catalysed by cysteine desulfhydrylase (EC 4.4.1.1).

Conversion of 3-chloro-L-alanine and sodium hydrogen sulfide into L-cysteine (modified from Dhillon et al. 1987).

In this process, cells were first grown in a medium containing the substrate 3-chloro- L-alanine. Then, cells were harvested and incubated with a reaction mixture containing 3-chloro-L-alanine, sodium hydrosulfide, *N*-cyclohexyl-3-aminopropanesulfonic acid buffer and acetone. Due to the incubation of the cells with the reaction mix, L-cysteine production was initiated. The reaction was stopped by addition of trichloroacetic acid (Dhillon et al. 1987). This procedure points out that bacteria may be grown for subsequent enzyme isolation and use in L-cysteine production.

2.3.1.2.2. L-cysteine production using the genus Pseudomonas

As a bioconversion process, bacteria from the genus *Pseudomonas* were shown to hydrolyse the substrate DL-2-amino-Δ²-thiazoline-4-carboxylic acid (DL-ATC) leading to L-cysteine production relying on three distinct steps.

As shown in figure 12, D-ATC was first racemized into L-ATC. Second, a ring-opening reaction of L-ATC via L-ATC hydrolase led to the formation of the intermediate N-carbamoyl-L-cysteine (L-NCC). Third, L-NCC was hydrolyzed via L-NCC amidohydrolase into L-cysteine with further optimizations for increased L-cysteine yields as reviewed (Wada and Takagi 2006). Enzymatic conversion of thiazolines may present an option in L-cysteine production.

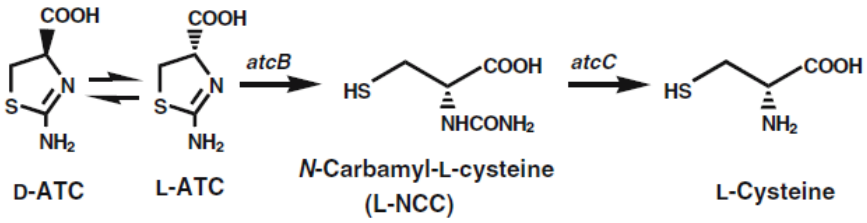

Figure 12: Enzymatic L-cysteine production catalysed by L-ATC acid hydrolase and L-NCC amidohydrolase.

Racemisation of D-2-amino-Δ²-thiazoline-4-carboxylic acid (D-ATC) into L-2-amino-Δ²-thiazoline-4-carboxylic acid (L-ATC) with subsequent enzymatic hydrolysis of L-ATC into N-carbamoyl-L-cysteine (L-NCC) and further enzymatic conversion into L- cysteine (modified from Wada and Takagi 2006).

2.3.1.2.3. L-cysteine production using *Corynebacterium glutamicum*

As a biosynthetic process for L-cysteine generation, cultivation of the genetically manipulated *Corynebacterium glutamicum* resulted in increased formation of L-cysteine.

Therefore, genetic manipulation needed to be achieved first by disrupting the gene encoding for cysteine desulfhydrase (CysD). CysD was responsible for the conversion of L-cysteine into pyruvate, NH_3 and H_2S. By disrupting the CysD gene, the protein for the enzyme CysD was not produced anymore thus accumulating the desired product L-cysteine.

Since increased L-cysteine levels impacted serine acetyltransferase (SAT) in *Corynebacterium glutamicum* activity due to feedback inhibition, the second genetic manipulation was the introduction of an *Escherichia coli* SAT gene altered by site directed mutagenesis. After its introduction into *Corynebacterium glutamicum*, the feedback inhibition effect was stopped and L-cysteine production was optimized as shown in figure 13.

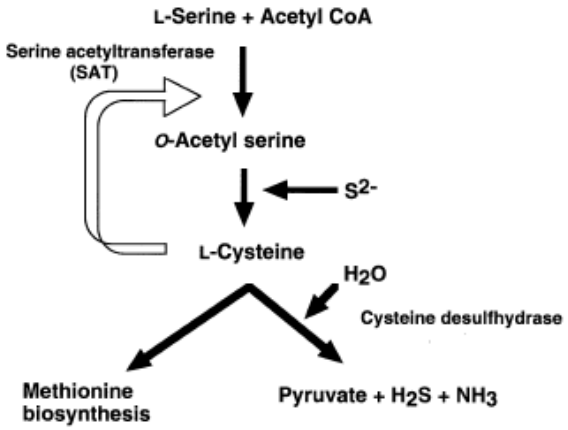

Figure 13: Enzymes serine acetyltransferase (SAT) and cysteine desulfhydrase in *corynebacterium glutamicum* as genetic manipulation options.

SAT is feedback inhibited by increasing L-cysteine levels. L-cysteine is degraded enzymatically by cysteine desulfhydrase into pyruvate, hydrogen sulfide (H_2S) and ammonia (NH_3) (modified from Wada et al. 2002).

Both manipulations increased the final L-cysteine concentrations in *C. glutamicum* (Nakamori et al. 1998; Wada et al. 2002). This emphasized that cultivation of genetically manipulated and improved cells is now an efficient method for L-cysteine production.

2.3.2. The physicochemical properties of L-cysteine

2.3.2.1. Structure and reactivity of L-cysteine

L-cysteine ((R)-2-amino-3-mercaptopropionic acid)) is an amino acid. To the asymmetrical carbon atom, one carboxy group, one amino group, one hydrogen atom and one rest are linked. In case of L-cysteine, the rest residue contains one methylen group linked to a thiol group as shown in figure 14 A.

The nucleophilic reactive thiol group allows addition and substitution reactions (Piste 2013). Due to its three reactive groups, L-cysteine contains three possible coordination sites for chelation (Shindo and Brown 1965). The thiol-group based reactivity is responsible for the dimerisation of two L-cysteine molecules leading to the formation of L-cystine ((R,R)-3,3´-Dithiobis(2-aminopropionic acid)) via a disulfide bridge as shown in figure 14 B.

This dimerisation behaviour is based on oxidation in the presence of air or metal ions but is reversible by reduction.

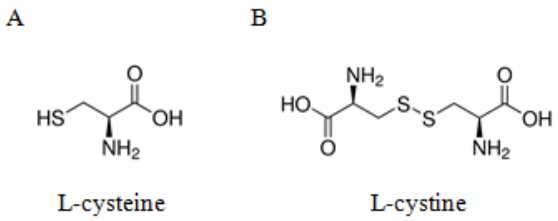

Figure 14: Structures of L-cysteine and L-cystine.

As an amino acid, L-cysteine is present in aqueous solution as a dipolar ion acting either as an acid or base. Since it contains three ionizable side chains (carboxyl, thiol and amine group), these three groups may be titrated as shown in figure 15 leading to three different pKa values of each ionization group. In proteins, pKa values for L-cysteine might be different due to the local environment e.g. surrounding by positively charged amino acids or L-cysteine location at the N-terminus of an α-helix as reviewed (Paulsen and Carroll 2012).

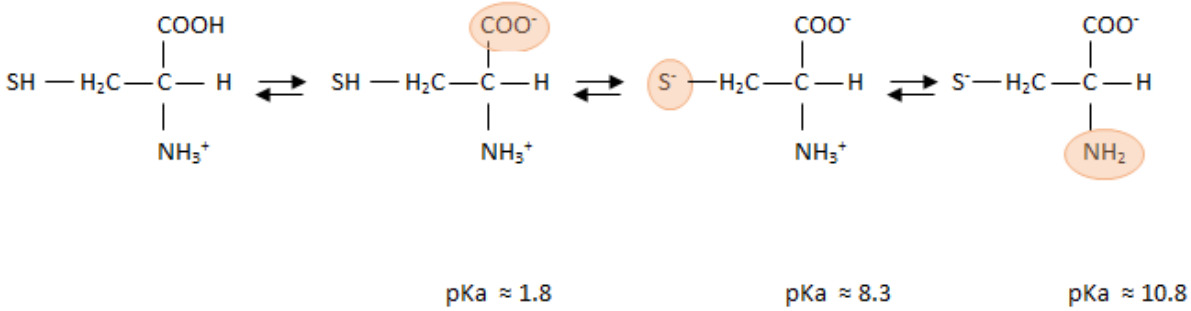

Figure 15: Titration reactions for pKa determination of L-cysteine.

After first titration, pKa of carboxyl group is determined followed by pKa of thiol group after second titration and pKa of amine group after third titration.

2.3.2.2. Solubility and stability of L-cysteine and L-cystine

L-cysteine and L-cystine differ in their solubility and stability behavior in aqueous media. L-cysteine was reported to be soluble in water at 25°C at a concentration of 2.3 mol/L (M). In contrast, at 25°C, L-cystine showed reduced solubility in aqueous media of 0.46 mM. The solubilized L-cystine concentration may be increased when being dissolved in acidic aqueous media such as 2 mol/L hydrochloric acid as reviewed (Ralph et al. 1994 (a)). These data point out that L-cysteine shows higher solubility compared with L-cystine. L-cysteine is highly reactive and is rapidly oxidized into L-cystine.

2.3.3. Reaction behavior of L-cysteine in complex formulations of CDM

The complexity of cell culture media as nutrient cocktails serves as a source for multiple cell-free reactions with L-cysteine being a reactive component.

2.3.3.1. L-cysteine oxidation by copper ions

Due to the presence of copper salts in CDM formulations, L-cysteines´ auto-oxidation in aqueous media was reported to be catalyzed by copper ions. The generated L-cystine may further form chelate-precipitates with copper ions.

Catalyzed auto-oxidation of L-cysteine by copper ions was studied extensively. L-cysteine was oxidized into L-cystine in the presence of Cu (II) while the latter was reduced to Cu (I) in aqueous solution. The generated Cu (I) reacted with L-cysteine forming a stable complex (Ahmed et al. 2011). A reaction cycle for the aerobic Cu (II) catalysed oxidation of L-cysteine in phosphate buffer at pH 7.4 was proposed. Therein, the catalyst bound a second L-cysteine leading to the formation of the bis-cysteine complex (Pecci et al. 1997). Reaction of excess L-cysteine and Cu (II) in the presence of phosphate in aqueous solution showed an one electron oxidation of L-cysteine via a free radical mechanism at neutral pH (Rigo et al. 2004).

With regard to the poorly stable L-cystine, metal-ligand-complex formation was reported in the presence of Cu (II) in aqueous solution (Berthon 1995).

Consequently, L-cysteine is able to be rapidly converted into L-cystine via redox reactions when copper ions are present. Due to the presence of copper in CDM, these reactions are expected to take place after media preparation and storage.

2.3.3.2. L-cysteine oxidation by iron ions

The catalytic effect of iron with excess L-cysteine was also under investigation. It was proposed that one iron ion and three L-cysteine molecules form an octahedral complex which dissociated in two L-cysteinyl species leading to L-cystine formation (Taylor et al. 1966). Potassium ferrate reacted with L-cysteine in an 1:1 ratio resulting in the formation of sulfinate anion whereas the reaction with L-cystine took place in a 4:3 stoichiometry leading to the production of thiosulfonate (Read et al. 2000). Moreover, nanomolar concentrations of Fe (III) were shown to inhibit Cu (II) catalysed oxidation of L-cysteine in aqueous solution at pH 7.25 (Munday et al. 2004). Figure 16 summarizes reactions of L-cysteine and L-cystine with iron or ferrate ions.

Due to the co-existence of iron and copper salts in CDM, those reactions are able to take place in prepared and stored media with interconnections of the undergoing reactions.

A

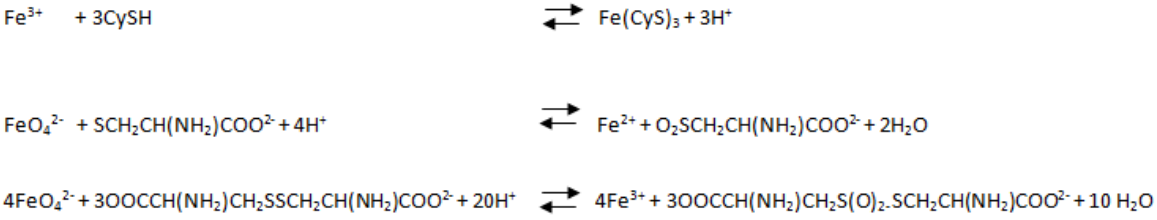

Figure 16: Reactions of L-cysteine with iron ions and reactions of L-cysteine and L-cystine with ferrate ions.
(A) Complex formation of three L-cysteine molecules and one iron (III) ion. (B) Reactions of ferrate ions with L-cysteine (1:1) and L-cystine (4:3) leading to sulfinate ion and thiosulfonate production, respectively (modified from Taylor et al. 1966; Read et al. 2000).

2.3.3.3. L-cysteine and other trace metals

Also, reactions of zinc (II), cadmium (II), lead (II) and mercury (II) with L-cysteine were described resulting in poorly soluble complexes in diverse solvents (Shindo and Brown 1965). Moreover, vanadate and oxovanadium (IV) underwent reactions with L-cysteine and L-cystine, respectively as reviewed (Baran 2003).

Since media formulations always contain inorganic salts based on the above mentioned metal ions, it is possible that these reactions with L-cysteine may lead to loss of free available L-cysteine. This might impact cell culture performance.

2.3.3.4. L-cysteine and glucose

Moreover, reactions of L-cysteine and the monosaccharide D-glucose have been reported in nutrition infusates leading to the formation of D-glucocysteine as reviewed (Soghier and Brion 2006). Since CDM contain high concentrations of carbohydrates, possible reactions between L-cysteine and D-glucose might be possible in prepared and stored liquid media which might impact availability of free L-cysteine for cell cultivation.

2.3.4. Reactive species (RS) - ROS, reactive nitrogen species and reactive sulfur species

Many reactive molecules *in vivo* are non-radicals and become even more reactive when e.g. a single electron is added. Several species are clustered into this group called ROS such as e.g. superoxide, hydroxyl, hydroperoxyl and peroxyl radicals. But radicals may also be transformed into non-radical species as reviewed (Halliwell 2006). When radicals are formed, chain reactions will be initiated serving as a source for continuous and diverse radical and non-radical species formation.

Hydrogen peroxide (H_2O_2) as a non-radical molecule and hydroxyl radicals may be formed after administration of L-cysteine pointing out that L-cysteine is able to form reactive species.

L-cysteine is sensitive towards ROS attack. H_2O_2 oxidized this amino acid to sulfenic acid which was itself the base for production of sulfinic and sulfonic oxyacids in the presence of excess H_2O_2.

When L-cysteine residues are chemically changed in a protein, this may affect biological activity and might be a source for intracellular redox signaling when L-cysteine modifications may be reversible. This is the case for e.g. L-cysteines with –SOH groups which may be reduced with a –SH donor to form a disulfide as reviewed (D`Autréaux and Toledano 2007).

But also reactive nitrosylated species may interact with L-cysteine. In this case, L-cysteine groups of proteins may react with S-nitrosoglutathione to produce mixed disulfides (Jacob et al. 2003).

Besides oxygen and nitrogen based reactive radicals, formation of sulfur centered radical species was found to occur *in vivo* and *in vitro*. The dominant member of reactive sulfur species was the thiyl radical as reviewed (Jacob et al. 2003). Since enzymatic thiyl generation from L-cysteine was reported to occur (Harman et al. 1984), harmful effects resulting from thiyl radical presence may be possible.

2.3.4.1. RS generation by reactions of L-cysteine with HCO_3^- and GSH

Alone or in combination with different CDM components, L-cysteine may provoke the production of highly reactive species. The formation of ROS as reactive radicals is critical since rapid multiple reaction series are prompted by their presence and may further initiate rapid reaction mechanisms of other components. As a member of ROS, H_2O_2 generation was studied in interaction studies with CDM components and L-cysteine.

H_2O_2 was reported to be generated in presence of L-cysteine and HCO_3^-. Since HCO_3^- is used to stabilize pH in cell culture media, this essential component may not be easily excluded from media formulation. The reaction of the amino acid and the buffer system resulted in the oxidation of L-cysteine and generation of the oxidant H_2O_2 (Regino and Richardson 2007). Addition of L-cysteine, GSH, γ-glutamylcysteine and cysteinylglycine to the media formulations RPMI, MEM and DMEM resulted in the formation of H_2O_2 (Long and Halliwell 2001). The nitrogen based reactive molecule nitric oxide (NO) was reported to react aerobically with L-cysteine and glutathione leading to the formation of S-nitrosothiols with subsequent NO release (Sheu et al. 2000).

2.3.4.2. RS generation by L-cysteine and reactions of RS with vitamins

Since L-cysteine was able to generate RS, reports stated the instabilities of vitamins towards produced RS.

As such, incubation of riboflavin, thiamine and pyridoxine with H_2O_2 resulted in decreasing vitamin concentrations indicating that the mentioned vitamins show sensitivity towards oxidation mediated by H_2O_2 (Ribeiro et al. 2011). Further, the susceptibility of thiamine was supported by studies made by Dwivedi and Arnold. In presence of H_2O_2, thiamine was shown to be oxidized forming a disulfide derivative (Dwivedi and Arnold 1973).

2.3.5. Effects of L-cysteine on cell cultivation

In presence of L-cysteine in excess, cultured neurons and developing animals show neurotoxic effects since L-cysteine may act as an excitotoxin as reviewed (Janáky et al. 2000).

Addition of 1 M L-cysteine to different cell culture media and further cultivation of different mammalian cell lines in these media led to growth differences. For several cell lines, cell death was observed. When the L-cysteine containing media were heated to 37 °C before starting the cultivation, cultures showed improved cell growth. This was connected to increased L-cysteine oxidation in pre-warmed media leading to decreased free L-cysteine concentrations. Another method for overcoming L-cysteine toxicity was the addition of pyruvate leading to thiazolidine structures and decreased free L-cysteine concentrations. These data point out that the concentration of free L-cysteine may be harmful to cultured cells without specifying toxicity mechanisms (Nishiuch et al. 1976).

Further experiments with renal epithelial cells exposed to 0.5 mM L-cysteine showed increased lactate dehydrogenase (LDH) release after 16 hours in culture pointing out a cellular damage. The LDH release was further stimulated in the presence of 100 µmol/L (µM) copper (II) sulfate ($CuSO_4$). Cell damage was shown to be a result of lipid peroxidation which was caused by produced H_2O_2 and hydroxyl radicals (Nakanishi et al. 2005). The effect of lipid peroxidation by L-cysteines´ auto-oxidation was increased in the presence of copper (Nakanishi et al. 2005). L-cysteine-based lipid peroxidation was also observed in liver microsomes being intensified by the presence of iron (Searle and Willson 1983).

This points out that L-cysteine application in cell culture leads to the generation of reactive molecules impacting cell viability and cell culture performance. Their production is accelerated by CDM since they contain trace metals such as copper.

2.3.6. L-cysteine stabilization in CDM

Due to the auto-oxidation of L-cysteine and the consequences in cell culture, L-cysteine stabilization is necessary to limit L-cysteine auto-oxidation. Addition of pyruvate was shown to decrease H_2O_2 concentrations due to scavenging properties of pyruvate (Nath and Salahudeen 1993). Pyruvate supplementation is an option for stabilizing L-cysteine in CDM to prevent L-cysteine from being oxidized into L-cystine and therefore its decrease in concentration in prepared and stored media (Nishiuch et al. 1976). Evidence for direct H_2O_2 scavenging by pyruvate was given since decarboxylation of pyruvate was detected after H_2O_2 treatment indicating protection mechanisms of pyruvate against H_2O_2 (Salahudeen et al. 1991). Similar decarboxylation reactions of α-ketoglutarate (α-KG) were determined after H_2O_2 treatment indicating anti-oxidative properties not only of pyruvate but also of α-KG (Salahudeen et al. 1991).

The reaction of L-cysteine with pyruvic acid was reported to yield a thiazolidine structure which is a dissociable ring structure protecting the reactive thiol group from oxidation and other reactions (Schubert 1937). Thiazolidines may undergo non-enzymatic and enzymatic ring opening reactions (Wlodek et al. 1993) to release both compounds for further metabolic use. Thiazolidines have been reported to be prodrugs for L-cysteine (Nagasawa et al. 1984).

Summarised, L-cysteine is involved in multiple reactions with different component classes. These components are part of CDM formulations. It is therefore likely that reactions of L-cysteine and these various CDM components may occur.

2.3.7. Cellular L-cysteine and L-cystine uptake

2.3.7.1. Cellular L-cysteine uptake

Amino acids usually are taken up from the extracellular medium in a balanced manner for e.g. intracellular protein synthesis and energy metabolism responding on cellular nutritional requirements as reviewed (Shotwell and Oxender 1983). Amino acids are transported via transporters being located in the cellular membrane. They transport amino acids from the extracellular into the intracellular space down their electrochemical gradient (Hediger et al. 2004). But amino acid transporters serve also as cellular signaling tools evaluating intra-and extracellular amino acid availability as reviewed (Hundal and Taylor 2009), thus controlling the uptake adapted to cellular need. They are distinguished on the base of their properties such as e.g. function/mode, pH dependence, sodium ion dependence or regulation.

Extracellular L-cysteine may be taken up by mammalian cells via different transporters belonging to distinct transporter systems. Table 1 summarizes transport proteins from literature data which are reported to be involved in L-cysteine uptake in mammalian cells.

As an essential remark, substrate specificities may be overlapping. In the case of L-cysteine uptake in CHO cells, different transporter systems such as the sodium-dependent systems A and ASC as well as the sodium-independent system L are able to transport this amino acid dependent on differences in substrate concentrations (Shotwell et al. 1981). Summarized, in eukaryotic cells, one amino acid may be a substrate for different transporters as reviewed (Hundal and Taylor 2009).

Table 1: Summary of literature-based L-cysteine transport systems

Transport proteins, transport system type, function and substrates as well as references for L-cysteine uptake are listed; n.m. = not mentioned

Transport protein	Transport system type	Function	Substrates	Reference for L-cysteine uptake
EAAT3 (SLC1a1, EAAC1)	X^-_{AG}	3 Na^+ : 1 H^+ : 1 glutamate (in) : 1 K^+ (out) (Alexander et al. 2013)	L-glutamic acid, L-aspartic acid (Alexander et al. 2013) L-cysteine (Zerangue and Kavanaugh 1996)	Zerangue and Kavanaugh 1996; Himi et al. 2003; Chen and Swanson 2003; Watts et al. 2014
EAAT2 (SLC1a2, GLT1)	X^-_{AG}	3 Na^+ : 1 H^+ : 1 glutamate (in) : 1 K^+ (out) (Alexander et al. 2013)	L-glutamic acid, L-aspartic acid (Alexander et al. 2013), L-cysteine (Chen and Swanson 2003)	Chen and Swanson 2003
ASCT1 (SLC1a4)	ASC	1 Na+ : 1 amino acid (in) : 1 Na+ : 1 amino acid (out) (homo –or hetero exchange) (Alexander et al. 2013)	L-cysteine > L-alanine = L-serine > L-threonine (Alexander et al. 2013)	Tamarappoo et al. 1996
ASCT2 (SLC1a5)	ASC	1 Na+ : 1 amino acid (in) : 1 Na+ : 1 amino acid (out) (homo –or hetero exchange) (Alexander et al. 2013)	L-alanine = L-serine = L-cysteine = L-threonine = L-glutamine = L-asparagine >> L-methionine ≅ L-glycine ≅ L-leucine > L-valine > L-glutamic acid (Alexander et al. 2013)	Utsunomiya-Tate et al. 1996
n.m.	ASC	1 Na+ : 1 amino acid (in) : 1 Na+ : 1 amino acid (out) (homo –or hetero exchange) (Alexander et al. 2013)	L-serine, L-alanine, L-cysteine, L-threonine (Christensen et al. 1967) L-cysteine (Kilberg 1979; Shanker et al. 2001) L-alanine, L-serine, L-cysteine, L-leucine, L-phenylalanine (Shotwell et al. 1981) L-alanine,L-serine, L-cysteine (Franchi-Gazzola et al. 1982)	Christensen et al. 1967; Kilberg et al. 1979; Shotwell et al. 1981; Franchi-Gazzola et al. 1982; Shanker et al. 2001
$hATB^{0+}$	B^{0+}	2 or 3 Na^+, 1Cl^-, and 1 amino acid (Sloan and Mager 1999)	Neutral and cationic amino acids (Sloan and Mager 1999)	Sloan and Mager 1999
LAT-2	L (Alexander et al. 2013)	1 amino acid (in) : 1 amino acid (out) (Verrey 2003)	L-isomers of neutral α- amino acids (Segawa et al. 1999)	Segawa et al. 1999

2.3.7.1.1. L-cysteine transport via high affinity glutamate transport proteins

High affinity glutamate transporters, also called excitatory amino acid transporters, belong to the solute carrier (SLC) family 1 being represented by five members: excitatory amino acid transporter 1 (EAAC1, SLC1a1 or EAAT3), glutamate transporter 1 (GLT1, SLC1a2 or EAAT2), glutamate-aspartate transporter (GLAST, SLC1a3 or EAAT1), EAAT4 (SLC1a6) and EAAT5 (SLC1a7). Preferably, they are involved in the uptake of one glutamate molecule accompanied by the import of three sodium ions and one proton (co-transport), while one potassium ion is released (counter-transport). These five members are clustered in the transport system X^-_{AG} as reviewed (Kanai et al. 2013). Besides high affinity uptake of glutamate, L-cysteine transporting properties are reported for members of the SLC1 family and multiple experiments with SLC1a1 are described.

In particular SLC1a1 is reported to transport L-cysteine in a sodium-dependent manner in voltage-clamped experiments with *Xenopus laevis* oocytes expressing the human transporter (Zerangue and Kavanaugh 1996). This indicates that this transporter being predominantly responsible for glutamate uptake may also transport L-cysteine. Experiments with neuronal cells showing strong SLC1a1 expression revealed neuronal L-cysteine transport via this transporter (Himi et al. 2003). Blocking of EAAT transporter systems resulted in decreased L-cysteine uptake and consequently slowed GSH production (Chen and Swanson 2003). HEK293 cells expressing SLC1a1 showed L-cysteine transport leading to an intracellular, cytoplasmic alkalization opposite to the results obtained with glutamate. It is proposed that intracellular alkalization may be connected with extracellular acidification due to glutamate and proton efflux (Watts et al. 2014).

This points out that transporters belonging to the system X^-_{AG} predominantly move glutamate from the extracellular to the intracellular space but may also transport L-cysteine. This demonstrates that limited and restricted amino acid uptake systems do not exist; substrate variability is ensured by nature.

2.3.7.1.2. L-cysteine transport via neutral amino acid transport proteins

Due to amino acid sequence similarity with high affinity glutamate transporters, two neutral amino acid transporters namely **a**lanine-**s**erine-**c**ysteine transporter 1 (ASCT1 or SLC1a4) and ASCT2 (SLC1a5) are also grouped in the SLC1 family but rely on ASC transport system properties which are discussed later as reviewed (Kanai 1997). The amino acid identity between members of the X^-_{AG} and the ASC transport system is around 40-44 % and both transport system are characterized by sodium ion dependence as reviewed (Kanai and Hediger 2004). As members of the SLC1 family, ASCT1 and ASCT2 preferably transport the neutral amino acids L-alanine, L-serine and L-cysteine relying on an exclusive sodium-dependent exchange of amino acids without showing counter transport of potassium ions as reviewed (Kanai and Hediger 2004).

ASC transport systems have been determined in different cell types such as e.g. Ehrlich cells and rat hepatocytes (Christensen et al. 1967; Kilberg et al. 1979). Primary cultures of hippocampal neurons and cerebrocortical astrocytes showed participation of the L-cysteine transporting systems X^-_{AG} and ASC in L-cysteine transport (Shanker et al. 2001). In human fibroblasts, L-cysteine was reported to be mainly transported in the cells via ASC transport system with participation of a different system, namely system A, only after starvation (Franchi-Gazzola et al. 1982). As a member of the ASC transport system, ASCT2 expression was found to be rich in proliferating tissue such as mouse testis, where high amino acid concentrations were necessary for cellular events like cell division. ASCT2 expressed in *Xenopus laevis* oocytes showed high affinity for L-alanine, L-serine, L-cysteine and was also capable to transport glutamate with lower affinity at lower extracellular pH. Via ASCT2, L-alanine transport was inhibited by L-cysteine. Amino acid import via ASCT2 was suggested to rely on mechanisms similar to high affinity glutamate transporters (Utsunomiya-Tate et al. 1996).
This points out that different cell types possess the transport system ASC being highly specific for L-cysteine. Further, connections between members of the SLC1 family exist although they belong to different transport systems. This reflects overlapping substrate specificities.

2.3.7.1.3. Other L-cysteine transporter proteins

Belonging to the transporter type, B^{0+}, the human $hATB^{0+}$ gene expressed in oocytes was reported to transport L-cysteine. This transport system was characterized to be sodium and chloride ion dependent and inward currents occurred when neutral amino acids were taken up (Sloan and Mager 1999).
Xenopus oocytes expressing rat **L**-type **a**mino acid **t**ransporter 2 (LAT-2) transporter protein were reported to transport L-cysteine with higher affinity. In rat tissues like placenta, brain and kidney, LAT-2 was natively detected. This transporter belongs to the L-type amino acid transport systems. It displays no sodium nor chloride ion dependence and shows broad substrate specificity. Transport function was reported to be dependent on pH (Segawa et al. 1999). System L is a sodium ion-independent obligate amino acid exchange transporter which is responsible for the transport of large neutral amino acids. This transporter was found in epithelial barriers of organs such as placenta, kidney and intestine, for both rodent and human LAT-2 mRNAs and also ovary expression in rodents was reported as reviewed (Verrey 2003).
Summarizing, several transport proteins belonging to different transport systems are able to recognize L-cysteine as a substrate and transport this amino acid via the presented membrane located carriers. Different cell types express these transport systems and they share similarities in function and show overlapping substrate specificity.

2.3.7.2. Cellular L-cystine uptake

Outside the cell, L-cysteine is predominantly oxidized into L-cystine. In human plasma, 10- 20 % of the L-cystine concentration may be determined as free L-cysteine as reviewed (Bannai 1984). To be able to take up both forms for survival, cells possess L-cysteine and L-cystine transporters.

Historically, early evidence for distinct transport systems for L-cysteine and L-cystine in humans was reported. Early studies of L-cystine transport indicated the presence of different L-cystine transport systems in rat kidney cortex slices (Segal and Crawhall 1968). Impacted L-cystine uptake was observed in rat kidney slices in the presence of ornithine, L-lysine, L-arginine, L-valine and L-glycine (Schwartzman et al. 1966). Later, studies of primary isolated rat hepatocytes revealed sodium-dependent L-cystine transport in early culture phases while L-cystine transport became sodium-ion independent in the late culture phase (Takada and Bannai 1984).

One of the most studied L-cystine transporters is the sodium-independent, obligatory exchange transport protein xCT which belongs to the transport system x_C^-. The transport system x_C^- was found in a variety of tissues as reviewed (Bridges and Patel 2009). In cell cultures, transporter expression levels may be altered and may not be necessarily comparable with those of native cells as reviewed (Lo et al. 2008). This transporter is known to import anionic L-cystine for anionic L-glutamate export in a 1:1 stoichiometry. The import of L-cystine is proposed to be the base for GSH production and subsequently be related to protection against oxidative stress. Increased x_c^- transporter activity was shown to protect neuronal cells against oxidative stress by increased L-cystine uptake for maintenance of GSH levels (Lewerenz et al. 2006).

Experiments with HEK cells revealed L-cystine uptake via high affinity glutamate transporters GLT1, GLAST and EAAT3. These cells were manipulated to individually overexpress these high-affinity glutamate transporters. These tests did not study L-cystine uptake via the x_C^- system and consequently the authors did not exclude a possible connection of glutamate export via x_C^- stimulating L-cystine import via representatives of the X^-_{AG} system (Hayes et al. 2005). Table 2 summarizes literature-based L-cystine transporters.

Table 2: Summary of literature-based L-cystine transport systems

Transport proteins, transport system type, function and substrates as well as references for L-cystine uptake are listed; n.m. = not mentioned

Transport protein	Transport system type	Function	Substrates	Reference for L-cystine uptake
n.m. (Takada and Bannai 1984)	n.m.	1 L-cystine (in) : 1 L-glutamate (out) (Bridges and Patel 2009)	L-cystine (Takada and Bannai 1984)	Takada and Bannai 1984
xCT (Lewerenz et al. 2006)	x_C^-	1 L-cystine (in) : 1 L-glutamate (out) (Bridges and Patel 2009)	L-cystine (Lewerenz et al. 2006)	Lewerenz et al. 2006
xCT/rBAT, rBAT-$b^{0,+}$AT (Wang et al. 2013)	x_C^-, $b^{0,+}$	1 L-cystine (in) : 1 L-glutamate (out) (Bridges and Patel 2009) Dibasic amino acids (in) : neutral amino acids (out) (Pineda et al. 2004)	L-cystine (Wang et al. 2013)	Wang et al. 2013
rBAT (Magagnin et al. 1992)	$b^{0,+}$	Dibasic amino acids (in) : neutral amino acids (out) (Pineda et al. 2004)	L-cystine (Magagnin et al. 1992)	Magagnin et al. 1992
rBAT-$b^{0,+}$AT (Fernandez et al. 2002)	$b^{0,+}$	Dibasic amino acids (in) : neutral amino acids (out) (Pineda et al. 2004)	L-cystine (Fernandez et al. 2002)	Fernandez et al. 2002
EAAT3	X^-_{AG}	3 Na^+ : 1 H^+ : 1glutamate (in) : 1 K^+ (out) (Alexander et al. 2013)	L-cystine (Hayes et al. 2005)	Hayes et al. 2005
EAAT2	X^-_{AG}	3 Na^+ : 1 H^+ : 1glutamate (in) : 1 K^+ (out) (Alexander et al. 2013)	L-cystine (Hayes et al. 2005)	
EAAT1 (Hayes et al. 2005)	X^-_{AG}	3 Na^+ : 1 H^+ : 1glutamate (in) : 1 K^+ (out) (Alexander et al. 2013)	L-cystine (Hayes et al. 2005)	

Summarized, L-cystine transport is preferably carried out via the x_C^- system. Import of L-cystine is connected to simultaneous export of L-glutamate. Several cell lines possess this transport system for L-cystine uptake. This offers the cell all possibilities for L-cysteine uptake either in its reduced or oxidized form minimizing intracellular L-cysteine starvation. These transport systems contribute therefore mostly to GSH synthesis.

2.3.7.3. Transport systems in CHO cells

As shown above, different transport systems are distributed in a broad range of cell types. The sodium-dependent ASC transport system was determined to be present in CHO cells. L-cysteine was determined to be the predominantly transported via ASC system amongst the neutral amino acid transport systems (Shotwell et al. 1981). In CHO-K1 cells, L-alanine transport was strongly inhibited by L-cysteine, both being substrates for the ASC systems pointing out the existence of this transport system in CHO-K1 (Bass et al. 1981). Further investigations of transport systems in CHO cells revealed existence of X^-_{AG} - like and x_C^- system in CHO-K1 (Ash et al. 1993). Cooperation of x_C^- and X^-_{AG} transport systems for GSH maintenance was suggested (Igo and Ash 1996).

Figure 17 summarizes essential L-cysteine and L-cystine transport systems and their action of mode.

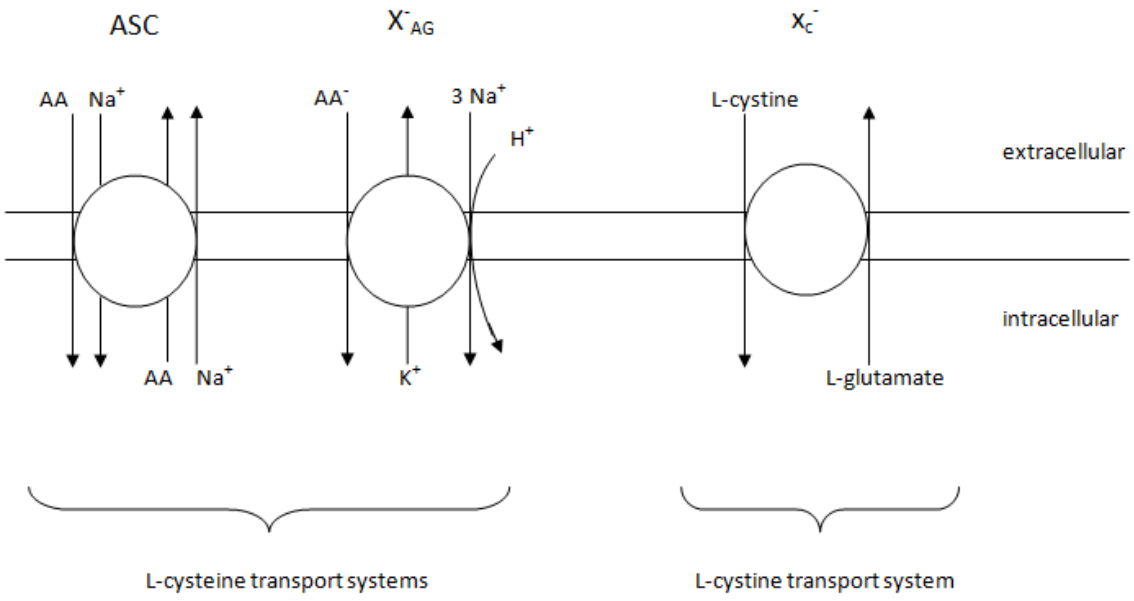

Figure 17: Schematic function of selected import L-cysteine and L-cystine transporters.

Alanine-serine-cysteine (ASC) systems co-transport sodium ions and amino acids, while the X^-_{AG} system takes up one sodium ion, one proton and one amino acid molecule and exports one potassium ion. x_C^- shows L-cystine uptake and coupled L-glutamate export.

This section was dedicated to the different uptake systems allowing intake of L-cysteine and L-cystine. Next, we want to focus on the intracellular metabolism of L-cysteine after its entry in the cell.

2.3.8. Intracellular metabolism of L-cysteine

2.3.8.1. Intracellular L-cysteine production

L-cysteine may be produced from homocysteine (HCy) as summarized in figure 18. HCy is the branch-point for three pathways: transmethylation, remethylation and transsulfuration with transsulfuration comprising L-cysteine generation which will described in the next section.

2.3.8.1.1. Transsulfuration

Based on two pyridoxalphosphate dependent enzymes, cystathionine β-synthase (CBS) and cystathionine γ-lyase (CSE), HCy is irreversibly used for L-cysteine formation. First, CBS catalyzes the condensation of L-serine and HCy under release of water leading to the production of cystathionine. Second, cystathionine is hydrolyzed via CSE resulting in L-cysteine, NH_3 and α-ketobutyrate formation. The latter compound may undergo oxidative decarboxylation to propionyl-CoA boosting the TCA as reviewed (Stipanuk and Ueki 2011).

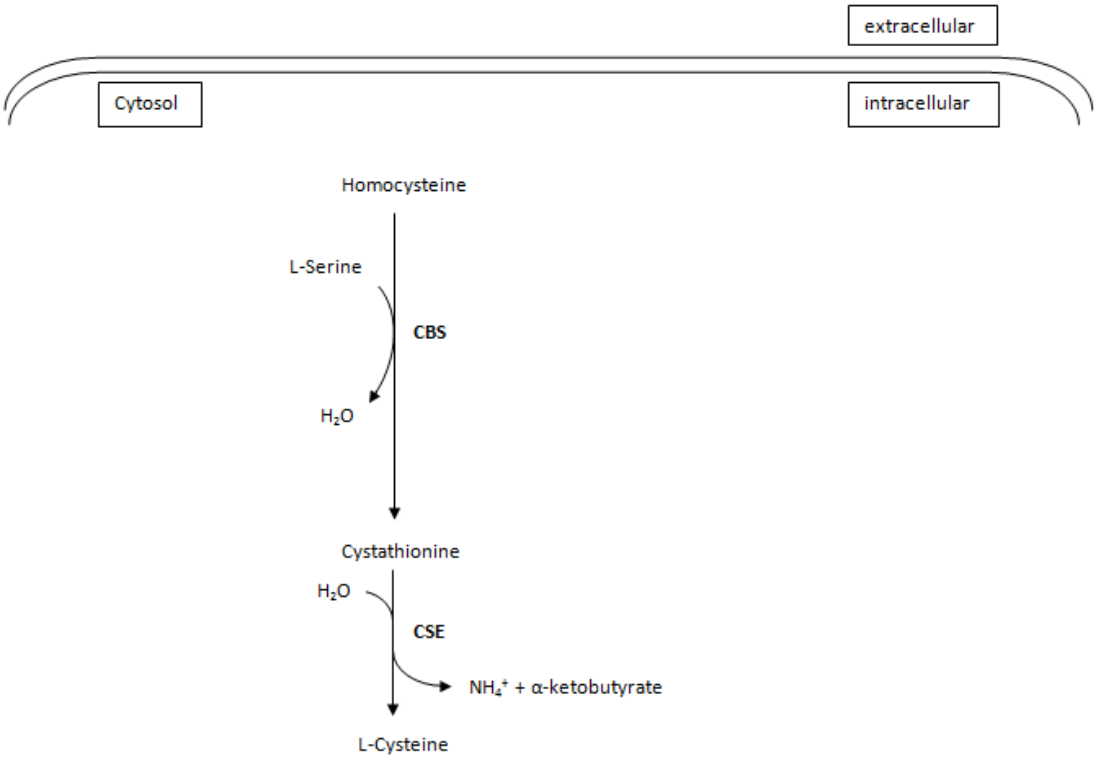

Figure 18: Intracellular L-cysteine anabolism.

Based on homocysteine, L-cysteine is produced in two enzyme reactions via cystathionine formation. CBS: cystathionine β-synthase, CSE: cystathionine γ-lyase (modified from Stipanuk and Ueki, 2011).

2.3.8.2. L-cysteine catabolism

Intracellular L-cysteine undergoes two catabolic pathways: the oxidative pathway relying on the formation of cysteine sulfinate and the non-oxidative pathway.

The oxidative pathway relies on the oxidation of L-cysteine into cysteinesulfinate catalyzed by cysteine dioxygenase (CDO). This enzyme is regulated by diet and its activity is the base for favoring one or the other catabolic pathway. Since the extracellular dietary availability of L-cysteine determines the route of cysteine degradation, low dietary L-cysteine levels may favor the non-oxidative pathway while high diet L-cysteine concentrations may support the oxidative pathway as reviewed (Stipanuk and Ueki 2011).

As summarized in Figure 19, different metabolites of each pathway are generated and both pathways are schematically presented.

2.3.8.2.1. The non-oxidative catabolic pathway

As mentioned above, if the dietary L-cysteine concentrations are low, the non-oxidative pathway is chosen for L-cysteine degradation. Here, L-cysteine is the substrate for two PLP -dependent enzymes: CBS and CSE. These enzymes catalyze non-specific degradation reactions of L-cysteine and produce reduced sulfur as reviewed (Stipanuk and Ueki 2011). In the transsulfuration pathway, the enzyme CBS is shown to catalyze the reaction of HCy with serine yielding cystathionine via release of water. But L-cysteine may replace serine. This leads to the reaction of L-cysteine with HCy generating cystathionine and H_2S (figure 19, reaction 1) and contributes to desulfuration.

As another enzyme of the transsulfuration pathway, CSE may accept L-cysteine instead of cystathionine as a substrate. In this reaction, L-cysteine is hydrolyzed which is catalyzed by CSE leading to the formation of L-serine and H_2S (figure 19, reaction 2). Moreover, CSE may also recognize L-cystine as a substrate although intracellular L-cystine concentrations are low due to reduced environment. Rat CSE is able to catalyze the β-disulfide elimination of L-cystine leading to the formation of pyruvate, NH_3 and thiocysteine (figure 19, reaction 3). Thiocysteine may be further partially transformed into H_2S as reviewed (Stipanuk and Ueki 2011).

The reactions in the non-oxidative pathway give rise to L-cysteine desulfuration leading to the release of H_2S. Due to toxic effects initiated by H_2S, its concentration needs to be kept minimal. The next section deals with H_2S. The consequently evolving detoxification reactions are described.

2.3.8.2.2. H_2S detoxification

H_2S is a biological gas. At physiological pH, the molecule exists mostly as hydrosulfide anions. The minority is present in the undissociated form. It is lipid soluble and it may freely penetrate cell membranes as reviewed (Qu et al. 2008; Mathai et al. 2009). H_2S has positive and toxic effects dependent on its concentration.

As a biological signaling molecule, sulfhydration of proteins by H_2S is known to occur and to alter their biological activity as reviewed (Stipanuk and Ueki 2011). In vasorelaxation, H_2S is reported to be a signaling molecule (Zhao et al. 2001; Mustafa et al. 2011). Also, H_2S is reported to function as an endogenous neuromodulator in the brain as reviewed (Kamoun 2004). As an example for toxic effects, H_2S is known to react with cytochrome C oxidase leading to the inhibition of mitochondrial electron transport. As a positive example of H_2S, the combination of intramitochondrial produced H_2S and succinate led to increased mitochondrial ATP production in isolated liver mitochondria (Módis et al. 2013). This points out that generated H_2S shows double-edged, concentration dependent effects which show beneficial and crucial phenomena.

Due to its toxic effects, detoxification of H_2S into inorganic sulfur (sulfate) must be achieved. H_2S oxidation is achieved in mammalian mitochondria based on three enzymatic reactions (figure 19, reactions 5, 6, 7) finally leading to sulfate production.

Consequently, generated toxic H_2S is detoxified in mitochondria. This sulfur coming from L-cysteine is released as inorganic sulfate which is than stored in the activated form PAPS for further processes.

2.3.8.2.3. The oxidative L-cysteine catabolism

The oxidative L-cysteine catabolism relies essentially on the enzyme CDO. In this pathway, the sulfur in the thiol group of L-cysteine is oxidized into a sulfinate group catalyzed by CDO before the sulfur is cleaved off or metabolized into hypotaurine as reviewed (Stipanuk and Ueki 2011).

CDO oxidizes L-cysteine into cysteine sulfinate via conversion of the thiol into a sulfinate group (figure 19, reaction 8). Secondly, cysteine sulfinate is transported into the mitochondria wherein aspartate aminotransferase (AST) catalyzes its conversion into β-sulfinylpyruvate (figure 19, reaction 9). Thereby, α-KG is transformed into glutamate. β-sulfinylpyruvate dissociates spontaneously into pyruvate and sulfite (figure 19, reaction 10), the latter being further oxidized by sulfite oxidases described above (figure 19, reaction 7) as reviewed (Stipanuk and Ueki 2011).

Cysteine sulfinate may be decarboxylated by cysteine sulfinate decarboxylase into hypotaurine (figure 19, reaction 11) with subsequent oxidation into taurine (figure 19, reaction 12) as reviewed (Stipanuk and Ueki 2011).

L-cysteine may be directly converted in the mitochondria via AST into 3`-mercaptopyruvate. This transamination relies on the conversion of α-KG into L-glutamate. Further, 3`-mercaptopyruvate is converted via zinc-dependent 3`-mercaptopyruvate sulfurtransferase generating H_2S while releasing pyruvate. H_2S is further converted into thiosulfate which is then transformed into sulfite and finally sulfate as described before (Kamoun 2004).

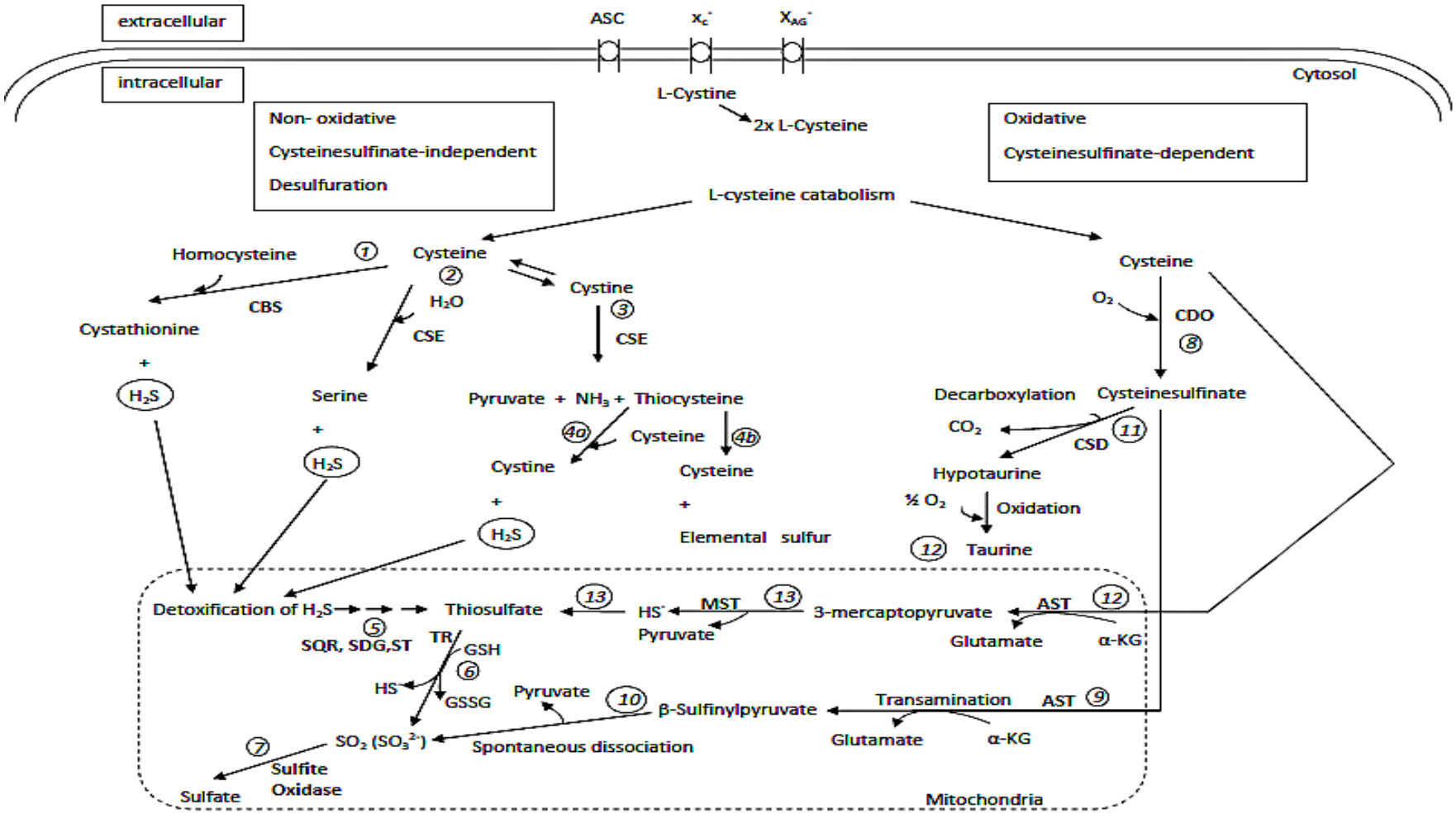

Figure 19 : Intracellular catabolic pathways of L-cysteine.

Oxidative L-cysteine catabolism is presented on the right while non-oxidative l-cysteine catabolism is presented on the left. CBS: cystathionine β-synthase, CSE: cystathionine γ-lyase, CDO: cysteine dioxygenase, CSD: cysteinesulfinate decarboxylase, AST: aspartate amino transferase, MST: 3`-mercaptopyruvate sulfurtransferase, TR: Thiosulfate reductase, SQR: sulfide quinine oxidoreductase, SDG: sulfur dioxygenase, ST: sulfurtransferase (based on data reviewed in Stipanuk and Ueki, 2011; Kamoun 2004).

In summary, L-cysteine is catabolized into essential metabolites. As such, the carbon chain of L-cysteine is released as pyruvate. The carboxyl atom of L-cysteine is released as carbon dioxide while the L-cysteines` carbon backbone, nitrogen and sulfur atom remain in the final product taurine. $H_2S$ is generated as a signaling molecule and its subsequent detoxification is achieved via generation of inorganic sulfate. Thus, L-cysteines` sulfur is stored in inorganic sulfate and its amino group is released as NH_3 or transferred to an α-keto-acid acceptor.

In the next section, we highlight specifically the meaning of L-cysteine in mAb pointing out its role in the final product in mammalian fed-batch cell cultivation.

2.3.9. L-cysteine based PTMs

L-cysteine residues in therapeutical proteins may be altered due to PTMs with consequences for protein structure and function pointing out the importance of PTM characterization in mAb.

2.3.9.1. Disulfide bond based PTMs

2.3.9.1.1. Disulfide shuffling

Disulfide rearrangement was reported in CHO cells expressing a recombinant human IgG2. Three isoforms of this antibody were reported to occur in cell culture showing differences in specific disulfide linkage. *In vivo*, interconversion of the IgG2 disulfide bridges was observed while circulating in humans. Changes in IgG2 isoform distribution were observed *in vitro* in L-cysteine containing medium linking this change in isoform composition to disulfide exchange mechanisms. Disulfide shuffling may impact activity changes of the antibody and may serve as an antibody age marker (Liu et al. 2008).

2.3.9.1.2. Trisulfide bonds

Trisulfide bonds were reported to occur in fed-batch cultivation of a CHO DG44 expressing a human monoclonal IgG1. Cell cultivation with feeds comprising higher L-cysteine concentrations resulted in higher trisulfide bond levels pointing out a concentration-dependent relationsship between L-cysteine and trisulfide modification being even more pronounced in late phase culture. Moreover, H_2S generation by L-cysteine was shown to react with the antibody leading to trisulfide modification (Kshirsagar et al. 2012). Although studies with two mAb containing different levels of trisulfide modification in their LC5-HC5 linkage showed no change in binding activity (Gu et al. 2010), it may not be automatically concluded that trisulfide bond formation has no effect on biological activity of the antibody. In case of trisulfide bond formation in e.g. biosimilars, it needs to be demonstrated that no change in biological activity is observed to ensure a functional and safe product.

This points out that cell culture conditions may impact trisulfide bond formation. Balanced feeding strategies are necessary with focus on L-cysteine for maintenance of mAb product quality.

2.3.9.1.3. Thioether links and β-elimination

A non-reducible thioether bond between L-cysteine 223 of the HC and L-cysteine 213 of the LC was reported to occur in an monoclonal IgG1 with increasing thioether link contents oberved in heat-stressed conditions (Tous et al. 2005). Thioether bond containing antibodies were reported to occur also in their native state. It suggested that the shortening in bond length by thioether bond formation may lead to decreased antibody binding since Fab orientation in this process may be affected but needs to be determined case by case (Zhang et al. 2013).

Thioether bond generation may be also generated from β-elimination of the disulfide bond between LC and HC. This reaction leads to persulfide and dehydroalanine formation. Dehydroalanine may be hydrolysed leading to antibody fragmentation in the hinge region as reviewed (Liu and May 2012). Destruction of the hinge region by β-elimination may result in impacted antigen binding since the flexibility of the hinge region may be impaired.

2.3.9.1.4. Loss of disulfide bridges

Conformational changes in the quarternary structure of an IgG were observed caused by single disulfide reduction between the HCs. By reducing one disulfide bond in the hinge region, separation of the C_{H2} domains occurred in favor of prolonged Fab arms. Due to these conformational changes, effector functions might be impacted (Seegan et al. 1979). No loss in function was reported for a L-cysteine-free intrinsically stable single chain variable fragment. Both disulfide bridges in the HC and LC of this fragment were replaced by the amino acid combination valine-alanine fulfilling similar steric needs. These hydrophobic amino acids integrated well in the hydrophobic interior of the antibody domains therefore ensuring slight stabilization of the structure. Biological function measured via antigen binding was not altered implying no change in native structure (Wörn and Plückthun, 1998). This points out that loss in disulfide bond not necessarily affects biological function. Case by case decisions need to be considered.

2.3.9.2. Free L-cysteine levels

In a recombinant monoclonal IgG1 free L-cysteine residues (Cys- 22 and Cys-96) were found in the hydrophobic core of the v_H domain leading to free thiol Fab. To determine the effect of the free thiol Fab on biological functions of the mAb, antigen binding tests and Fc effector function were evaluated. These tests revealed slightly increased antigen binding and unchanged CDC activity compared with

the intact Fab (Zhang et al. 2012). Although showing no impacts on biological activity, impacts on other parameters such as e.g. shelf life, stability or serum half-life need may not be excluded.

2.3.10. L-cysteine and its derivatives in cell culture

As discussed above, L-cysteine is able to undergo different reactions with several reaction partners. This reactivity of L-cysteine may impact cell culture efficiency since changes in available free L-cysteine concentration may occur or toxic side products may impact cell culture outcome. One possibility is the application of exogenous L-cystine.

It is reported that combined exogenous application L-cystine showed beneficial effects on cell proliferation and GSH levels in colorectal adenocarcinoma cells and *spodoptera frugiperda* (Sf) cells (Noda et al. 2002; Doverskog et al. 1998). Since cellular transport mechanisms for this compound exist, exogenous L-cystine supplementation as a L-cysteine source might be an option although L-cystines` solubility is so low that its application in cell culture is not favorable. To overcome L-cysteines` reactivity, its replacement by chemically modified L-cysteine derivatives is a strategy discussed below.

2.3.10.1.N-acetyl-L-cysteine (NAC) and its derivatives

2.3.10.1.1 Chemical properties of NAC

NAC is the acetylated form of L-cysteine and serves as a L-cysteine source. As shown in figure 20, the acetyl group is attached to L-cysteines` nitrogen atom and the molecule possesses a free thiol group. Since it is a thiol, it may be oxidized and may react with radicals as reviewed (Samuni et al. 2013).

At physiological pH, the pK_a value of NACs´ thiol group (pK_a=9.51) is higher compared with the one of L-cysteine (pK_a=8.18) and GSH (pK_a=8.7) indicating that its reactivity towards most oxidants is lower than that of the mentioned thiols as reviewed (Samuni et al. 2013).

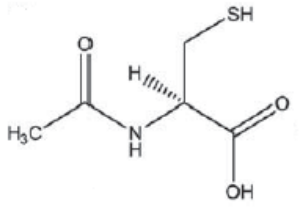

Figure 20: Structure of N-acetyl-L-cysteine (NAC)

(modified from Sunitha et al. 2013)

Since the reactive thiol group is not protected, reaction with different trace metals such as chrome (III), Fe (III), nickel (II) and cobalt (II) were reported (Güzeloğlu et al. 1998). Moreover, the extracellular environment was oxidizing pointing out dimerization behavior of the thiol groups in NAC molecules. Symmetric and asymmetric interaction products of NAC, L-cysteine and proteins may be predicted such as e.g. NAC-NAC, the mixed disulfide L-cysteine-NAC and protein-NAC (Giustarini et al. 2012).

2.3.10.1.2. Biological function of NAC

NAC is reported to contribute to intracellular GSH build-up. When NAC is de-acetylated, L-cysteine is produced which will be further used for GSH synthesis. Due to its effect on GSH concentrations, the cellular radical scavenging potential may be increased pointing out its antioxidant activity although it might also act as a radical generator as reviewed (Samuni et al. 2013; Atkuri et al. 2007).

Historically, NAC was used as a mucolytic agent. NAC disrupted the disulfide bonds in mucolytic proteins leading to smaller, less viscous mucus particles. Moreover, it was used to treat intoxication by acetaminophen (paracetamol) as reviewed (Samuni et al. 2013). *In vivo* studies showed that hepatic GSH depletion after acetaminophen treatment was decreased after NAC administration (Lauterburg et al. 1983) indicating protection mechanisms by increasing GSH levels rather than a direct scavenge effect of acetaminophen.

Other studies indicate the connection of NAC administrations and GSH increase. Mice fed with NAC show an increase in intracellular GSH possibly due to an intracellular increase in L-cysteine levels. Suggestions point out NAC participation in an indirect manner such as e.g. thiol-exchange with protein-bound L-cysteine causing increased intracellular L-cysteine levels (Zhou et al. 2015). In cell culture application, simultaneous supplementation of L-cystine and NAC in CHO cell culture is reported to induce L-cystine uptake by the cells. The increased L-cystine uptake was possibly due to participation of mixed disulfides of L-cystine and NAC and their further uptake leading to increased intracellular GSH levels (Issels et al. 1988). This indicates the intracellular antioxidant machinery was boosted when NAC was applied.

Although NAC may serve as a L-cysteine source in cell culture models, NACs bioavailability is reported to be low since it is negatively charged at physiological pH. Because cellular membranes are negatively charged, membrane passage of the negatively charged molecule at physiological pH is hindered. Therefore, chemical modification is introduced to NAC making it more susceptible for cellular uptake.

2.3.10.1.3. NAC derivatives

The introduction of a positively charged amide group at the carboxyl group of NAC neutralizes their negative charge making the molecule more lipophilic and able to pass cell membranes. The created NAC derivative is known to be N-acetylcysteine amide (NACA) as reviewed (Sunitha et al. 2013).

A protective effect in red blood cells towards oxidative stress is reported to occur after NACA administration. Changes in GSH/oxidized glutathione (GSSG) ratio point out the beginning of oxidative stress. After its cell entry, thiol exchange with GSSG is proposed to happen, thereby regenerating GSH. The newly formed GSH is then able to protect cells from further stress (Grinberg et al. 2005). Besides increase in intracellular GSH content, reduced lipid peroxidation is observed under NACA administration in brain endothelial cells (Price et al. 2006) pointing out an effective antioxidant machinery preventing different oxidative stresses.

Another mechanism to increase lipophilicity is the esterification of NACs carboxyl group leading to N-acetylcysteine ethyl ester (NACET). *In vivo* studies in rats confirm higher bioavailability of NACET compared with NAC. Moreover, the passaging of NACET through the blood brain barrier was increased compared with NAC. After its cell-entry, NAC and L-cysteine formation are observed with the latter being involved in GSH synthesis. This suggests the cleavage of the NACETs ester group by esterases leading to the formation of NAC with subsequent N-de-acetylation resulting in L-cysteine production (Giustarini et al. 2012).

With regard to direct effects of NAC, after NAC administration, increased p53-dependent apoptosis was observed in transformed human fibroblast cells and tumor cell lines but not in normal fibroblasts or keratinocytes (Havre et al. 2002) indicating possible NAC application in cancer treatment.

2.3.10.2. Thiazolidines and their derivatives

2.3.10.2.1. Chemical properties of thiazolidines

L-cysteine may react with a variety of carbonyl compounds such as e.g. carbohydrates, PLP and pyruvate to form fully saturated heterocyclic ring systems. This allows the thiol group in L-cysteine to be protected from oxidation therefore enhancing its stability. To release L-cysteine and therefore being a useful L-cysteine delivering tool, ring-opening may undergo non-enzymatic and enzymatic processes discussed in the next section.

2.3.10.2.2. Biological functions of thiazolidines

In thiazolidine ring systems, the thiol group of L-cysteine is protected from oxidation. Both, non-enzymatic and enzymatic processes may open the ring structure thereby releasing L-cysteine

(Wlodek et al. 1993). As a prodrug approach, non-enzymatic ring opening and further hydrolysis leads to liberation of one molecule L-cysteine and one aldehyde as shown in figure 21 (Wlodek et al. 1993).

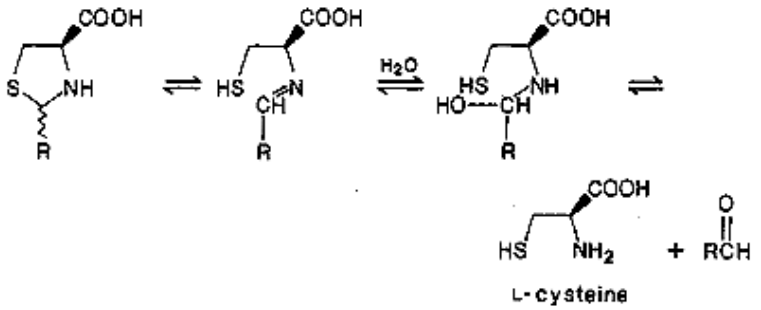

Figure 21: 2-substituted thiazolidine-4(R)-carboxylic acids as a prodrug for L-cysteine release.

Non-enzymatic ring opening and further hydrolysis liberates the L-cysteine (modified from Roberts et al. 1987)

Released L-cysteine may be further used for GSH production (Roberts et al. 1987) pointing out its protective effects relying on its connection to GSH. This application method of thiazolidines as an exogenous indirect L-cysteine source is an option for protected L-cysteine delivery to cultured cells.

Enzymatic degradation of (R)-thiazolidine-4-carboxylic acid was observed in mitochondria. It was suggested that the L-cysteine derivative was first oxidized leading to the formation of (R)Δ^2-thiazoline-4-carboxylic acid. This compound was further hydrolyzed yielding N-acyl-cysteine. The produced N-acyl-cysteine was further hydrolyzed in the cytosol producing L-cysteine and an acid (Wlodek et al. 1993).

2.3.10.2.3. Thiazolidine derivatives

The L-cysteine prodrug L-2-oxothiazolidine-4-carboxylic acid (OTC) is reported to serve as a L-cysteine source and shows to have beneficial effects on GSH levels. OTC is enzymatically transformed by 5-oxoprolinase to give S-carboxy-L-cysteine which is further decarboxylated to L-cysteine being available for GSH synthesis. OTC application *in vivo* shows increased L-cysteine concentrations in plasma of rats compared to control animals (Bjelton and Fransson 1990) pointing out that OTC may serve as an L-cysteine donor in an animal model without showing toxic impacts.

2-methyl-thiazolidine-2,4-dicarboxylic acid is the condensation product of L-cysteine and pyruvate. In an acetaminophen-induced hepatotoxicity mouse model, its administration alone prevents hepatic damage and increases free L-cysteine levels. Increasing GSH levels and decreasing ROS levels in the liver are reported (Wlodek and Rommelspacher 1997).

Moreover, application of 2-alkyl- and 2-aryl-substituted thiazolidine-4(R)-carboxylic acid in mouse model confirms the observation of protection against acetaminophen-induced toxicity by boosted GSH levels (Nagasawa et al. 1984).

Coupling of aldose monosaccharides such as e.g. glucose, ribose or galactose to L-cysteine results in the formation of carbohydrate based thiazolidines (Wlodek et al. 1993). Colitis mice pre-treated with D-ribose-L-cysteine (RibCys) showed increased intestine L-cysteine levels compared with not pre-treated colitis mice (Oz et al. 2007) indicating that RibCys may serve as a L-cysteine source *in vivo*.
Application of thiazolidines for L-cysteine delivery is efficient since enzymatic and non-enzymatic L-cysteine release mechanisms exist. Due to non-enzymatic degradation, stability of this compound class is suggested to be low.

2.3.10.3. SSC

2.3.10.3.1. Chemical properties of SSC

SSC belongs to the class of alkyl thiosulfates. Its structure is presented in figure 22. The reactive thiol group is esterified and therefore protected from oxidation. But its structure may be also regarded as disulfide-like (Yang and Wells 1991).
SSC may be either synthesized by the conversion of L-cystine with sodium sulfite or by the transformation of L-cysteine with sodium tetrathionate (Lundblad 2005). Also, thiols may be converted via sulfurous acid in presence of iodine as an oxidant (Distler 1967).

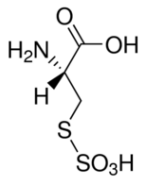

Figure 22: Structure of S-sulfocysteine (SSC)

2.3.10.3.2. Biological function

SSC showes structure similarity with L-glutamate. SSC is determined to occur natively in whole rat brain tissues as an excitotoxic metabolite being present in lower concentrations compared with L-glutamate and L-cysteine (Abbas et al. 2008).
Neurotoxic effects were reported after SSC administration as it was observed in a rat model. Therein, subcutaneous SSC administration led to neurotoxicity which is known to result also from L-glutamate application (Olney et al. 1975).
SSC was observed to impact L-glutamate uptake in mouse synaptic vesicles. Both D- and L-enantiomers of SSC were able to inhibit significantly L-glutamate uptake and it was suggested that SSC was tolerated in the L-glutamate recognition site of the synaptic vesicle glutamate carrier (Dunlop et al. 1991). L-glutamate uptake inhibition by SSC is confirmed in purified bovine synaptic

vesicles. It is proposed that SSC sulfonates an essential thiol residue in the transport protein thereby leading to non-competitive L-glutamate uptake inhibition rather than being a substrate for the L-glutamate transport system itself (Winter and Ueda1993). The L-enantiomer of SSC was reported to inhibit weakly and competitively D-aspartate uptake in mouse synaptosome fractions pointing out stereospecificity of the transport system (Griffiths et al. 1989).

Cell free *in vitro* SSC synthesis was reported to be carried out by transamination of cystine disulfoxide (CDS) via AST. In this reaction presented in figure 23, one amide group of CDS was transferred on α-KG therefore generating L-glutamate and sulfinylpyruvic acid. Further non-enzymatic dissociation of the latter compound results in release of pyruvate and formation of SSC (Ubuka et al. 1979).

$$\textbf{Cystine disulfoxide} + \propto - \textbf{ketoglutarate} \overset{\textbf{AST}}{\rightarrow} \textbf{Sulfinylpyruvate} \rightarrow \textbf{Pyruvate} + \textbf{S} - \textbf{sulfocysteine}$$

Figure 23: Cell free production of S-sulfocysteine from cystine disulfoxide.

Transamination of cystine disulfoxide by aspartate amino transferase (AST) leads to sulfinylpyruvate which further degrades non-enzymatically to pyruvate and S-sulfocysteine (modified from Ubuka et al. 1979)

A second example for enzymatic, cell free *in vitro* SSC production was based on S-sulfoglutathione transformation. As shown in figure 24, conversion of S-sulfoglutathione with inorganic sulfite via thioltransferase (TT) resulted in the formation of an intermediate. The intermediate was further transformed into S-sulfocysteinylglycine via γ-glutamyltranspeptidase (GT). Finally, S-sulfocysteinylglycine was hydrolysed into SSC and L-glycine via a dipeptidase (DP) (Kågedal et al. 1986). This cell-free reaction points out to be metabolically possible due to native occurrence of S-sulfoglutathione and the used enzymes.

$$\textbf{Glutathione disulfide} + \textbf{Sulfite} \overset{\textbf{TT}}{\rightarrow}$$

$$\textbf{S} - \textbf{sulfoglutathione} \overset{\textbf{GT}}{\rightarrow} \textbf{S} - \textbf{sulfocysteinylglycine} \overset{\textbf{DP}}{\rightarrow} \textbf{S} - \textbf{sulfocysteine}$$

Figure 24: Cell free production of S-sulfocysteine from S-glutathione.

Reaction of glutathione disulfide with sulfite catalyzed by thioltransferase (TT) led to the formation of S-sulfoglutathione. The latter was converted into S-sulfocysteinylglycine by γ-glutamyltranspeptidase (GT). S-sulfocysteinylglycine was finally transformed in to S-sulfocysteine by dipeptidase (DP) (modified from Kagedål et al. 1986).

Besides SSC generation and hypothesized transporter interaction, SSC was shown to be enzymatically converted *in vitro* by rat liver homogenate. Pyruvate, NH_3 and thiosulfate formation were reported (Sörbo 1958) pointing out the enzymatic usage of SSC in rodent cell lysates.

Further experiments point out that SSC may be used as a substrate in cell-free enzymatic reactions. Isolated and purified TT from rabbit liver cytosol was reported to catalyze the thiol: disulfide exchange

mechanism between GSH and SSC (Hatakeyama et al. 1985). The activity in this exchange mechanism of rat liver TT was tested i*n vitro* relying on the use of SSC as a substrate based on the reactions shown in figure 25 (Gan and Wells 1986).

$$\mathbf{CysSO_3^- + 2\,GSH \rightleftarrows Cysteine + HSO_3^- + GSSG} \qquad \text{(catalyzed by TT)}$$

$$\mathbf{GSSG + NADPH + H^+ \rightleftarrows 2\,GSH + NADP^+} \qquad \text{(catalyzed by GR)}$$

Figure 25: In vitro reaction of S-Sulfocysteine with reduced glutathione into L-cysteine, oxidized glutathione and inorganic sulfite for thioltransferase activity determination

Reaction of S-sulfocysteine ($CysSO_3^-$) and glutathione (GSH) catalyzed by thioltransferase (TT) yielding L-cysteine, inorganic sulfite and oxidized glutathione (GSSG).TT: Thioltransferase, GR: glutathione reductase (modified from Gan and Wells 1986).

To further identify the thioltransferase mediated mechanism, incubation of the enzyme with the alkylating reagent iodoacetamide (IAM) led to enzyme inhibition relying on the blockage of a L-cysteine residue necessary for substrate binding. Pretreatment of the enzyme with SSC before IAM treatment showed protection from IAM inactivation possibly relying on an intramolecular disulfide bridge formation. This indicated involvement of an important L-cysteine residue in the enzyme responsible for IAM and SSC binding which is proposed to be Cys22 (Yang and Wells 1991).
As shown above, SSC was able to undergo thiol: disulfide exchange with GSH. As such, reaction of excess SSC and GSH was shown to form a mixed disulfide by releasing inorganic sulfite via a non-enzymatic reaction (Swan 1957; Eriksson and Eriksson 1967).

2.3.10.4. GSH and its derivatives

2.3.10.4.1. Chemical properties of GSH and intracellular GSH formation

GSH is a tripeptide composed of L-cysteine, L-glycine and L-glutamate. Intracellular GSH production is carried out in two steps. First, the γ-carboxyl group of L-glutamate and the amino group of L-cysteine are linked with each other in an ATP-dependent reaction catalyzed by γ-glutamylcysteine ligase. This results in the formation γ-linked dipeptide γ-glutamylcysteine (γ-GluCys). The formation of γ-GluCys is shown to be feedback inhibited by GSH as reviewed (Cacciatore et al. 2010; Meister 1988). Second, linkage of L-glycines` amine to the L-cysteine carboxyl group of the generated γ-GluCys leads to GSH production as reviewed (Cacciatore et al. 2010). This reaction is catalyzed by glutathione synthetase in an ATP-dependent manner. The availability of L-cysteine is the key factor in the formation of GSH and determines its intracellular synthesis rate catalyzed as reviewed (Aoyama and Nakaki 2013). Figure 26 shows the structure of reduced GSH.

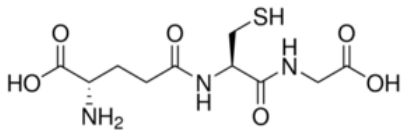

Figure 26: Structure of reduced L-glutathione (GSH)

2.3.10.4.2. Biological function of GSH

The synthezised glutathione is available for e.g. intracellular scavenging reactions of ROS leading to its oxidation (GSSG) as reviewed (Meister 1988) and is the major defense system against oxidative stress. This property is related to its free thiol group shown in figure 26. Since it contains L-cysteine, its application as an exogenous source for this thiol containing amino acid may be favorable. Exogenous GSH application is restricted only to a few cell phenotypes which possess the outer surface membrane bound enzyme γ-glutamyltranspeptidase. Extracellular GSH is enzymatically degraded and the constituents are taken up by individual transporters followed by intracellular GSH re-synthesis as reviewed (Bachhawat et al. 2013). Therefore, chemical modification of GSH is used for employing its use as a L-cysteine donor.

2.3.10.4.3. GSH derivatives

GSH monoethyl ester is a GSH derivative being reported to act as a L-cysteine donor. After administration to rats, GSH monoethyl ester was found to have an increased half-life in plasma compared with GSH and L-cysteine pointing out its function as a GSH prodrug. But its poor uptake in rat model suggested that it was taken up by cells only to a low extent (Grattagliano et al. 1995).

As shown above, GSH monoethyl ester showed limited cell permeability which leads to the need for optimized chemical modification of GSH for optimal uptake in exogenous administration.

N-butanoyl α-glutamyl-cysteinyl-glycine (GSH-C4) is another chemically modified GSH derivative. An aliphatic chain is attached to the α-NH_2 group of glutamic acid in GSH. The introduction of a hydrophobic part allows the molecule to pass the membrane. The length of the chain needs to be considered carefully since short aliphatic chains may not show any effect while too long chains may induce toxicity. Administration of GSH-C4 to Madine Darby canine kidney monolayer cultures showed no cytotoxicity in the tested concentrations ranging from 0.1-10 mM and antiviral activity was reported (Palamara et al. 2004). This modification makes the molecule to overcome its low potential for membrane diffusion.

Further modification of GSH with fatty acids led to the production of S-acyl-GSH wherein the thiol group of GSH was coupled to the carboxylic group of the fatty acid. Examples for successful coupling was the linkage of the linoleic acid (C18:2) and palmitic acid (C16:0) to GSH. Linkage of fatty acids to GSH was suggested to enhance membrane passage and GSH delivery. Cellular uptake of the generated GSH derivatives was observed in different cell types such as primary skin fibroblasts and neuroblastoma cells. After cell entry, the GSH derivatives were hydrolysed by thioesterases releasing GSH for intracellular use therefore protecting the cell against oxidative stress (Zampagni et al. 2012). The combination of the antioxidant GSH with unsaturated fatty acids was a double strategy for protection of oxidative stress since both, GSH and unsaturated fatty acids (linoleic acid), may scavenge RS. In contrast, fatty acid supplementation in aqueous media would be complicated due to their low solubility.

3. Motivation

The state-of-the-art fed-batch process at Merck relies on the use of two separate highly concentrated nutrient solutions: one main feed and one separate feed. The main feed comprises all feed components such as vitamins, amino acids and inorganic salts except L-cysteine and L-tyrosine. L-cysteine was shown to dimerise rapidly to insoluble L-cystine at neutral pH thereby leading to precipitations. L-tyrosine was shown to be poorly soluble at neutral pH. In the standard fed-batch process, both amino acids need to be kept separately at alkaline pH since L-cysteine and L-tyrosine were shown to be stable and soluble at this pH compared with neutral pH. To compensate pH differences while feeding, the main feed is kept at slight acidic pH.

The application of two feeds with different pH in cell culture is detrimental due to possible culture pH peaks resulting in the process of feeding. With regard to bioreactor cultivation, often the same tubes for the slightly acidic and the alkaline feed are used leading to the interaction of both feeds in the same tube. Precipitations of L-cystine in bioreactor tubes may thereby occur leading to bioreactor tube blocking. L-cystine precipitation might also occur in the cell broth. Handling inefficiencies may be a consequence when the two-feed-strategy is applied.

To overcome this, the development of a single feed was initiated and it was shown to be subject of other working groups, too (Ma et al. 2009). The single feed in this study needed to comprise all nutrients in one complex, highly concentrated neutral pH feed. By this, culture pH peaks while feedings and handling inefficiencies may be avoided. To do so, derivatives for L-tyrosine and L-cysteine needed to be established.

As a source for L-tyrosine, the previously established L-tyrosine derivative phosphotyrosine disodium salt ($PTyr2Na^+$) was used. It was shown that this derivative was soluble at neutral pH in complex, highly concentrated, chemically defined feed. Further, the derivative was used by the cells as a prodrug for L-tyrosine without impacting culture performance, titer and mAb characteristics (Zimmer et al. 2014).

With regard to L-cysteine derivatives, their use was reported in CHO fed-batch processes being implemented in chemically defined feed with improvements in titer (Kishishita et al. 2015). In this work, it was aimed to establish a L-cysteine derivative which might have been integrated in the single feed together with $PTyr2Na^+$ without impacting or even improving culture performance, final titer and cQAs of the produced mAb compared to the antibody produced in the state-of-the-art fed-batch process.

4. Material and Methods

4.1. Chemicals and reagents

Standard chemicals, tested L-cysteine derivatives and substances used for cell transporter tests are summarized in alphabetical order.

Standard chemicals:

6-carboxy-2',7'-dichlorodihydrofluorescein diacetate (carboxy-H_2DCFDA) (C400, Life technologies, Carlsbad, US), copper (II) sulfate penta hydrate (1.02788.5000, Merck, Darmstadt, Germany), L-cysteine (1.02838, Merck, Darmstadt, Germany), L-cysteine hydrochloride monohydrate (CysHCl*H_2O) (1.02735, Merck, Darmstadt, Germany), dimethylsulfoxide (1.02931, Merck, Darmstadt, Germany), D(+)-glucose (1.37048, Merck, Darmstadt, Germany), L-glutamine (1.00286, Merck, Darmstadt, Germany), hydrogen chloride (HCl) (109057, Merck, Darmstadt, Germany), CellPrime®r insulin (4512-01, Merck, Darmstadt, Germany), IAM (A3221, Sigma Aldrich, St Louis, US), MSX (M5379, Sigma Aldrich, St Louis, US), norvaline (04-11-020, Novabiochem, Darmstadt, Germany), phosphate buffered saline (PBS) 10x (14200-067, Gibco, Carlsbad, US), PTyr2Na^+ (2.01385, Merck, Darmstadt, Germany), poloxamer 188 (S10307, BASF, Ludwigshafen, Germany), puromycine dihydrochloride (540411, Calbiochem, Darmstadt, Germany), simethicone emulsion USP (30 %) (Antifoam) (7-9245, Dow Corning®, Midland, US), sodium carbonate (1.06398, Merck, Darmstadt, Germany), sodium hydroxide (NaOH) (1.09136, Merck, Darmstadt, Germany), sodium L-glutamate monohydrate (1.06445, Merck, Darmstadt, Germany), L-tyrosine disodium salt (RES3156T-A103X, SAFC, St Louis, US).

L-cysteine derivatives:

L-cysteine ethyl ester hydrochloride (C121908, Sigma Aldrich, St Louis, US), L-cysteine sulfinic acid monohydrate (C4418, Sigma Aldrich, St Louis, US), Di-(PTyr)-cystine-tetrasodium salt (Merck, Darmstadt, Germany, intern synthesis), 2-(D-glucopentylhydroxypentyl)-4(R)-1,3-thiazolidine-4-carboxylic acid (282730A, Santa Cruz Biotechnology, Dallas, US), NACA (A0737, Sigma Aldrich, St Louis, US), NACET (Merck, Darmstadt, Germany, intern synthesis), S-sulfocysteine mono sodium salt (SSC*Na) as two external synthesis products (SSC*Na-A and SSC*Na-B, 4016588, Bachem AG, Bubendorf, Switzerland) and as seven internal synthesis products (SSC*Na-C, SSC*Na-D, SSC*Na-E, SSC*Na-F, SSC*Na-G, SSC*Na-H and SSC*Na-I, Merck, Darmstadt, Germany, intern synthesis), (2RS, 4R)-1,3-thiazolidine-2,4-dicarboxylate sodium salt (Merck, Darmstadt, Germany, intern synthesis), 1,3-thiazolidine-2,4-dicarboxylic acid (3J-939, Key Organics Ltd, Camelford, UK), (R)-2-((1R,2R,3R)-1,2,3,4-tetrahydroxy-butyl)-thiazolidine-4-carboxylic acid (Merck, Darmstadt, Germany, intern synthesis),

enantiomer mix (2R,4R)-(2-methyl)-1,3-thiazolidine-2,4-dicarboxylate disodium salt and (2S,4R)- (2-methyl)-1,2-thiazolidine-2,4-dicarboxylate disodium salt (Merck, Darmstadt, Germany, intern synthesis).

Inhibitors and activators of different transporters:
2-amino-5,6,7,8-tetrahydro-4-(4-methoxyphenyl)-7-(naphthalen-1-yl)-5-oxo-4H-chromene-3-carbonitrile (UCPH-101) (3490, Tocris, Minneapolis, US), dihydrokainic acid (0111, Tocris, Minneapolis, US), (3S)-3-[[3-[[4-(trifluoromethyl)benzoyl]amino]phenyl]methoxy]-L-aspartic acid (TFB-TBOA) (2532, Tocris, Minneapolis, US), (S)-4-carboxy-phenylglycine (0323, Tocris, Minneapolis, US).

4.2. Characterization of different SSC

Different synthesis routes for SSC production were carried out at performance material operation department at Merck. Due to these differences in synthesis, differences in product properties were generated. Purity of the synthesized batches was determined via quantitative nuclear magnetic resonance (NMR) or capillary electrophoresis (CE). Copper concentration was quantified via inductively coupled plasma mass spectrometry (ICP-MS). Sulfate and thiosulfate were measured via CE as described in off-line analytics.

4.3. Physicochemical tests

4.3.1. Solubility tests

4.3.1.1. Solubility tests in L-cysteine derivative screening process

Cellvento™ Feed 220 was prepared following manufacture guidelines (Merck Millipore, Darmstadt, Germany) with subsequent addition of 30 mM $PTyr2Na^{+}$. The pH of the feed medium was adjusted to neutral pH using 2 M NaOH. In a final volume of each 100 mL neutral pH feed, different concentrations of SSC*Na-A (5, 10, 15, 20, 30, 50, 60, 70, 80 and 100 mM) were each solubilized and pH was re-adjusted to neutral pH. Evaluation of solubility was carried out visually.

4.3.1.2. Residual mass determination

To determine the maximum solubility of SSC*Na, residual mass determination was carried out. A saturated SSC*Na solution was prepared in water at room temperature. After sedimentation, the solution was dried using infrared and the residual mass was determined.

4.3.2. Stability tests

Cellvento™ Feed 220 was prepared following manufacture guidelines (Merck Millipore, Darmstadt, Germany). 15 mM SSC*Na-A and 30 mM PTyr2Na$^+$ were solubilized in a final feed volume of 50 mL and pH was re-adjusted to neutral pH. Stability was evaluated over three months at room temperature and 4°C, both protected from light. SSC*Na-A containing feed was compared to feed supplemented with 30 mM PTyr2Na$^+$ or 15 mM CysHCl*H_2O, respectively. The stability was evaluated through visual observation of the feed (color and precipitation) and via quantification of L-cysteine, L-cystine and the derivative SSC*Na-A using the ultra performance liquid chromatography (UPLC) method described in offline analysis. The feed medium was considered stable if the standard deviation of the measured concentrations over time was below 10 %.

4.4. Cell culture

4.4.1. Thawing

Three CHO suspension clones each expressing a human monoclonal antibody were used: while clone 1 and clone 2 both express the same human mAb and were both transfected with a plasmid containing the gene for GS, clone 3 was transfected with the ubiquitous chromatin opening elements plasmid containing the gene for puromycine resistance. Vials from a working bank were thawed in a water bath at 37°C, resuspended in 29 mL medium in spin tubes (Techno Plastics Products AG (TPP), Trasadingen, Switzerland) and centrifuged (1200 rpm, 5 min). The supernatant was discarded and the pellet was resuspended in 30 mL and incubation was carried out at 37°C, 5 % CO_2, 80 % humidity and an agitation of 320 rpm.

4.4.2. Passaging and cell expansion

Depending on the expression system, different expansion media for each CHO clone were used. Cellvento™ CHO-220 supplemented with 25 µM MSX was used for passaging of clones 1 and 2 while Cellvento™ CHO-220 supplemented with 6 mM L-glutamine and 5 mg/L puromycine dihydrochloride was used for passaging of clone 3. Cells were seeded either at 3*10^5 C/mL every three days for cultivation over the weekend, while cells were seeded at 2*10^5 C/mL every two days for cultivation in the week, respectively. Cell passaging and expansion for spin tube experiments was carried out in 50 mL spin tubes (Techno Plastics Products AG (TPP), Trasadingen, Switzerland) in a culture volume of 30 mL. Incubation was carried out at 37°C, 5 % CO_2, 80 % humidity and an agitation of 320 rpm. Samples were taken for cell counting as described in offline-analytics.

4.4.3. Batch experiments

Batch experiments were carried out with all three CHO clones. As batch medium, neutral pH L-cysteine deficient Cellvento™ CHO-220 (Merck Millipore, Darmstadt, Germany) supplemented with 1.5 mM SSC*Na-B was used. In the control condition, the same concentration of CysHCl*H_2O was added. Depending on the used CHO clone, medium supplementation with 6 mM L-glutamine was carried out.

Batch experiments were performed in triplicates using 50 mL spin tubes (Techno Plastics Products AG (TPP), Trasadingen, Switzerland) with or without pH sensors (Presens GmbH, Regensburg, Germany) in a starting culture volume of 30 mL with a seeding density of $2*10^5$ C/mL. Incubation was carried out at 37°C, 5 % CO_2, 80 % humidity and an agitation of 320 rpm.

Samples were taken for cell counting, metabolite measurements, amino acid quantification and vitamin quantification as described in offline-analytics. On-line pH was measured when necessary as described in off-line analytics.

4.4.4. Small scale fed-batch experiments

Small scale fed-batch experiments were carried out with all three CHO clones. As fed-batch medium, Cellvento™CHO-220 medium containing 1.5 mM CysHCl*H_2O was used. Depending on the used CHO clone, medium supplementation with 6 mM L-glutamine was carried out. 15 mM or 20 mM SSC*Na-A or SSC*Na-B were added to neutral pH Cellvento™ Feed 220 (Merck Millipore, Darmstadt, Germany) containing 30 mM PTyr2Na^+. In the control condition, a separate feed containing 150 mM L-cysteine and 288.5 mM L-tyrosine disodium salt at pH 11 and a neutral pH Cellvento™ Feed 220 (Merck Millipore, Darmstadt, Germany) were used. Feeding was carried out in all conditions at days 3, 5, 7, 10 and 14 at the following v/v ratios (3, 6, 6, 6 and 3 %). Glucose was quantified daily and adjusted to 4 g/L using a 400 g/L D(+)- glucose solution. Starting culture volume in small scale fed-batches using spin tubes (Techno Plastics Products AG (TPP), Trasadingen, Switzerland) was 34 mL with a seeding density of $2*10^5$ C/mL. Five replicates for each condition was performed. Incubation was carried out at 37°C, 5 % CO_2, 80 % humidity and an agitation of 320 rpm.

Samples were taken for cell counting, metabolite measurements, amino acid quantification and vitamin quantification as described in offline-analytics. On-line pH was measured when necessary as described in off-line analytics.

4.4.5. Bioreactor fed-batch experiments

Bioreactor runs were carried out with clone 2. Fed batch experiments in bioreactors were carried out in 1.2 L glass vessels (DasGip, Eppendorf, Hamburg, Deutschland) using DASGIP Control 4.0 software (DasGip, Eppendorf, Hamburg, Deutschland). Probes for determination of DO concentration (DasGip,

Eppendorf, Hamburg, Deutschland), pH (Mettler Toledo, Columbus, US) and temperature (DasGip, Eppendorf, Hamburg, Deutschland) were used. Single-point calibration for the DO probe and three-point calibration for the pH probe were carried out. DO concentration was controlled at 50 % air saturation by sparging with pure oxygen and air via an open pipe sparger. pH was controlled at 6.95 +/- 0.15 using 0.5 M sodium carbonate and CO_2.

Verification of pH was carried out with a blood gas analyzer (Radiometer GmbH, Willich-Schiefbach, Germany) and one point pH calibration was done, if necessary. Temperature was set at 37°C and shifted from 37°C to 33°C on day 5 of culture. Heating was either achieved by heating jackets or by heating blocks. Agitation was maintained at 140 rpm using a clockwise oriented marine impeller. As fed-batch medium, Cellvento™ CHO-220 medium containing 1.5 mM CysHCl*H_2O was used. 15 mM or 20 mM SSC*Na-A were added to a neutral pH Cellvento™ Feed 220 (Merck Millipore Darmstadt, Germany) containing 30 mM PTyr2Na^+. In the control condition, a separate feed containing 150 mM L-cysteine and 288.5 mM L-tyrosine disodium salt at pH 11 and a neutral pH Cellvento™ Feed 220 (Merck Millipore, Darmstadt, Germany) were used. Feeding was carried out in all conditions at days 3, 5, 7, 9 and 14 at the following v/v ratios (3, 6, 6, 6 and 3 %). Glucose was quantified daily and adjusted to 4 g/L using a 400 g/L D(+)- glucose solution whereas glucose was adjusted to 10 g/L on day 7. To control foam generation, 1 % antifoam solution was added when necessary without overcoming 300 parts per million (ppm) in the whole cultivation process. An initial culture volume of 800 mL were used and cells were seeded in $2*10^5$ C/mL.

Samples were taken for cell counting, metabolite measurements, amino acid quantification and vitamin quantification as described in offline-analytics.

4.4.6. Specific productivity

For bioreactor experiments, the productivity per cell per day was calculated following the formula:

$$\mathbf{pcd_t} = \left(\frac{\mathbf{titer_t}}{\mathbf{cIVC_t}}\right)$$

Figure 27: Formula for the calculation of the specific productivity (l pg/(cell.day)) at Merck

with $pcd_t \equiv$ productivity per cell per day at day ´t´ (in pg/ (cell.day)), $titer_t \equiv$ titer at day ´t´ (in mg/L), $cIVC_t \equiv$ corrected integral viable cell concentration at day ´t´ (in mio VC.day/mL). Corrected IVC (cIVC) is calculated here with a correction factor in order to take in mind the culture dilution by feeds or pH regulation. The formula presented below was used for cIVC calculation:

$$\mathbf{cIVC_t} = [(\mathbf{VCD_{t-1}} + \mathbf{VCD_t}) * \mathbf{\Delta t/2}] * \mathbf{D_{-t}} + \mathbf{cIVC_{t-1}} * \mathbf{D_t}$$

Figure 28: Formula for the calculation of the corrected integral viable cell concentration (cIVC) (mio.V.day/mL) at Merck

with $cIVC_0$ =0 ≡ cIVC at day zero, $cIVC_{t-1}$ ≡ cIVC at day ´t-1´ (in mioCV.day/mL), $cIVC_t$ ≡cIVC at day ´t´ (in mioV.day/mL), VCD_{t-1} ≡ viable cell density at day ´t-1´ (in mio viable cells per mL), VCD_t ≡ viable cell density at day´t´ (in mio viable cells per mL), Δt ≡ time (in days) between two points of cell counting, between ´day t-1´ and ´day t´, D_t ≡ dilution factor due to feed or pH regulation solution added between ´day t-1´ and ´day t´; (always < or= 1.00); equal to bioreactor volume at ´day t-1´ divided by bioreactor volume at ´day t´.

To estimate the overall specific productivity of the cells during the run, the linear regression curve between the titer and cIVC was applied, the slope factor corresponding to the overall specific productivity (pcd).

4.5. mAb characterization

In the department of R&D at Merck Millipore, IgG were purified from cell culture supernatants using PureProteome™ protein A magnetic beads (Merck Millipore, Darmstadt, Germany). Briefly, beads were washed three times in PBS. Cell culture supernatants containing the IgG were added to the bead solution leading to antibody binding. After incubation at room temperature for 30 minutes, beads were washed four times to remove unbound antibodies. Beads were resuspended in 90 % 200 mM L-glycine pH 3 for elution of antibodies. For neutralization, 10 % 1 M Tris(hydroxymethyl)aminomethane (Tris) pH 8.5 was added. Quantification of mAb was performed via protein quantification relying on the Bradford method as described in section 4.7.6 of this chapter. Purified mAb were used for N-glycosylation, charge variant analyses and peptide mapping as described below.

4.5.1. N-glycosylation

N-glycosylation patterns of mAb produced from control process (two feed strategy) and single feed strategy were compared and interpreted at the department of central analytics at Merck.

Briefly, samples were denatured using dodecyl sulfate sodium salt and mercaptothanol. Enzymatic N-glycan cleavage was carried out with peptide- N-glycosidase F (P0704S, New England Biolabs, Ipswitch, US). Proteins were removed using Microcon Ultracel YM-10 centrifugal filter devices (42407, Amicon) and after centrifugation the collected N-glycan filtrate was dried. Further, N-glycans were de-salted via Glyco Clean columns (GKI-4025, Prozyme, Hayward, US) and dried again. Freshly prepared 2-amino benzamide (2-AB) solution was mixed with dried N-glycans and excess 2-AB was removed via Glyco Clean S columns (GKI-4726, Prozyme, Hayward, US). Dried samples were dissolved in 70 % (v/v) acetonitrile and analysis was carried out on an Agilent Series 1100 using a Glyco N HPLC column and an injected sample volume of 45 µL. 2-AB labeled samples were excited at 330 nm and fluorescence was detected at 420 nm. Data were interpreted with Chemstation software

(Agilent, Santa Clara, US) relying on the integration of total peak area. Total peak area was set to 100 %. The percentage of each peak area was calculated based on the total peak area.

4.5.2. Charge variant

The isoform profile of mAb produced from control process (two feed strategy) and single feed strategy were compared with capillary isoelectric focusing (cIEF) and interpreted at the department of central analytics at Merck.

To determine the isoelectric points (pI) of the produced mAb, cIEF was used. To do so, the sample was mixed with ampholytes, stabilizers and pI markers. Ampholytes are used for the establishment of the pH gradient. Anodic and cathodic stabilizers are high-conductivity molecules being necessary for minimization of distortions of the pH gradient at the anodic and cathodic capillary sides. Also, stabilizers force the sample to focus before the detection window. As internal standards, pI markers were used.

Briefly, samples were diluted to 1 mg/mL in eCap Tris Buffer pH 8.0 (477427, Beckman) and de-salted using Microcon*Ultracell YM 10 (PN A11530, Millipore, Billerica, US) relying on size exclusion centrifugation. The retentates containing the mAbs were resuspended in eCap Tris buffer pH 8.0 (477427, Beckman). The cIEF reagent mix was prepared containing urea - cIEF gel (U0631, Sigma Aldrich, St Louis, US; 477497, Beckman, Fullerton, US), pharmalyte 3-10 carrier ampholytes (17-0456-01, GE Healthcare, St Giles, UK), arginine (A5006, Sigma Aldrich, St Louis, US) as cathodic stabilizer, iminodiacetic acid (220,000, Sigma Aldrich, St Louis, US) as anodic stabilizer, pI markers 10.0 (A58481[a], Beckman, Fullerton, US), 9.5 (A58481[a], Beckman, Fullerton, US) and 5.5 (A58481[a], Beckman, Fullerton, US). cIEF reagent mix was mixed with samples. With overpressure, gel-sample mixtures were loaded in the neutral coated capillary (Beckman). As anolyte, phosphoric acid (345, 245, Sigma Aldrich) was used while as catholyte NaOH (722082, Sigma Aldrich) was applied. Focusing was carried out at 25 kV voltage for 15 minutes followed by chemical mobilization at 30 kV for 30 minutes. Due to the last step, the samples passed the detection window where detection was done at 280 nm. Analysis was done based on the linear regression of the migration time of the pI markers. Due to the migration time of the sample compared with the migration time of the pI markers, the isoelectric point was calculated.

4.5.3. Peptide mapping

Peptide mapping of mAb produced from control process (two feed strategy) and single feed strategy were compared via mass spectrometry (MS) in electrospray ionization (ESI) positive mode and interpreted at the department of central analytics at Merck.

Peptide mapping was carried out aiming to determine the incorporation of SSC containing peptides in the mAb produced from single feed strategy process. Tryptic peptides generated from enzymatic digestion were analysed for SSC incorporation using non-reducing conditions. Treatment with the alkylating reagent IAM leads to no modification of intact disulfide bridges and peptides containing SSC residues.

Free L-cysteine residues undergo alkylation. In MS analysis using ESI positive mode, intact disulfide bridges are detected as such. Free L-cysteine residues are alkylated. Peptides containing SSC residues lose the $–SO_3H$ modification in the ionisation process leading to free L-cysteine residues.

Briefly, sample preparation was carried out using a slightly modified RapiGest^{TM} SF based protocol (Waters, Milford, US). Briefly, 50 µg of each sample were mixed with a final concentration of 0.1 % RapiGest^{TM} SF. Alkylation was performed with 20 mM IAM. For maintaining disulfide bridges intact, no reduction was performed. Trypsin solution was added, followed by an overnight incubation. After digestion, the sample was acidified by addition of trifluoroacetic acid and analyzed by liquid chromatography-mass spectrometry (LC-MS) using the ESI positive mode. NanoLC-MS analysis was accomplished using a nanoAcquity UPLC coupled to a Synapt G1 HDMS (Waters, Milford, US). 0.1 % formic acid in water was used as solvent A and 0.1 % formic acid in acetonitrile as solvent B. Tryptic peptides were injected and trapped for 4 minutes on a Symmetry C18 pre-column (Waters, Milford, US) with a flow rate of 10 µL/minutes. Separation was performed using an UPLC 1.7 µm BEH130 column (Waters, Milford, US) with a flow rate of 450 nL/minutes, one linear gradient (3-45 % B for 70 min) and holding at 95 % B for a further 5 minutes before returning to 3 % B for 15 min. MS spectra were acquired from m/z 50 to 1600. Extracted ion chromatograms were analyzed manually for each L-cysteine containing peptide. Since no reduction was performed, most of the peptides were found linked through disulfide bridges. Relative intensities of alkylated peptides (corresponding to free L-cysteine containing peptides of the mAb) and free L-cysteine containing peptides (resulting from the in-source fragmentation of putative SSC containing peptides of the mAb) were calculated with the average of the 3 highest peptide intensities.

4.6. Mechanistic studies

4.6.1. Cell-free interactions of SSC with GSH

In the department of R&D at Merck, interaction of GSH either with SSC*Na-A, CysHCl*H_2O or L-cystine was tested at different pH in distilled water, 1x PBS and Cellvento™ CHO-220 medium at a final concentration of 1 mM each. Moreover, at acidic, neutral and alkaline pH, mixtures of GSH with SSC*Na-A, L-cystine or CysHCl*H_2O were tested at concentrations of 1 mM each. The incubation was done at room temperature and 500 rpm for 3 hours. As controls, the single raw materials were

tested alone in different matrices (water, PBS, medium) at different pH to determine if degradation over time (instability) or matrix dependent events (interactions) occurred.

Amino acid quantification was carried out after different time points via UPLC while analyte identification was carried out using liquid chromatography-high resolution mass spectrometry (LC-HRMS) as described in off-line analytics.

4.6.2. Cell spiking experiments

In the department of R&D Merck Millipore, clone 2 was used for an enzymatic cleavage test of SSC. Cells were counted and cell lysis based on $15*10^7$ C/ mL Phospho Safe Extraction reagent (71296-2, Novagen, Durham, US) was carried out on ice. Samples were incubated at room temperature for 5 minutes and centrifuged (10 min, 14000 rpm, 4°C). Supernatants were transferred in new tubes. 100 µL cell lysate were spiked with 1 mM SSC*Na-B. Samples were incubated at room temperature for 10 minutes. For pre-treatment with IAM, 100 µL cell lysate were treated with 0.05 M IAM and incubated for 30 minutes at room temperature in the absence of light. Addition of 1 mM SSC*Na-B followed and samples were again incubated for 30 minutes at room temperature in the absence of light. Subsequent, detection of L-cysteine, L-cystine and SSC was performed via UPLC as described in offline analytics.

To mimic intracellular behavior, $5*10^6$ cells were lysed in PhosphoSafe™ (71296, Merck Millipore, Darmstadt, Germany) containing four phosphatase inhibitors (sodium fluoride, sodium vanadate, β-glycerophosphate and sodium pyrophosphate) preserving the proteins phosphorylation state. Cell lysates were spiked to the mixtures of GSH/L-cysteine hydrochloride or GSH/SSC*Na-B at a final concentration of 1 mM each. Reactions were stopped by addition of IAM. After different incubation intervals, samples were taken for amino acid analysis via UPLC and MS/MS as described in offline analytics.

4.6.3. Inhibition experiments of selected L-glutamate transporter

To determine if transporter(s) were participating in SSC uptake in clone 2, two glutamate transporters (SLC1a2, SLC1a3) and the L-cystine/L-glutamate transporter (SLC7a11) were chosen for inhibition experiments in cell passaging.

SLC1a3 was blocked by using 1 µM UCPH 101, SLC1a2 by 10 µM dihydrokainic acid and both by 0.3 µM TFB-TBOA. SLC7a11 was blocked by 25 µM (S)-4-carboxy-phenylglycine. Blocking experiments were carried out in L-cysteine deficient Cellvento™CHO-220 medium supplemented with 1.5 mM SSC*Na-B and 25 µM MSX. Passage experiments were performed in triplicates using 50 mL spin tubes (Techno Plastics Products (TPP), Trasadingen, Switzerland) in a culture volume of 30 mL. Cells were seeded either at $3*10^5$ C/mL every three days for cultivation over the weekend, while cells

were seeded at $2*10^5$ C/mL every two days for cultivation in the week, respectively, and VCD and viability were monitored. Incubation was carried out at 37°C, 5 % CO_2, 80 % humidity and an agitation of 320 rpm. After three passages in SSC containing media with inhibitors, cells were used for a batch culture in the same media without MSX supplementation in a higher seeding cell density of $6*10^5$ C/mL.

4.6.4. Intracellular ROS measurements

Carboxy-H_2DCFDA was used for intracellular ROS detection in small scale fed-batch experiments with clone 2. Intracellular ROS levels of cells cultured in single feed strategy using 15 mM SSC*Na-B and 30 mM PTyr2Na^+ in neutral pH feed were compared to those cultured in two feed strategy (control) using a separate alkaline L-cysteine/L-tyrosine disodium salt feed over time. Three replicates á $3*10^6$ C per condition per day were centrifuged (1200 rpm, 10 minutes). Supernatants were discarded. For autofluorescence, cells were resuspended in 200 µL 1x PBS and analysed as negative control. For ROS determination, cell pellets were loaded with 200 µM 50 µM carboxy-H_2DCFDA and incubated for 20 minutes at 37°C, 1000 rpm. After centrifugation (1200 rpm, 10 minutes), supernatants were discarded and cell pellets were each resuspended in 200 µL 1x PBS and transferred into a black microtiter plate. Green fluorescence was analysed with Envision 2104 Multilabel Reader (Perkin Elmer, Waltham, US) at an excitation wavelength of 475 nm and an emission wavelength of 520 nm.

4.6.5. RNA isolation and quantification

All three clones were harvested from routine cell passaging in passage 12. RNA isolation was carried out with RNeasy® Mini Kit (74106, Qiagen, Veno, Netherlands) according to manufacturer instructions relying on disruption of biological samples with subsequent homogenization and inactivation of RNases. After RNA column binding and washing, RNA is eluted in RNase free water.
Briefly, $1*10^7$ C of each clone were harvested and diluted 1:2 in RNase-free water. Cells were centrifuged at 300 g for 5 minutes and the supernatant was aspired. Pellets were carefully resuspended in 600 µL RLT buffer. Further, 600 µL 70 % ethanol were added and mixed by pipetting. Samples were transferred on RNeasy Mini spin columns, centrifuged at maximum speed for 15 seconds. Columns were used for next steps. Addition of 700 µL buffer RW1 was carried out and columns were centrifuged at maximum speed at 15 seconds Eluates were discarded. Addition of 500 µL buffer RPE was carried out and columns were centrifuged at maximum speed at 15 seconds. Eluates were discarded. Addition of 500 µL buffer RPE was carried out and columns were centrifuged at maximum speed at 2 minutes. Eluates were discarded. Columns were centrifuged dry at maximum speed for 1 minute. 40 µL of RNase free water were added and columns were centrifuged at maximum speed for 1 minute. RNA containing eluates were kept on ice and later stored at -80°C.

RNA quantification was carried out on a NanoDrop2000c UV-Vis spectrophotometer (Thermo Fisher Scientific, Waltham, US) with NanoDrop 2000/2000c software (Thermo Fisher Scientific, Waltham, US). For RNA quantification, 1 µL of freshly, isolated RNA was applied with RNase free water as blank. RNA was quantified at 260 nm. Nucleic acid quantification relies on the Lambert-Beer equation which uses here a modified extinction coefficient of 40 ng-cm/µL for RNA and a absorbance was measured over 10 mm normalized pathway.

RNA concentrations were calculated via $\boldsymbol{c = (A * \varepsilon)/b}$ with c ≡ RNA concentration (ng/µL), A ≡ absorbance (AU), ε ≡ wavelength-dependent extinction coefficient (ng-cm/µL) and b ≡ path length (cm).

Absorbance ratios of 260/280 nm and 260/230 nm were used to assess nucleic acid purity.

4.6.6. Quantitative Real-Time polymerase chain reaction (RT-PCR)

4.6.6.1. Taq-Man based RT-PCR- expression levels of selected glutamate transporters

For complementary DNA (cDNA) synthesis, 1.5 µg RNA of all three clones was used. RNA was mixed with RNase free water to give a volume of 14 µL per sample. Synthesis of cDNA was carried out based on TaqMan®Reverse Transcription Reagents (N8080234, Applied Biosystems, Waltham, US). The reaction mix for cDNA synthesis of one sample contained 15.4 %(v/v) 10x RT buffer (100025924, Applied Biosystems, Waltham, US), 33.8 % (v/v) magnesium chloride (100020476, Applied Biosystems, Waltham, US), 30.8 % (v/v) desoxyribonucleosidtriphosphates mix (100023382, Applied Biosystems, Waltham, US), 7.7 % (v/v) random hexamer (100026484, Applied Biosystems, Waltham, US), 3.1 % (v/v) RNase inhibitor (100021540, Applied Biosystems, Waltham, US) and 9.2 % (v/v) MultiScribe ™ Reverse Transcriptase (100024128, Applied Biosystems, Waltham, US) in a final volume of 26 µL mix per sample. PCR was carried out in a final volume of 40 µL being composed of 14 µL sample and 26 µL PCR mix. For cDNA synthesis, samples were incubated in a GeneAmp ® PCR system 9700 (Applied Biosystems, Waltham, US) using the following program: 25°C for 10 minutes, 37°C for 60 minutes, 95°C for 5 minutes and samples were stored at 4°C. For Real-Time PCR, 80 µL of cDNA sample was diluted with 40 µL RNase free water and mixed.

The Real-Time PCR reaction mix per sample contained: 66.7 % (v/v) TaqMan® Fast Universal Master Mix (2x) (4352042, Applied Biosystems, Waltham, US), 6.7 % (v/v) primer and 26.7 % (v/v) RNase free water (1017979, Qiagen, Veno, Netherlands) in a final volume of 15 µL per sample. 15 µL Real-Time PCR reaction mix were added to 5 µL cDNA. Cells were incubated in a 7500 Fast Real-Time PCR System (Applied Biosystems, Waltham, US). For enzyme activation, incubation at 95°C for 20 seconds for was carried out. 45 cycles were run in the following program: 95°C for 3 seconds and 60°C for 30 seconds.

Gene expression of several genes was determined using mouse primers against SLC1a1 (Mm00436590_m1, Applied Biosystems, Waltham, US), SLC1a2 (Mm00441457_m1, Applied Biosystems, Waltham, US), SLC1a3 (Mm00600697_m1, Applied Biosystems, Waltham, US), SLC1a6 (Mm01173279_m1,Applied Biosystems, Waltham, US), SLC1a7 (Mm00525562_m1, Applied Biosystems, Waltham, US) and SLC7a11 (Mm00442530_m1, Applied Biosystems, Waltham, US) and the house keeping gene glycerinaldehyde-3-phosphate-dehydrogenase (GAPDH) (Mm99999915_g1, Applied Biosystems, Waltham, US).

Data were interpreted for each target gene in comparison with endogenous GAPDH levels as control. The relative amount of target genes in each sample was calculated in comparison with the calibrator sample (expression levels in clone 3) applying the ΔΔCt method. The magnitude of gene induction was calculated using the formula $2^{-\Delta\Delta Ct} = 2^{-(\Delta Ct \text{ clone } 1,2 \text{ - } \Delta Ct \text{ clone } 3)}$ and a difference in relative mRNA expression level of at least 2 fold was considered as differentially expressed.

4.6.6.2. SYBR-Green based RT-PCR – microarray tests

For cDNA synthesis, 1 µg RNA of clone 2 was used. First, genomic DNA (gDNA) elimination mix was prepared as follows: 20 % (v/v) buffer GE and 1 µg RNA were mixed and replenished with RNase free water to give a final volume of 10 µL per sample. Reaction mixtures were incubated at 42°C for 5 minutes and put on ice for at least one minute. For cDNA synthesis, reverse transcription mix using the RT² First Strand Kit (330401, Qiagen, Veno, Netherlands) was prepared as follows: 40 % (v/v) 5x Buffer BC3, 10 % (v/v) Control P2, 20 % (v/v) RE3 Reverse Transcriptase Mix, and 30 % (v/v) RNase-free water were mixed to give a final volume of 10 µL per sample. 10 µL gDNA elimination mix was subsequently mixed with 10 µL reverse transcription mix. Samples were incubated at 42°C for 15 minutes (Thermomixer, Eppendorf, Hamburg, Germany) and 95°C for 5 minutes (Thermomixer, Eppendorf, Hamburg, Germany). Subsequently, samples were mixed with 91 µL RNase free water and put on ice.

For the preparation of the Real-Time PCR Mix, 92.6 % (v/v) RT²SYBR® Green ROX™ qPCR Mastermix (330523, Qiagen, Veno, Netherlands) and 7.4 % (v/v) Primer were mixed in a final volume of 13.5 µL per sample. cDNA was diluted 1:11.5 in RNase free water. For RT-PCR, 11.5 µL diluted cDNA were added to 13.5 µL RT-PCR reaction mix per sample. Cells were incubated in a 7500 Fast Real-Time PCR System (Applied Biosystems, Waltham, US). For enzyme activation, incubation at 95°C for 10 minutes was carried out. 40 cycles were run in the following program: 95°C for 15 seconds, 60°C for 1 minute. To exclude potential contamination with gDNA or non-specific amplification such as primer-dimer formation, melt curve analysis was carried out following the program: 95°C for 15 seconds, 60°C for 1 minute, 95°C for 30 seconds and 60°C for 15 seconds.

Gene expression was determined using hamster primers against genes encoding several enzymes (e.g. Glutathione Peroxidases, Peroxiredoxins, SODs) (PAJJ065, Qiagen) and the house keeping gene GAPDH (PPJ00327A-200, Qiagen, Ven, Netherlands).

Data were interpreted for each target gene in comparison with endogenous GAPDH levels as control. The relative amount of target genes in each sample was calculated in comparison with the calibrator sample (control process with clone 2) applying the ΔΔCt method. The magnitude of gene induction was calculated using the formula $2^{-\Delta\Delta Ct} = 2^{-(\Delta Ct \text{ clone 2, SSC process} - \Delta Ct \text{ clone 2, control process})}$ and a difference in relative mRNA expression level of at least 2 fold was considered as differentially expressed.

4.6.7. Western Blot

In the department of R&D Merck Millipore, western blotting was carried out. Briefly, clone 2 cells from fed-batch experiments were harvested daily in late phase culture. Cells were washed three times with cold PBS. After centrifugation (1200 rpm, 5 minutes), cell pellets were lysed in a buffer containing 8.3 M urea (U4883, Sigma Aldrich, St Louis, US), 2 M thiourea (T8656, Sigma Aldrich, St Louis, US), 4 % 3-((3-cholamidopropyl) dimethylammonio)-1-propanesulfonate (C9426, Sigma Aldrich, St Louis, US), 50 mM 1,4-dithiothreitol (DTT) (43815, Sigma Aldrich, St Louis, US) and 24 mM spermine (S3256, Sigma Aldrich, St Louis, US). After centrifugation (16 000 g, 1 hour, 20°C), supernatants were recovered and stored at -80°C. Proteins were quantified using a Bradford assay as described in off-line analytics. NuPAGE-western blotting was carried out according to standard procedures (Life technologies, Carlsbad, US). 8 µg of protein samples were separated on 4 to 12 % Bis-Tris NuPAGE gels and blotted on a polyvinylidene difluoride (PVDF) membrane using the iBlot system applying program 3 (20 V, 7 minutes) following manufacturer instructions. This dry blotting principle relies on shortened electrode distances, high field strength and currents leading to reduced transfer times. Briefly, the transfer membrane was placed on the iBlot® Anode Stack. The latter was in contact with the copper anode. The pre-run gel was placed bubble-free on the transfer membrane which was covered with a presoaked iBlot® Filter Paper. The copper cathode was placed on top of the filter paper. After blotting, PVDF membranes were placed in pure water. For western detection, the iBind™ Flex Western System (Thermo Fisher Scientific) was used following manufacturer instructions. This technique utilizes sequential lateral flow to perform automated blocking, antibody binding and washing steps using mechanical pressure generated by iBind™ Flex Cards. Homogenous flow in washing, blocking and antibody binding steps is achieved by iBind™ Flex. Briefly, wetting of the iBind™ Flex Card, washing, blocking and antibody dilution was carried out with the iBind™ Flex Solution Kit (SLF2020, Thermo Fisher Scientific). The following primary antibodies were used for immunoblotting analyses: anti SOD-1 (TA343111, Origene, Rockville, US) and anti SOD-2 (13141S, 1:1000, Cell Signaling Technology, Danvers, US) both antibodies being diluted 1:1000 in iBind™

Flex Solution. For recognition of the primary antibody, a peroxidase-conjugated goat anti-rabbit secondary antibody used (1:20000) (Jackson Immunoresearch Laboratories, West Grove, US). Briefly, pre-activation of PVDF membranes was carried out in methanol followed by rinsing with pure water. Blotted membranes were immersed in iBind^{TM} Flex Solution. The membrane was placed bubble-free on the wet iBind^{TM} Flex Card with its protein-side down. Antibody and washing solutions were added sequentially to the iBind^{TM} Flex Wells and membranes were incubated overnight. After incubation, membranes were rinsed in pure water. Chemiluminescence was detected via the chemiluminescence detection kit from Pierce (Life technologies, Carlsbad, US) relying on blot incubation with a stable peroxide solution and an enhanced luminol solution.

Western blot signals were acquired with a charge-coupled device camera (Chemidoc XRS, Biorad, Munich, Germany) and band volume was quantified using the Biorad Quantity One software. GAPDH (2118, Cell Signaling Technology, Danvers, US) was diluted 1:1000 and was used as loading control.

4.7. Offline analytics

4.7.1. Characterization of SSC batches

4.7.1.1. Quantitative NMR

NMR spectra were measured and interpreted at the NMR laboratories within the central analytical department at Merck. The purity (w %) was calculated against the internal standard maleic acid (99.99 w % purity of standard). The sample and the standard were exactly weighted, dissolved in DMSO-d6, the solution was checked for clarity and subsequently a ^{1}H-NMR was recorded. The purity of the sample was calculated via the formula:

$$\mathbf{w_x = w_{st} \frac{z_{st} I_x M_x m_{st}}{z_x I_{st} M_{st} m_x}}$$

Figure 29: Formula for the calculation of purity (w %) using data obtained from NMR spectra measurements at Merck

with $w_x \equiv$ purity of sample, $w_{st} \equiv$ purity of standard, $z_{st} \equiv$ integrated protons per integral of the standard, $z_x \equiv$ integrated protons per integral of the sample, $I_x \equiv$ value of integral for the sample, $I_{st} \equiv$ value of integral for the standard, $M_x \equiv$ molecular weight of the sample, $M_{st} \equiv$ molecular weight of the standard, $m_{st} \equiv$ weighted amount of the standard, $m_x \equiv$ weighted amount of the sample.

4.7.1.2. Capillary electrophoresis (CE)

CE measurements were carried out and interpreted at the molecule analytics laboratory within the central analytical department at Merck. Samples were run on an Agilent CE G1600 instrument (Agilent, Santa Clara, US). The capillary had an inner diameter of 50 µm and a length of 120 cm. Samples were injected with 50 mbar and injection lasted 40 seconds. An Agilent basic anion buffer at

pH 12.1 was used. Detection was carried out using indirect UV detection at 275 nm. To develop this analytical method, SSC samples of different concentrations and purities were measured and the method was refined until a sufficient separation of the signals and signal-to-noise ratio were achieved. Standard solutions of suspected impurities were spiked in and their retention times were assigned. To unambiguously assign thiosulfate, this signal was additionally verified by another method employing direct UV detection at 200 nm. This approach verified that the signal assigned to thiosulfate is definitely distinct from the close by signals of chloride in the indirect detection mode and nitrate in the direct and in the indirect detection mode. For the quantification, standard solutions of the determined analytes were measured as external standards together with each sample run. Amounts in w % were calculated via comparison of the integrals. Standard deviation was determined to be 100 % +/- 0.3 %**.**

4.7.1.3. Inductively coupled plasma high resolution mass spectrometry (ICP-HR-MS)

ICP-HR-MS measurements were carried out and interpreted at the element analytics laboratory within the central analytical department at Merck. Samples were dissolved in nitric acid and diluted with pure water to the required volume. A copper standard was spiked to the sample at varying concentrations to calibrate the measurement with the exclusion of matrix effects. Measurements were carried out with ELEMENT 2^{TM} ICP-MS (Thermo Fisher Scientific, Waltham, US) using a medium resolution of 4000. The result is given in µg/g together with the recovery rate to estimate the precision of each measurement.

4.7.2. Measurement of cell concentration and viability

VCD and viability were measured in 500 µL cell suspension using an automatic cell counting device based on trypan blue exclusion method with 0.4 % trypan blue solution (Vicell™ XR, Beckman Coulter, Fullerton, US). Viable cells differ from dead cells in their membrane permeability. Intact viable cells exclude the dye while damaged or dead cells take up the dye due their decreased membrane integrity. Moreover, the viability of the cells was determined. Cell counts and viability measurements are based on 30 taken pictures, respectively.

4.7.3. Measurement of metabolites

Quantitative measurements of NH_3, iron and titer were carried out in 250 µL cell culture supernatant or feed volume, respectively, with an automatic system based on photometric and turbidimetric tests, UV detection and established standard curves (Cedex BIO HT, Roche, Mannheim, Germany). Photometrical measurement of solved NH_3 relies on its conversion together with α-KG and NADPH catalyzed by glutamate dehydrogenase by reductive amination. L-glutamine and $NADP^+$ are formed. NADPH decrease is proportional to NH_3 concentration. Complexed iron is liberated at acidic pH to

give free Fe (III) ions which are further reduced to Fe (II) ions in the presence of ascorbate. Fe (II) ions react subsequently with FerroZine to form a colored complex and its measured absorbance is directly proportional to the iron concentration in the sample. IgG quantification is carried out via immunoturbidimetric measurements in which the antibody precipitates with a specific antiserum and precipitation is turbidimetrically quantified.

4.7.4. Measurement of online pH

Online-measurement of pH was carried out in cultivation tubes (Techno Plastics Products AG (TPP), Trasadingen, Switzerland) having integrated non-invasive, pre-calibrated pH sensor patches (Presens GmbH, Regensburg, Germany). These pH sensor patches rely on the dual lifetime referencing method which is used to quantify pH shifts. The method is based on combination of two fluorescent dyes (luminophores), one being the pH sensitive indicator and the other being the reference standard. Simultaneous excitation of both dyes is carried out and the pH-dependent overall phase shift resulting from the ratio of the two intensities is measured (Boniello et al. 2012). Generated data were handled with ITRS V1.0.2.5534 software. Intervals of measurements were 5, 10 or 30 minutes, respectively. Determination of pH was carried out over the whole cultivation.

4.7.5. Measurement of sulfate and thiosulfate

In the department of central analytics, sulfate and thiosulfate were determined in stability studies, cell culture supernatants of batch and fed-batch experiments via ion chromatography (IC) using an ICS 1100 (Thermo Fisher Scientific, Waltham, US). Samples were diluted 1:10 in pure water and mixed. Samples were injected and separated during 1 hour on a HPIC Ionpac-AG14 pre-column (Thermo Fisher Scientific, Waltham, US) and a HPIC-Ionpac-AS14 separation column (Thermo Fisher Scientific, Waltham, US) with a flow rate of 1.5 mL/min. Detection was performed using a suppressed conductivity detector. Sulfate and thiosulfate concentrations were calculated from obtained conductivity signals based on a four point calibration curve of sodium thiosulfate and sulfate standard solution, respectively. Data were handled with Chromeleon 6.80 software (Thermo Fisher Scientific, Waltham, US).

4.7.6. Protein quantification via Bradford Assay

For intracellular protein quantification, supernatants of lysed clone 2 cells were diluted 1:10, 1:20 and 1:40 in pure water. The standard curve ranging from 0 to 1000 µg/mL was prepared with an albumin standard (P0834, Sigma Aldrich, St Louis, US) in pure water. For quantification of purified IgG, the standard curve was prepared with a human serum IgG (I4506, Sigma Aldrich) in pure water. 10 µL sample were mixed with 200 µL BIOQUANT ® Protein (Bradford Method) reagent solution

(1.10306.0500, Merck, Darmstadt, Germany). Samples were incubated 5 minutes at room temperature and absorbance was measured at 595 nm via Envision Alpha Reader (Perkin Elmer, Waltham, US).

4.7.7. Amino acid quantification

Quantification of L-cysteine, L-cystine and SSC was achieved via ultra high pressure liquid chromatography (UHPLC) (Acquity™ Ultra performance LC, Waters, Milford, US).

Cell free cell culture supernatants were diluted 1:10 in 0.1 M HCl (109057, Merck Millipore, Darmstadt, Germany) while feeds from stability study were diluted of 1:200 and 1:500 in 0.1 M HCl. For intracellular amino acid quantification, clone 2 cells were washed three times in cold 1x PBS. For extraction of cytosolic proteins, $12*10^6$ cells were lysed in 100 µL PhosphoSafe™ reagent (Merck Millipore, Darmstadt, Germany) containing four phosphatase inhibitors (sodium fluoride, sodium vanadate, β-glycerophosphate and sodium pyrophosphate) preserving the proteins phosphorylation state.

Samples were alkylated with 20 mM IAM solution (A3221, Sigma Aldrich, St Louis, US) for 45 minutes in the dark. Alkylation with IAM inhibited further conversion of L-cysteine in L-cystine, therefore enabling the quantification of both amino acids. In intracellular samples, L-cysteine residues in the active site of enzymes were alkylated and blocked by IAM. 250 µM norvaline was used as internal standard.

Pre-column derivatisation of diluted samples was carried out using AccQ Tag Ultra® reagent (Waters, Milford, US). Samples were incubated for ten minutes at 55°C. AccQ Tag Ultra® reagent is an N-hydroxysuccinimide-activated heterocyclic carbamate responsible for the conversion of both primary and secondary amino acids leading to stable derivatives. Followed separation was carried out with a reversed phase column RP C18 130A (1.7 µm particles) and eluents A and B (Waters, Milford, US) following a gradient presented in table 3.

Detection was carried out using UV light. Derivatization, chromatography and data analysis were carried out following suppliers recommendations (Waters, Milford, US). Quantification of each amino acid was based on standard curves. For analysis, Empower software 3 was used. Standard deviation of the method was determined to be 10 %.

Table 3: Gradient parameters of UHPLC for amino acid and SSC quantification

Time (min)	Flow (mL/min)	% Eluent A	% Eluent B	Curve
Initial	0.7	99.9	0.1	6
0.54	0.7	99.9	0.1	7
5.74	0.6	90.9	9.1	6
7.74	0.6	78.8	21.2	6
8.04	0.7	40.4	59.6	6
8.05	0.7	10	90	6
8.64	0.7	10	90	6
8.73	0.7	99.9	0.1	6
9.5	0.7	99.9	0.1	6
11	0.7	99.9	0.1	6

4.7.8. Intracellular total glutathione quantification

In the R&D department of Merck Millipore, intracellular total glutathione was quantified in clone 2 cells. Cells were washed three times in cold 1x PBS. For extraction of cytosolic proteins, $12*10^6$ cells were lysed in 100 µL PhosphoSafe™ reagent (Merck Millipore, Darmstadt, Germany) containing four phosphatase inhibitors (sodium fluoride, sodium vanadate, β-glycerophosphate and sodium pyrophosphate) preserving the proteins phosphorylation state. Total glutathione concentrations (GSH+GSSG) were determined using the UHPLC method as described in section 4.7.7 of this chapter. Data were normalized with the total protein concentrations as described in section 4.7.6 of this chapter.

4.7.9. Vitamin quantification

In the department of central analytics at Merck, the determination of vitamins in cell culture supernatants and feeds from stability study was carried out. Vitamin quantification was performed with ultra-high pressure liquid chromatography-MS-MS (UHPLC-MS/MS) analysis. For vitamin separation, reversed phase chromatography relying on an Acquity UPLC HSS T3 (Waters, Milford, US) was used. AB Sciex 4000 QTrap system supported MS/MS analysis. Multiple reaction monitoring was applied for MS/MS detection. ESI was used to create charged aerosol. After injection into MS/MS, analytes were detected according to their specific mass to charge (m/z) ratio in the first quadrupole Q1 while in the second quadrupole Q2 m/z corresponding to the analyzed vitamins were selected. Specific fragments for each vitamin were quantified in quadrupole Q3. Standard deviation of the method was determined to be 10 %.

4.7.10. LC-HRMS for analyte identification generated by interaction studies

Samples generated from cell-free interaction studies were injected into an Ultimate 3000 UPLC system (Thermo Fisher Scientific, Waltham, US) using a reversed phase Hypercarbcolumn (Thermo Fisher

Scientific, Waltham, US). Samples were eluted with mobile phase A and B. Mobile phase A contained water, ammonium formate and formic acid while mobile phase B comprised acetonitrile. The applied flow rate was 1.5 mL/minute and a linear gradient from aqueous to organic phase was adjusted. Samples were injected in a volume of 10 µL.

Separated molecules entered a Q Exactive MS (Thermo Fisher Scientific, Waltham, US). ESI was carried out using collision energy of 35 % in both positive and negative ionization mode. Deviation of 5 ppm was allowed. Resolution in MS was 7000 while resolution in MS/MS was 35000.

4.7.11. Statistics

Data are expressed as means ± standard error of the mean (SEM). For cell culture experiments, the area under the curve of each technical replicate was calculated and statistical differences between groups were assessed by using a 2-tailed nonparametric Mann-Whitney test for single comparison, or a Kruskall-Wallis test for multiple comparisons. P-values of less than 0.05 were considered significant. Statistical and graphic analyses were performed with Prism 6 software (GraphPad Software Inc, La Jolla, US).

5. Results

The state of the art fed-batch process at Merck uses two separate feeds. In the slightly acidic main feed, all feed components except L-cysteine and L-tyrosine are included. These two amino acids were kept in an alkaline second separate feed due to stability and solubility issues of L-cysteine and L-tyrosine, respectively. Due to the pH differences of both feeds and resulting pH peaks in cell culture, a single feed at neutral pH comprising all nutrients is aimed. For L-tyrosine, the chemically modified tyrosine derivative PTyr2Na$^+$ was developed being able to be integrated in the main feed and to replace tyrosine in fed-batch processes (Zimmer et al. 2014). In this work, the search for a L-cysteine derivative was started. As desired, the L-cysteine derivative should possess similar solubility and increased stability at neutral pH feed compared to the control L-CysHCl*H_2O. In the next sections, different L-cysteine derivatives were evaluated for the physicochemical properties meaning similar solubility and increased stability of derivative compared with control.

5.1. L-cysteine derivative screening

To evaluate different L-cysteine derivatives concerning physicochemical properties and use in batch and fed-batch cell tests, 11 L-cysteine derivatives belonging to different chemical classes were tested as summarized in table 4. Due to their structures, the chosen L-cysteine derivatives showed differences in protecting the thiol group from further reactions. Out of these 11 L-cysteine derivatives, it was aimed to find at least one candidate fulfilling the desired properties.

As a class being already described in different cell studies present in the literature, thiazolidines were chosen. They are heterocycles including one thioether and one amine group in their 5-membered saturated ring structure. Due to the generated thiazolidine structure, the thiol and the amine group of L-cysteine were protected preventing the reactive thiol group to interact quickly with other compounds.

Reactions of L-cysteine with reaction partners having aldehyde or ketone character were carried out here to form the appropriate thiazolidines. Belonging to the group of reaction partners with aldehyde character, the aldoses glucose and ribose, methanal (formaldehyde) and glyoxylic acid were used. As a substance with ketone character, pyruvate was used.

After condensation reactions of L-cysteine with glucose, 2-(D-glucopentylhydroxypentyl)-4(R)-1,3-thiazolidine-4-carboxylic acid was produced. The reaction of L-cysteine with ribose resulted in the condensation product (R)-2-((1R,2R,3R)-1,2,3,4-tetrahydroxy-butyl)-thiazolidine-4-carboxylic acid. Reaction of L-cysteine and methanal led to condensation product 1,3-thiazolidine-2,4-carboxylic acid. The molecule (2RS, 4R)-1,3-thiazolidine-2,4-dicarboxylate sodium salt was obtained from the condensation reaction of glyoxylic acid with L-cysteine.

Reaction of L-cysteine and pyruvate led to the condensation enantiomer mix (2R,4R)-(2-methyl)-1,3-thiazolidine-2,4-dicarboxylate disodium salt and (2S,4R)-(2-methyl)-1,2-thiazolidine-2,4-dicarboxylate disodium salt.

Further known from literature, the NAC derivatives NACA and NACET were tested. The mucolytic agent NAC is described in the literature to reduce mucus viscosity by breaking disulfide bridges involved in protein linkage via its free thiol group as reviewed (Sunitha et al. 2013). At physiological pH, it loses a proton making thereby the compound negatively charged. The negatively charged molecule limits the cell permeability making NAC poorly bioavailable. To overcome this, the carboxylic group was neutralized in the amide form of NAC, leading to the formation of NACA. By esterification of the carboxylic group of NAC, the molecule NACET was formed. Both NAC derivatives were designed to enhance lipophilicity and cell permeability of NAC while possessing an unprotected, free thiol group. Further, L-cysteine ethyl ester hydrochloride shows an unprotected, free thiol group and was tested as a L-cysteine derivative in this study.

Di-(PTyr)-cystine-tetrasodium salt was chosen as a peptide of one L-cystine and two phosphotyrosine disodium molecules. Since L-cystine possesses a disulfide bridge wherein the reactive thiol group is not reactive anymore, the linkage of two highly soluble $PTyr2Na^+$ molecules was thought to increase the low solubility of L-cystine to overcome physicochemical limitations. Both phosphotyrosine molecules were each linked via one peptide bond to L-cystine framing the disulfide.

As sulfur group modified derivatives, L-cysteine sulfinic acid monohydrate and SSC*Na salt were chosen. L-cysteine may be oxidized by direct oxygen addition leading to cysteine sulfinic ($-SO_2H$) and –sulfonic ($-SO_3H$) acid. Due to the oxidation, the thiol group is not free and reactive anymore. As a representative of oxidized L-cysteine molecules, cysteine sulfinic acid monohydrate was tested. SSC*Na comprises a disulfide bridge with the outer sulfur atom being oxidized leading to the sulfonic group and was also tested as a representative of sulfur group modified derivatives.

As summarized in figure 30, solubility of all 11 L-cysteine derivatives was tested first in a complex matrix, a concentrated, neutral pH feed. L-cysteine derivatives were excluded from following screening steps when L-cysteine derivatives failed the applied criteria. Secondly, stability in complex, concentrated neutral pH feed over one month of the remaining L-cysteine derivatives was determined. L-cysteine derivatives which failed the applied criteria were excluded from following screening steps. Third, pre-passaging of CHO clone 1 cells was carried out with the remaining L-cysteine derivatives in L-cysteine deficient medium. L-cysteine derivatives in which no cell growth was observed in pre-passages were excluded from following cell tests. Finally, batch tests with in L-cysteine derivatives pre-passaged CHO clone 1 cells were carried out to investigate if the remaining L-cysteine derivatives had the potential to replace L-cysteine in short time cell cultures. L-cysteine derivatives were excluded

from further steps when cell death, lowered maximum VCD or no cell growth was observed. As a consequence, after these screening steps one derivative was chosen to go further with.

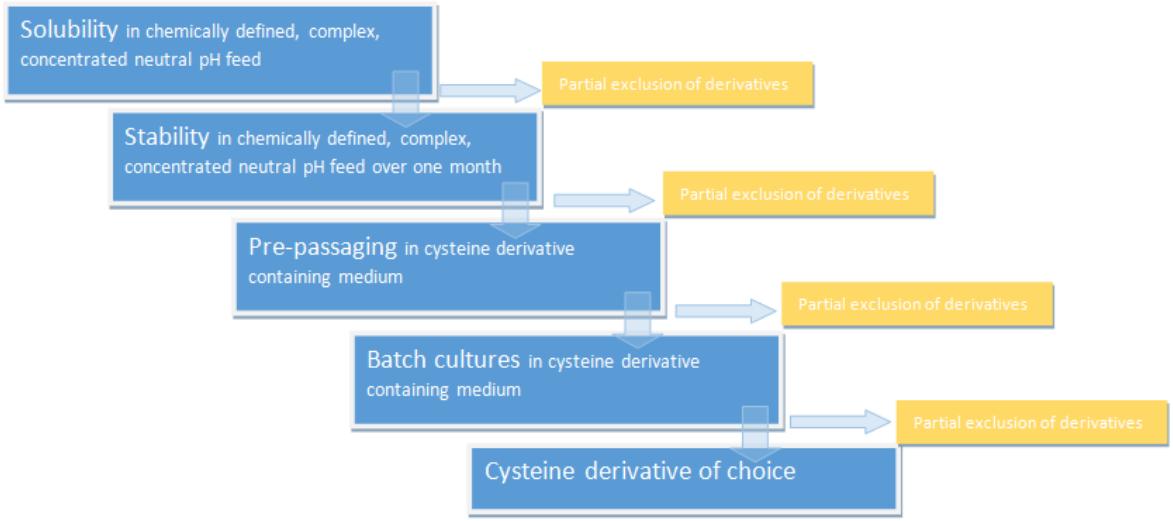

Figure 30: Schematic representation of the workflow in the L-cysteine derivative screening process.

First, solubility was tested in neutral pH Cellvento™ Feed 220. Secondly, over a period of one month, stability of the L-cysteine derivatives was evaluated in neutral pH Cellvento™ Feed 220. Thirdly, pre-passaging of CHO clone 1 cells was carried out in L-cysteine deficient Cellvento^{TM} CHO-220 medium supplemented with 1.5 mM L-cysteine derivatives. Fourthly, batch cultures with CHO clone 1 cells were carried out in L-cysteine deficient Cellvento^{TM} CHO-220 medium supplemented with 1.5 mM L-cysteine derivatives. After each screening step, failed L-cysteine derivatives were excluded from further tests.

As shown in table 4, data obtained from physico-chemical studies (solubility, stability) and short-term cell cultures (pre-passaging and batch tests) were summarized.

To successfully choose L-cysteine derivatives in solubility study, the desired concentration needed to be determined as the test criterion. In the standard process, 150 mM L-cysteine was used in the separate, alkaline feed. Since the applied volume of separate, alkaline L-cysteine containing feed in standard fed-batch cultures was 1:10 of the fed main feed volume, the L-cysteine concentration in the main feed equals 15 mM L-cysteine. In the future single feed strategy, the L-cysteine derivatives were thought to be integrated in the main feed. When using L-cysteine derivatives in the main feed, their utilization rate in cell culture might be lower compared with the utilization rate of L-cysteine. Consequently, a higher L-cysteine derivative concentration (30 mM) was chosen to cover possible cellular requirements. L-cysteine derivatives were excluded from the following stability studies when insolubility or lower maximum concentrations for complete solubilization were observed. L-cysteine ethyl ester hydrochloride was only soluble in neutral pH feed when being applied in concentrations below 30 mM. 2-(D-glucopentylhydroxypentyl)-4(R)-1,3-thiazolidine-4-carboxylic acid, NACET and Di-(PTyr)-cystine-tetrasodium salt were insoluble in the complex matrix of concentrated, neutral pH feed while L-cysteine ethyl ester hydrochloride was only soluble in concentrations < 30 mM.

Table 4: Summary of physico- chemical tests (solubility and stability in concentrated, neutral pH feed) and short term batch cultures in L-cysteine replacement strategy using clone 1 with 11 chemically modified L-cysteine derivatives.

Solubility and stability were evaluated visually while batch tests using clone 1 were evaluated by automatic cell counting based on trypan blue staining.

Substance	Structure	Protection	CAS	Tested concentrations (mM) in Feed 220 (pH 7)	Solubility in Feed 220 (pH 7)	Stability in Feed 220 (pH 7)	Batch culture (Cysteine replacement)
Di-(PTyr)-cystine-tetrasodium salt	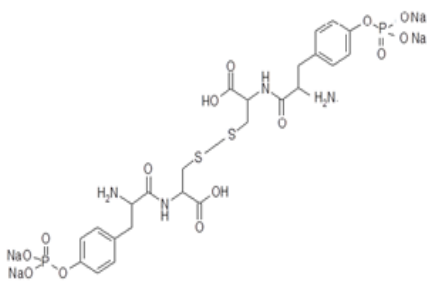	-SH and -NH_2		30, 20, 15, 10	Insoluble in all concentrations	----	----
2-(D-glucopentylhydroxypentyl)-4(R)-1,3-thiazolidine-4-carboxylic acid	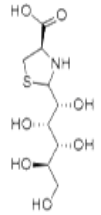	-SH and -NH_2	88271-29-8	30, 20, 15, 10	Insoluble in all concentrations	----	----
N-acetylethylester (NACET) (R)-2-acetylamino-3-mercapto-propionic acid ethyl ester	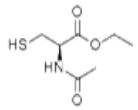	-NH_2 and -COOH	59587-09-6	30, 20, 15, 10	Insoluble in all concentrations	----	----

L-cysteine ethyl ester hydrochloride	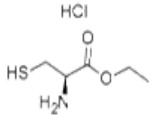	-COOH	868-59-7	30, 20, 15, 10	Soluble < 30 mM	----	----
(R)-2-((1R,2R,3R)-1,2,3,4-tetrahydroxy-butyl)-thiazolidine-4-carboxylic acid	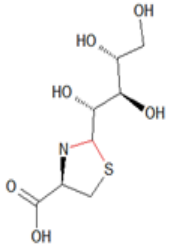	-NH_2 and -SH		30	soluble	Precipitations and browning in < 4 weeks	
N-acetylcysteine amide (NACA)	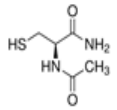	-SH and-NH_2	38520-57-9	30	soluble	Browning in < 4 weeks	0
1,3-thiazolidine-2,4-dicarboxylic acid	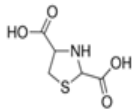	-NH_2 and -SH	30097-06-4	30	soluble	Browning in < 4 weeks	
(2RS, 4R)-1,3-thiazolidine-2,4-dicarboxylate sodium salt	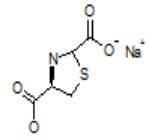	-NH_2 and -SH		30	soluble	Browning in > 4 weeks	1.5mM shows lower max VCD as 1.5mM CysHCl*H2O
L-cysteine sulfinic acid monohydrate	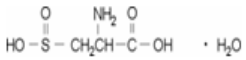	-SH (Oxidation)	207121-48-0	30	soluble	No precipitations nor browning in > 4 weeks	Cells did not survive prepassages

Enantiomer mix (2R,4R)-(2-methyl)-1,3-thiazolidine-2,4-dicarboxylate disodium salt and (2S,4R)- (2-methyl)-1,2-thiazolidine-2,4-dicarboxylate disodium salt		-NH_2 and -SH		30	soluble	Precipitations and browning in > 4 weeks	1.5mM shows similar max VCD as 1.5mM CysHCl*H2O
S-sulfocysteine mono sodium salt (SSC*Na)	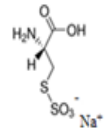	-SH (Disulfide)	7381-67-1	30	soluble	No precipitations nor browning in > 4 weeks	1.5mM shows similar max VCD as 1.5mM CysHCl*H2O with clone 1

Consequently, the primary excluded L-cysteine derivatives were L-cysteine ethyl ester hydrochloride, 2-(D-glucopentylhydroxypentyl)-4(R)-1,3-thiazolidine-4-carboxylic acid, NACET and Di-(PTyr)-cystine-tetrasodium salt.

To determine the stability in neutral pH feed over one month, stability studies using 30 mM of the remaining L-cysteine derivatives were carried out. The time frame of one month was set up as desired since a complete fed batch process may comprise one month including media and feed preparation as well as the culture itself. Over this period, the L-cysteine derivative containing complex, concentrated neutral pH feed needed to be free from precipitations and color change. The presence of insoluble complexes and color changes in prepared liquid feed may be related to reactions of feed components possibly impacting the formulated feed component concentrations. L-cysteine derivatives were excluded from following steps of the screening, when precipitations or browning alone, respectively, or both together occurred in the stability study in an interval shorter than one month. Both, precipitations and color change, were observed in stability studies using (R)-2-((1R, 2R, 3R)-1, 2, 3, 4-tetrahydroxy-butyl)-thiazolidine-4-carboxylic acid. Browning alone was observed in stability studies using NACA and 1,3-thiazolidine-2,4-dicarboxylic acid. Consequently, the secondary excluded L-cysteine derivatives were (R)-2-((1R, 2R, 3R)-1, 2, 3, 4- tetrahydroxy-butyl)-thiazolidine-4-carboxylic acid, NACA and 1,3-thiazolidine-2,4-dicarboxylic acid.

To determine if L-cysteine may be replaced by L-cysteine derivatives in short term cultures, pre-passaging and batch cultures were carried out. In both cell culture experiments, 1.5 mM L-CysHCl*H_2O originally formulated in the Cellvento^{TM} CHO-220 medium was replaced by the same concentration of L-cysteine derivatives. Since clone 1 was the first one being available for cell tests, this clone was used in L-cysteine replacement pre-passaging and batch studies to evaluate possible cell growth in L-cysteine derivative containing medium.

To exclude L-cysteine and L-cystine from cell culture tests, cells were pre-passaged two times in L-cysteine deficient medium containing 1.5 mM L-cysteine derivatives before starting the actual batch culture. Since cells did not survive pre-passages in medium containing 1.5 mM L-cysteine sulfinic acid monohydrate, this derivative was excluded from batch studies although its stability study outcome fulfilled the criteria.

The remaining L-cysteine derivatives were applied in batch cultures with clone 1. L-cysteine derivatives were excluded from further studies when cells showed no growth or lowered maximum VCD in batch mode compared with L-CysHCl*H_2O containing control. Although (2RS,4R)-1,3-thiazolidine-2,4-dicarboxylate sodium salt showed no feed color change over one month, lower similar maximum VCDs were observed in this derivative condition compared with the control.

Similar maximum VCDs were observed in batch cultures using 1.5 mM of the enantiomer mix (2R,4R)-2-methyl-thiazolidine-2,4-dicarboxylate-disodium salt and (2S,4R)-2-methyl-thiazolidine-2,4-dicarboxylate-disodium salt and SSC*Na compared with 1.5 mM L-CysHCl*H_2O containing batch cultures as controls. Since the condensation product of L-cysteine and pyruvate was already protected by a patent, the use of the enantiomer mix (2R,4R)-2-methyl-thiazolidine-2,4-dicarboxylate-disodium salt and (2S,4R)-2-methyl-thiazolidine-2,4-dicarboxylate-disodium salt was not permitted anymore. Consequently, the derivatives (2RS,4R)-1,3-thiazolidine-2,4-dicarboxylate sodium salt and the enantiomer mix (2R,4R)-2-methyl-thiazolidine-2,4-dicarboxylate-disodium salt and (2S,4R)- 2-methyl-thiazolidine-2,4-dicarboxylate-disodium salt were excluded from further studies. Only SSC*Na showed higher maximum VCD compared with 1.5 mM L-CysHCl*H_2O containing batch cultures in first batch tests.

SSC*Na showed the desired physical chemical characteristics. It was soluble at the desired concentration of 30 mM in chemically defined, complex, highly concentrated, neutral pH feed. Over a period of one month, no precipitations nor color change were observed with the L-cysteine derivative in this matrix indicating stability of the molecule. Pre-passaging of clone 1 cells was successful in a L-cysteine deficient medium containing 1.5 mM SSC*Na. Batch cultures of clone 1 cells using 1.5 mM SSC*Na in a L-cysteine deficient medium revealed similar growth and similar maximum VCD compared with the L-CysHCl*H_2O containing control. Consequently, out of the 11 tested derivatives, SSC*Na was the only derivative chosen to go further with.

5.2. Maximum solubility of SSC*Na in two different matrices

To further characterize SSC*Na physicochemically, its maximum solubility was tested at room temperature in two matrices: water and concentrated, neutral pH feed. As shown in table 5, SSC*Na reached its maximum solubility at 1300 mM in water while in concentrated neutral pH feed its maximum solubility was reached at 60 mM.

Table 5: Maximum solubility of SSC*Na in water and concentrated, neutral pH feed.

Solubility of SSC*Na in water was determined using infrared-based residual mass determination, whereas solubility of SSC*Na in the feed was carried out by dissolving increasing SSC*Na concentrations in neutral pH feed

	S-sulfo-L-cysteine sodium salt
Molecular weight (g/mol)	223.21
Formula	$C_3H_6NNaO_5S_2$
Solubility in water (25 °C)	300 g/L (= 1300 mM)
Solubility in concentrated feed at pH 7.0 (25 °C)	13,4 g/L (= 60 mM)

The maximum solubility of SSC*Na was determined to be 60 mM in complex concentrated neutral pH feed. In conclusion, the derivative satisfied the solubility requirements. Since L-cysteines` poor stability in concentrated, neutral pH feed was the reason for derivative screening, its replacement by an appropriate L-cysteine derivative candidate was aimed. With L-cysteines` stability issue in mind, next, stability of the L-cysteine replacing derivative SSC*Na was evaluated over three months in concentrated, neutral pH feed.

5.3. Stability study of SSC*Na in concentrated, chemically defined neutral pH feed

First, stability of SSC*Na was evaluated in complex, neutral pH feed. As a second readout, the impact of SSC*Na on different feed component classes such as e.g. amino acids, vitamins, metals such as iron and on released NH_3 was monitored. As seen in stability studies with L-CysHCl*H_2O, impacts on L-cystine, iron, NH_3, folic acid, riboflavin, vitamin B12 and thiamine were observed. By replacing L-CysHCl*H_2O with SSC*Na, these feed components were monitored. Amino acids were monitored using UPLC. Vitamins were quantified using UHPLC-MS/MS analysis. Iron and NH_3 were measured automatically via photometry. Chosen and herein presented data showed changes due to SSC*Na application.

5.3.1. Amino acid and SSC*Na quantification

To further characterize SSC*Na physico-chemically, stability of the L-cysteine derivative was tested in rich, complex, chemically defined neutral pH feed stored at 4°C protected from light over three months. Since the separate, alkaline feed in the standard process contained 150 mM L-cysteine and its applied volume was 1:10 of the main feed volume in the standard process, the L-cysteine concentration in the main feed equaled 15 mM L-cysteine. In order to compare the stability of SSC*Na with L-cysteine, the 15 mM SSC*Na was tested in complex, neutral pH feed and was compared to feed containing 15 mM L-CysHCl*H_2O and L-cysteine free feed.

Over three months, no precipitations nor color change were observed visually in SSC*Na supplemented feed. As shown in figure 31 A, no change in SSC concentration (15.2 +/- 0.27 mM) was observed in neutral pH feed after three months at 4 °C protected from light. No concomitant release L-cystine was observed after three months storage period in the SSC*Na containing feed as shown in figure 28 B. No L-cysteine was detected in the SSC*Na containing feed (data not shown). In contrast, the positive control condition using 15 mM L-CysHCl*H_2O showed a brownish precipitation after less than 24 hours indicating rapid reaction of L-cysteine with metals such as iron to insoluble complexes. No free L-cysteine was detected in the positive control (data not shown). L-cystine was quantified (2.3 +/- 0.05 mM) in the L-CysHCl*H_2O containing feed after three months at 4°C protected from light as shown in figure 31 B. In the control condition, 84 % of the applied L-cysteine was not detected as L-cystine nor L-cysteine after three months indicating reactions of L-cysteine with other feed components such as metals like iron and copper. Consequently, SSC*Na was considered to be stable over three months at 4°.

5.3.2. Sulfate quantification

Since any instability of the derivative may lead to molecule cleavage by liberating sulfate and L-cysteine, sulfate was quantified by using IC to determine if SSC*Na was stable in concentrated, chemically defined neutral pH feed stored at 4°C protected from light. As shown in figure 31 C, no change in sulfate concentration was observed in SSC*Na containing (107.6 +/- 2.1 %), L-CysHCl*H_2O containing (95 +/- 2.4 %) and L-cysteine free feed (93.6 +/- 1.9 %) after three months at 4°C. These data indicate no cleavage of SSC*Na after storage in complex feed supporting the molecules` stability shown with UPLC.

5.3.3. NH_3 release

Since L-cysteine was shown to be deaminated non-enzymatically to form NH_3 amongst others (Metzler and Snell 1952), the effect of L-cysteine on NH_3 production in complex feed was determined

here. With replacing L-cysteine by SSC*Na in mind, the effect of SSC*Na on NH_3 concentration was evaluated.

To determine if SSC*Na application in concentrated, chemically defined neutral pH feed stored at 4°C protected from light had an impact on NH_3 generation, solved NH_3 was quantified using photometrical measurements. As shown in figure 31 D, no change in NH_3 levels after three months was observed in SSC*Na containing feed (0.5 +/- 0.02 mM) and in L-cysteine free feed (0.5 +/- 0.03 mM). In contrast, the L-CysHCl*H_2O containing feed showed seven times higher final NH_3 concentrations (3.4 +/- 1.3 mM) compared with L-cysteine free feed. These data indicate no effect of SSC*Na on NH_3 levels compared to L-cysteine free feed. With replacing L-cysteine by SSC*Na in mind, low NH_3 concentrations may be beneficial since NH_3 may cause toxic effects in cell cultures.

5.3.4. Iron concentration

Since L-cysteine was shown to react with iron to form complexes (Taylor et al, 1966), the effect of L-cysteine on iron concentration in complex feed was studied here. With replacing L-cysteine by SSC*Na in mind, the effect of SSC*Na on iron concentration was monitored. To determine if SSC*Na application in concentrated, chemically defined neutral pH feed stored at 4°C protected from light had an impact on iron concentration, iron was quantified using photometry.

As shown in figure 31 E, similar and higher iron concentrations in both SSC*Na containing feed (101 +/- 0.5 %) and L-cysteine free feed (112 +/- 0.4 %) were detected after three months compared with the L-CysHCl*H_2O containing feed (83.3 +/-2.4 %). The deviation was connected to interference of feed components with the assay or due to technical variation of the assay. A significant reduction of absolute 28.7 % in iron concentration was observed in L-CysHCl*H_2O containing feed after three months compared with L-cysteine free feed. These data may have indicated that SSC*Na had no effect on iron concentration in concentrated neutral pH feed after three months compared with L-cysteine free feed.

5.3.5. Vitamin quantification

To determine if SSC*Na application in concentrated, chemically defined neutral pH feed stored at 4°C protected from light had an impact on vitamins, they were first separated by using reversed phase chromatography and subsequently quantified via UHPLC-MS/MS.

The chosen and herein presented data of folic acid, riboflavin, vitamin B12 and thiamin concentrations showed changes due to SSC*Na application while the concentrations of biotin, myo-inositol, pyridoxine, choline chloride, nicotinamide and calcium pantothenate were unchanged.

5.3.5.1. Folic acid

All three feeds showed reduced folic acid concentrations from the beginning of the stability study. After three months at 4°C in complex feed, all three feeds showed reduced folic acid concentrations as presented in figure 31 F. Among the three feeds, SSC*Na containing feed showed significantly higher final folic acid concentrations (79.1 +/- 1.9 %) compared with L-cysteine free feed (66.5 +/- 1.7 %) and significantly lower final folic acid concentrations in L-CysHCl*H_2O containing feed (42.2 +/- 2.9 %). These data may indicate that folic acid interacted with other feed components from the beginning of the study. Moreover, these data possibly indicate a stabilizing effect of SSC*Na on folic acid concentration compared with L-CysHCl*H_2O containing feed and basal formulation feed.

5.3.5.2. Riboflavin

As shown in figure 31 G, higher riboflavin concentrations were determined in the SSC*Na containing feed (97.4 +/- 1.9 %) compared with L-cysteine free feed (89.5 +/- 0.9 %). In the L-CysHCl*H_2O containing feed, significant lower final riboflavin concentrations (74.1 +/- 5.5 %) were observed compared with L-cysteine free feed representing a reduction of absolute 15 % in final riboflavin concentration. These data may indicate a stabilizing effect of SSC*Na on riboflavin concentrations compared with basal formulation feed.

5.3.5.3. Vitamin B12

As shown in figure 31 H, SSC*Na containing feed showed significantly decreased final vitamin B12 concentrations (87.2 +/- 0.8 %) compared with L-cysteine free feed (93.5 +/- 1 %). In contrast, the L-CysHCl*H_2O containing feed showed highly significant lower final vitamin B12 concentrations (12.1 +/- 1.1 %) compared with L-cysteine free feed representing a reduction of absolute 81 % in vitamin B12 concentration. These data may indicate slight instability of vitamin B12 concentrations in SSC*Na containing feed compared with basal formulation feed.

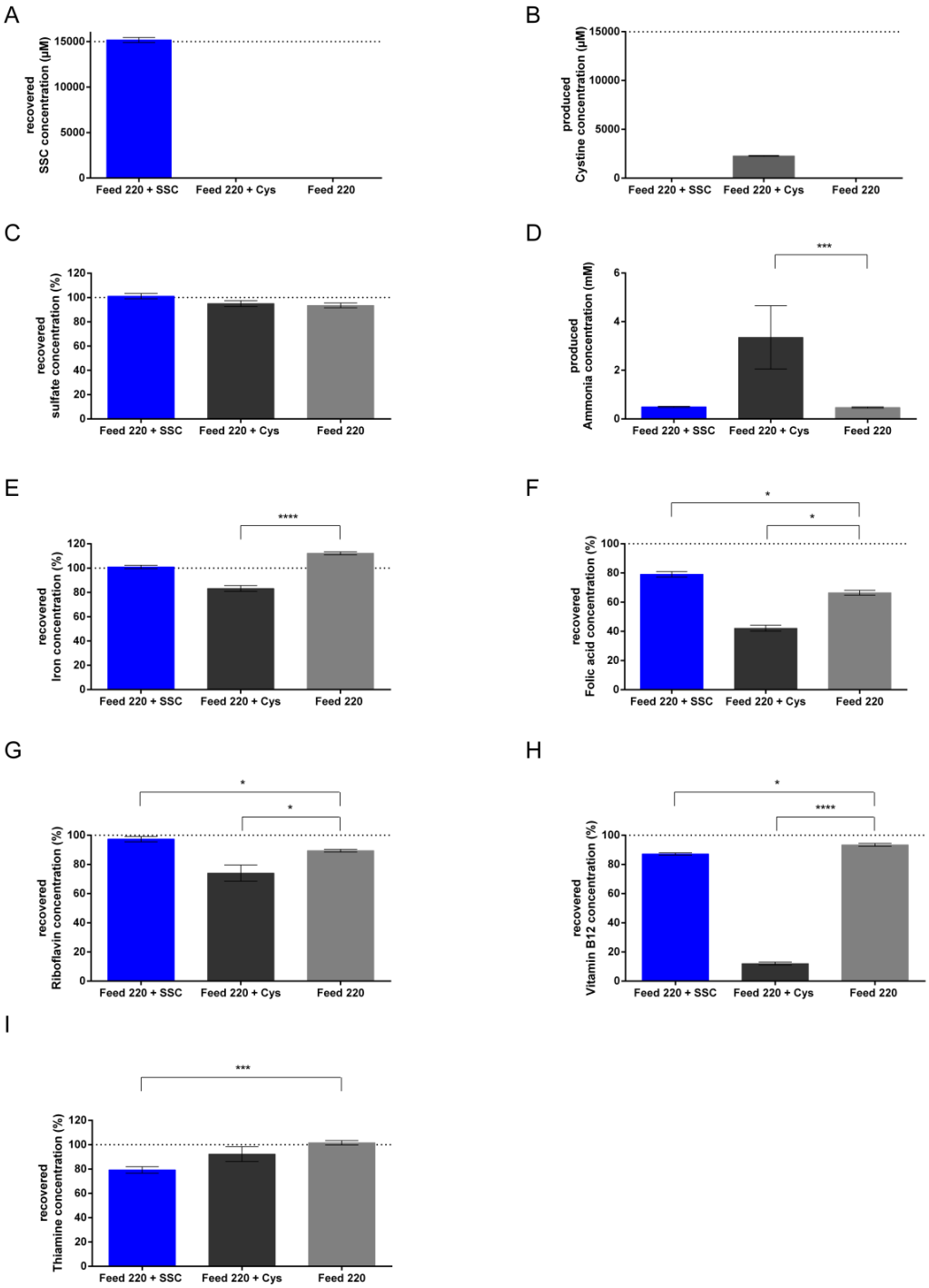

Figure 31: Stability study of SSC*Na in concentrated, chemically defined neutral pH feed after three months at 4°C protected from light.

15 mM SSC*Na was added to chemically defined, complex, neutral pH Cellvento™ CHO-220 Feed and comparison with Cellvento™ CHO-220 Feed containing 15 mM L-CysHCl*H_2O and Cellvento™ CHO-220 Feed was carried out (n=8). (A) recovered SSC concentration (µM) in the feed measured by UPLC after IAM treatment and AccQ●Tag derivatization (B) produced L-cystine concentration (µM) in the feed measured by UPLC after IAM treatment and AccQ●Tag derivatization. (C) recovered, normalized sulfate concentration measured by ion chromatography. (D) produced NH_3 concentration (mM) in the feed measured by photometry. (E) recovered, normalized iron concentration in the feed measured by photometry. (F) recovered, normalized folic acid concentration in the feed measured by UHPLC-MS/MS. (G) recovered, normalized riboflavin concentration in the feed measured by UHPLC-MS/MS. (H) recovered, normalized vitamin B12 concentration in the feed measured by UHPLC-MS/MS. (I) recovered, normalized thiamin concentration in the feed measured by UHPLC-MS/MS. SSC was considered stable if the standard deviation of the measured concentrations over three months was below 10 % in figures 1A and 1C. Kruskal-Wallis test followed by Dunn`s multiple comparisons test were performed ($p < 0.05$). Values are means +/- SEM.

5.3.5.4. Thiamin

As shown in figure 31 I, L-cysteine free feed (101.7 +/- 1.8 %) and L-CysHCl*H_2O containing feed (92.3 +/- 6.1 %) showed no change in thiamin concentration. SSC*Na containing feed showed reduced thiamin concentrations (79.3 +/- 2.7 %) compared with L-cysteine free feed representing a reduction of absolute 22 % in thiamin concentration. These data possibly indicate direct reactions of SSC*Na with thiamin.

Concluding physical chemical properties, the maximum solubility of SSC*Na fulfilled the applied criteria. SSC*Na containing neutral pH feed showed no change in SSC*Na concentration over three months. Further, the stability of the derivative was confirmed by sulfate quantification. Although decreased vitamin B12 and thiamine concentrations were observed in SSC*Na containing feed compared with basal formulation feed, no impacts of SSC*Na on NH_3 and iron concentration were observed. Further, higher final folic acid and riboflavin concentrations were detected in SSC*Na containing feed compared with L-cysteine free feed.

5.4. Characterization of SSC*Na batches produced from different synthesis routes

Different SSC*Na batches were purchased or synthesized inhouse. Since the dependency on an external SSC*Na supplier bared the risk of possible lot-to-lot inconsistencies and supply bottlenecks, own internal synthesis routes were developed. The characterization of several used SSC*Na batches was carried out and results were summarized in table 3. Purity and traces were followed. The impurities of the SSC*Na batches presented here were chosen due to the syntheses characteristics.

Both external batches SSC*Na-A and SSC*Na-B were synthesized by Bachem AG. Their synthesis relyed on the tetrathionate method based on the conversion of L-cysteine with sodium tetrathionate leading to the formation of SSC*Na and thiosulfate. After regular analysis of trace elements and purity, higher sulfate and thiosulfate concentrations were found in the externally synthesized batches SSC*Na-A and SSC*Na-B indicating possible carry-overs of the synthesis materials into the final product. Based on these observations, the internal synthesis routes were checked for sources of contaminations.

The internally used synthesis routes for the production of SSC*Na research batches relied on tetrathionate free methods. The reaction of L-cystine with sodium sulfite was catalysed by copper finally leading to the formation of SSC*Na via oxidative sulfitolysis of L-cystine. Since the internal synthesis routes were based on the use of copper as a catalyst, the copper concentration was measured to determine if and how much of the catalyst was carried over from the synthesis process into the final product. With regard to synthesis starting raw materials, L-cystine contaminations were measured and chosen to be presented here.

5.4.1. Purchased SSC*Na batches

As shown in table 6, both externally synthesized batches SSC*Na-A and SSC*Na-B showed differences in impurities compared with the internally synthesized batches. With regard to purity, SSC*Na-B (85.3 % (m/m)) was more pure compared with SSC*Na-A (81.3 % (m/m)) indicating possible inefficient external synthesis routes or ineffective purification processes of the final product. In both externally synthesized SSC*Na batches, similar low copper concentrations were found for SSC*Na-A (0.3 µg/g) and SSC*Na-B and (0.4 µg/g) possibly indicating copper containing raw materials. L-cystine was not detected in both SSC*Na batches. Similar sulfate concentrations were found for SSC*Na-A (1.8 % (w/w)) and SSC*Na-B (1.3 % (w/w)) possibly indicating partial carry-over of sulfate from the synthesis into the final product or sulfate containing raw materials in a SSC*Na lot independency. Higher thiosulfate concentrations were found for SSC*Na-B (12.8 % (w/w)) compared with SSC*Na-A (9.1 % (w/w)) indicating carry-over of thiosulfate from synthesis into the final product leading to SSC*Na. Differences in thiosulfate concentrations were

determined in both SSC*Na batches being possibly related to lot-to-lot-inconsistencies due to synthesis or process variations at Bachem AG.

5.4.2. Internally synthesized SSC*Na research batches

As shown in table 6, all internally synthesized SSC*Na research batches showed higher purities compared with the purchased SSC*Na batches. Highest purity of all internal SSC*Na batches was measured for SSC*Na-I and SSC*Na-G (99.6 % (w/w)) followed by SSC*Na-F (98.5 % (w/w)), SSC*Na-H (96 % (w/w)), SSC*Na-C and SSC*Na-D (91.3 % (w/w)) compared with SSC*Na-E (88.2 % (w/w)) indicating more efficient synthesis routes or purification processes inhouse. The majority of the synthesized SSC*Na batches showed higher copper concentrations compared with the purchased batches. Highest copper concentrations were determined in SSC*Na-E (800 µg/g) followed by SSC*Na-D (600 µg/g), SSC*Na-H (460 µg/g), SSC*Na-C (280 µg/g), SSC*Na-F (60 µg/g), SSC*Na-I (2 µg/g) and SSC*Na-G (< 0.2 µg/g) indicating differences in residual copper concentration in the final product due to optimization of inhouse synthesis and process purification. No L-cystine was determined in batch SSC*Na-C. L-cystine concentrations below the limit of quantification (LOQ < 0.2 % (w/w)) were detected in batches SSC*Na-F, SSC*Na-G and SSC*Na-I. Highest L-cystine concentrations were measured in SSC*Na-D (2.2 % (w/w)), followed by SSC*Na-E (2 % (w/w)) and SSC*Na-H (0.5 % (w/w)) indicating L-cystine carry-overs resulting from internal synthesis routes and raw materials. Similar sulfate concentrations were determined for SSC*Na-D (2.7 % (w/w)), SSC*Na-E (2.6 % (w/w)) and SSC*Na-H (2.8 % (w/w)) while low concentrations were found in batches SSC*Na-F (0.2 % (w/w)), SSC*Na-G and SSC*Na-I (< 0.2 % (w/w)). SSC*Na-C showed sulfate concentrations in the range of 2 to 8 % (w/w). These data represent slightly higher sulfate contaminations for SSC*Na batches C, D, E, H compared with externally synthesized SSC*Na batches A and B and negligible sulfate carry-overs for the internal SSC*Na batches F, G and I. These data indicate possible optimization steps in the purification process may be reflected in SSC*Na batch dependent sulfate carry-overs and final, residual sulfate concentrations. Thiosulfate was not measured in SSC*Na batches C and H while no thiosulfate was quantified in the internally synthesized SSC*Na indicating thiosulfate absence in internal SSC*Na syntheses and raw materials.

All herein presented SSC*Na batches show in sum no total recovery of 100 % indicating that losses in detection may be related to not quantified substances or to insufficient characterization methods since applied measuring methods were not double checked with different techniques.

Table 6: Different SSC*Na batches synthesized from different methods showing purities and all contaminations coming from syntheses.

Purity and impurities (copper, sulfate, thiosulfate, L-cystine) are listed. Purity was determined using NMR, copper was quantified using ICP-HR-MS (LOQ < 0.1 µg/g). Sulfate (LOQ < 0.2 % (w/w)), thiosulfate (LOQ < 0.3 % (w/w)) and L-cystine (LOQ < 0.2 % (w/w)) were quantified using CE.

SSC batch	Synthesis route	Purity of S-sulfocysteine variant in % (w/w)	[Cu] in µg/g	[Cystine] in % (w/w)	[Sulfate] in % (w/w)	[Thiosulfate] in % (w/w)
SSC*Na-A	Bachem AG (external)	81.3	0.3	0	1.8	9.1
SSC*Na-B	Bachem AG (external)	85.3	0.4	0	1.3	12.8
SSC*Na-C	Merck KGaA (inhouse)	91.3	280	Not measured	2-8	Not measured
SSC*Na-D	Merck KGaA (inhouse)	91.3	600	2.2	2.7	0
SSC*Na-E	Merck KGaA (inhouse)	88.2	800	2	2.6	0
SSC*Na-F	Merck KGaA (inhouse)	98.5	60	Not quantified	0.2	0
SSC*Na-G	Merck KGaA (inhouse)	99.6	Not quantified	Not quantified	Not quantified	0
SSC*Na-H	Merck KGaA (inhouse)	96	460	0.5	2.8	Not measured
SSC*Na-I	Merck KGaA (inhouse)	99.6	2	Not quantified	Not quantified	0

In conclusion, the differences in production methods of the different SSC*Na batches were reflected in their contaminations coming from their particular syntheses routes. Since the externally produced batches relied on the conversion of L-cysteine with sodium tetrathionate yielding SSC*Na, thiosulfate was only present in the externally produced SSC*Na batches. Internally produced synthesis products relied on the reaction of L-cystine with sodium sulfite catalysed by copper yielding SSC*Na. Consequently, higher copper, L-cystine and sulfate concentrations were determined in the internally produced SSC*Na batches.

5.5. Replacement strategy

5.5.1. L-cysteine replacement by SSC*Na-A in batch mode

As previously shown, SSC*Na was shown to be stable over three months in chemically defined complex, neutral pH feed.

In the following experiments, L-CysHCl*H_2O was replaced by SSC*Na in batch mode using clone 1 to determine if SSC*Na might be used as a L-cysteine source.

5.5.1.1. Viable cell densities and viabilities

As shown in figure 32 A, 1.5 mM SSC*Na-A showed similar growth and similar maximum VCD on day 6 of culture (143 +/- 2*10^5 C/mL) compared with control (156 +/- 2 *10^5 C/mL) indicating the use of SSC*Na-A as L-cysteine source for cell growth comparable to control. No cell growth was observed when cells were cultivated in a L-cysteine-free medium (data not shown). Lowered and delayed maximum VCD on day 7 of culture (122 +/- 4*10^5 C/mL) was observed with 3 mM SSC*Na-A indicating temporally impaired cell growth in a SSC*Na-A concentration dependency. Reduced cell growth was observed with 6 mM SSC*Na-A. Maximum VCD was reached on day 5 of culture (51 +/- 1*10^5 C/mL) followed by rapid cell death indicating SSC*Na-A concentration dependent toxicity.

As shown in figure 32 B, on day 7 of culture, when VCD were similar in control and 1.5 mM SSC*Na-A, prolonged high viability was observed in 1.5 mM SSC*Na-A (94 +/- 0.2 %) compared with control (41 +/- 1.7 %) indicating improved cellular viability in 1.5 mM SSC*Na-A. Since the cells grew more slowly in 3 mM SSC*Na-A, their viability on day 7 was similarly high (97 +/- 0.1 %) compared with 1.5 mM SSC*Na-A. A rapid drop in cellular viability from day 5 (97 +/- 0.3 %) to day 6 (0.2 +/- 0.1 %) in 6 mM SSC*Na-A was observed indicating toxicity of 6 mM SSC*Na-A.

5.5.1.2. Spent media analysis - SSC*Na quantification

As shown in 32 C, SSC*Na-A concentration in the cell culture supernatants over time was quantified. Decreasing SSC*Na-A concentration in all derivative conditions were observed over the whole culture period indicating the use of SSC*Na-A as a L-cysteine source. On day 5 and 6 of culture, 42 % and 90 % of SSC*Na-A were consumed in the 1.5 mM SSC*Na-A, respectively, indicating an intense use of the L-cysteine derivative between these days.

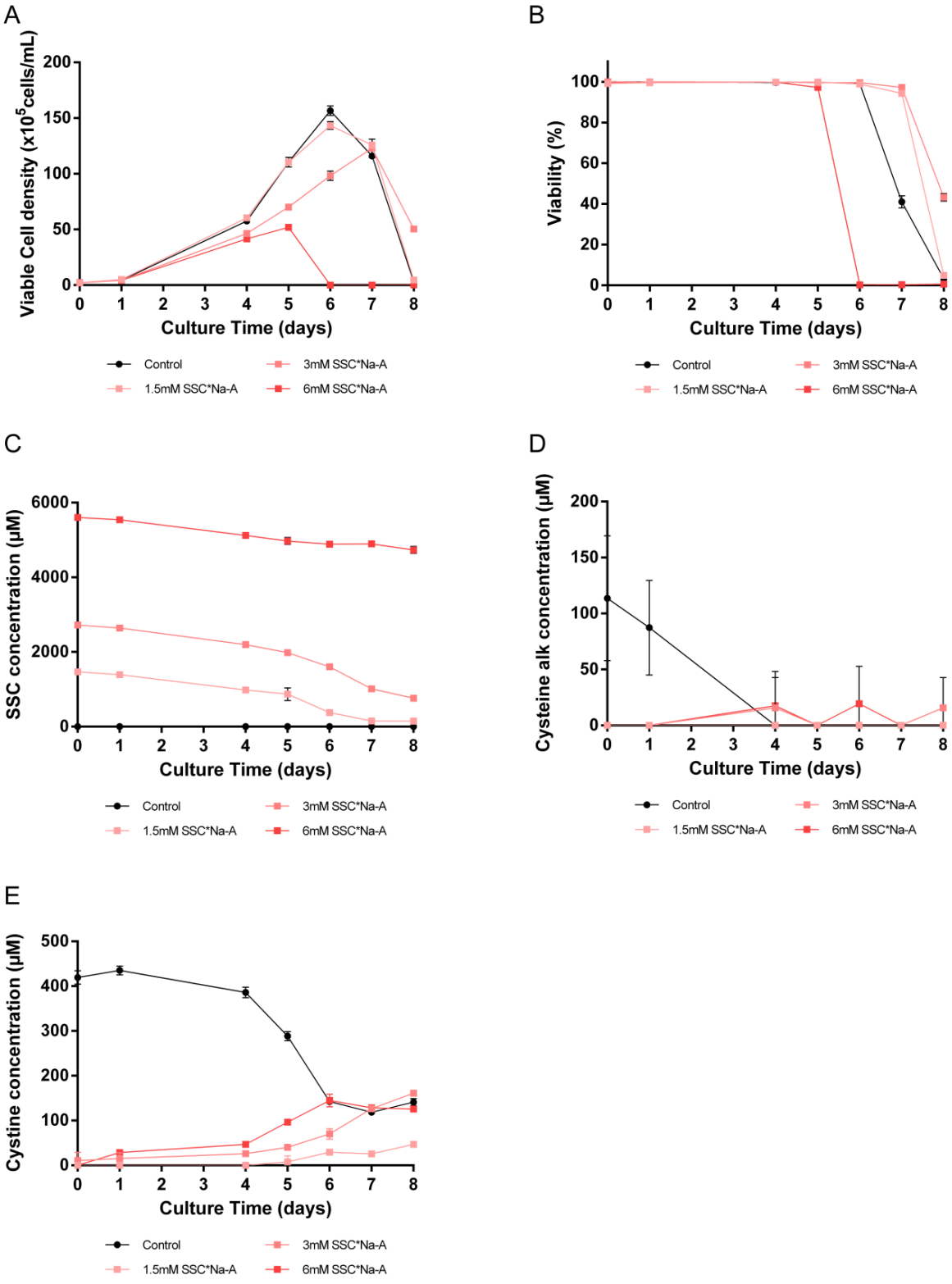

Figure 32: L-cysteine replacement by dose response of SSC*Na-A in L-cysteine deficient medium using spin tube batch processes with clone 1.

1.5, 3 and 6 mM SSC*Na were added to a L-cysteine depleted Cellvento^{TM} CHO-220 and the performance was compared to the medium supplemented with 1.5 mM L-CysHCl*H_2O (n=3). Suspension CHO clone 1 cells were seeded at 2*10^5 C/mL, incubated at 37 °C, 5 % CO_2, 80 % humidity and agitated at 320 rpm. (A) VCD. (B) Cellular viability. (C) SSC concentration in the supernatant (µM) measured by UPLC after IAM treatment and AccQ•Tag derivatization. (D) L-cysteine concentration in the supernatant (µM) measured by UPLC after IAM treatment and AccQ•Tag derivatization. (E) L-cystine concentration in the supernatant (µM) measured by UPLC after IAM treatment and AccQ•Tag derivatization. Mann-Whitney test of AUC (Area under the curve) was performed ($p < 0.05$). Values are means +/- SEM.

5.5.1.3. Spent media analysis - L-cysteine quantification

As shown in figure 32 D, lower starting concentration of L-cysteine (113.6 +/- 32.2 µM) compared with the theoretical concentration of 1.5 mM was detected in the control indicating possible reactions of L-cysteine with other media components and partial oxidation into L-cystine after media preparation.

No free L-cysteine was detected over the whole culture period in 1.5 mM SSC*Na-A condition. In the conditions 3 mM and 6 mM SSC*Na-A, free L-cysteine concentrations were detected over the whole time in several replicates but they were too close to the LOD making L-cysteine not quantifiable.

These data possibly indicate that SSC*Na-A was used as a L-cysteine source for growth.

5.5.1.4. Spent media analysis - L-cystine quantifcation

As shown in figure 32 E, L-cystine was present in the control condition (419.3 +/- 8.7 µM) from the beginning of the culture representing 28 % of the initial L-cysteine concentration in the medium. Since the control medium was free from L-cystine and only supplemented with 1.5 mM L-CysHCl*H_2O, these data indicate that L-cysteine was partially converted into L-cystine in liquid media after media preparation. Over the whole culture time, a steady decrease of L-cystine concentration was observed in the control condition. When all L-cysteine was consumed, increased L-cystine use started to take place beginning from day 4 indicating L-cystine as a possible source for L-cysteine in cellular metabolism. In all SSC*Na-A conditions, an increase in L-cystine concentration was observed in a SSC*Na-A concentration dependency over the whole culture time indicating possible cellular metabolic transformation of SSC*Na-A and partial release of L-cystine.

In conclusion, SSC*Na-A was able to replace L-cysteine in CHO suspension clone 1 batch cultures. In a concentration of 1.5 mM, cells cultured in SSC*Na-A showed similar growth and slightly prolonged viability compared with cells cultured in L-cysteine. SSC*Na-A was shown to be used as a L-cysteine source. As a consequence from these data, 1.5 mM was determined to be the optimal SSC*Na-A concentration with clone 1.

5.6. Application of single feed strategy in spin tube fed-batch processes using SSC*Na-A and PTyr2Na$^+$ with clone 2

To evaluate if the reported effects for CHO suspension clone 1 were reproducible with a different clone, the effects on growth, IgG production and metabolites were determined in fed-batch processes. Since the produced titer was determined to be the criterion for the choice of an optimal SSC*Na concentration, the high antibody producer CHO suspension clone 2 was used. To evaluate an optimal SSC*Na-A concentration for clone 2, different concentrations of SSC*Na-A were tested. As previously mentioned, fed-batch media in control and SSC*Na-A conditions were both supplemented with 1.5 mM L-CysHCl*H_2O to ensure cellular requirements for initial growth between days 0 and 3 of culture. With feedings starting from day 3, different SSC*Na-A concentrations were integrated with PTyr2Na$^+$ in the single feed of test conditions while L-cysteine and L-tyrosine were kept in an alkaline, separate feed in the control (two feed strategy).

5.6.1. VCD

As shown in figure 33 A, similar growth of all tested SSC*Na-A concentrations was observed until day 6 of culture compared with control. Starting from day 6, similar growth profiles for 2.5 mM SSC*Na-A and control were observed. Prolonged growth of 5, 10 and 15 mM SSC*Na-A compared with control condition was observed. Significant higher final VCD were detected in 5 mM (64 +/- 1*10^5 C/mL), 10 mM (88 +/- 3*10^5 C/mL), and 15 mM (83 +/- 4*10^5 C/mL) compared with control (23 +/-1*10^5 C/mL) indicating beneficial effects of SSC*Na-A concentrations ≥ 5 mM on VCD. Rapid cell death occurred with 20 mM SSC*Na-A from day 7 (84 +/- 2*10^5 C/mL) to day 10 (0.8 +/- 0.2 *10^5 C/mL) indicating toxicity of 20 mM SSC*Na-A on cell growth.

5.6.2. Viabilities

As shown in figure 33 B, similar viabilities of all conditions were observed until day 7. Starting from day 7, similar viability profiles were observed for 2.5 mM SSC*Na-A and control. Significant higher final viabilities of 5 mM (39 +/- 0.8 %), 10 mM (53 +/- 1.3 %) and 15 mM (49.8 +/- 2.3 %) SSC*Na-A were measured compared with control (12.9 +/- 0.8 %) representing prolonged growth indicating beneficial effects of SSC*Na-A concentrations ≥ 5 mM on cellular state in a SSC*Na-A concentration dependency. Rapid decrease in viability leading to cell death was observed with 20 mM starting from day 10 (0.85 +/- 0.15 %) indicating toxic effects of SSC*Na-A on cell viability.

5.6.3. Spent media analysis - IgG concentration

As shown in figure 33 C, similar IgG production was observed in all conditions until day 7. Since cells died in 20 mM SSC*Na-A from day 7 to 10, no further antibody production starting from day 10 was detected in this condition. Similar antibody production profiles of 2.5 mM SSC*Na-A and control were observed. Starting from day 10, cultivated cells in all SSC*Na-A conditions ≥ 5 mM produced overall higher IgG levels compared with the control. Higher final antibody concentrations were detected in 5 mM (1390 +/- 38 mg/L), 10 mM (1385 +/- 61 mg/L) and 15 mM (1265 +/- 45 mg/L) SSC*Na-A compared with control (1026 +/- 11 mg/L) indicating beneficial effects of improved cellular state on antibody production.

5.6.4. Spent media analysis - NH_3 concentration

As shown in figure 33 D, similar NH_3 production was observed in all conditions until day 5 of culture. Starting from day 6, all SSC*Na-A conditions showed overall increasing NH_3 concentrations in a SSC*Na-A concentration dependency compared with control. In this SSC*Na-A concentration dependency, highest final NH_3 concentrations were detected with 15 mM SSC*Na-A (7.2 +/- 0.2 mM), followed by 10 mM SSC*Na-A (5.7 +/- 0.2 mM), 5 mM SSC*Na-A (3.9 +/- 0.2 mM) and 2.5 mM SSC*Na-A (5.1 +/- 0.1 mM) compared with control (3.82 +/- 0.1 mM). These data indicate possibly increased cellular metabolic NH_3 production or breakdown of nitrogen containing compounds such as amino acids, vitamins or supplements in SSC*Na-A application.

5.6.5. Spent media analysis - Vitamin B12 concentration

As shown in figure 33 E, similar increasing vitamin B12 profiles in all conditions were observed until day 5 of culture due to feedings. Starting from day 6, vitamin B12 decrease in all SSC*Na-A conditions was observed compared with control. Final vitamin B12 concentration was highest for control compared with 1.2 fold for 2.5 mM and 5 mM, 1.6 fold for 10 mM and 3.2 fold for 15 mM SSC*Na-A reduced vitamin B12 levels representing an inverse SSC*Na-A concentration dependency of vitamin B12 levels detected in the supernatants. These data possibly indicate interactions of SSC*Na-A with vitamin B12 or boosted vitamin B12 dependent metabolic pathways such as purine and pyrimidine synthesis.

5.6.6. Spent media analysis - SSC*Na quantification

As shown in figure 33 F, similar low concentrations of SSC*Na-A was observed in all SSC*Na-A conditions until day 5 of culture. Starting from day 6, overall increases in SSC*Na-A concentration were detected in all SSC*Na-A conditions in a SSC*Na-A concentration dependency.

Final SSC*Na-A concentrations were measured with 15 mM SSC*Na-A (803.2 +/- 96 µM), 10 mM SSC*Na-A (270.3 +/- 18.5 µM), and SSC*Na-A limitations in 5 and 2.5 mM SSC*Na-A. Decreases in SSC*Na-A concentration especially after feedings was observed in 5, 10 and 15 mM SSC*Na-A indicating cellular consumption of SSC*Na-A.

5.6.7. Spent media analysis - L-cysteine quantification

As shown in figure 33 G, similar low concentrations of L-cysteine were measured in all tested conditions since the medium contained 1.5 mM L-CysHCl*H_2O ensuring initial cell growth. The measured L-cysteine concentrations of control (102.7 +/- 0.7 µM) and 2.5 mM SSC*Na-A (109.7 +/- 6.3 µM), 5 mM SSC*Na-A (136.3 +/- 30.8 µM), 10 mM SSC*Na-A (101.0 +/- 0.6 µM), 15 mM SSC*Na-A (103.7 +/- 0.9 µM) and 20 mM SSC*Na-A (101.3 +/- 1.2 µM) were similar to each other but lower as the theoretical starting concentration indicating partial dimerisation of L-cysteine into L-cystine and reactions of L-cysteine with other media components. Between day 0 and 3 similarly decreasing L-cysteine concentrations were observed in all conditions leading to L-cysteine limitation starting from day 3.

5.6.8. Spent media analysis - L-cystine concentration

As shown in figure 33 H, similar L-cystine starting concentrations were measured in all test conditions indicating partial dimerisation of medium L-cysteine into L-cystine. Until day 3 of culture, no change in L-cystine concentration was observed in all conditions indicating first the use of L-cysteine in the medium. With the first feeding on day 3, separately fed L-cysteine led to increasing L-cystine concentrations in the control indicating L-cystine generation from fed L-cysteine. After L-cysteine feedings, consumption of L-cystine was observed in the control condition until day 10.

Between 2.5 and 15 mM SSC*Na-A, similar and overall decreasing L-cystine concentrations were observed until reaching maximum VCD on day 7 of culture indicating use of L-cystine for cell growth in this period. After feedings of SSC*Na-A, no increases in L-cystine concentrations were observed until day 7 possibly indicating no extracellular L-cystine formation out of SSC or the L-cystine generated by SSC*Na was directly uses by the cells. Final L-cystine concentrations in 15 mM SSC*Na-A (200.3 +/- 3.5 µM), 10 mM SSC*Na-A (116 +/- 5.7 µM), 5 mM SSC*Na-A (7 +/- 7 µM) and in 2.5 mM SSC*Na-A were lower or limited compared with control (275.3 +/- 8.2 µM) indicating direct cellular use of the L-cystine generated by SSC*Na in a SSC*Na-A concentration dependency.

5.6.9. Spent media analysis - L-alanine quantification

As shown in figure 33 I, similar increasing concentrations of L-alanine in the supernatants were observed for all conditions until day 5 of culture.

Starting from day 6, overall increase in L-alanine concentration was observed in the control condition indicating export of L-alanine over the whole cultivation period. Increasing L-alanine concentrations were observed in SSC*Na-A conditions ≤ 10 mM starting from day 7 whereas no change in L-alanine concentration was observed for 15 mM SSC. Final decreased L-alanine concentrations were observed 1.37 fold for 5 mM, 1.87 fold for 10 mM and 2.61 fold for 15 mM SSC*Na-A in an inverse SSC*Na-A concentration dependency compared with control. These data possibly indicate inhibition of metabolic L-alanine production pathways such as L-alanine production from pyruvate by increasing SSC*Na-A concentrations or reactions of SSC*Na-A with L-alanine.

5.6.10. Spent media analysis - Sulfate quantification

As shown in figure 33 J, similar increasing concentrations of sulfate in the supernatants were observed for all conditions over the whole culture time. Final increased sulfate concentrations of 1.28 fold for 5 mM, 1.54 fold for 10 mM and 1.66 fold for 15 mM SSC*Na-A in a SSC*Na-A concentration dependency were observed compared with control condition. Besides basal cellular sulfate export detected in the control, additionally sulfate was detected in all SSC*Na-A conditions indicating SSC breakdown and release of generated sulfate in a SSC*Na-A concentration dependency.

5.6.11. Spent media analysis - Thiosulfate quantification

As shown in figure 33 K, thiosulfate containing SSC*Na-A resulted in thiosulfate detection in all SSC*Na-A conditions. Increasing thiosulfate concentration were observed for all SSC*Na-A conditions in a SSC*Na-A concentration dependency over the whole cultivation phase. Since all SSC*Na-A conditions showed comparable VCD on day 6, thiosulfate concentrations in all SSC*Na-A conditions were compared to the theoretical thiosulfate concentration on that day. Lower thiosulfate concentrations were found in 10 mM (12 mg/L), 5 mM (7 mg/L) and 2.5 mM (3 mg/L) SSC*Na-A compared with the theoretical thiosulfate concentration (13.77 mg/L) indicating possible metabolism of thiosulfate by the cells or interaction of thiosulfate with other metabolites. Higher thiosulfate concentrations were found in 20 mM (26 mg/L) and in 15 mM (19 mg/L) SSC*Na-A compared with the theoretical thiosulfate concentration (13.77 mg/L) indicating export of thiosulfate by the cells in these SSC*Na-A conditions.

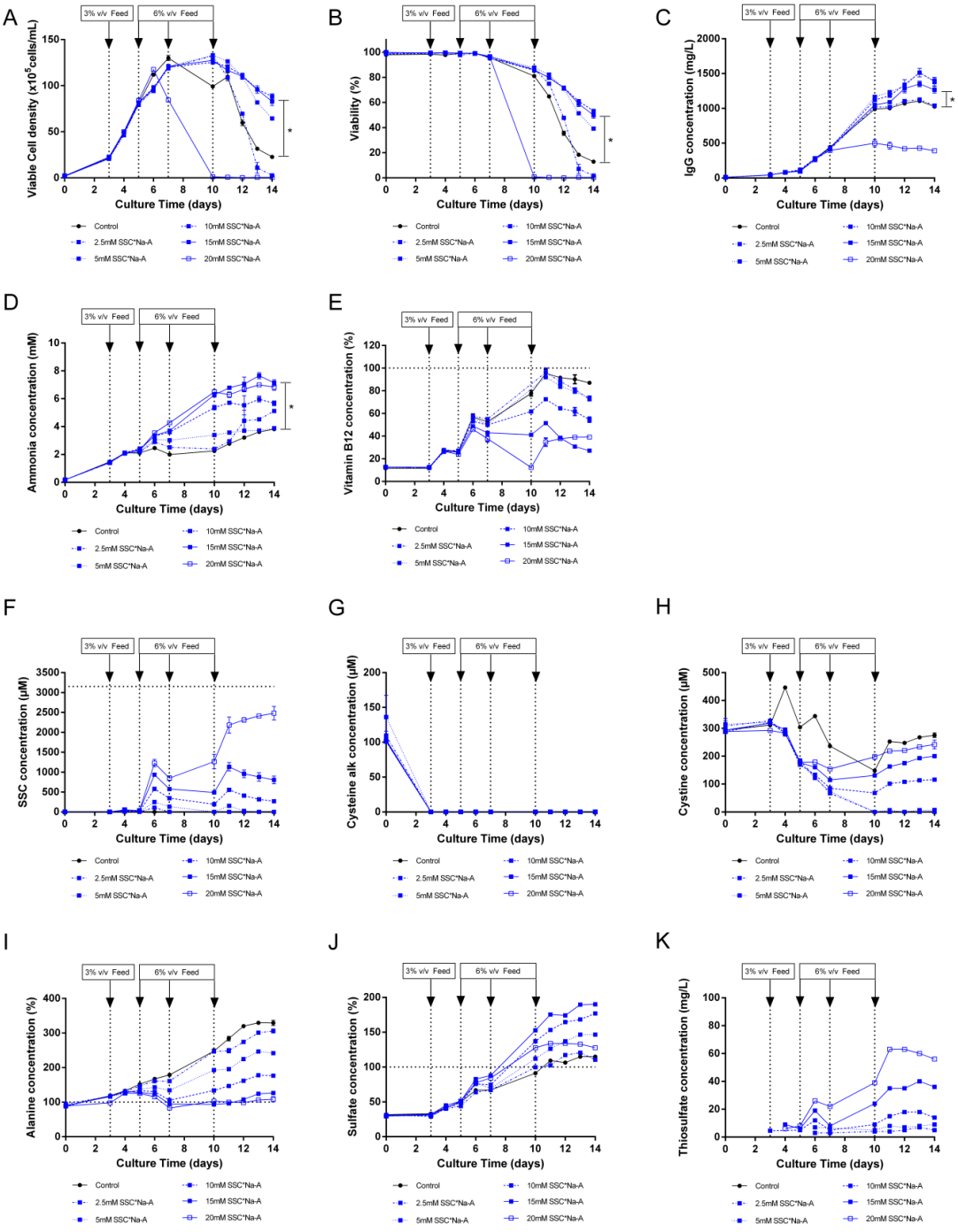

Figure 33: Spin tube fed-batch process with neutral pH feed containing SSC*Na-A using CHO suspension clone 2.

Different SSC*Na-A concentrations (2.5, 5, 10, 15 and 20 mM) were integrated in the main feed with 30 mM $PTyr2Na^+$ at neutral pH (single feed system). To ensure initial growth, medium containing 1.5 mM L-CysHCl*H_2O was used. In the control condition, L-cysteine was added separately in an alkaline feed (n=4). Suspension CHO clone 2 cells were seeded at $2*10^5$ C/mL, incubated at 37 °C, 5 % CO_2, 80 % humidity and agitated at 320 rpm. Feed was added at 3 % (v/v) at day 3 and 6 % (v/v) at days 5, 7 and 10. (A) VCD (B) Cellular viability (C) Produced IgG concentration (mg/L) in SSC*Na-A condition measured by a turbidometric method. (D) Produced NH_3 concentration (mM) in SSC*Na-A condition measured by photometry. (E) Normalized vitamin B12 concentration measured with UHPLC-MS/MS. (F) SSC concentration (µM) in the supernatant measured by UPLC after IAM treatment and AccQ•Tag derivatization. (G) Alkylated L-cysteine concentration (µM) in the supernatant measured by UPLC after IAM treatment and AccQ•Tag derivatization. (H) L-cystine concentration (µM) in the supernatant measured by UPLC after IAM treatment and AccQ•Tag derivatization. (I) Normalized L-alanine concentration in the supernatant measured by UPLC after IAM treatment and AccQ•Tag derivatization. (J) Normalized sulfate concentration in the supernatant measured by ion chromatography. (K) Thiosulfate concentration (mg/L) in the supernatant measured by ion chromatography. Mann-Whitney test of AUC was performed ($p < 0.05$). Values are means +/- SEM.

Between day 7 and 10, thiosulfate concentration increased from 22 mg/L on day 7 to 39 mg/L on day 10 in the 20 mM SSC*Na-A condition due to SSC*Na-A feeding. On day 10, higher thiosulfate concentration was monitored in 20 mM SSC*Na-A (39 mg/L) compared with the theoretical thiosulfate concentration (22.95 mg/L). Between days 7 and 10, rapid cell death was observed possibly indicating impacts of exported thiosulfate concentration on cell viability after overcoming a potential thiosulfate threshold concentration.

In conclusion, the application of the single-feed strategy integrating SSC*Na as a L-cysteine source and PTyr2Na^{+} as a L-tyrosine source was demonstrated in spin tube fed-batch processes. It was shown that application of 15 mM SSC*Na-A led to prolonged growth, viability and increased titers compared with the state-of-the-art fed-batch process (two feed strategy). SSC*Na-A was shown to be used as a L-cysteine source. In 20 mM SSC*Na-A, rapid cell death between days 7 and 10 was observed. As a consequence from these data, 15 mM was determined to be the optimal SSC*Na-A concentration with clone 2 in spin tube fed-batch processes.

5.7. Application of single feed strategy in bioreactor fed-batch processes using SSC*Na-A and PTyr2Na$^+$ with clone 2

To evaluate if the reported positive effects on growth and titer in the theoretic applied SSC*Na concentration of 15 mM were reproducible under controlled and regulated conditions, lab scale bioreactor experiments were carried out.

5.7.1. VCD, viabilities and IgG concentration

As shown in figure 34 A, similar growth and VCDs were observed until day 7 of culture for 15 mM SSC*Na-A and control. Lower maximum VCDs on day 9 of culture were observed for 15 mM SSC*Na-A (158.2 +/- 4.2*10^5 C/mL) compared with control (190.9 +/- 8.9*10^5 C/mL). No change in maximum VCDs was observed in both conditions until day 12 of culture. Starting from day 13, the control started to die while VCD in 15 mM SSC*Na-A did not change until day 14 of culture. Until the end of culture, prolonged cell growth was observed in 15 mM SSC*Na-A compared with control. Final VCDs were higher for 15 mM SSC*Na-A (74.4 +/- 7.4*10^5 C/mL) compared with control (32.2 +/- 2.2*10^5 C/mL) representing an increase of 2.3 fold for 15 mM SSC*Na-A compared with control. These data indicate that 15 mM SSC*Na-A may have had a beneficial effect on VCD by improving cell health.

As shown in figure 34 B, from day 13 on, the control started to die while cells cultivated in 15 mM SSC*Na-A showed prolonged viabilities. Final viabilities in 15 mM SSC*Na-A were higher (50.8 +/- 4.3 %) compared with control (17.1 +/- 0.4 %) representing an increase of 3 fold for 15 mM SSC*Na-A compared with control. These data supported the above presented prolonged growth in 15 mM SSC*Na-A compared with control possibly indicating beneficial effects of 15 mM SSC*Na-A on viability by improving cell health.

As shown in figure 34 C, until day 11 of culture, similar IgG concentrations were observed for 15 mM SSC*Na-A and control. Starting from day 12, strongly increasing IgG concentrations were detected with 15 mM SSC*Na-A compared with control. Significantly higher final titers were detected in 15 mM SSC*Na-A (3413 +/- 76.2 mg/L) compared with control (1913.5 +/- 18.5 mg/L) representing an increase of 1.8 fold. These data may indicate that the specific productivity was increased in 15 mM SSC*Na-A or possible beneficial effects on cell health related to impurity profiles were responsible for increased titers.

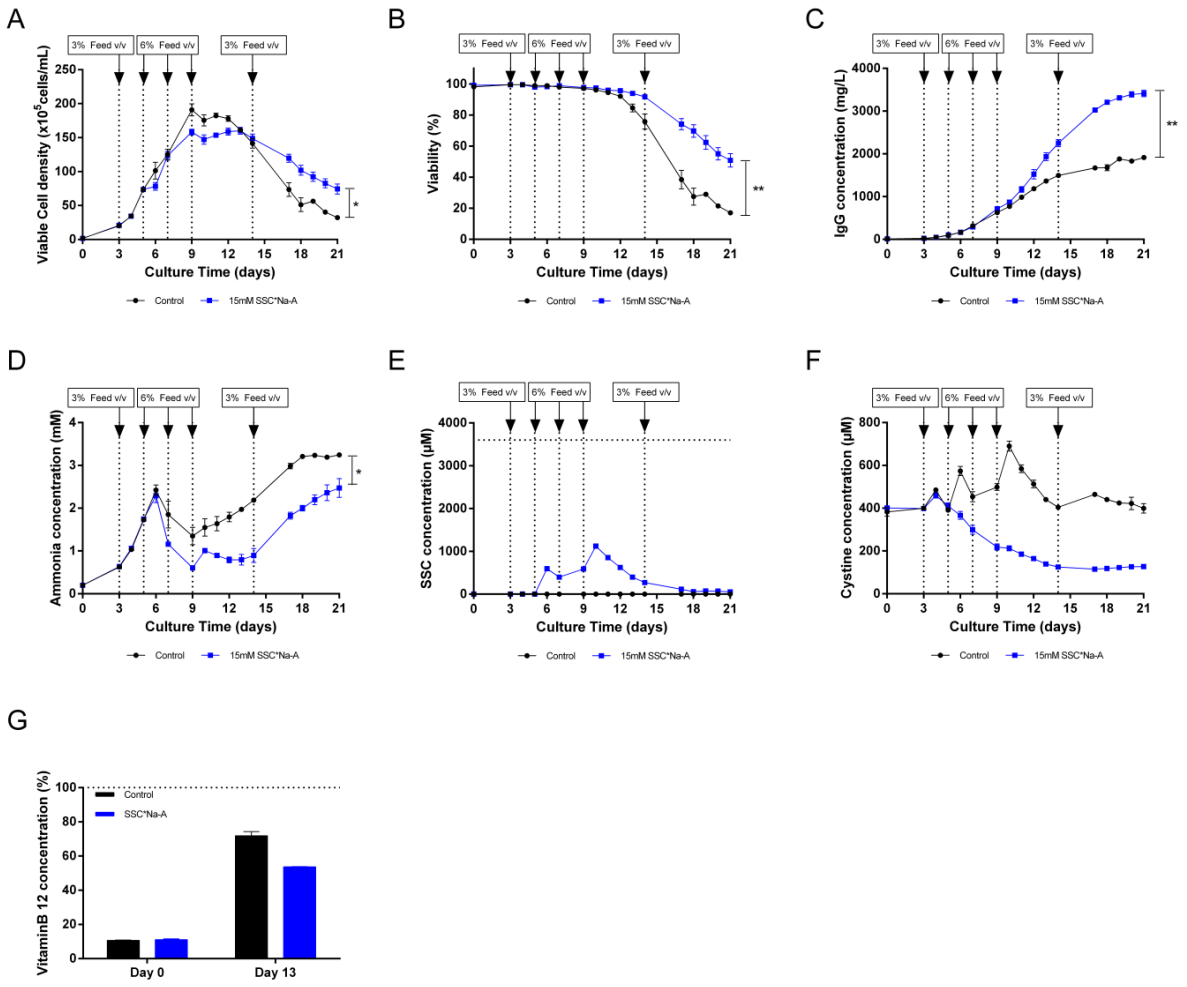

Figure 34: Bioreactor fed-batch experiment with neutral pH feed containing SSC*Na-A using CHO suspension clone 2.

15 mM SSC*Na-A was integrated in the main feed with 30 mM PTyr2Na$^+$ at neutral pH (single feed system). To ensure initial growth, medium containing 1.5 mM L-CysHCl*H_2O was used. In the control condition, L-cysteine was added separately in an alkaline feed (n=5). Suspension CHO clone 2 cells were seeded at 2*10^5 C/mL. Feed was added at 3 % (v/v) at day 3 and 6 % (v/v) at days 5, 7, 9 and 14. (A) VCD. (B) Cellular viability. (C) IgG concentration over time in the supernatants measured by turbidometric method. (D) NH_3 concentration in the supernatants measured by photometry. (E) SSC concentration over time in the supernatants measured by UPLC after IAM treatment and AccQ•Tag derivatization. (F) L-cystine concentration in the supernatants measured by UPLC after IAM treatment and AccQ•Tag derivatization. (G) Normalized vitamin B12 concentration in the supernatants measured with UHPLC-MS/MS. Mann-Whitney test of AUC was performed ($p < 0.05$). Values are means +/- SEM.

5.7.2. Spent media analysis - NH_3 quantification

As shown in figure 34 D, similar increases in NH_3 production were observed until day 6 in 15 mM SSC*Na-A and control. Between day 6 and 9 of culture, NH_3 concentration decreased in both conditions.

From day 9 until the end of culture, strongly increasing NH_3 concentrations were detected in the control. Starting from day 15, NH_3 concentrations started to increase in SSC*Na-A. Final lower NH_3 concentrations were detected in SSC*Na-A (2.5 +/- 0.2 mM) compared with control (3.2 +/- 0.1 mM).

These results were in contrast with results obtained from spin tube experiments indicating impacts of the controlled and regulated system on NH_3 production in both conditions.

5.7.3. Spent media analysis - SSC*Na, L-cystine and vitamin B12 quantification

As shown in figure 34 E, free SSC*Na-A concentrations in the supernatants started to be detected starting from day 6 of culture. After feedings on days 5, 7 and 9, increases in SSC*Na-A concentrations were detected on days 6, 9 and 10. The detected SSC*Na concentration on days 6, 9 and 10 represented decreases of 56 %, 73.9 % and 72.8 % of the theoretical SSC*Na-concentrations on these days. These data supported the observations made in spin tube experiments and possibly indicated SSC*Na-A consumption or reaction with other metabolites.

As shown in figure 34 F, L-cystine was present in both conditions from the beginning of the culture since both media contained 1.5 mM L-CysHCl*H_2O ensuring initial cell growth indicating partial oxidation of L-cysteine into L-cystine supporting the observations from spin tube fed-batch processes. Over the whole culture time, decreasing L-cystine concentrations were observed in the SSC*Na-A condition compared with control possibly indicating cellular use of L-cystine for cell growth and metabolism. In the control condition, increasing L-cysteine concentrations were observed on day 6, 9, 10 and 17 due to L-cysteine feedings. Final lower L-cystine concentrations were detected in the SSC*Na-A condition (127.2 +/- 7.7 µM) compared with the control (399 +/- 22 µM) representing a 3.1 fold decrease in L-cystine concentration compared with control. These data supported the observations made in spin tube experiments.

As shown in figure 34 G, similar starting concentrations of vitamin B12 were detected in the control (10.7 +/- 0.2 %) and in the SSC*Na-A condition (11.1 +/- 0.5 %). On day 13 of culture, when both conditions showed similar VCDs, lowered free vitamin B12 concentration was observed in the SSC*Na-A condition (53.7 +/- 0.2 µM) compared with control (71.9 +/- 2.4 %) representing a decrease of 25 % in vitamin B12 concentration compared with control. These data indicate possible interactions of SSC*Na-A with vitamin B12 or boosted vitamin B12 dependent metabolic pathways such as purine and pyrimidine synthesis. These data supported the observations made in spin tube experiments.

In conclusion, the application of the single-feed strategy integrating SSC*Na as a L-cysteine source and PTyr2Na^{+} as a L-tyrosine source was demonstrated in lab scale bioreactor fed-batch processes. The data obtained in bioreactors supported the findings made in spin tube fed-batch experiments. The application of 15 mM SSC*Na-A led to prolonged growth, viability and significantly increased titers compared with the state-of-the-art fed-batch process (two feed strategy). SSC*Na-A was shown to be used as a L-cysteine source. As a consequence from these data, 15 mM SSC*Na-A was determined to be the optimal derivative concentration with clone 2 independent of the used scale.

5.8. Characterization of antibodies produced from bioreactor fed-batch processes using the single feed strategy with clone 2

To evaluate the impact of SSC*Na-A containing feeds on the mAb quality attributes, glycosylation and charge variants in antibodies produced from control (two feed strategy) and single feed strategy were compared with each other. Since viabilities needed to be high and similar for comparison, antibodies produced until day 12 were chosen. On day 12, similar viabilities were found in the control (92.1 +/- 1.2 %) and in the SSC*Na-A condition (95.6 +/- 0.4 %).

5.8.1. Charge variant distribution

As shown in figure 35 A, charge variant distribution of antibodies produced from control and 15 mM SSC*Na-A were determined. The main peak was slightly higher in antibodies produced from the control (68.5 +/- 0.5 %) compared with antibodies produced from the 15 mM SSC*Na-A condition (66 +/- 2 %). Both, acidic and basic forms were determined to be similar in the control (25.5 +/- 0.5 % and 6 +/- 1 %, respectively) and in the SSC*Na-A condition (27.5 +/- 1.5 % and 6.5 +/- 0.5 %).

5.8.2. N-glycosylation pattern

As shown in figure 35 B, the N-glycosylation pattern of antibodies produced from control and 15 mM SSC*Na-A were determined. For the minor form GlcNAc3Man3Fuc, similar data were obtained in the control (3.7 +/- 0.01 %) and for the SSC*Na-A condition (3.8 +/- 0.3 %). Regarding the second minor form G2F/Man6, similar data were obtained for control (1.2 +/- 0.04 %) and for SSC*Na-A (1.3 +/- 0.01 %). For the third minor form Man5, similar data were obtained in the control (4.6 +/- 0.1 %) and for the SSC*Na-A condition (6.3 +/- 0.1 %). Regarding the fourth minor form Man7, similar data were obtained in the control (2.9 +/- 0.3 %) and for the SSC*Na-A condition (3.9 +/- 0.9 %).

The main glycoforms G0F and G1F varied slightly between antibodies produced from both conditions. Slightly higher data were obtained for G0F in the control (61.4 +/- 1.4 %) compared with SSC*Na-A (55.6 +/- 3.5 %). Regarding G1F, slightly lower data were found for control (26.3 +/- 1.1 %) compared with SSC*Na-A (29.2 +/- 2.8 %). No significant changes were found in the main glycoforms G0F and G1F in antibodies produced from both conditions.

A

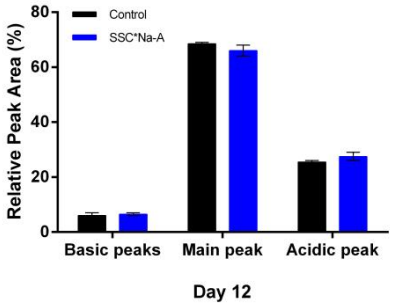

B

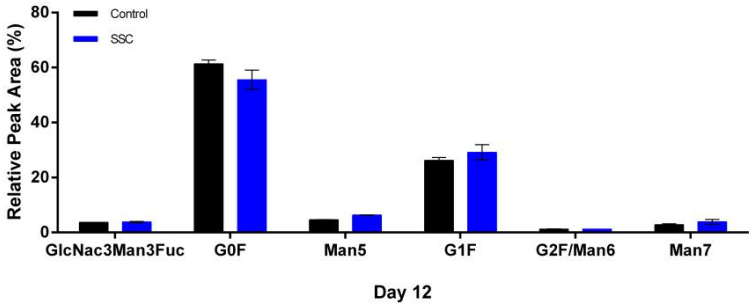

C

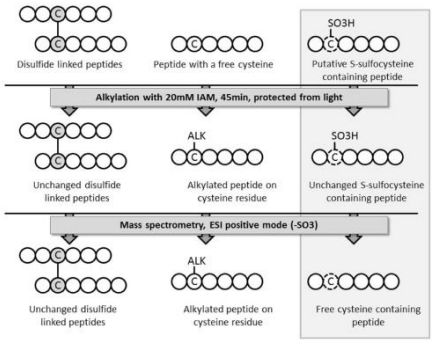

D

N°	Sequence of cysteine containing peptides	Control process $[M+H]^+$	Control process Alkylated peptide	SSC process $[M+H]^+$	SSC process Alkylated peptide
1	DYFPEPVTVSWNSGALTSGVHTFPAVLQSSGLYSLSSVVTVPSSSLG TQTYICNVNHKPSNTK	N.D.	N.D.	N.D.	N.D.
2	FSGSGSGTDFTLTISSLQAEDVAVYYCQQYYSYPFTFGQGTK	N.D.	N.D.	N.D.	N.D.
3	WQQGNVFSCSVMHEALHNHYTQK	N.D.	1.0	N.D.	2.1
4	THTCPPCPAPPVAGPSVFLFPPKPK	N.D.	N.D.	N.D.	N.D.
5	LSCAASGYSITAEYMNWVR	N.D.	N.D.	N.D.	0.1
6	TPEVTCVVVDVSHEDPEVK	0.3	1.75	0.2	2.95
7	VYACEVTHQGLSSPVTK	N.D.	N.D.	N.D.	N.D.
8	SGTASVVCLLNNFYPR	N.D.	N.D.	N.D.	0.1
9	STSGGTAALGCLVK	N.D.	0.15	N.D.	0.5
10	AEDTAVYYCAR	N.D.	0.45	N.D.	1
11	NQVSLTCLVK	N.D.	1.45	N.D.	3.1
12	ATINCK	N.D.	N.D.	N.D.	N.D.
13	SCDK	N.D.	N.D.	N.D.	N.D.
14	GEC	N.D.	N.D.	N.D.	N.D.
15	CK	N.D.	N.D.	N.D.	N.D.

Figure 35: Impact of SSC*Na-containing feed on key quality attributes charge variant distribution, N-glycosylation pattern and peptide mapping.

(A) N-glycosylation pattern determined using the 2-AB labeling method. (B) Charge variant distribution obtained using IEF. (C) Strategy used to detect putative SSC integration into the sequence of the mAb using a modified peptide mapping experiment and ESI positive mass spectrometry analysis. (D) Sequence analysis of L- cysteine containing peptides using a modified peptide mapping experiment and ESI positive mass spectrometry analysis.

5.8.3. SSC integration in the mAb sequence

To evaluate if the molecule SSC which contained $–SO_3H$ modification, might be integrated in the mAb sequence, peptide mapping experiments were performed. To develop the method for SSC with peptide mapping and ESI positive may spectrometry analysis, first a positive control needed to be used for the conception. Experiments with this positive control revealed that the sulfate moiety on the L-cysteine residue was released in source in electrospray positive ionization mode.

This observation confirmed results for tyrosine O-sulfation from literature (Önnerfjord et al. 2004; Salek et al. 2004). To overcome this technical limitation, a new sample preparation was developed based on a subtractive strategy being already used to determine the sites of tyrosine O-sulfation in proteins (Yu et al. 2007). As summarized in figure 35 C, first, tryptic peptides were produced from enzymatic digestion and analysis of SSC incorporation was carried out under non-reducing conditions. Non-reduced conditions and IAM treatment were used to alkylate only free L-cysteine residues. Intact disulfide bridges and peptides containing SSC residues were not modified by this procedure. An in source fragmentation of the sulfate moiety of putative SSC containing peptides leading to free L-cysteine containing peptides was carried out via mass spectrometry analysis of peptides in ESI positive mode. With this method, most of the L-cysteine containing peptides were found to be involved in disulfide bridges, whereas several L-cysteine containing peptides where found alkylated (e.g. free L-cysteine containing peptides in the mAb).

The relative intensities of these peptides were below 3.5 % when compared to the average of the 3 highest peptide intensities. To detect possible SSC containing peptides, extracted ion chromatograms were performed manually for all L-cysteine containing peptides. This procedure revealed one positive hit with a relative intensity below 0.5 % as shown in figure 35 D. This peptide was found in both conditions indicating that it may correspond to an endogenous S-sulfation, independent of the culture condition (see Hecklau et al. 2016).

In conclusion, no impacts on N-glycosylation pattern, charge variant nor mAb sequence were observed in conditions using SSC*Na-A as a L-cysteine source and $PTyr2Na^+$ as a L-tyrosine source in the single feed strategy compared with the established state-of-the-art (two feed strategy) fed-batch process. Consequently, SSC*Na-A may be used as a L-cysteine derivative to replace L-cysteine in feeds of fed-batch processes without the need for changing production processes.

5.9. Determination of mechanisms being responsible for positive effects of SSC*Na-A on cell culture performance

5.9.1. Spiking of SSC*Na-A to cell lysates

To determine if SSC*Na-A was consumed and metabolized by cellular enzymes, cell lysates were treated with SSC*Na-A and amino acid quantification was carried out.

As shown in figure 36, after quantification by UPLC, recovery of SSC alone in pure water was found to be 100 %. After addition of SSC*Na-A to clone 2 cell lysates, no free SSC and L-cystine were detected while free L-cysteine (28.6 %) was quantified. 71.4 % of the initial SSC*Na-A concentration applied was not detected as SSC, L-cysteine nor L-cystine. Since the total, initial concentration of SSC*Na-A was not detected after spiking of SSC*Na to cell lysates, these data might indicate enzymatic breakdown of SSC*Na.

Based on these observations, the participation of at least one enzyme was considered. Since the alkylating reagent IAM reacts with free L-cysteine residues, IAM was used to block free L-cysteine residues in the enzymes` active center to create dysfunctional enzymes. In this case, the recovered SSC*Na-A concentration would have been similar to the total, initial SSC*Na-A concentration.

As shown in figure 36, pre-treatment of clone 2 cell lysates with IAM and subsequent SSC*Na-A administration resulted in higher SSC recovery (96.4 %) and reduced L-cysteine recovery (1.8 %) compared with cell lysates not treated with IAM. These data possibly indicated the active enzymatic breakdown of SSC*Na-A by participation of enzymes containing L-cysteine residues in their active center.

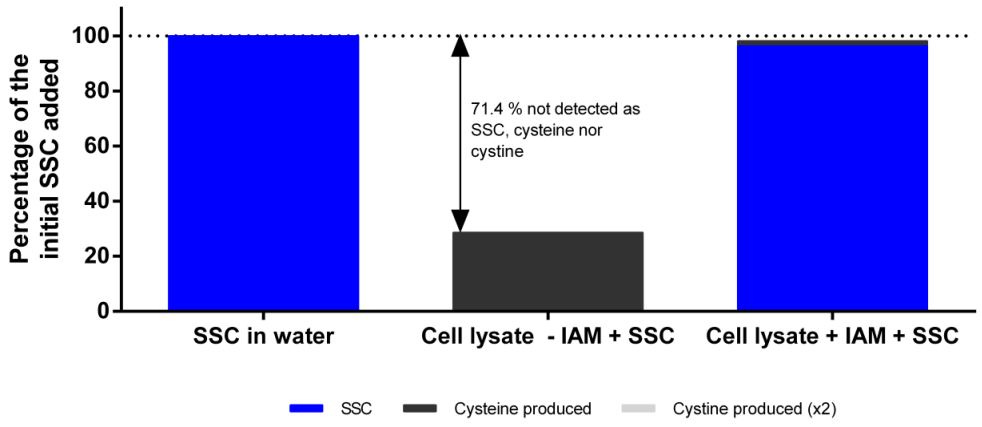

Figure 36: Cell lysate spiking with SSC*Na alone and pre-treatment of cell lysates with IAM followed by SSC*Na spiking.

Spiking of cell lysates with 1 mM SSC and subsequent quantification of SSC, L-cysteine and L-cystine via UPLC after iodoacetamide (IAM) treatment and AccQ•Tag derivatization. Values are shown as percentages of the initial applied SSC concentration.

5.9.2. Mechanism of SSC*Na function

Previous spiking of SSC*Na-A to not pre-treated cell lysates resulted in no recovery of SSC*Na-A possibly indicating SSC*Na-A cleavage or reactions of SSC*Na-A with intracellular components. Data from cell culture supernatants of fed-batch experiments showed neither L-cysteine, nor L-cystine detected at significant levels, whereas a dose dependent increase in sulfate was monitored indicating that SSC*Na-A was actively cleaved. This loss in SSC*Na-A recovery raised the question for interactions of SSC*NaA-A with other reaction partners. GSH as the major intracellular thiol was chosen for further interaction studies since it was intracellular ubiquitously present and highly concentrated.

5.9.2.1. Cell-free interaction studies

As the base for interaction studies of SSC and GSH, first their respective pH dependence needed to be determined to evaluate possible instabilities of both molecules and probable break down product formation. As follows, the controls for the cell-free interaction studies of SSC*Na and GSH were tested at different pH in water.

5.9.2.1.1. SSC*Na in water at different pH

To determine if SSC*Na was stable at different pH, the derivative was dissolved in water and the different pH were adjusted. Subsequently, UPLC analysis was carried out to monitor SSC recovery and possible formation of other metabolites.

As shown in figure 37 A, high recovery of SSC (98 %) was determined at acidic pH with concomitant detection of low amounts of L-cystine (2 %). No change in recovery of SSC (100 %) was observed at neutral pH and no generation of L-cysteine nor L-cystine was detected indicating stability of the derivative at neutral pH. At alkaline pH, 71.8 % SSC was recovered while concomitantly L-cystine (26.2 %) and L-cysteine (2 %) were detected. These data possibly indicated SSC*Na instability in an alkaline environment.

5.9.2.1.2. GSH in water at different pH

To determine if GSH was stable at different pH, the thiol was dissolved in water and the different pH were adjusted. Subsequently, UPLC analysis was carried out to monitor total GSH recovery and LC-HRMS/MS analysis was used to detect possible interaction products.

As shown in figure 37 B, 98.7 % GSH was recovered at acidic pH while concomitantly low amounts of GSSG (1.2 %) were detected. This trend was also observed at alkaline pH with slightly lower recovered amounts of GSH (95.2 %) and slightly higher amounts of GSSG (4.8 %).

At neutral pH, lowest GSH recovery (74.3 %) of the tested conditions was observed with highest GSSG detection (25.7 %). These data indicated possible instability of GSH at neutral pH accompanied by concomitant formation of GSSG.

5.9.2.1.3. Cell-free interaction of SSC*Na and GSH

Previously, stability of SSC*Na and GSH was each determined in water at different pH. Next, interaction of SSC*Na and GSH together at different pH was followed. Therefore, equal concentrations of SSC*Na and GSH were dissolved and mixed. Subsequently, UPLC analysis was carried out to monitor SSC, L-cysteine, L-cystine, GSH and interaction products.

As shown in figure 37 C, interactions of SSC*Na and GSH were detected at acidic, neutral and alkaline pH.

At acidic pH, molecules representing the L-cysteine moiety were determined to be SSC (95.8 %) and L-cysteine (1.3 %). No free L-cystine was detected. Molecules representing the GSH moiety were monitored to be GSH (82.3 %) and GSSG (6.6 %).The produced interaction product GS-Cys represented both moieties in similar concentrations (8.4 % and 6.1 %, respectively) while the interaction product sulfoglutathione (GS-SO_3) represented the GSH moiety with 2.6 %. These data indicated that interaction of SSC*Na and GSH in an acidic environment resulted in the formation of the mixed disulfides GS-Cys and GS-SO_3 based on thiol-disulfide exchange.

At neutral pH, molecules representing the L-cysteine moiety were determined to be SSC (53.4 %), L-cysteine (23 %), L-cystine (6.5 %). Molecules representing the GSH moiety were monitored to be GSH (43 %) and GSSG (22.9 %) with GSSG formation resulting from GSH instability at neutral pH as described previously. The produced interaction product GS-Cys represented both moieties in similar concentrations (15.3 % and 12.5 %, respectively) while the interaction product GS-SO_3 represented the GSH moiety with 22.3 %. These data indicated that interaction of SSC*Na and GSH led to mixed disulfides based on thiol-disulfide exchange in a neutral environment. At pH 7, 2 fold and 8.5 fold increased GS-Cys and GS-SO_3 levels, respectively, were detected compared with GS-Cys and GS-SO_3 levels obtained at acidic pH indicating pH-dependent GS-Cys formation.

At alkaline pH, molecules representing the L-cysteine moiety were determined to be SSC (6.1 %), L-cysteine (22.6 %) and L-cystine (30.9 %) with L-cystine formation being related to SSC*Na instability at alkaline pH.

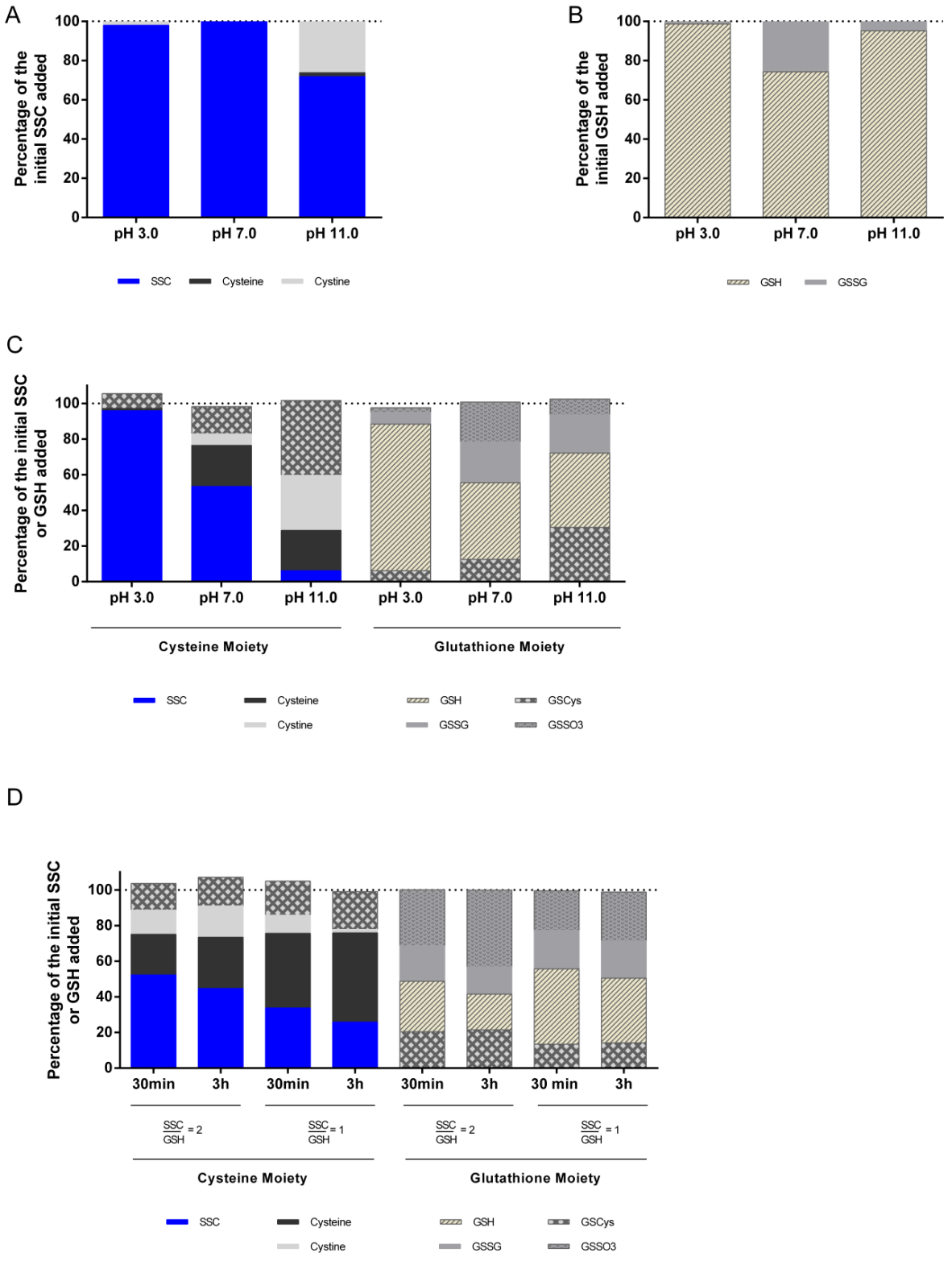

Figure 37: Cell-free interaction studies of SSC*Na and GSH at different pH alone and together.

(A) Stability of SSC at different pH in water and quantification of SSC, L-cysteine and L-cystine. (B) Stability of GSH at different pH in water and quantification of GSH and GSSG.(C) Interaction of SSC with GSH at different pH in water and quantification of SSC, GSH, L-cysteine, L-cystine and interaction products. (D) Interaction of different SSC/GSH ratios over time at neutral pH and quantification of SSC, GSH, L-cysteine, L-cystine and interaction products. Quantification was carried out using UPLC after IAM treatment and AccQ•Tag derivatization. Values are shown as percentages of the initial applied SSC or GSH concentration.

Although L-cysteine was previously shown to be produced from SSC*Na at pH 11, its increase is related to GSH-SSC*Na interaction. Molecules representing the GSH moiety were monitored to be GSH (41.6 %) and GSSG (21.5 %).

Although GSSG was previously shown to be produced from GSH at pH 11, its increase is related to GSH-SSC*Na interaction. The produced interaction product GS-Cys represented both moieties in similar concentrations (30.5 % and 42.1 %, respectively) while the interaction product GS-SO_3 represented the GSH moiety with 8.8 %. These data indicated that interaction of SSC*Na and GSH led to mixed disulfides based on thiol-disulfide exchange in an alkaline environment. At pH 13, 2.4 fold increased GS-Cys levels were detected compared with GS-Cys levels obtained at neutral pH indicating pH-dependent GS-Cys formation.These data indicated that interaction of SSC*Na and GSH led to mixed disulfides based on thiol-disulfide exchange in an alkaline environment. At pH 13, 2.4 fold increased GS-Cys levels were detected compared with GS-Cys levels obtained at neutral pH indicating pH-dependent GS-Cys formation.

Summarized, with increasing pH, increasing concentrations of the mixed disulfide GS-Cys were detected in interaction studies of SSC*Na and GSH. A second mixed disulfide (GS-SO_3) was monitored in all three tested environments with highest recovery at neutral pH. These data indicate cell-free interaction of SSC*Na and GSH generating mixed disulfide formation based on thiol-disulfide exchange.

5.9.2.1.4. Interaction of SSC*Na and GSH over time

Previously, interaction of equal SSC*Na and GSH concentration with each other was determined in water at different pH. To determine if different SSC*Na/GSH ratios and incubation times had an impact on interactions and product formation, two ratios and two incubation periods were chosen to be tested at neutral pH. Subsequently, UPLC analysis was carried out to monitor SSC, L-cysteine, L-cystine, GSH and interaction products.

As shown in figure 37 D, at higher SSC*Na/GSH ratios, increased incubation times resulted in a tendency of slightly decreased SSC (52.2 % and 44.7 %, respectively) and GSH concentrations (28.3 % and 20 %, respectively) while similar GS-Cys concentrations (20.4 % and 21.5 %, respectively) and slightly increased GS-SO_3 concentrations (31.5 % and 43 %) were observed by trend. Concomitantly, slightly increased L-cysteine (22.8 % and 28.7 %) and L-cystine levels (13.7 % and 17.6 %) were detected by trend.

At equal SSC*Na and GSH concentrations, increasing the incubation time from 30 minutes to 3 hours resulted in a tendency of slightly decreased SSC (33.7 % and 25.8 %, respectively) and GSH

(42.3 % and 36.3 %, respectively) concentrations while similar GS-Cys concentrations (13.4 % and 14.2 %, respectively) and slightly increased GS-SO_3 concentrations (22.2 % and 27.4 %) were observed by trend. Concomitantly, a tendency of slightly increased L-cysteine (41.9 % and 50.1 %) and decreased L-cystine levels (10.2 % and 1.9 %) were detected by trend.

These data possibly indicated that interaction product concentrations were similar after 30 minutes and 3 hours indicating rapid cell-free SSC-GSH interactions. Since higher GS-SO_3 levels were detected in conditions using lower GSH concentrations, the formation of mixed disulfides might have been dependent on the GSH concentration.

5.9.2.1.5. Interaction studies of SSC*Na and GSH with cell lysates

Previously, cell-free interaction of SSC and GSH was proven. This raised the question if consumption of the SSC-GSH mix, already containing mixed disulfides, by clone 2 lysates may be observed. Equal concentrations of SSC*Na and GSH were mixed at neutral pH without cells to generate mixed disulfides. Then, after different incubation times, cell lysates were added to the SSC-GSH reaction mix. Subsequently, UPLC and LC-HRMS/MS analysis were carried out to monitor SSC and GSH recovery and identification of possible interaction products.

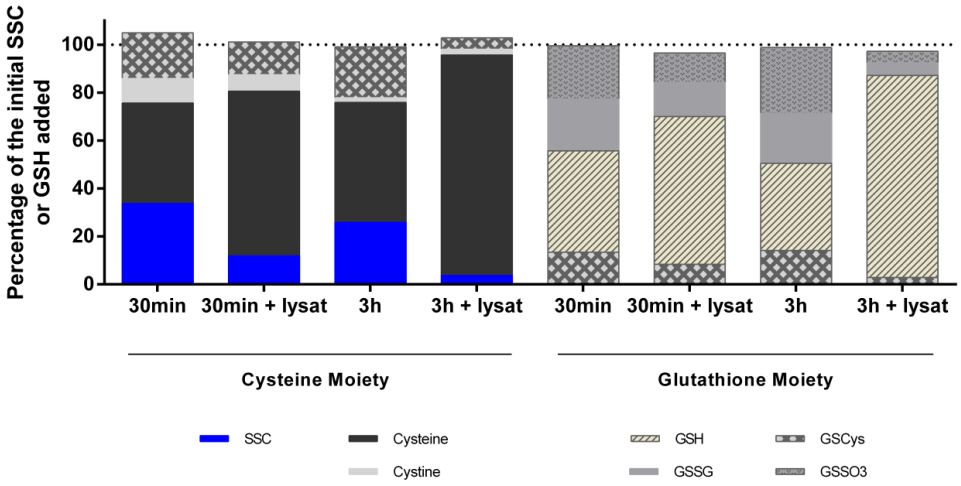

Figure 38: Fate of SSC in presence of GSH and after spiking with cell lysate.

Released products were quantified by UPLC after IAM treatment and AccQ•Tag derivatization. Identification of GS-Cys, GSH, GS-SO_3 and GSSG was confirmed by LC-MS/MS.

As shown in figure 38, after 30 minutes of incubation, 33.7 % SSC, 41.9 % L-cysteine and 10.2 % L-cystine were recovered representing the L-cysteine moiety. For molecules representing the GSH moiety, 42.3 % GSH, 21.6 % GSSG and 22.2 % GS-SO_3 were recovered.

Recovered GS-Cys represented both moieties in similar portions, 19.1 % and 13.4 %, respectively. Similar observations were found after 3 hours. After 3 hours of incubation, 25.8 % SSC, 50 % L-cysteine and 1.9 % L-cystine were recovered as molecules representing the L-cysteine moiety. For molecules representing the GSH moiety, 36.3 % GSH, 20.9 % GSSG and 27.4 % GS-SO_3 were recovered. Recovered GS-Cys represented both moieties in similar portions, 21.2 % and 14.2 %, respectively. These data supported the previously shown cell-free interaction of SSC and GSH after 30 minutes and 3 hours.

After addition of cell lysates, different incubation times showed different recoveries of the particular molecules. After 30 minutes, 11.9 % SSC, 68.6 % L-cysteine and 6.9 % L-cystine were recovered representing the L-cysteine moiety. For molecules representing the GSH moiety, 61.6 % GSH, 14.3 % GSSG and 22.2 % GS-SO_3 were recovered. Recovered GS-Cys represented both moieties at 13.7 % and 8.4 %, respectively. After 3 hours of incubation, 3.7 % SSC, 92 % L-cysteine and 4.8 % L-cystine were recovered as molecules representing the L-cysteine moiety. For molecules representing the GSH moiety, 84.3 % GSH, 5.2 % GSSG and 4.8 % GS-SO_3 were recovered. Recovered GS-Cys represented both moieties in 4.8 % and 2.9 %, respectively. These data indicated that reactions have been nearly completed after 3 hours of incubation of cell lysates and SSC-GSH mixtures. Further, reduced recoveries were detected for SSC, GS-Cys, GS-SO3, GSSG while increased recoveries were observed for L-cysteine and GSH. These data indicate that cell lysates were able to break the mixed disulfides generated from interaction of SSC*Na and GSH into its components L-cysteine and GSH. Finally, the presented results suggested an intracellular cleavage of SSC *via* interaction with GSH to produce mixed disulfides. These interaction products may have served as a L-cysteine pool being recovered through the enzyme activity of e.g. oxidoreductases.

In conclusion, SSC*Na may be broken down by intracellular enzymes containing L-cysteine residues in their active center. Cell-free interaction of the major intracellular thiol GSH and SSC*Na was determined leading to the formation of mixed disulfides relying on thiol-disulfide exchange. Incubation of cell lysates with SSC*Na/GSH mixtures led to reduced recoveries of mixed disulfides in favor for L-cysteine and L-cystine. SSC*Na may be intracellularly cleaved *via* interaction with GSH to produce mixed disulfides serving as a L-cysteine pool and being recovered through enzymatic activity.

5.9.2.2. Antioxidative effects of SSC*Na

To further understand the mechanism of prolonged growth and increased productivity in fed-batch processes using SSC*Na, evaluation of intracellular ROS was performed using a reactive fluorescent dye (carboxy-H_2DCFDA). Since ROS are involved in cellular oxidative stress, measurements of increasing intracellular ROS levels may reflect increasing intracellular oxidative stress. To determine SSC*Na batch dependency of ROS levels, two SSC*Na batches were chosen. Both chosen batches differ highly in their purity as well as in the type and concentrations of their impurities with SSC*Na-I being the more pure batch compared with SSC*Na-B.

5.9.2.2.1. Evaluation of oxidative stress levels via intracellular ROS determination

As shown in figure 39 A, similar fluorescence intensities were observed for control and both SSC*Na batch conditions until day 10. Starting from day 11 of culture, strongly increasing fluorescence intensities were determined in the control condition compared with both SSC*Na conditions. Final fluorescence intensities were lower in SSC*Na-B (1339.7 +/- 56.2) and SSC*Na-I (1105.7 +/- 20.3) compared with control (2888 +/- 125.8) representing a decrease of 2.1 fold for SSC*Na-B and 2.6 fold for SSC*Na-I compared with control, respectively. These data indicate that SSC*Na increased culture duration and produced titer in CHO suspension clone 2 either through activation of anti-oxidative mechanisms or through lower oxidative properties.

5.9.2.2.2. Intracellular total glutathione quantification

Since increased intracellular oxidative stress levels would be reflected in decreased intracellular anti-oxidant levels, the major intracellular anti-oxidant glutathione was quantified in its total form (GSH+GSSG) via UPLC in SSC containing fed-batch cultures obtained from bioreactor cultivation.

As shown in figure 39 B, higher intracellular total glutathione levels were observed throughout the whole culture with SSC*Na-B compared with control. On day 11 of culture, when intracellular ROS levels started to decrease in SSC*Na conditions compared with control (see figure 13A), intracellular total glutathione concentrations were higher in the SSC*Na-B condition (729.6 +/- 194.2 µM) compared with control (123.9 +/- 123.9 µM) representing 5.8 fold higher total glutathione levels in SSC*Na condition compared with control. These data indicate a higher free total glutathione pool when using SSC*Na, giving further evidence supporting the anti-oxidative properties of SSC.

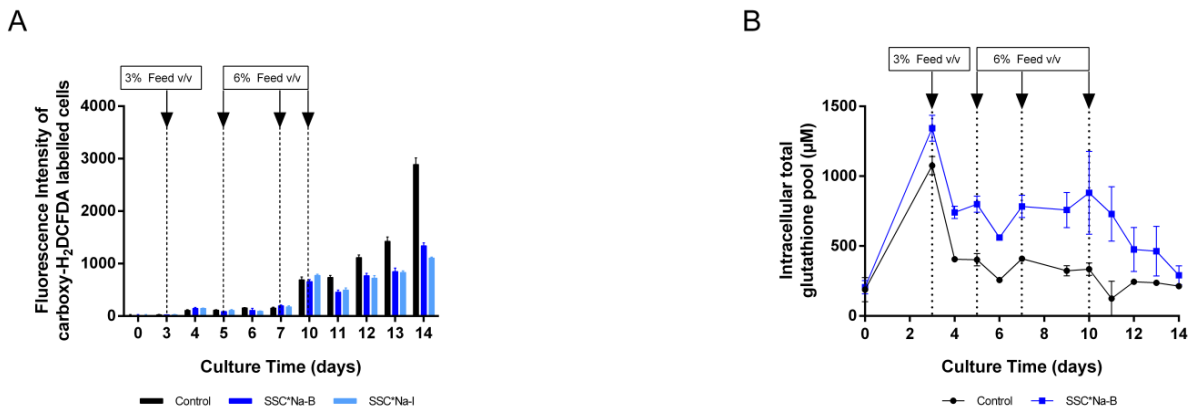

Figure 39: Anti-oxidative properties of two SSC*Na batches in fed-batch cell cultures.

(A) Intracellular reactive species were quantified during fed-batches using 15 mM SSC*Na-B and SSC*Na-I compared with control by labeling the cells with carboxy-H_2DCFDA. Alower fluorescence intensity indicates a lower intracellular reactive potential. (B) Total free glutathione (GSH + GSSG) was quantified in cell lysates using UPLC after IAM treatment and AccQ•Tag derivatization.

5.9.2.2.3. Anti-oxidative effects of SSC*Na on enzyme transcripts and enzyme protein levels

To further understand the mechanism of action of SSC*Na, microarrays for anti-oxidative, sulfur- or cysteine-related enzyme transcripts were performed. Out of the 122 genes assessed with qPCR, 16 genes exhibited a low or undetectable mRNA expression level (defined as Ct > 35) including genes involved in L-cysteine synthesis or anti-oxidative mechanisms (data not shown).

From the measurable gene transcripts presented in figure 40 A and figure 40 B, the expression levels of the vast majority were highly similar between the conditions. No change in expression of *e.g.* GSH or sulfur-related enzymes was observed. No transcriptional regulation of AST, 3-mercaptopyruvate sulfurtransferase and cysteine sulfinic acid decarboxylase, three enzymes involved in the degradation of L-cysteine to form the anti-oxidative molecules pyruvate and taurine, was determined as shown in figure 40 A. No change in expression of the antioxidant enzymes from the peroxiredoxin family was observed as shown in figure 40 B (see Hecklau et al. 2016).

Finally, this screening indicated an up-regulation of a thioredoxin-interacting protein (see figure 40 B). As shown in figure 41 A, two SOD enzymes involved in ROS elimination showed time dependent SOD-1 and SOD-2 expression changes in a bioreactor fed-batch process.

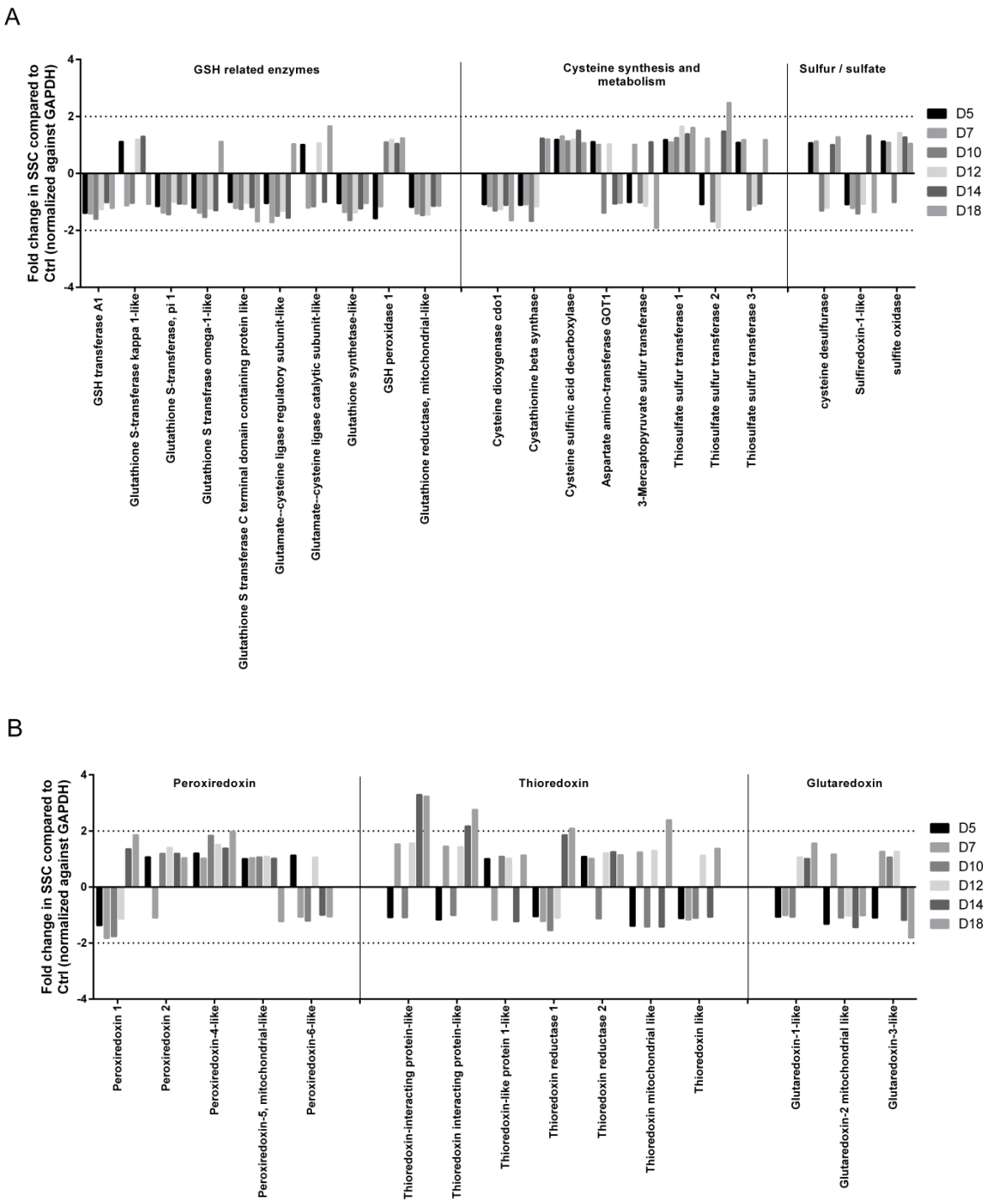

Figure 40: Microarray studies of transcript levels of different enzymes in fed-batch cultures using 15 mM SSC*Na compared with control.

(A) Expression of GSH-related, L-cysteine synthesis and metabolism-related and sulfur-related enzymes quantified by qPCR (SYBR Green). (B) Expression of peroxiredoxin-related, thioredoxin-related and glutaredoxin-related enzymes quantified by qPCR (SYBR Green).

Similar mRNA levels of SOD-1 and SOD-2 were determined in the control and in the SSC*Na condition until day 10 of culture, the early culture phase. Starting from day 11, higher transcript levels of both enzymes were observed in the SSC*Na condition compared with control. On day 11, higher

SOD-1 (8.2 fold change) and higher SOD-2 transcription levels (4.1 fold change) were determined in the SSC*Na condition compared with the control.

From that day on, prolonged growth and higher titers were monitored in the SSC*Na condition compared with the control indicating possible contributions of increased SOD-1 and SOD-2 transcription levels in the later culture phase on beneficial cell culture effects in the SSC*Na condition.

The impact of SSC*Na on the SOD family was further validated using western blot analysis of different time points in a fed-batch process. Protein levels of SOD-1 and SOD-2 were determined in a fed-batch process using SSC*Na compared with control process. As shown in figure 41 B, time-dependent increased SOD-1 and SOD-2 protein levels were detected in the SSC*Na containing process compared with control.

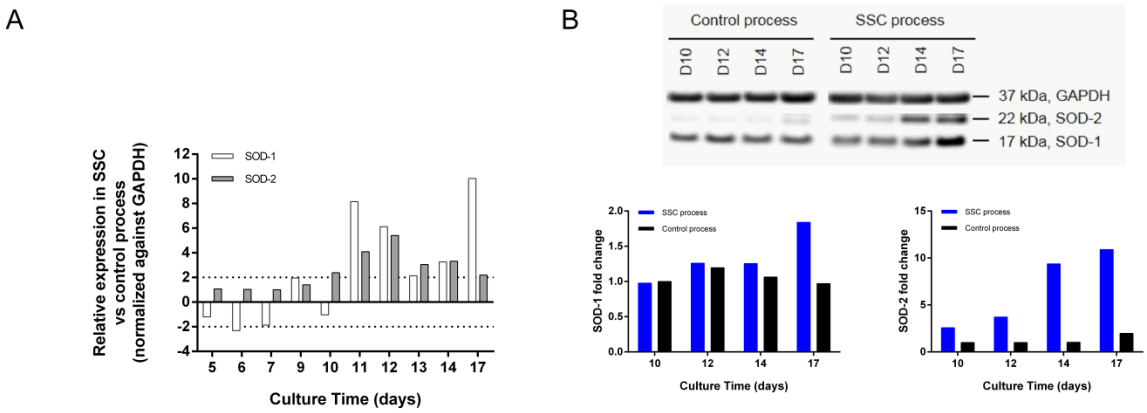

Figure 41: Antioxidative properties of SSC*Na on enzymatic expression levels and enzyme protein levels.

(A) Relative expression of SOD-1 and SOD-2 over time in SSC*Na and control fed-batch processes monitored using a RT^2 Profiler PCR Array (SYBR Green) normalized against GAPDH. Dotted lines represent the threshold of ± 2 fold change. (B) Validation of the SOD-1 and SOD-2 protein levels in the late culture phase in SSC*Na and control process normalized against GAPDH using Western Blot.

While in the control process no change in SOD-1 protein levels was observed over time, increasing SOD-1 protein levels were determined in the SSC*Na process without showing significant changes in protein levels (< 2 fold change). Higher final SOD-1 protein levels were detected in the SSC*Na process (1.8 fold change) compared with the control. Starting from day 10 of culture, increased SOD-2 protein levels were observed in the SSC*Na process compared with control. Higher final SOD-2 protein levels were detected in the SSC*Na process (10.9 fold) compared with the control indicating possible stronger contribution of SOD-2 to prolonged growth and increased titers compared with SOD-1.

In conclusion, use of SSC*Na reduced the intracellular ROS levels thereby lowering intracellular stress levels compared with cells cultured in the state-of-the-art fed-batch process. Higher intracellular total glutathione levels were observed in cells cultured in SSC*Na compared with control cultures supporting the findings of lowered intracellular stress. Higher transcript levels of SOD-1 and SOD-2 were observed in late phase cultures of SSC*Na compared with state-of-the-art fed-batch cultures. Prolonged viabilities in SSC*Na may be connected to reduced intracellular stress levels and increased enzyme transcripts in late phase cultures.

5.10. Determination of mechanisms being responsible for toxic effects of SSC*Na on cell culture performance

5.10.1. Application of single feed strategy in spin tube fed-batch processes using 20 mM of SSC*Na-A together with PTyr2Na$^+$ using clone 3

As previously shown, cell death occurred with 20 mM SSC*Na-A in spin tube fed-batch experiments using clone 2. To determine if SSC*Na-A might show toxic impacts on cell growth of a different clone, small scale spin tube fed-batch experiments were carried out using clone 3.

5.10.1.1. VCD, viabilities and IgG concentration

As shown in figure 42 A, similar VCD were observed in control and 20 mM SSC*Na-A until day 4 of culture. While increasing VCD were observed in the control until reaching its maximum VCD on day 10 (118.8 +/- 1.5 *10^5 C/mL), cells cultured in 20 mM SSC*Na-A started to reach a plateau from day 5 until the end of the culture. Final VCD in 20 mM SSC*Na-A were similar (33.1 +/- 0.8*10^5 C/mL) compared with control (37.3 +/-1.5*10^5C/mL) although the area under the curve (AUC) of 20 mM SSC*Na-A was reduced 2 fold compared with the AUC of control. These data possibly indicate that SSC*Na-A might have inhibited growth of clone 3 cells.

As shown in figure 42 B, cell viabilities started to decrease in the SSC*Na-A condition from day 7 compared with control. Final viabilities of the control were lower (35.7 +/- 1.7 %) compared with the SSC*Na-A condition (53.4 +/- 0.7 %) although the AUC of 20 mM SSC*Na-A was significantly reduced compared with the control. These data support the possible toxic effect of SSC*Na-A on clone 3 cells.

As shown in figure 42 C, IgG concentrations were similar in both conditions until day 10. Starting from day 11, higher IgG concentrations were detected in the control compared with the SSC*Na-A condition. Final higher IgG concentrations were detected in the control (1613.8 +/- 26.3 mg/L) compared with 20 mM SSC*Na-A (1123 +/- 21.4 mg/L) representing a reduction of 1.4 fold compared with the final titer of the control. These data possibly indicate decreased specific productivity in 20 mM SSC*Na-A or impacts on cell health.

5.10.1.2. Spent media analysis - NH_3 concentration

As shown in figure 42 D, starting from day 6, increased NH_3 concentrations were observed in the SSC*Na-A condition compared with control. Higher final NH_3levels were detected in 20 mM SSC*Na-A (13.5 +/- 0.1 mM) compared with the control (11.4 +/- 0.1 mM) representing an increase of 1.2 fold. This effect was observed clone independently and may indicate a molecule specific behavior.

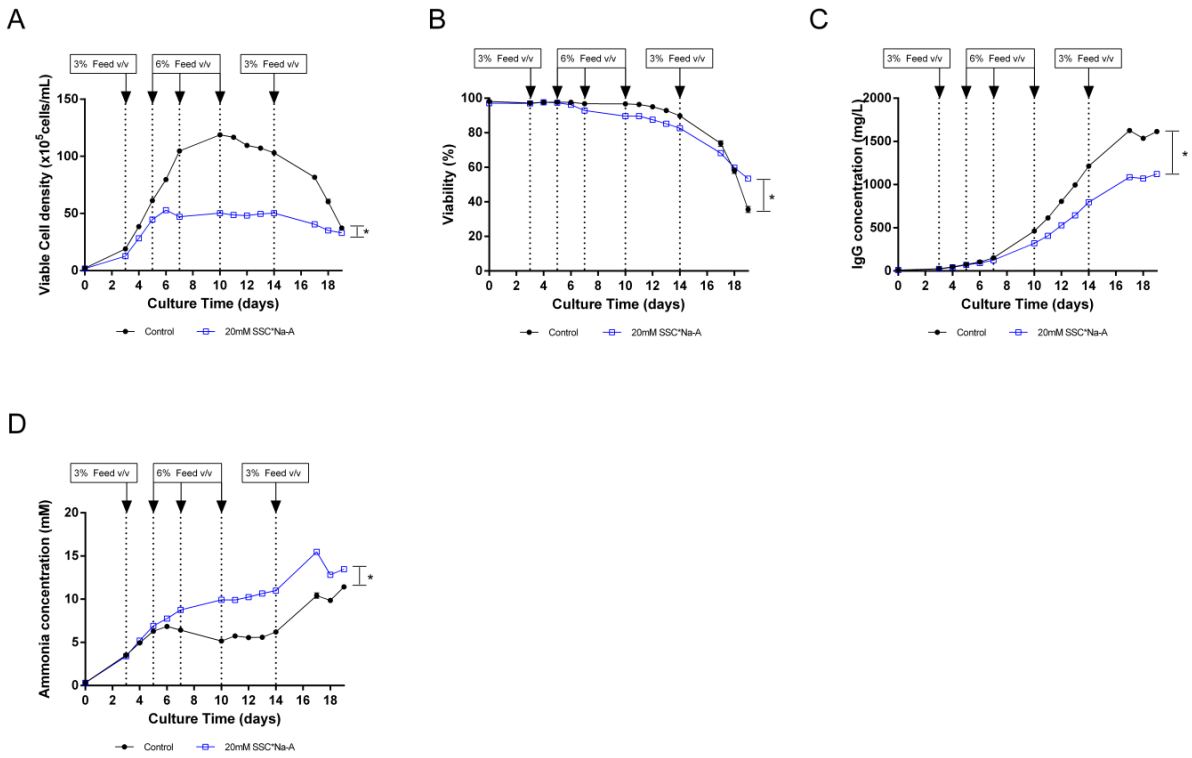

Figure 42: Spin tube fed-batch experiment with neutral pH feed containing 20 mM SSC*Na-B using CHO suspension clone 3.

20mM SSC*Na-B was integrated in the main feed with 30 mM $PTyr2Na^+$ at neutral pH (single feed system). To ensure initial growth, medium containing 1.5 mM L-CysHCl*H_2O was used. In the control condition, L-cysteine was added separately in an alkaline feed (n=5). Suspension CHO clone 3 cells were seeded at 2*10^5 C/mL, incubated at 37 °C, 5 % CO_2, 80 % humidity and agitated at 320 rpm. Feed was added at 3 % (v/v) at day 3 and 6 % (v/v) at days 5, 7, 10 and 14. (A) VCD. (B) Cellular viability. (C) IgG concentration in the supernatants measured by turbidometric method. (D) NH_3 concentrations in the supernatants measured by photometry. Mann-Whitney test of area under the curve (AUC) was performed ($p < 0.05$). Values are means +/- SEM.

These data possibly indicate increased cellular metabolic NH_3 production or breakdown of nitrogen containing compounds such as amino acids, vitamins or supplements in SSC*Na-A application.

5.10.2. Application of single feed strategy in spin tube fed-batch processes using different SSC batches together with $PTyr2Na^+$ using clone 2

As previously shown, SSC*Na-A in a concentration of 20 mM impacted negatively cell growth of clones 2 and 3 in spin tube fed-batch processes. To evaluate if the reported effects of cell death with 20 mM SSC*Na-A with the high producer clone 2 were reproducible with different SSC*Na batches, the effects on cell growth, viability and IgG concentration were determined. The second externally synthesized SSC*Na-B batch as well as several internally synthesized SSC*Na-batches C, D, E, F, G, H and I possessing different purity and impurity profiles were tested. The following table summarized the different batches and their applied test concentration with corresponding pure SSC*Na concentration.

Since crystal structure analysis at Merck of the first used, externally produced SSC*Na-batches A and B revealed the presence of SSC*Na as dimers each linked with three water molecules and 2 sodium ions, the molecular weight given by Bachem differed from the molecular weight internally determined. Consequently, the molecular weight needed to be corrected. Since all fed-batch tests were carried out before this analysis was done, the theoretical applied SSC*Na concentration needed to be calculated into the real applied pure SSC*Na concentration.

Due to purity differences of the particular SSC*Na batches, differences in the real, pure applied SSC*Na concentration were observed. With increasing purities of the SSC*Na batches, increasing real applied SSC*Na concentrations were calculated with all corrected SSC*Na concentrations being lower as the theoretical used SSC*Na concentration. Besides the previously summarized impurity profile differences (see table 6), the real applied SSC*Na concentration might be kept in mind.

Table 7: Purity, corrected molecular weight, theoretical and real SSC*Na concentrations of different externally and internally synthesized SSC*Na batches.

Molecular weight was determined by crystal structure analysis, the real SSC*Na concentration was calculated based on the SSC*Na batch purity, applied SSC*Na concentration in g/L and corrected molecular weight.

SSC*Na batch	Purity % (w/w)	Molecular weight$_{corrected}$ (g/mol)	Theoretical SSC*Na concentration (mM)	Real SSC*Na concentration (mM)
SSC*Na-A	81.3	250.26	20	14.5
SSC*Na-B	85.3	250.26	20	15.2
SSC*Na-C	91.3	250.26	20	16.3
SSC*Na-D	91.3	250.26	20	16.3
SSC*Na-E	88.2	250.26	20	15.7
SSC*Na-F	98.5	250.26	20	17.6
SSC*Na-G	99.6	250.26	20	17.8
SSC*Na-H	96	250.26	20	17.1
SSC*Na-I	99.6	250.26	20	17.8

5.10.2.1. VCD, viabilities and IgG concentration with SSC*Na-C

As one of the first internally synthesized SSC*Na batches, SSC*Na-C was used in cell culture performance evaluation. Compared with the previously used batch SSC*Na-A, the internally synthesized SSC*Na-C research batch showed higher copper concentrations of 280 µg/g and higher sulfate concentrations of 2-8 % (w/w) while thiosulfate and L-cystine were not measured. Although not measured, no thiosulfate in the final synthesis product was expected to be present since the internal

synthesis routes for SSC*Na did not rely on tetrathionate. The real SSC*Na concentration in SSC*Na-C was calculated to be 7 % higher compared with the real calculated SSC*Na concentration in SSC*Na-B.

As shown in figure 43 A, similar growth curves of 20 mM SSC*Na-C and control were observed until day 10 of culture. Starting from day 10, the control started to die and decreasing VCD were measured while 20 mM SSC*Na-C showed prolonged growth until the end of culture. Final higher VCD were observed in 20 mM SSC*Na-C (103.4+/- $2.2*10^5$ C/mL) compared with control (9.9 +/- $0.4*10^5$ C/mL). These data possibly indicate beneficial effects of this batch on cell health in 20 mM possibly due to the major impurity copper or the absence of thiosulfate.

As shown in figure 43 B, prolonged cell viability was observed in 20 mM SSC*Na-C compared with control starting from day 10. Final higher viabilities were observed in 20 mM SSC*Na-C (61.1 +/- 0.4%) compared with control (6.4 +/- 0.2 %). No cell death was observed 20 mM SSC*Na-C compared with 20 mM SSC*Na-A indicating that possibly SSC*Na-C batch characteristics such as its high copper concentration or the absence of thiosulfate may beneficially impact the cell health.

As shown in figure 43 C, higher final titers were measured in 20 mM SSC*Na-C (1529.5 +/- 25.2 mg/L) compared with control (727.8 +/- 4.8 mg/L) possibly indicating beneficially impacted antibody concentration relying on prolonged viability or increased specific productivity.

5.10.2.2. VCD, viabilities and IgG concentration with SSC*Na-B, SSC*Na-D, SSC*Na-E, SSC*Na-H

As shown before, the cell death in 20 mM SSC*Na-A was not reproduced in 20 mM SSC*Na-C. Since the molecule did not differ chemically in both batches, possible impacts on prolonged growth and higher final titers in 20 mM SSC*Na-C may have resulted from the impurity profile. To evaluate if previously observed prevention from cell death with 20 mM SSC*Na-C might be reproduced with other SSC*Na batches, the second externally delivered batch SSC*Na-B and the next internally synthesized research batches SSC*Na-D, E and H were tested in cell culture. The real SSC*Na concentrations in SSC*Na-D, E and H were calculated to be 7 %, 3 % and 12.5 % higher, respectively, compared with the real calculated SSC*Na concentration in SSC*Na-B.

Since SSC*Na-D, E, and H batches were the next products in the process of synthesis and purification optimization, higher copper concentrations were found in SSC*Na-D (600 µg/g), SSC*Na-E (800 µg/g) and SSC*Na-H (460 µg/g) compared with SSC*Na-B (0.3 µg/g) and SSC*Na-C (280 µg/g). No thiosulfate was detected in these batches. Similar higher sulfate concentrations were detected in SSC*Na-D (2.7 % (w/w)), SSC*Na-E (2.6 % (w/w)) and SSC*Na-H (2.8% w/w)) compared with SSC*Na-B (1.3 % (w/w)). Higher L-cystine concentrations were monitored in

SSC*Na-D (2.2 % (w/w)), SSC*Na-E (2 % (w/w)) and SSC*Na-H (0.5 % (w/w)) compared with L-cystine-free SSC*Na-B.

As shown in figure 43 D, lower maximum VCDs were observed with all four SSC*Na batches tested here compared with control. Cell death from day 7 to 10 started to occur only with 20 mM SSC*Na-B compared with the other SSC*Na batches and the control. These data indicate that both externally synthesized batches SSC*Na-A and SSC*Na-B led to time defined cell death possibly related to their impurity profiles. Prolonged cell growth was detected in 20 mM using SSC*Na batches D, E, H compared with control. Higher final VCD were obtained for 20 mM SSC*Na-D (92.8 +/- $1.2*10^5$ C/mL), 20 mM SSC*Na-E (94.9 +/-$0.6*10^5$ C/mL) and 20 mM SSC*Na-H (88.9 +/- $0.9*10^5$ C/mL) compared with control (28.8* +/- $1.7*10^5$ C/mL) and 20 mM SSC*Na-B (0.9 +/- $0.2*10^5$ C/mL) indicating beneficial effects on cell health possibly relying on the impurity profiles of the SSC*Na batches.

As shown in figure 43 E, prolonged cell viability was observed with 20 mM SSC*Na-D, SSC*Na-E and SSC*Na-H compared with control and 20 mM SSC*Na-B. Final higher viabilities were observed in 20 mM SSC*Na-D (48.8 +/- 0.6 %), 20 mM SSC*Na-E (48.7 +/- 0.2 %) and 20 mM SSC*Na-H (46.2 +/- 0.1 %) compared with control (14 +/- 0.7 %) and 20 mM SSC*Na-B (0.5 +/- 0.1%). Cell death between day 7 and 10 was observed with SSC*Na-B as it was previously shown with 20 mM SSC*Na-A. No cell death was observed in 20 mM SSC*Na-D, SSC*Na-E and SSC*Na-H as previously shown with SSC*Na-C. These data may indicate that beneficial effects on cell health possibly connected to the impurity profiles of SSC*Na-D, E, H such as e.g. copper, L-cystine and sulfate levels or the absence of thiosulfate.

As shown in figure 43 F, final higher titers were measured in 20 mM SSC*Na-D (1358 +/- 19 mg/L), 20 mM SSC*Na-E (1349.6 +/- 20.8 mg/L) and 20 mM SSC*Na-H (1164 +/- 83.7 mg/L) compared with control (1031.8 +/-17.2 mg/L) and 20 mM SSC*Na-B (571.3 +/- 2.7 mg/L). Increases in final antibody concentration of 1.3 fold for 20 mM SSC*Na-D and SSC*Na-E as well as 1.12 fold for 20 mM SSC*Na-H were found compared with control. These data may indicate that the specific productivity was increased in SSC*Na-D, E, H or possible beneficial effects on cell health related to impurity profiles were responsible for increased titers.

5.10.2.3. VCD, viabilities and IgG concentration with SSC*Na-F, SSC*Na-G

As shown before, the culture time dependent cell death in 20 mM of the externally synthesized batches SSC*Na-A and B was not reproduced in 20 mM of the previously internally synthesized batches SSC*Na-C, D, E, and H. Since the molecule did not differ chemically in all previously tested batches, possible impacts on prolonged growth and higher final titers in 20 mM SSC*Na-C, D, E and H may have resulted from the impurity profiles.

To evaluate if previously observed prevention from cell death with 20 mM SSC*Na-C, D, E and H might be reproduced with other SSC*Na batches, the next internally synthesized research batches SSC*Na-F and G were tested in cell culture.

The real SSC*Na concentration in SSC*Na-F and SSC*Na-G were calculated to be 15 % and 17.1 % higher, respectively, compared with the real calculated SSC*Na concentration in SSC*Na-B. As products of further synthesis and purification optimization steps, copper was monitored to be 60 µg/g in SSC*Na-F and < 0.2 µg/g in SSC*Na-G. No thiosulfate was found to be present in these batches since the internal synthesis route did not rely on tetrathionate. No L-cystine was quantified. Sulfate concentrations were determined to be 0.2 % (w/w) for SSC*Na-F and < 0.2 % (w/w) for SSC*Na-G. Compared with the previously tested SSC*Na-batches C, D, E and H, SSC*Na-F and G showed reduced copper and sulfate levels and consequently may be regarded as more pure. Since impurity profiles of internally synthesized SSC*Na batches may have impacted cell culture performance as shown before, the impact of more pure SSC*Na-batches F and G on cell culture performance was evaluated.

As shown in figure 43 G, lower maximum VCDs on day 7 were observed for all tested SSC*Na batches compared with control. Cell death started to occur between days 7 and 10 in 20 mM SSC*Na-G and 20 mM SSC*Na-F. This observation was consistent with cell culture performances 20 mM SSC*Na-A and B. These data may indicate that the impurity thiosulfate did not cause the herein observed cell death, since both batches SSC*Na-F and G were free from thiosulfate. Possibly, copper and sulfate were not sufficiently present in these batches compared with the previously tested SSC*Na-batches C, D, E and H or the molecule SSC itself might be toxic in batches with low copper and sulfate levels.

As shown in figure 43 H, the observed cell deaths in 20 mM SSC*Na-F and G were confirmed in viability. While slight decreasing viabilities were observed in the control between day 7 (98.9 +/- 0.1 %) and day 10 (90 +/- 0.2 %), viability dropped 20 mM SSC*Na-F from 97.8 +/- 0.1 % on day 7 to 0.3 % on day 10 and in 20 mM SSC*Na-G from 98.1 +/- 0.1 % on day 7 to 0.2 % on day 10. These data may indicate that SSC itself might be toxic in batches with low copper and sulfate levels.

As shown in figure 43 I, viability drops in SSC*Na-F and SSC*Na-G reflected decreased final titers in these conditions compared with control. Due to cell death G between day 7 and 10 of culture in 20 mM SSC*Na-F and 20 mM SSC*Na-G, no further increases in IgG concentration in both conditions was detected after day 7 leading to final lower titers in 20 mM SSC*Na-F (320 +/- 8.9 mg/L) and SSC*Na-G (326 +/- 6.2 mg/L) compared with control (1222.7 +/- 38 mg/L).

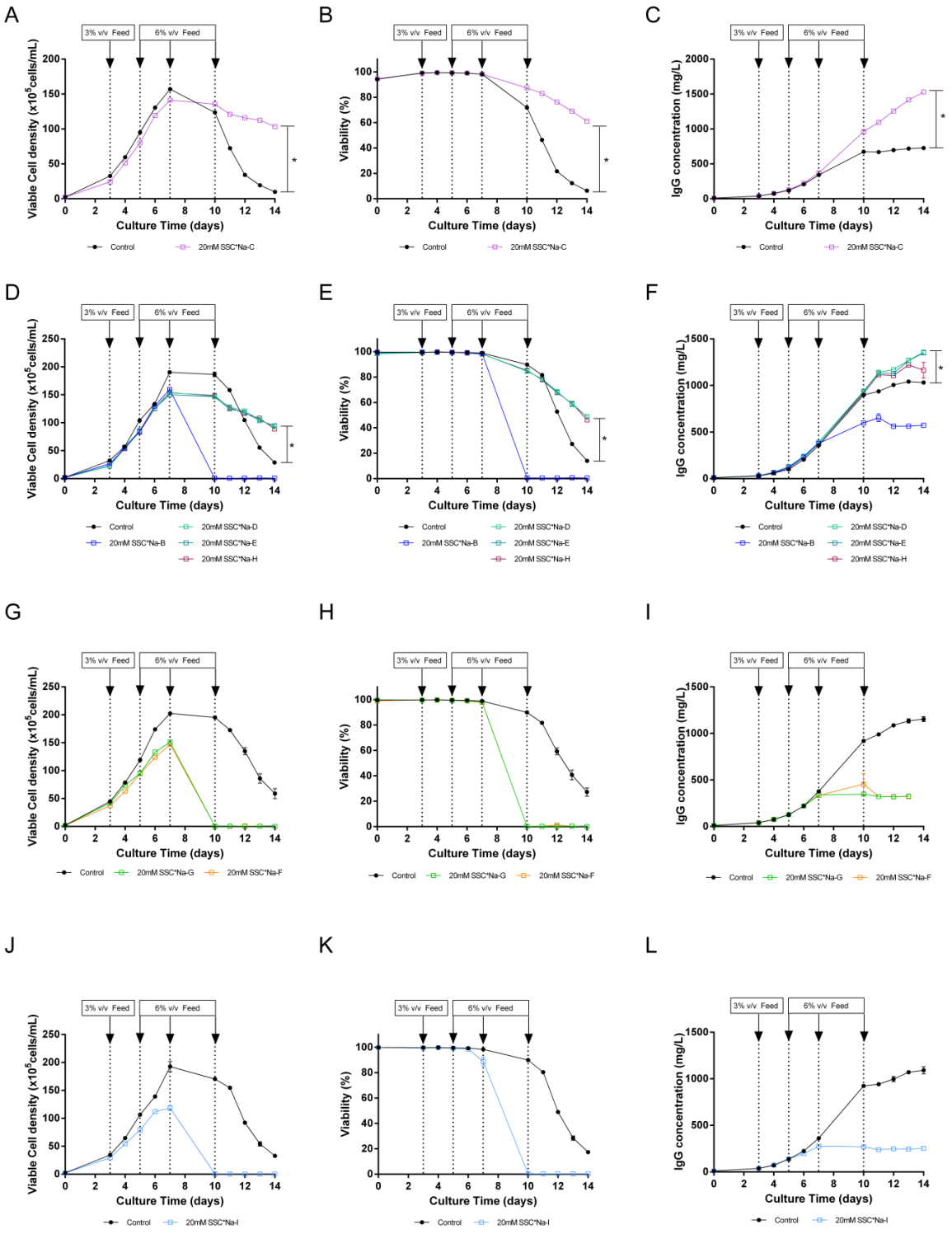

Figure 43: Spin tube fed-batch experiment with neutral pH feed containing 20 mM of different SSC*Na batches using CHO suspension clone 2.

20 mM of different SSC*Na batches (B,C,D, E, F, G, H and I) were integrated in the main feed with 30 mM $PTyr2Na^+$ at neutral pH (single feed system). To ensure initial growth, medium containing 1.5 mM L-CysHCl*H_2O was used. In the control condition, L-cysteine was added separately in an alkaline feed (n= 4). Suspension CHO clone 2 cells were seeded at $2*10^5$ C/mL, incubated at 37 °C, 5 % CO_2, 80 % humidity and agitated at 320 rpm. Feed was added at 3 % (v/v) at day 3 and 6 % (v/v) at days 5, 7 and 10. (A-C) VCD, viability and produced IgG concentration presented in 20 mM SSC*Na-C, respectively. (D-F) VCD, viability and produced IgG concentration of 20 mM SSC*Na-B, D, E and H, respectively. (G-I) VCD, viability and produced IgG concentration of 20 mM SSC*Na-F and G, respectively. (J-L) VCD, viability and produced IgG concentration of 20 mM of SSC*Na-I. Antibody concentrations were measured in the supernatants with a turbidometric method. Mann-Whitney test of area under the curve (AUC) was performed ($p < 0.05$). Values are means +/- SEM.

5.10.2.4. VCD, viabilities and IgG concentration using SSC*Na-I

As shown before, the culture time dependent cell death in 20 mM of the externally synthesized batches SSC*Na-A and B was reproduced in 20 mM of the previously internally synthesized batches SSC*Na-F and SSC*Na-G but not in SSC*Na batches C, D, E, and H. Since the molecule did not differ chemically in all previously tested batches and the purity increased from batches C,D,E H to batches F and G, the last internally synthesized SSC*Na batch I was tested for cell culture performance. The real SSC*Na concentration in SSC*Na-I was calculated to be 17 % higher, respectively, compared with the real calculated SSC*Na concentration in SSC*Na-B. Since differences in cell culture performance may have resulted from different impurity profiles, SSC*Na-I as the second most pure internally produced batch was evaluated in cell culture. The determined copper concentration was 2 µg/g and sulfate concentration was monitored to be < 0.2 % (w/w). L-cystine was not quantified. No thiosulfate was detected due to the tetrathiosulfate-free internal synthesis method. Consequently, SSC*Na-I is the second most pure internally produced SSC*Na batch after SSC*Na-G in the process development of synthesis and purification optimization.

As shown in figure 43 J, lower maximum VCDs on day 7 were observed in 20 mM SSC*Na-I (118.3 +/- $4.5*10^5$ C/mL) compared with control (192.5 +/- $9.3*10^5$ C/mL). Culture time dependent cell death started to occur from day 7 (112.8 +/- $1.6*10^5$ C/mL) to 10 (7.2 +/- $2.5*10^5$ C/mL) with 20 mM SSC*Na-I whereas slight decreases in VCD were observed from day 7 (192.5 +/- $9.3*10^5$ C/mL) to 10 (170.3 +/- 1.4 $*10^5$ C/mL) in control. This effect was also observed in 20 mM batches SSC*Na-A, B, F and G. These data possibly indicate that impurities were not sufficiently present in these batches compared with the previously tested SSC*Na-batches C, D, E and H or the molecule itself might be toxic in batches with low copper and sulfate levels.

As shown in figure 43 K, the observed cell death was supported by viability data. While the control slightly showed decreasing viabilities from day 7 (98.4 +/- 0.1 %) to 10 (89.9 +/- 0.1 %), viability dropped from day 7 (88.8 +/- 3.4 %) to 10 (0.4 +/- 0.1 %) in 20 mM SSC*Na-I. These data possibly indicate insufficient present batch impurities or toxicity of SSC*Na in conditions with low copper and sulfate levels.

As shown in figure 43 L, higher final titers were found in the control (1091.8 +/- 38.6 mg/L) compared with 20 mM SSC*Na-I (253.7 +/- 15 mg/L) due to early cell death. These data possibly indicate insufficient present batch impurities or toxicity of SSC*Na in conditions with low copper and sulfate levels.

5.10.2.5. Spent media analysis - NH_3 concentration with SSC*Na-C

As shown in figure 44 A, similar NH_3 concentrations were observed in 20 mM SSC*Na-C compared with control until day 5. Starting from day 6, strongly increasing NH_3 concentrations were observed 20 mM SSC*Na-C compared with control as shown in figure 43 A. Final higher NH_3concentrations were observed in 20 mM SSC*Na-C (5.7 +/-0.2 mM) compared with control (4 +/- 0.1 mM) representing an increase of 1.4 fold, respectively.

These data possibly indicate that SSC*Na-C may increased cellular metabolic NH_3 production or breakdown of nitrogen containing compounds such as amino acids, vitamins or supplements. Since higher NH_3 levels might be toxic to CHO suspension clones, SSC*Na application might impact culture performance negatively.

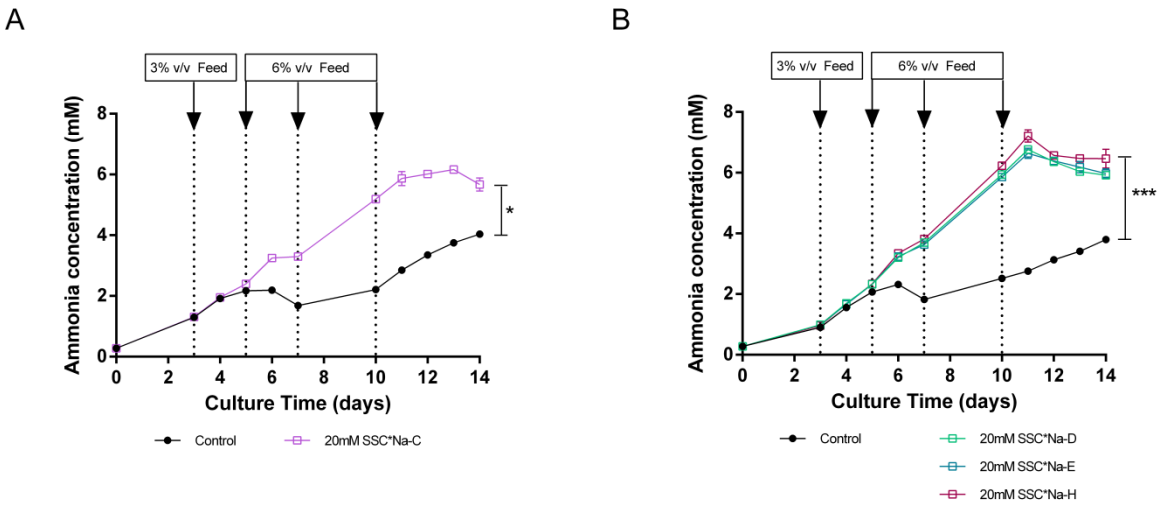

Figure 44: NH_3 **concentrations from spin tube fed-batch experiment with neutral pH feed containing 20 mM SSC*Na using CHO suspension clone 2.**

20 mM of SSC*Na batches C, D, E and H were integrated in the main feed with 30 mM PTyr2Na^+ at neutral pH (single feed system). To ensure initial growth, medium containing 1.5 mM L-CysHCl*H_2O was used. In the control condition, L-cysteine was added separately in an alkaline feed (n= 4). Suspension CHO clone 2 cells were seeded at 2*10^5 C/mL, incubated at 37 °C, 5 % CO_2, 80 % humidity and agitated at 320 rpm. Feed was added at 3 % (v/v) at day 3 and 6 % (v/v) at days 5, 7 and 10. (A) NH_3 concentration over time in the supernatants of 20 mM with SSC*Na-C. (B) NH_3 concentration over time in the supernatants in 20 mM SSC*Na- D, E and H. NH_3 concentrations in the supernatants were measured by photometry. Mann-Whitney test or Kruskal- Wallis test with Dunn`s multiple comparison test were applied ($p < 0.05$). Values are means +/- SEM.

5.10.2.6. Spent media analysis - NH_3 concentrations with SSC*Na- D, E and H

As shown in figure 44 B, similar NH_3 concentrations of the 20 mM SSC*Na batches D, E and H and control were observed until day 5 of culture. Starting from day 6, strongly increasing NH_3 concentrations were observed in all herein presented SSC*Na batches D, E and H compared with control.

Final higher NH_3 concentrations were observed in 20 mM SSC*Na-D (5.9 +/- 0.1 mM), 20 mM SSC*Na-E (6 +/- 0.2 mM), 20 mM SSC*Na-H (6.5 +/- 0.3 mM) compared with control (3.8 mM +/- 0.1 mM) representing an increase of 1.5 fold, 1.6 fold and 1.7 fold for SSC*Na-D, SSC*Na-E and SSC*Na-H compared with control, respectively. These data possibly indicate that SSC*Na batches D, E and H may increase cellular metabolic NH_3 production or breakdown of nitrogen containing compounds such as amino acids, vitamins or supplements. Final NH_3 concentrations measured in viable cell cultures using 20 mM SSC*Na-C, D, E and H were comparable with each other and higher compared with the control conditions. These data indicate batch impurity independent NH_3 production and SSC*Na molecule dependent NH_3 formation. Since higher NH_3 levels might be toxic to CHO suspension clones, SSC*Na application might impact culture performance negatively.

5.10.2.7. Overview of cell culture fed-batch results in cell cultures using 20 mM of different SSC*Na batches

As previously shown, different SSC*Na batches in a theoretical applied concentration of 20 mM led to different cell culture performances. Since the impurities and the real applied SSC concentration may have impacted cell culture performance, the following table 8 summarized these parameters and the observations from small scale fed-batch processes using 20 mM of different SSC*Na batches.

The real applied SSC*Na concentrations of batches F and H were similar (17.6 and 17.1 mM, respectively) and copper concentrations differed (60 and 460 µg/g, respectively). In SSC*Na-batches B and E, similar lower real SSC*Na concentrations were calculated (15.2 and 15.7 mM, respectively) compared with batches F and H. Copper concentrations varied (800 and 0.4 µg/g, respectively) in SSC*Na batches B and E, too. In both SSC*Na batch comparisons, cell culture performances varied (cell death (batches F and B) and prolonged growth (H and E), respectively). These data may indicate that the amount of SSC*Na alone might not be crucial whereas the present copper concentration in the SSC*Na batches may impact performance.

When comparing the sulfate concentrations in different SSC*Na batches, the sulfate concentrations of e.g. SSC*Na batches F, G and I (0.2, < 0.2, < 0.2 % (w/w), respectively) were lower compared with sulfate concentrations in SSC*Na batches C, D, E and H (2-8, 2.7, 2 and 2.8 % (w/w)), respectively). On average, in the latter SSC*Na batches, 2-3 % (w/w) sulfate were detected. Over a fed-batch cultivation period of 14 days, theses sulfate contaminations coming from SSC*Na increased the total sulfate concentration of ~8 % and ~12 %, respectively.

In SSC*Na batches C/D, E and H containing higher sulfate contaminations prolonged growth was observed compared with batches A, B, F, G and I possibly indicating that low sulfate concentrations may have impacted cell culture performance leading to cell death.

The presence of L-cystine was synthesis route dependent. Since only the internally produced SSC*Na batches relied on L-cystine as a starting material, only the internally produced batches SSC*Na showed L-cystine impurities. Since L-cystine was present in the three SSC*Na batches D, E and H and showing prolonged viability in the theoretical concentration of 20 mM, these data possibly indicate that L-cystine presence may be responsible for prolonged growth.

The presence of thiosulfate was synthesis route dependent. Since only the externally produced SSC*Na batches A and B relied on the tetrathionate method, only the externally produced batches SSC*Na-A and B showed thiosulfate impurities. Thiosulfate was quantified to be 1.8 and 1.3 % (w/w) for SSC*Na batches A and B, respectively. Since the internally synthesized batches were synthesized free from tetrathionate, no thiosulfate was present in SSC*Na batches C, D, E, F, G, H and I. Cell death occurred in internally synthesized, thiosulfate-free batches e.g. SSC*Na-F, G, I and in the externally synthesized, thiosulfate containing batches SSC*Na-A and B. These data indicate that thiosulfate alone may not have caused cell death.

Table 8: Externally and internally synthesized and tested SSC*Na research batches showing impurities coming from synthesis method (copper, sulfate, L-cystine, thiosulfate), real applied SSC*Na concentrations and observations from small scale fed-batch processes using the theoretical concentration of 20 mM.

Copper was quantified using ICP-HR-MS (LOQ < 0.1 µg/g), L-cystine (LOQ < 0.2 % (w/w)), sulfate (LOQ < 0.2 % (w/w)) and thiosulfate (0.3 % (w/w)) were measured using CE. Real applied SSC*Na batch concentrations were calculated. * n.q. – not quantified, **n.m. – not measured

Order in respect of real, applied SSC*Na concentration (highest to lowest)	I,G	>	F	>	H	>	C,D	>	E	>	B	>	A
Real applied SSC concentration (mM)	17.8, 17.8		17.6		17.1		16.3, 16.3		15.7		15.2		14.5
Batch produced	internally		internally		internally		internally		internally		externally		externally
Observation with theoretical 20 mM SSC*Na batch in FB culture	dead		dead		viable		viable		viable		dead		dead
Copper content (µg/g)	2, n.q*		60		460		280, 600		800		0.4		0.3
Sulfate content (% (w/w))	n.q.*, n.q.*		0.2		2.8		2-8, 2.7		2		0		0
Cystine content (% (w/w))	n.q.*, n.q.*		n.q.*		0.5		n.m.*, 2.2		2		0		0
Presence of thiosulfate	no		no		no		no		no		yes		yes

In conclusion, different SSC*Na batches may cause different cell culture performances with different clones when using the theoretical concentration of 20 mM SSC*Na. Cell growth was inhibited in clone 3. Improved cell culture fed-batch performance was observed in the theoretical concentration of 20 mM SSC*Na of batches C, D, E and H compared with cell culture performance in SSC*Na-A. These internally synthesized batches showed higher concentrations of contaminants coming from synthesis route relying on L-cystine and sulfite catalysed by copper. Higher copper, L-cystine or sulfate concentrations in combination with or without higher real SSC*Na concentrations may beneficially impact cell culture performance. Thiosulfate as a contamination of externally produced SSC*Na batches was not shown to be alone responsible for cell death in the theoretical concentration of 20 mM SSC*Na.

5.10.3. Toxic effects in batch mode with two different clones

As previously shown, applying a theoretic concentration of 20 mM SSC*Na-A in fed-batch experiments using clone 2, led to cell death starting from day 7 to 10. Further, this SSC*Na-A concentration inhibited growth of clone 3 in spin tube fed-batch experiments.

Since batch experiments were only carried out with clone 1 due to limitations in clone availability, the question of possible toxic effects of SSC*Na on different, later available clones in short-term batch cultures emerged. Since the optimal SSC*Na concentration of 1.5 mM was determined in batch mode with clone 1, batch cultures with this SSC*Na concentration were carried out using clones 2 and 3. Since SSC*Na-A and B differed only in thiosulfate concentration and thiosulfate was shown to be not responsible for toxic effects observed in fed-batch studies, SSC*Na-B was used for further studies.

5.10.3.1. L-cysteine replacement by 1.5 mM SSC*Na-B in batch cultures using clones 2 and 3

5.10.3.1.1. VCD

As shown in figure 45 A, when using clone 2, lower cell growth was observed in SSC*Na-B until day 3 compared with control. Between days 3 and 4 of culture, rapid cell death was observed in the SSC*Na-B condition compared with control. Higher VCD were observed on day 4 of culture in the control (87.1 +/- 2.1*10^5 C/mL) compared with SSC*Na-B (9.7 +/- 0.5*10^5 C/mL). These data indicate toxic effects of SSC*Na-B on clone 2 cells in batch mode.

As shown in figure 45 B, when using clone 3, only slight cell growth was observed in SSC*Na-B compared with control starting from day 4 pointing out inhibition of cell growth by SSC*Na-B. Final VCD were higher in control (93 +/- 0.6*10^5 C/mL) compared with 1.5 mM SSC*Na-B (9.1 +/- 2.3*10^5 C/mL) possibly indicating toxic effects of SSC*Na-B on clone 3 in batch mode.

5.10.3.1.2. Viabilities

As shown in figure 45 C, initial viabilities of control and SSC*Na-B in clone 2 were similar until day 3. Between days 3 and 4, viability of cells cultured in SSC*Na-B dropped rapidly leading to cell death on day 4 of culture. Viabilities in control were higher (99.5 +/- 0.1 %) on day 4 compared with SSC*Na-B (22.1 +/- 1.9 %). These data possibly indicate toxic effects of SSC*Na-B on clone 2 cells in batch mode.

As shown in figure 45 D, initial viabilities in SSC*Na-B were lower (84.4 +/- 2.2 %) compared with control (98.6 +/- 1 %). Over the whole culture time, lower viabilities were detected in SSC*Na-B compared with control. Final viabilities were higher in control (97 +/- 0.1 %) compared with SSC*Na-B (92.9 +/- 2 %). These data possibly indicate that SSC*Na-B had a toxic effect on cell viability *ab initio*.

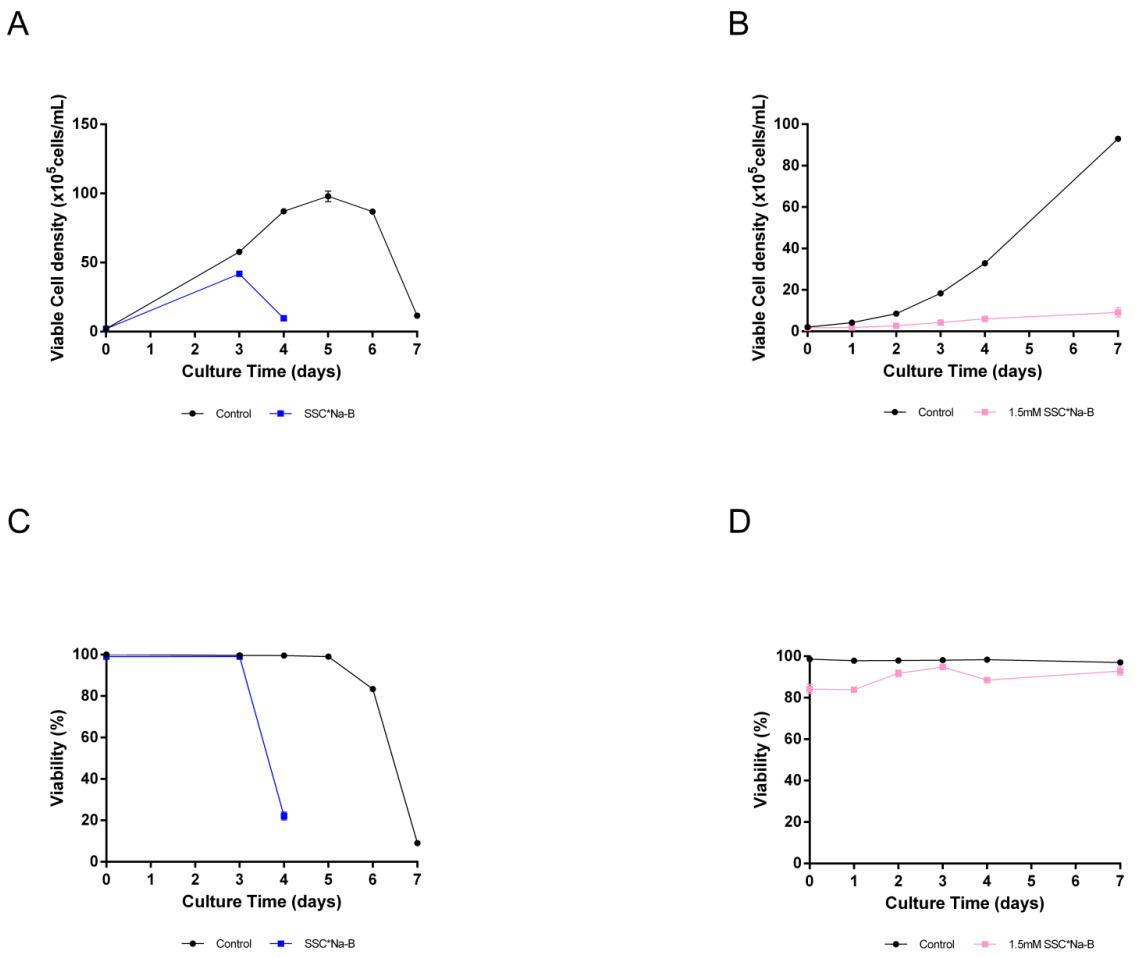

Figure 45: L-cysteine replacement by 1.5 mM SSC*Na-B in L-cysteine deficient medium in spin tube batch processes using CHO suspension clones 2 and 3.

1.5 mM SSC*Na-B were each added to a L-cysteine depleted Cellvento^{TM} CHO-220 and the performance was compared to the medium non-modified Cellvento^{TM} CHO-220 and to non-modified Cellvento^{TM} CHO-220 supplemented with puromycine and glutamine (n=3). Suspension CHO clones 2 and 3 cells were seeded at 2*10^5 C/mL, incubated at 37 °C, 5 % CO_2, 80 % humidity and agitated at 320 rpm. (A) VCD of clone 2. (B) VCD of clone 3. (C) Cellular viability of clone 2. (D) Cellular viability of clone 3. Values are means +/- SEM.

In conclusion, 1.5 mM SSC*Na-B impacted cell growth in two different CHO suspension clones. Two scenarios were observed showing clone-dependency. After initial cell growth, rapid cell death was observed between days 3 and 4 of culture with one high producing clone while growth inhibition *ab initio* was monitored with a glutamine-dependent clone.

5.10.4. L-glutamate transporter studies

As previously shown, in batch experiments with 1.5 mM SSC*Na-B, cell death between days 3 and 4 of culture were observed with clone 2 while inhibited cell growth was monitored in batch cultures using clone 3. In fed-batch experiments, it was shown that in a theoretical SSC*Na concentration of 20 mM of batches A,B,F,G and I showed cell death between days 7 and 10 with clone 2. Inhibited cell growth of clone 3 was observed in fed-batch experiments. With these observations in mind, questions of disturbed amino acid uptake leading to impaired cell growth arose.

Since reports described SSC*Na to be an analogue of glutamate with regard to its structural similarity (Belaidi and Schwarz 2013), it was hypothesized that SSC*Na might compete with glutamate for one or more glutamate transporters. By this hypothesized scenario, glutamate or SSC*Na might not have been entered the cell efficiently and cell growth might be impaired.

To further evaluate if the clones 2 and 3 showed expression of glutamate transporters belonging to two glutamate transporter classes, first RT-PCR of isolated mRNAs of both clones was carried out. Therefore, regular passaging experiments using the basal formulated medium Cellvento™ CHO-220 were performed and cells were harvested after passage 12 for mRNA isolation.

5.10.4.1. Expression levels of L-glutamate transporters in all three CHO suspension clones

As shown in figure 46, three transporters belonging to the high affinity glutamate transporter class (SLC1a2, SLC1a3, SLC1a6) and one L-cystine/L-glutamate transporter (SLC7a11) were evaluated concerning their expression levels in clones 2 and 3. The herein presented SLC1 transporters represented members belonging to the transport system type X^-_{AG} whereas the L-cystine/L-glutamate transporter represented a member of the transport system type x_C^-.

As shown in figure 46, highest fold changes were found in clone 2 for SLC1a2 (312 +/- 45.2 fold), SLC1a3 (47.5 +/- 34.3 fold), SLC1a6 (7 +/- 1.8 fold) and SLC7a11 (2.5 +/- 0.1 fold) compared with those found in clone 3. In both presented clones, no expression of glutamate transporters SLC1a1 and SLC1a7 was detected (data not shown).

Since clone 3 showed the lowest expression levels of all tested transporters amongst the three clones and cell growth in batch and fed-batch mode was inhibited, these data may indicate a correlation of low glutamate transporter expression levels and impacted cell culture performances in batch and fed-batch mode.

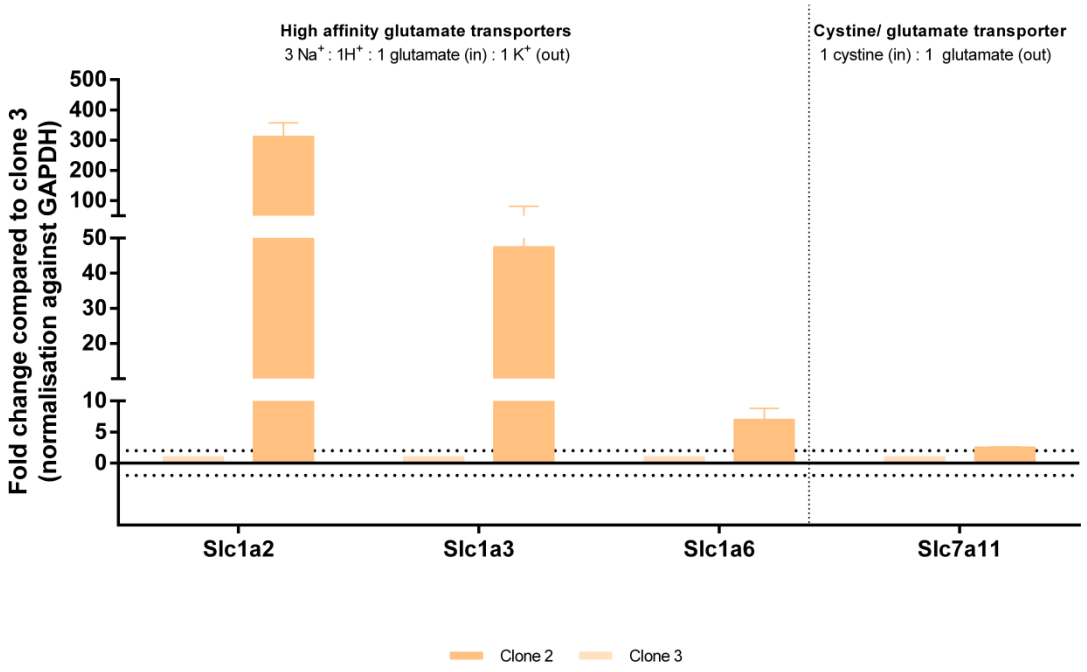

Figure 46: Expression levels of five high affinity glutamate transporters (SLC1a2, SLC1a3, SLC1a6 and SLC7a11) in CHO suspension clones 2 and 3.

Both clones were cultured and passaged regularly in Cellvento^{TM} CHO-220. For passaging of clone 3, medium was supplemented with glutamine and puromycine (n=3). Both CHO suspension clones were either seeded at 2 or $3*10^5$ C/mL, incubated at 37 °C, 5 % CO_2, 80 % humidity and agitated at 320 rpm. RNA was isolated via column binding and washing steps. Eluted RNA was quantified via spectrophotometry. TaqMan based generation of cDNA was used. Endogenous GAPDH levels were used as control. Target genes in samples were calculated and compared with expression levels in clone 3. The relative amounts of target genes were calculated applying the ΔΔCt method. Differences in relative mRNA expression level of at least 2 fold was considered as differentially expressed. Values are means +/- SEM.

Since clone 2 showed optimal performance in fed-batch but not in batch mode and highest glutamate transporter expression levels amongst the tested clones were detected, these data may indicate uptake differences of SSC*Na via differences in culture mode dependent glutamate transporter participation. Summarized, the high producing clone 2 showed highest expression levels of all herein presented glutamate transporters amongst the three tested clones and was used for further studies.

5.10.4.2.L-glutamate transporter inhibition tests using clone 2

With this information in mind, the question of impacts on growth in SSC*Na containing medium together with L-glutamate transporter inhibitors arose. Based on the hypothesis that L-glutamate and SSC*Na competed for one or more L-glutamate transporters due to structural similarity of both molecules, it was assumed that addition of L-glutamate transporter blockers to SSC*Na containing medium may have led to strikingly impaired amino acid uptake and cell growth.

To test this hypothesis, first dose response tests of selective L-glutamate transport inhibitors in batch experiments using basal formulated CHO 220™ medium were carried out to determine their appropriate concentrations for future experiments. It was aimed to monitor comparable growth of clone 2 cells in control media and media supplemented with transporter inhibitors.

The blocker dihydrokainic acid was used to block specifically SLC1a2 while the inhibitor UCPH-101 was applied to inhibit specifically SLC1a3. Aiming out to block both high affinity transporters simultaneously, SLC1a2 and SLCa3, TFB-TBOA was used for inhibition studies. For SLC7a11, (S)-4-carboxyphenylglycine was used to efficiently inhibit its transporter function. Since most of the literature showed only data from short-lasting pharmacological L-glutamate transporter inhibition experiments, first, higher inhibitor concentration ranges were tested in longer-lasting batch using L-cysteine deficient Cellvento™CHO-220 medium supplemented with 25 µM MSX. Dose response tests were carried out before the actual batch experiment to determine the appropriate inhibitor concentrations aiming out to find those inhibitor concentrations wherein cell growth was not impacted (data not shown). The determined inhibitor concentrations were 1 µM for UCPH-101, 10 µM for dihydrokainic acid, 0.3 µM for TFB-TBOA and 25 µM for (S)-4-carboxyphenylglycine. These concentrations were added to a L-cysteine depleted medium supplemented with 1.5 mM SSC*Na-B to investigate if L-glutamate transport blocking may have additionally impacted growth in SSC*Na containing medium.

As shown in figure 47, three different controls were used: the positive control using basal formulated CHO 220™ medium containing L-cysteine and L-glutamate, the negative control L-glutamate-free CHO 220™ medium and L-cysteine deficient CHO 220™ medium supplemented with 1.5 mM SSC*Na-B. The latter two controls were used to monitor possible effects of inhibitors on L-glutamate or L-cysteine derivative uptake.

Cell growth was observed in the positive control with reaching its maximum VCD on day 4 of culture (99.2 +/- $1*10^5$ C/mL). No cell growth was observed in L-glutamate-free medium possibly indicating that L-glutamate may be needed as a necessary nutrient for cell growth. Lowered cell growth was observed in inhibitor free SSC*Na containing medium with reaching its maximum VCD on day 3 (33.1 +/- $0.5*10^5$ C/mL). Maximum VCDs were similar in UCPH 101 (28 +/- $1.3*10^5$ C/mL), dihydrokainic acid (29.5 +/- $1*10^5$ C/mL), TFB-TBOA (31.1 +/- $1*10^5$ C/mL) and (S)-4-carboxyphenylglycine conditions (38.7 +/- $0.1*10^5$ C/mL) compared to inhibitor free SSC*Na on day 3 of culture.

Rapid cell death was observed in the inhibitor free SSC*Na condition between days 3 (33.1 +/- $0.5*10^5$ C/mL) and 4 (9.8 +/- $0.3*10^5$ C/mL) of culture representing a 3.4 fold VCD reduction in the SSC*Na condition. In the inhibitor containing SSC*Na conditions, rapid cell death was also observed in this period of culture.

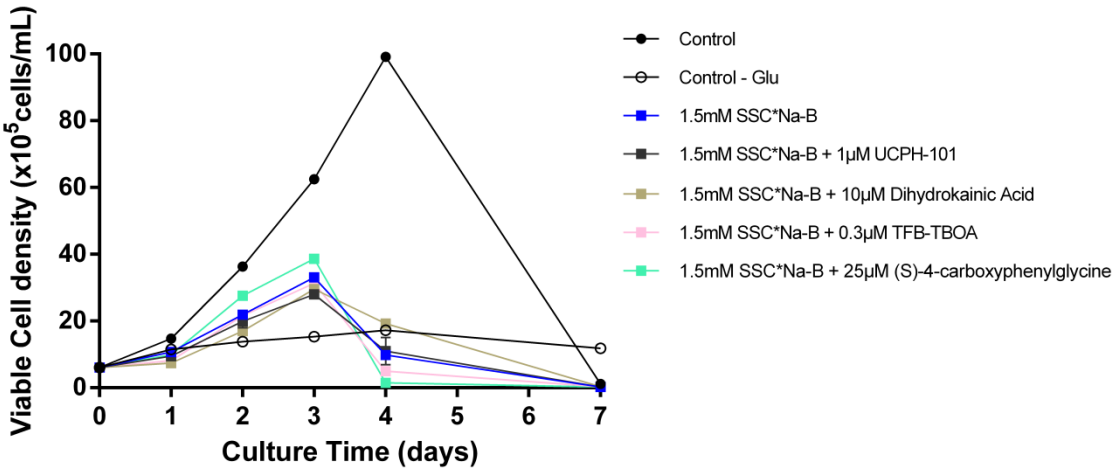

Figure 47: Evaluation of L-glutamate transporter inhibition of cells grown in L-cysteine depleted medium supplemented with 1.5 mM SSC*Na in batch test using clone 2.

L-cysteine depleted medium was supplemented with 1.5 mM SSC*Na-B and different inhibitors in different concentrations (1 µM UCPH-101, 10 µM dihydrokainic acid, 0.3 µM TFB-TBOA, 25 µM (S)-4-carboxyphenylglycine. After pre-passaging clone 2 cells twice in these media, batch process was started. Clone 2 cells were seeded in $6*10^5$ C/mL. Incubation was carried out at 37°C, 5 % CO_2, 80 % humidity and at 320 rpm. VCD of batch experiments using glutamate transporter inhibitor concentrations determined in preliminary experiments. Values are means +/- SEM.

On day 4 of culture, similar low VCD were observed in UCPH 101 (11 +/- $4*10^5$ C/mL), dihydrokainic acid (19.2 +/- $0.6*10^5$ C/mL), TFB-TBOA (5 +/- $0.2*10^5$ C/mL) and (S)-4-carboxyphenylglycine conditions (1.5 +/- $0.4*10^5$ C/mL) compared with the inhibitor-free SSC*Na condition. No significant differences in AUC of all SSC*Na containing conditions were observed. No additional effect on cell death of clone 2 in batch experiments using SSC*Na containing medium was observed when L-glutamate inhibitors were added. These data possibly indicate that the hypothesis of competition of L-glutamate and SSC*Na for one or several L-glutamate transporters leading to strikingly impaired growth might not be maintained in the tested inhibitor concentrations and in the used culture mode.

5.10.5. Evaluation of extracellular pH in batch and fed-batch experiments using 15 and 20 mM SSC*Na

Since the previously shown data did not support the hypothesis of transporter competition of SSC*Na and L-glutamate strikingly impairing amino acid uptake and cell growth, another hypothesis was considered. Since cell death in batch and fed-batch mode between days 3 and 4 and 7 and 10, respectively, was rapid and drastic, it was decided to direct the focus on a culture parameter which might change quickly. Therefore, the measurement of the culture broth pH was used as a readout.

As shown in figure 48 A, rapid cell death was reproduced between in 1.5 mM SSC*Na-B days 3 and 4 compared with control in batch experiments using clone 2. With regard to fed-batch experiments,

prolonged growth and cell death were reproduced with theoretically 15 mM and 20 mM SSC*Na-B, respectively, compared with control as shown in figure 48 B. With regard to batch experiments, culture broth pH dropped rapidly within 7 hours on day 3 from pH 6.31 to pH 5.81 +/- 0.01 in 1.5 mM SSC*Na-B compared with unchanged pH in control (pH 6.36 and pH 6.3 +/- 0.01, respectively) as shown in figure 48 C.

With regard to fed-batch experiments, two pH drops between days 5 and 6 and 6 and 7 were monitored in 20 mM SSC*Na-B compared with 15 mM SSC*Na-B and control as shown in figure 48 D. The first extracellular pH drop between days 5 and 6 in 20 mM SSC*Na-B was observed ranging from pH 6.67 +/-0.01 to pH 6.18 +/- 0.01 within 10.5 hours, respectively, while pH in 15 mM SSC*Na-B (pH 6.71 and pH 6.73 +/- 0.01, respectively) and control (pH 6.76 +/- 0.03 and pH 6.8 +/- 0.04, respectively) did not change. Higher pH differences were observed in 20 mM SSC*Na-B in this period (ΔpH=0.49) compared with 15 mM SSC*Na-B (ΔpH=0.02) and control (ΔpH=0.04). After this first pH drop, the extracellular pH increased and no cell death was observed after this first pH shift.

The second pH drop between days 6 and 7 in 20 mM SSC*Na-B was observed from pH 6.56 +/- 0.01 to pH 6.31 +/- 0.01 within 18.5 hours, respectively, while pH in 15 mM SSC*Na-B (pH 6.77 +/- 0.01 and pH 6.71, respectively) and control (pH 6.93 +/- 0.04 and pH 6.77 +/- 0.03, respectively) did not change. Higher pH differences were observed in 20 mM SSC*Na-B (ΔpH=0.25) in this period compared with 15 mM SSC*Na-B (ΔpH=0.06) and control (ΔpH=0.16). Possibly, the cells did not survive the series of pH shifts. These data possibly indicate that the observed cell death in 1.5 mM SSC*Na in batch and in 20 mM SSC*Na in fed-batch mode may result from rapid and drastic pH drops.

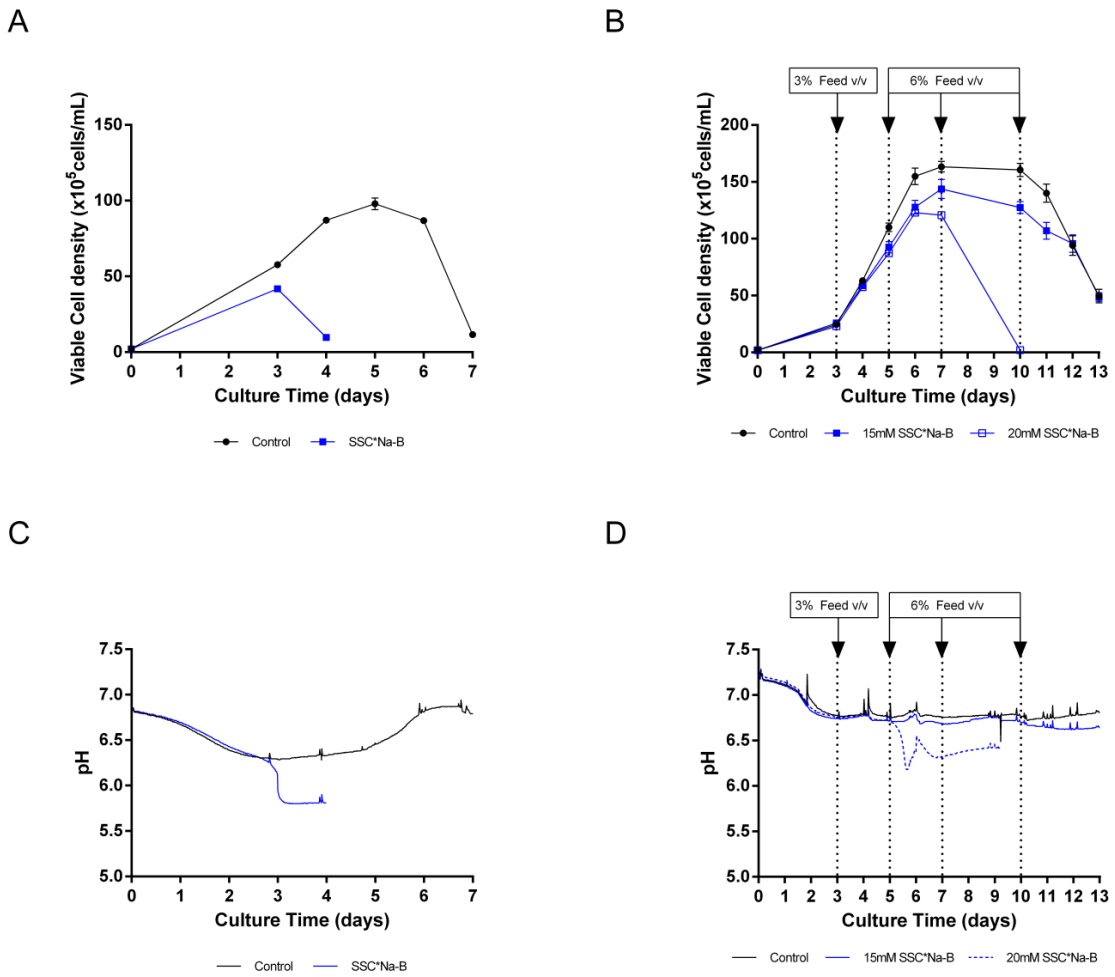

Figure 48: Spin tube batch and fed-batch experiments with neutral pH feed containing different SSC*Na-B concentrations using CHO suspension clone 2.

For batch experiments, 1,5 mM SSC*Na-B was added to a L-cysteine depleted Cellvento^{TM} CHO-220 medium. Performance was compared to the medium supplemented with 1.5 mM L-CysHCl*H_2O (n=3). For fed-batch experiments, different theoretic SSC*Na-B concentrations (15 and 20 mM) were integrated in the main feed with 30 mM PTyr2Na$^+$ at neutral pH (single feed system). To ensure initial growth, medium containing 1.5 mM L-CysHCl*H_2O was used. In the control condition, L-cysteine was added separately in an alkaline feed (n=5). Suspension CHO clone 2 cells were seeded at 2*10^5 C/mL, incubated at 37 °C, 5 % CO_2, 80 % humidity and agitated at 320 rpm. Feed was added at 3 % (v/v) at day 3 and 6 % (v/v) at days 5, 7 and 10. (A) VCD of batch experiment. (B) VCD of fed-batch experiments. (C) Culture broth pH in batch experiments over time. (D) Culture broth pH in batch experiments over time. Culture broth pH was measured using non-invasive, pre-calibrated pH sensor patches .Values are means +/- SEM.

In conclusion, the phenomena of reproducible and culture time-dependent rapid cell death in batch mode with 1.5 mM SSC*Na and in fed-batch with 20 mM SSC*Na may not be related to the hypothesis of L-glutamate transporter competition of SSC*Na and amino acids. The observed drastic decreases in VCD and viability in both modes may be rather correlated to the observed massive extracellular pH drops in the SSC*Na conditions in both modes when using clone 2.

5.10.6. Rescue options of toxic SSC*Na conditions in fed-batch mode

Since it was previously shown that drastic changes of culture broth pH in toxic SSC*Na conditions in batch and fed-batch mode may be correlated to the observed cell death, three rescue options were hypothesized to protect clone 2 cells from pH related cell death in fed-batch mode.

First, the obvious method to regulate culture broth pH was adding base. To test this, the base sodium carbonate was chosen since pH regulation in bioreactors was carried out with this base. To test if base addition rescued the culture, sodium carbonate was separately spiked in the culture broth in case of decreasing culture broth pH trends.

As previously mentioned, structural similarity of SSC*Na and L-glutamate was proposed (Belaidi and Schwarz 2013). Based on this fact, it was second hypothesized that SSC*Na might be taken up regularly by L-glutamate transporters belonging to the high affinity glutamate transporter class SLC1. Since these transporters were highly affine for L-glutamate, it was assumed that it was affine for SSC*Na, too, and they were highly expressed in clone 2 cells as previously shown. With this idea in mind, one idea was to exploit the function principle of these transporters in terms of extracellular pH regulation. Since three sodium ions and one proton were imported when one L-glutamate molecule (SSC*Na) was taken up, this effect might have been driven by applying high extracellular L-glutamate concentrations while feedings. Based on the hypothesized SSC*Na import via L-glutamate transporters, it was first assumed that extracellular L-glutamate addition might change the ratio of SSC*Na and L-glutamate for uptake via L-glutamate transporters. Due to this, possible toxic effects might be prevented. Second, increased extracellular L-glutamate concentrations might drive the import of protons leading to increased extracellular pH.

As previously shown, beneficial effects on culture performance with theoretically 20 mM SSC*Na were observed in SSC*Na batches containing copper concentrations > 60 µg/g. Moreover, the beneficial effects of 15 mM SSC*Na in fed-batch were correlated to increased SOD-1 and SOD-2 expression in the late culture phase compared with control. Due to this, it was hypothesized to augment their activity by increasing copper concentrations while feeding.

As shown in figure 49 A, cell death between days 7 and 10 was reproduced in theoretically 20 mM SSC*Na-B compared with control and rescue options. While cell death was observed in 20 mM SSC*Na-B between days 7 and 10, final VCD were similar in control (49.6 +/- $6*10^5$ C/mL) and 20 mM SSC*Na-B and 14 µM Cu (II) sulfate (46 +/- $2.6*10^5$ C/mL) while higher final VCDs were detected in 20 mM SSC*Na-B and sodium carbonate ($74.2*10^5$ C/mL), 20 mM SSC*Na-B and 203.2 mM sodium L-glutamate (58.5 +/- $3.6*10^5$ C/mL). These data possibly indicate that the applied rescue options protected the cells from cell death in 20 mM SSC*Na-B between days 7 and 10.

As shown in figure 49 B, no cell death was observed in the rescue conditions.

While cell death was observed in 20 mM SSC*Na-B between days 7 and 10, final viabilities of control (20.2 +/- 2.7 %), 20 mM SSC*Na-B and 203.2 mM sodium L-glutamate (25.3 +/- 0.5 %) and 20 mM SSC*Na-B and 14 µM Cu (II) sulfate (20 +/- 0.8 %) were similar while 20 mM SSC*Na-B and sodium carbonate showed higher final viabilities (58.4 %). These data possibly indicate that the rescue options prevented cell death in 20 mM SSC*Na-B with sodium carbonate spiking being the most efficient method.

As shown in figure 49 C, since cell death was observed in 20 mM SSC*Na-B between days 7 and 10, lowest final IgG were detected in this condition (273.6 +/- 3.6 mg/L) on day 10. Similar higher final IgG concentrations on day 13 were observed in 20 mM SSC*Na-B and sodium carbonate (1550.7 +/- 99.2 mg/L) and 20 mM SSC*Na-B and 203.2 mM sodium L-glutamate (1378.2 +/- 94 mg/L) compared with control (1087 +/- 35.4 mg/L) and 20 mM SSC*Na-B and 14 µM Cu (II) sulfate (895 +/- 82.1 mg/L). These data possibly indicate that prevented cell death in rescue conditions containing carbonate and L-glutamate improved the titer.

As shown in figure 49 D, similar NH_3 production profiles were obtained in control and 20 mM SSC*Na-B and sodium carbonate while the other rescue conditions showed increased NH_3 production. Final NH_3 levels in control (3.2 +/- 0.2 mM) and 20 mM SSC*Na-B and sodium carbonate (2.1 +/- 0.6 mM) were lower compared with 20 mM SSC*Na-B and sodium L-glutamate (6.9 +/- 0.2 mM) and 20 mM SSC*Na-B and Cu (II) sulfate (7.1 +/- 0.1 mM).

These data possibly indicate that NH_3 production was connected to pH: the higher the extracellular pH, the lower the produced NH_3 concentration. As shown in figure 49 E, two pH drops were reproduced in 20 mM SSC*Na-B compared with the other conditions. No pH drops were observed in the rescue conditions and in the control. Final pH was higher in 20 mM SSC*Na-B and sodium carbonate (pH 6.93) followed by control (pH 6.805 +/- 0.025), 20 mM SSC*Na-B and Cu (II) sulfate (pH 6.67 +/- 0.01) and 20 mM SSC*Na-B and sodium L-glutamate (pH 6.59 +/- 0.01). These data indicate that the rescue methods showed no pH drops and prevented the cells from death with carbonate being the most powerful option amongst the tested methods.

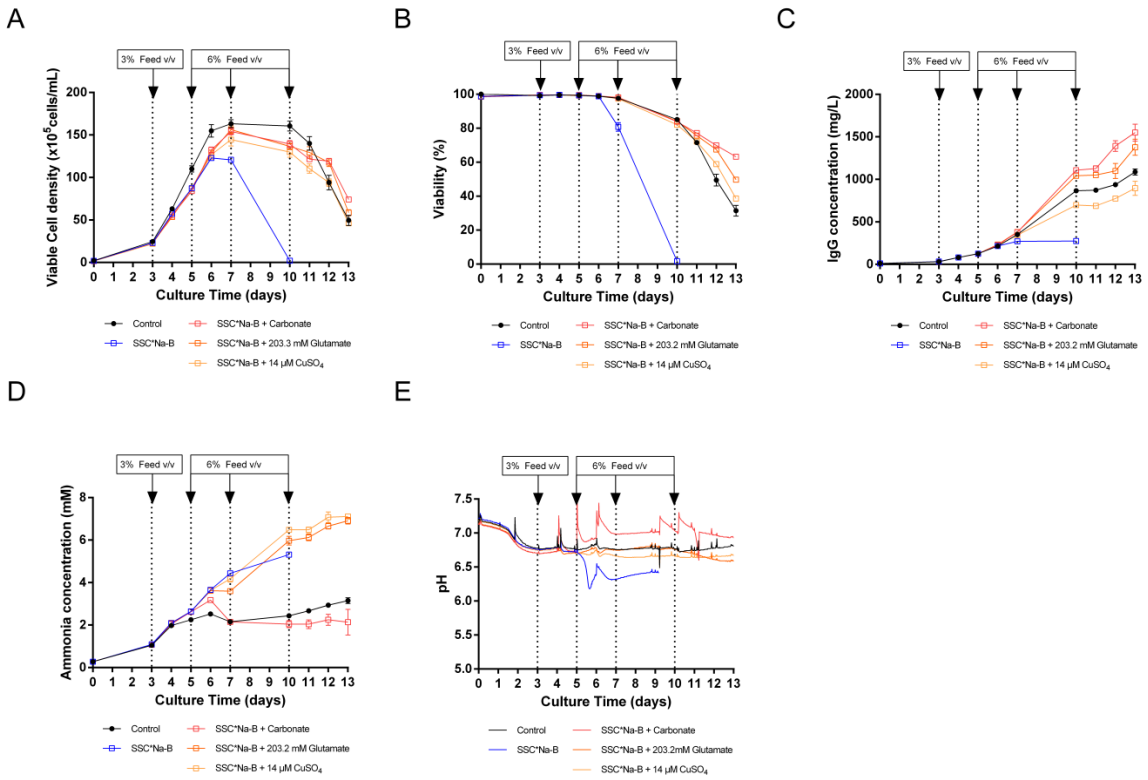

Figure 49: Rescue options of spin tube fed-batch experiments with neutral pH feed containing theoretically 20 mM SSC*Na-B using CHO suspension clone 2.

Theoretically 20 mM SSC*Na-B were integrated in the main feed with 30 mM PTyr2Na$^+$ at neutral pH (single feed system). To ensure initial growth, medium containing 1.5 mM L-CysHCl*H_2O was used. In the control condition, L-cysteine was added separately in an alkaline feed (n=5). In the carbonate condition, sodium carbonate was spiked in separately as necessary. In the L-glutamate condition, the single feed contained a final concentration of 203.2 mM sodium L-glutamate. In the copper sulfate condition, the single feed contained a final copper sulfate concentration of 14 µM. Suspension CHO clone 2 cells were seeded at 2*10^5 C/mL, incubated at 37 °C, 5 % CO_2, 80 % humidity and agitated at 320 rpm. Feed was added at 3 % (v/v) at day 3 and 6 % (v/v) at days 5, 7 and 10. (A) VCD. (B) Cellular viability. (C) IgG concentrations in the supernatants measured by turbidometric method. (D) NH_3 concentrations in the supernatants measured using photometry. (E) Culture broth pH was measured using non-invasive, pre-calibrated pH sensor patches. Values are means +/- SEM.

In conclusion, the phenomena of reproducible and culture time-dependent rapid cell death in fed-batch mode using 20 mM SSC*Na was prevented either by spiking of the base sodium carbonate, feeding of increased sodium L-glutamate or Cu (II) sulfate concentrations. The observed drastic decreases in extracellular pH were prevented with all three methods with sodium carbonate spiking being the most efficient amongst the tested options. Prolonged growth and increased titers were partially observed such as in rescue options with sodium carbonate and sodium L-glutamate.

6. Discussion and Perspectives

This study focused on the establishment of a single feed strategy for fed-batch processes using recombinant mAb producing CHO suspension clones. The state-of-the-art fed-batch process used L-cysteine and L-tyrosine in a separate alkaline feed since both amino acids showed stability and solubility issues at neutral pH, respectively. Therefore, this work aimed to screen for a L-cysteine derivative which might be integrated together with the L-tyrosine derivative PTyr2Na$^+$ (Zimmer et al. 2014) in one complex, chemically defined neutral pH feed, without impacting or even improving growth, titer and cQA of the produced mAb in CHO suspension fed-batch processes.

In the stability study of this work, besides stability of SSC*Na over three months in a complex, chemically defined neutral pH feed, lowered thiamine levels were observed in the SSC*Na containing feed compared with the L-cysteine containing feed and the control feed after three months of storage at 4°C. It was shown for the first time that the L-cysteine derivative SSC*Na might serve as a L-cysteine source in batch experiments using CHO suspension clone 1. SSC*Na was shown to work as a L-cysteine source in fed-batch tests using CHO suspension clone 2. Further, prolonged growth and increased titer were detected in fed-batch experiments with 15 mM SSC*Na using clone 2 compared with the state-of-the-art process. For the description of the positive effects by 15 mM SSC*Na, increased intracellular total glutathione concentration, increased SOD-1 and SOD-2 levels and lowered intracellular ROS levels were observed compared with the state-of-the-art process.

As a consequence of dose response studies with SSC*Na in fed-batch studies using clone 2, SSC*Na was found to be toxic in a theoretic concentration of 20 mM. Rapid and drastic cell death was reproduced between days 7 and 10 of culture when using 20 mM SSC*Na compared with control. Extracellular pH measurements revealed a drastic pH drop when using 20 mM SSC*Na in fed-batch mode compared with control as well as in batch mode when using 1.5 mM SSC*Na compared with control.

6.1. Use of SSC*Na as a replacement for L-cysteine

6.1.1. Stabilization of feed formulations

6.1.1.1. The L-cysteine containing complex, chemically defined, highly concentrated neutral pH feed

With regard to the L-cysteine containing feed, more vitamins were impacted with respect to their stability compared with SSC*Na containing and control feed. In this study, riboflavin, folic acid and vitamin B12 concentrations were lower in the L-cysteine containing feed compared with the control and the SSC*Na containing feed.

Auto-oxidation of L-cysteine was reported to take place leading to the generation of H_2O_2 (Nath and Salahudeen 1993) and may have occurred in the L-cysteine containing feed used in the stability study of this work. Several vitamins were reported to be sensitive towards H_2O_2 such as riboflavin and thiamine (Ribeiro et al. 2011) and vitamin B12 (Nazhat et al. 1989). In the presence of iron, hydroxyl radicals were reported to be produced from H_2O_2 at neutral pH in a Fenton-type reaction (Puppo and Halliwell 1988). Since feed contained iron salts, it may be speculated that hydroxyl radicals might have been produced from H_2O_2 in the L-cysteine containing feed of this study. The vitamin folic acid was reported to be susceptible towards hydroxyl radicals (Patro et al. 2005).
It may be assumed that vitamin loss in the L-cysteine containing feed presented in the stability study of this work may have been caused indirectly by L-cysteine.

6.1.1.2. The SSC*Na containing complex, chemically defined, highly concentrated neutral pH feed

Only thiamine concentration was significantly negatively affected in the SSC*Na containing feed compared with L-cysteine containing feed and control. It may thus be concluded that lowered thiamine recovery in SSC*Na feed is specifically related to the presence of the derivative.
Due to the use of SSC*Na in this study, its dissociation in sodium ion and Cys-SO_3^- in aqueous solution is concluded. To further speculate about i) direct interactions of thiamine with the -SO_3^- group of SSC or ii) SSC cleavage into L-cysteine and sulfite followed by reaction of thiamine with sulfite, one might highlight the quantification methods for thiamine, SSC and sulfate used herein. In this study, ~20 % of thiamine was lost in neutral pH feed containing SSC*Na after three months compared with the control as quantified by UHPLC-MS/MS. This method showed a standard deviation of 15 %. Since thiamine concentration in the feed is formulated to be in the nmol/L (nM) range, the technical variation of the UHPLC-MS/MS method is in the nM range. SSC and L-cysteine quantification was carried out using the UPLC method which has a standard deviation of 10 %. Sulfate was quantified using IC. Since the SSC*Na and sulfate concentrations in the feed are formulated to be in the mM range, the technical variations of the UPLC and IC methods are in the mM range. Consequently, it may be concluded that the UHPLC-MS/MS method for thiamine quantification is more sensitive compared with the UPLC and IC methods for SSC and sulfate quantification. Connecting the different sensitivities of the used quantification methods with the aforementioned assumed interactions of thiamine with SSC, one might detect changes in thiamine concentration while changes in SSC, sulfate or generated L-cysteine concentrations might not be followed.
Concerning possible direct interactions of SSC and thiamine, it may be assumed that the vitamin may have interacted with SSC via their sulfur atoms. Since in this work interaction of GSH with SSC was

shown to result in the formation of mixed disulfides in cell free studies, it may be hypothesized that the sulfur-containing vitamin thiamine may have interacted with SSC via thiol-disulfide exchange thereby generating mixed disulfides. Since the existence of the thiamine disulfide derivatives e.g. thiamine propyldisulfide, thiamine tetrahydrofurfuryl disulfide, thiamine disulfide was reported as reviewed (Kruglikova-L´vova, 1970), some of them might have exist in the SSC*Na containing feed of this study, too.

With regard to the assumed SSC cleavage and sulfite release, thiamine might have interacted with free sulfite. Cleavage of thiamine by sulfite at 25°C and pH 5 was reported to yield two structurally not further characterized species (Williams et al. 1935). It was proposed that the reaction of equimolar concentrations of thiamine with sulfite led to the formation of (6-amino-2-methylpyrimid-5-yl)methanesulfonic acid and 5-β-hydroxyethyl-4-methylthiazole. The underlying reaction mechanism was assumed to be a nucleophilic displacement reaction (Leichter and Joslyn, 1969) which was supported by other groups (Zoltewicz et al. 1984).

To confirm interactions of SSC with thiamine, one might study cell free interaction of both molecules with each other in a different, less complex matrix as the used neutral pH feed, such as water. To study possible interactions of SSC with thiamine, one might incubate 15 mM SSC*Na with thiamine in the concentration used in the Cellvento™ Feed 220 and vary incubation time, pH and temperature. Samples from the corresponding conditions might give information about the recovered vitamin concentration via UHPLC-MS/MS analysis and SSC concentration via UPLC analysis. Further, MS analysis might help to identify possible interaction products.

6.2. Simplification of fed-batch processes

The development of a neutral pH feed comprising SSC*Na and PTyr2Na$^+$ as L-cysteine and L-tyrosine derivatives allowed rapid and simplified feeding. In feeding periods with the neutral pH single feed containing SSC*Na, no intense pH regulation via CO_2 gassing in bioreactors has been needed compared with the standard process. Further, application of the two-feed strategy was based on the use of separate filters for the alkaline L-cysteine feed and the slightly acidic main feed. By this, mixing of both solutions and resulting L-cystine precipitations and blocking in the filters were avoided. However while feedings, both feed solutions became mixed in the bioreactor leading to precipitations in the broth.

By the use of the neutral pH single feed, only one filter was needed for feeding procedures. No precipitations occurred in the broth when using the single feed strategy thereby simplifying handling while feedings compared with the standard procedure.

The state-of-the-art control fed-batch process used in this work was characterized by the use of a separate alkaline L-cysteine feed. The addition of this alkaline L-cysteine feed to CHO suspension cultures resulted in culture broth pH peaks. By the use of the single feed strategy, no culture broth pH peaks were observed since this feed was kept at neutral pH. The feeding procedures in the state-of-the-art control fed-batch process took up to two hours since only careful and slow addition of the alkaline L-cysteine feed ensured moderate pH increases from the adjusted culture pH 6.95 +/- 0.15 to maximum allowed pH 7.4. Studies of recombinant CHO cultures at pH 7.6 in batch mode revealed premature decrease in VCD, viability and titer compared with cultures grown at pH 7.0 (Kim and Lee 2007) and exposure of mammalian cell to pH 9.6 for 10 minutes led to sustainable inhibited cell growth compared with cell cultured at pH 7.3 (Burroni and Ceccarini 1984). Based on these results, it might be hypothesized that impacts on cell cultivation and titer might have temporarily occurred when a moderately increased culture pH was present while feeding the alkaline L-cysteine feed in the state-of-the-art fed-batch process. To avoid an overshoot in culture pH while feeding the alkaline L-cysteine feed, the addition of the slightly acidic main feed was carried out. But CO_2 addition was the main factor to regulate culture pH. Due to this, negative impacts of increased partial pressure levels of CO_2 (pCO_2) on growth and titer while feedings might be hypothesized in the state-of-the-art fed-batch process. As reported, increased pCO_2 levels negatively impacted VCD, viability and specific productivity in bioreactor CHO suspension cell cultures compared with the standard process. Researchers suggested a relation between solubilized CO_2 concentration and imbalanced intracellular pH homeostasis (Gray et al. 1996). Further, with increased pCO_2, decreased VCD and viabilities were observed in a recombinant hybridoma cell line (deZengotita et al. 1998). In recombinant *Sf-9* bioreactor cultures, reduced protein production was observed in conditions with elevated dissolved CO_2 levels compared with control (Garnier et al. 1996). Based on these reported observations, one might not exclude impacts on VCD, viabilities and titer in the period of feeding in the state-of-the-art fed-batch process.

To study possible impacts of alkaline culture pH, one might carry out state-of-the-art fed-batch bioreactor cultures with differently allowed maximum pH while feeding starting from pH 7.4 as control up to pH 9.6 while applying one fixed CO_2 concentration at all tested pH. While testing different pH overshoots on growth and titer in feedings procedures, one might collect samples for quantification of VCD, viability and titer after different time points to follow possible changes. To investigate possible toxic effects of pCO_2 while feedings in the state-of-the-art fed-batch bioreactor process, one might allow the regularly accepted maximum pH 7.4 and regulate culture pH with varying CO_2 concentrations in the inlet keeping one O_2 concentration fixed. While testing different CO_2 concentrations on growth and titer in feeding procedures, one might collect samples for quantification of VCD, viability and titer after different time points to follow possible changes.

6.3. L-cysteine production from SSC

In this work, replacement of L-cysteine by SSC*Na was shown to be possible in CHO suspension clone 1 without impacting growth. In the SSC condition, only low L-cystine concentrations were detected in the supernatants of clone 1 cultures compared with control while in both conditions no extracellular L-cysteine was monitored. In fed-batch cultures of clone 2 using 15 mM SSC, higher extracellular sulfate concentrations were measured compared with control. These data may indicate intracellular SSC cleavage into L-cysteine and sulfate. Further, after spiking SSC*Na to cell lysates, no SSC was detected indicating enzymatic conversion of SSC. To mimic the fate of SSC in cells, cell-free interaction of the intracellular anti-oxidant GSH and SSC was studied *in vitro*. This study revealed interaction of SSC and GSH leading to the formation of GSSG and the mixed disulfides GS-Cys and GS-SO_3. These spontaneous thiol-disulfide exchange products were already described in the literature. GS-Cys is known to be an oxidation product of GSH and L-cysteine in PBS (Yoshiba-Suzuki et al. 2011). The mixed disulfide GS-SO_3 was found to be present *in vivo* in several studies (Robinson and Pasternak, 1964; Togawa et al. 1988; Waley 1959). Increasing amounts of mixed disulfides were detected over time suggesting that these compounds may have served as storage for L-cysteine equivalents in the cell (Togawa et al. 1988).

In this work, spiking of SSC or SSC-GSH mixtures to clone 2 lysates resulted in complete SSC metabolisation or decreased mixed disulfide concentrations, respectively, while L-cysteine was concomitantly produced. From this observation, it may be assumed that SSC and SSC-GSH mixed disulfides may serve as substrates for intracellular enzymes. Preceeded IAM treatment of clone 2 lysates before SSC spiking inhibited SSC metabolisation. Based on these data, it may be assumed that SSC metabolizing enzymes may be inhibited by IAM. Literature data revealed that thiol-disulfide oxidoreductase glutaredoxin (GRX) was able to cleave the mixed disulfide SSC-GSH (Gladyshev et al. 2001) via deglutathionylation (Gallogy and Mieyal, 2007). The enzymes activity was shown to be inhibited by IAM (Gladyshev et al. 2001). In *Escherichia coli*, SSC was reported to be a component in the L-cysteine biosynthetic pathway being reduced by GRX and thioredoxin (TRX) isoforms to yield L-cysteine (Nakatani et al. 2012). Although L-cysteine synthesis is highly different in bacteria and plants compared with mammalian cells, it may be suggested that cleavage mechanisms of mixed disulfides in mammalian cells expressing GRX and TRX oxidoreductases exist. Summarized, from the results presented in this study it may be assumed that SSC may be taken up the CHO suspension cells. After cell entry, SSC may interact with GSH leading to the formation of mixed disulfides. These molecules may be than reduced back by GRX and TRX oxidoreductases yielding L-cysteine (see Hecklau et al. 2016).

To study if GRX and TRX may be able to cleave the mixed disulfides GS-Cys and GS-SO_3, one might carry out cell-free incubation tests. To do so, one may test the following conditions in the absence of cells: i) incubation of GS-Cys with GRX, ii) incubation of pre-treated GRX with IAM and GS-Cys, iii) incubation of GS-SO_3 with GRX, iv) incubation of pre-treated GRX with IAM and GS-SO_3, v) incubation of GS-Cys with TRX, vi) incubation of pre-treated TRX with IAM and GS-Cys, vii) incubation of GS-SO_3 with TRX, viii) incubation of pre-treated TRX with IAM and GS-SO_3. For GRX tests, the cofactor GSH is needed and tests may be carried out in potassium phosphate buffer (pH 7.4) (Gladyshev et al. 2001). To test the thioredoxin system, NADPH and thioredoxin reductase are needed and tests may be carried out in potassium phosphate buffer at neutral pH (Holmgren 1979). After different incubation times, samples may be taken from the above suggested tests for UPLC analysis to quantify possibly generated L-cysteine/L-cystine.

6.4. Positive effects of SSC on culture performance

6.4.1. Anti-oxidant related mechanisms with SSC*Na use

The presented single-feed used in this study showed integration of the L-cysteine derivative SSC*Na together with $PTyr2Na^+$ (Zimmer et al. 2014) in a complex, chemically defined, highly concentrated neutral pH feed. In small scale fed-batch experiments using spin tubes and in 1.2 L bioreactor runs, the use of 15 mM SSC*Na showed prolonged cell growth and higher final titer with an overall increase in specific productivity compared with the standard fed-batch process. No SSC containing peptides were monitored in the IgG produced from single feed strategy compared with the standard process. This indicated no SSC integration in the native form of the mAb. To understand the mechanism of increased titer, several experiments were performed to monitor the oxidative status of the cells. Labelling of intracellular ROS by carboxy-H_2DCFDA in the 15 mM SSC*Na condition revealed lower intracellular ROS levels compared with the standard fed-batch. These data indicated an overall anti-oxidative effect of SSC. Several studies have already linked SSC to anti-oxidative mechanisms. SSC was shown to be involved in light-dependent redox regulation in the plant *Arabidopsis thaliana* (Bermudez et al. 2010). Disturbed ROS detoxification was observed in the absence of SSC synthase activity in chloroplasts. Due to this, the plant was not able anymore to protect itself from photochemical damage caused during long-day photoperiod (Gotor and Romero 2013). It was suggested that SSC might act as a mild anti-oxidant in the lumen inducing redox changes. By this, regulatory proteins may have been activated being important in the plant protection from photo-oxidative damage (Gotor and Romero 2013). For further investigation of the anti-oxidative potential of SSC, microarrays were performed on mRNA of CHO cells being extracted from different time points of small scale fed-batch cultures.

Performed microarrays showed highest up-regulation of the gene encoding for the anti-oxidant enzyme SOD-2 in the SSC*Na condition compared with the control. SODs are enzymes which catalyze the conversion of superoxide radicals into H_2O_2 and molecular oxygen (McCord and Fridovich 1969). SODs are involved in the decrease of intracellular ROS levels like glutathione peroxidase and catalase (Mannarino et al. 2011). Cs26 mutant plants which did not produce SSC were shown to be defective in photosynthesis. In these mutant plants, ROS production e.g. superoxide radical anions and H_2O_2 was increased (Gotor and Romero 2013). These data underline the positive effect of SSC on SOD activity. Although microarray tests did not reveal any gene expression modification of enzymes being involved in GSH synthesis, increased free intracellular total glutathione levels were higher in the SSC*Na condition throughout the cultures compared with control. This increased total glutathione pool in the SSC condition might explain prolonged viabilities in the SSC*Na condition compared with control since increased levels of the major intracellular anti-oxidant GSH may be used in detoxification processes. These detoxification processes might be based on direct radical or ROS scavenging or might rely on the conjugation of GSH to xenobiotics catalyzed by glutathione S transferase (Mari et al. 2009). Moreover, protection against oxidative damage may be achieved by the formation of reversible mixed disulfides of GSH with L-cysteine residues. This process of protein glutathionylation may reduce oxidative stress potentially leading to apoptosis and growth limitation in fed-batch cultures (Selvarasu et al. 2012). Further, protein glutathionylation was related to increased energy generation mediated by GSH- 5′-adenosine monophosphate-activated protein kinase (AMPK) or GSH-mitochondrial uncoupling protein 3 (UCP3) adducts (Mailloux et al. 2011; Zmijewski et al.2010). Further, the GSH pool, or more generally the intracellular redox status of the cells, may be responsible for the observed prolonged viability as reported (Banerjee 2012). Further, GSH may be responsible for the increased titer in the SSC condition. Up-regulation of the GSH pathway was shown to be present in high producing CHO cells monitored by -omics studies. As an example, CHO cells overexpressing the taurine transporter showed correlation of increased viabilities and titer with GSH metabolism confirmed by transcriptomic studies (Tabuchi et al. 2010). Proteins involved in the GSH pathway were shown to be up-regulated in high producers determined by proteomic approaches (Chong et al. 2012; Orellana et al. 2015). Besides correlated beneficial effects of GSH against oxidative stress, some additional factors such as the intracellular redox status may be connected to titer increases (Templeton et al. 2013). Limited productivity in CHO cells was linked to limitations in protein folding in the ER (Lappi and Ruddock 2011; Mohan and Lee 2010; Mohan et al. 2007). The environment of the ER is oxidizing thereby being able to introduce disulfide bridges into the secreted proteins. To assemble a functional mAb, a favorable GSH/GSSG ratio needs to be maintained. GSH may protect against hyperoxidizing conditions in the ER.

This is achieved by the consumption of excess oxidizing equivalents thereby correcting protein disulfide bond formation. Isomerization or reduction of incorrect generated disulfide bridges prior to degradation due to GSH may help to produce a correct mAb (Chakravarthi and Bulleid 2004; Cuozzo and Kaiser 1999; Kojer and Riemer 2014). Depletion of GSH may lead to aggregate formation and higher rate of incorrect folding of secreted proteins (Chakravarthi and Bulleid 2004; Molteni et al. 2004). The higher intracellular free GSH pool in the SSC*Na condition of this work may be correlated to increased folding of secreted proteins in the ER. Consequently, a higher secretory rate and higher final titers may be result. Summarized, the increased intracellular GSH pools in the SSC*Na condition might induce redox potential changes thereby impacting viabilities and mAb production machinery with special accentuation of protein folding in the ER (see Hecklau et al. 2016).

To further investigate the portion of different reactive species leading to oxidative stress in the cell, one might carry out intracellular ROS detection as described in this work by using different dyes for monitoring different reactive species. As an example, 2-[6-(4V-Hydroxy)phenoxy-3H-xanthen-3-on-9-yl]benzoic acid may be used in the detection of hydroxyl radicals while peroxide radicals may be detected by the use of e.g. cis-parinaric acid (Gomes et al. 2005). Superoxide radicals may be detected by e.g. hydroethidine. By the measurement of superoxide radicals, one might correlate hypothesized lower intracellular superoxide levels with the observed increased SOD levels in 15 mM SSC*Na. Further, one might follow the expression levels of transporters being involved in L-cysteine, L-cystine, L-glutamate and L-glycine uptake over time in fed-batches using 15 mM SSC*Na compared with control. These tests may help to investigate if uptake of these amino acids might be increased and might be consequently correlated to increased intracellular total glutathione levels in 15 mM SSC*Na compared with control. To understand the effect of protein glutathionylation on energy generation, one might measure intracellular ATP levels and expression levels of AMPK and/or UCP3 over the whole culture time in 15 mM SSC*Na compared with L-cysteine. To investigate a possible relation of increased titer, higher intracellular total glutathione pool and increased folding in 15 mM SSC*Na compared with control, one might carry out a dose response of non-toxic SSC concentrations (e.g. 5, 10 and 15 mM SSC*Na) compared with control. Daily intracellular total GSH measurements and supernatant antibody concentrations measurements over time in all conditions might help to support the connection of applied SSC*Na concentration, intracellular total GSH concentration and titer.

6.5. Toxic effects of SSC on culture performance

6.5.1. Relation of SSC*Na application and increased extracellular NH_3 and sulfate levels

As shown in this study, application of non-toxic SSC concentrations between 5-15 mM in fed-batch gave rise to increased extracellular NH_3 levels compared with control. Further, increased extracellular sulfate and thiosulfate concentrations were detected in non-toxic SSC*Na concentrations between 5-15 mM in fed-batch compared with control.

From the above described data it may be speculated that intracellular increased L-cysteine concentrations may have been present in cells being cultured with 15 mM SSC*Na compared with control. The metabolic conversion of 25 mM L-cysteine was studied in rat hepatocytes leading to the formation of increased NH_3 levels. This effect on NH_3 was not observed when using 25 mM cysteine sulfinate as a substrate. The authors suggested the involvement of cystathionine γ-lyase (cystathionase) in the metabolism of L-cysteine (Drake et al. 1987) as a mechanistic pathway leading to NH_3 generation.

Since higher extracellular sulfate concentrations were detected with SSC*Na compared with control, it might be speculated that more sulfate may be produced directly from SSC or from increased intracellular L-cysteine concentrations. With regard to sulfate production, early studies of L-cysteine oxidation in rat liver mitochondria revealed the conversion of L-cysteine yielding sulfate and pyruvate. Sulfate generation from L-cysteine decreased when L-cysteine was oxidized into L-cystine. This effect was partially overcome by addition of GSH (Wainer 1966). Increasing extracellular sulfate concentrations were detected in the supernatants of all SSC*Na conditions ≥ 5 mM compared with control. It may be assumed that the intracellular sulfate production in the SSC*Na conditions was in excess and the cells have transported excess sulfate outside of the cell. Individuals in rat experiments protected themselves against high sulfate concentrations. Feeding of rats with a diet containing higher sulfate concentrations resulted in increased sulfate concentrations in the urine compared with standard diet (Glazenburg et al. 1983). This adjustment of sulfate homeostasis may be achieved by sulfate transporter members of SLC classes e.g. SLC13 and SLC26 as reviewed (Alexander et al. 2013). An adaption of expression of SLC26a1 (sulfate/anion exchanger) expression in response to plasma sulfate concentration was demonstrated in the kidney of rainbow trout. An injection of increasing sulfate concentrations in the kidney resulted in a sulfate concentration peak accompanied by an increase in SLC26a1 expression (Katoh et al. 2006). This study indicates a transporter expression adaption in response to increased sulfate concentrations pointing out the importance of sulfate transporters in sulfate homeostasis which might have been also present in SSC*Na conditions.

To study the relation of excess sulfate and L-cysteine formation from SSC, one might carry out again fed-batch dose response tests using different non-toxic SSC concentrations (e.g. 5, 10 and 15 mM SSC*Na) compared with control.

In these conditions, one may follow intracellular L-cysteine, L-cystine and SSC concentrations as well as intracellular and extracellular sulfate concentrations. With regard to sulfate transporters, one may follow expression of sulfate transporters e.g. SLC26a1 and SLC13a1 (Markovich 2011) in SSC*Na conditions compared with control over time.

6.5.2. Types of acidosis

In this work, the use of SSC*Na either in batch or fed-batch mode led to a rapid drop in extracellular pH (acidosis) when using clone 2 cells. A connection between extracellular pH drop and drop in viability was assumed. The decrease in pH was suggested to be correlated with an extracellular acidosis. Patients suffering from diabetic ketoacidosis showed a decreased serum pH (Elisaf et al. 1996) and patients suffering from lactic acidosis showed low blood pH (Huckabee 1961). In any case, negative impacts of extracellular low pH (acidosis) on viability of different cultured cell lines were reported (Isaev et al. 2010; Lan et al. 1999; Stelmashuk et al. 2007). Since a rapid drop in culture pH was shown in batch mode with 1.5 mM SSC*Na using clone 2, it may be assumed that metabolically generated acids may have been present in toxic SSC*Na concentrations thereby affecting VCD and culture pH. With increasing added lactate concentrations, decreasing VCDs of a murine hybridoma cell culture were observed. Moreover, the intracellular drop in peak pH was more pronounced when lactate concentrations increased (Ozturk et al. 1991). In this work, different clones behaved differently to one SSC*Na concentration in one mode. While clone 1 grew similar in 1.5 mM SSC*Na compared with control, clone 2 died and clone 3 showed inhibited growth in the presence of 1.5 mM SSC*Na compared with control. Since a drop in external pH was observed with clone 2 in the presence of 1.5 mM SSC*Na, it may be assumed that the clones differed in their sensitivity towards metabolically generated acids in batch mode. Studies with isolated clones being resistant towards high lactate concentrations showed higher VCDs and prolonged growth in medium containing 60 mM lactate compared with the parental clone (Schumpp and Schlaeger 1992). Further, pH homeostasis regulating transporters may have been present differently in the used cell clones. As reported for mutant CHO fibroblasts lacking Na^+/H^+ transporter activity, cell death was more pronounced when extracellular pH decreased compared with wildtype cells (Pouysségur et al. 1984). Different levels of Na^+/H^+ transporter expression may have been present in the different clones in this study, assuming to impact behavior towards SSC*Na application in both batch and fed-batch experiments.

To investigate the production of metabolically generated acids, one may test the three clones in batch mode with different SSC*Na concentrations. Since clone 1 was shown to grow between 1.5 mM and 3 mM SSC*Na with observed cell death at 6 mM SSC*Na, one might test these SSC*Na concentrations again and follow intracellular and extracellular acidic metabolites such as lactic acid, 2-hydroxyisovaleric acid (Landaas and Jakobs 1977) and β-hydroxybutyrate

(Kamel and Halperin 2015). Further, intracellular oxaloacetate and acetyl-CoA levels might be followed since decreased oxaloacetate and increased acetyl CoA levels indicate diabetic ketoacidosis as reviewed (Stojanovich and Ihle 2011). Moreover, intracellular amino acids such as L-alanine, L-proline, L-valine and L-leucine may be followed since a relation of high levels of these amino acids and acidosis was reported in patients (Marliss et al. 1972). These compounds may be followed in experiments using clones 1 and 3 with SSC concentrations ≤ 1.5 mM SSC*Na (e.g. 0.5, 0.75, 1 and 1.5 mM SSC*Na). Further, one might evaluate the level of Na^+/H^+ transporter expression after a fixed number of pre-passages of all three clones to evaluate basal differences between them. This transporter is known to internalize sodium ions and extrude protons as reviewed (Malo and Fliegel 2006). Next, one may follow Na^+/H^+ transporter expression of all three clones in non-toxic and toxic SSC*Na conditions to investigate possible changes in relation to SSC*Na concentration.

6.5.3. Relation of extracellular pH drop to L-cysteine, sulfate, NH_3 and urea cycle in the application of toxic SSC*Na concentration

In this study, it was shown that the application of 20 mM and 1.5 mM SSC*Na led to a rapid and massive extracellular pH drop in fed-batch and batch cultures of clone 2 compared with the controls (15 mM CysHCl*H_2O and 1.5 mM CysHCl*H_2O), respectively. Moreover, different SSC*Na concentrations in fed-batch experiments with clone 2 showed SSC*Na concentration dependent extracellular sulfate concentrations compared with control.

In this study, higher extracellular sulfate concentrations were observed in SSC*Na conditions ≥ 5 mM compared with control. It might be first assumed that sulfate was generated from SSC cleavage. Secondly, SSC might have led to increased intracellular L-cysteine levels due to the presence of mixed SSC-GSH disulfides serving as a reservoir for L-cysteine. Increased L-cysteine in turn might have produced increased sulfate. The feeding of excess L-cysteine caused increased L-cysteine and L-cystine levels, increased plasma sulfate concentrations and an acute metabolic acidosis (Dilger and Baker 2008). Participation of Na^+/H^+ exchanger activity in the sulfate efflux in primary culture of renal proximal tubule epithelium in winter flounder was reported. Increased sulfate efflux was accompanied by an increased Na^+/H^+ exchanger activity in metabolic acidosis (Pelis et al. 2005). It might be speculated that the high extracellular sulfate concentrations observed in the toxic SSC conditions might be connected to increased sulfate export combined with increased Na^+/H^+ exchanger activity being responsible for extracellular acidification.

To investigate a relation between sulfate efflux, extracellular acidification and intracellular pH homeostasis, one might evaluate the expression levels of certain sulfate transporters e.g. SLC13a1 and SLC26a1 and Na^+/H^+ exchanger over time in batch and fed-batch mode in control, 15 and 20 mM SSC*Na.

This might be accompanied by the quantification of intracellular and extracellular sulfate concentrations. Further, to get information about Na^+/H^+ exchanger activity and function, one might follow intracellular pH by the use of the intracellular fluorescent probe 2',7'-bis(2-carboxyethyl)-5,6-carboxyfluorescein (BCECF) in control, 15 and 20 mM SSC*Na.

In all tested SSC concentrations, extracellular NH_3 levels were higher in SSC*Na concentrations $\geq$ 5 mM compared with control. Since higher NH_3 levels in fed-batch did not impact growth of clone 2 in 15 mM SSC*Na compared with control, it might be speculated that NH_3 itself might not be toxic to the cells. This effect was reported in a murine hybridoma cell line over 275 hours of cultivation. With increasing added NH_3 concentrations, VCDs decreased without initiation of cell death (Ozturk et al. 1991).

Since detoxification of NH_3 is primarily carried out via the urea cycle as reviewed (Dimski 1994), other studies tried to examine deeper the relation of acidosis, NH_3 and urea cycle. The urea cycle enzymes carbamoyl phosphate synthetase and ornithine transcarbamylase being responsible for the first two steps in NH_3 detoxification via urea cycle were reported to be present in CHO cells (Kim and Kim 2006). Further, extracellular ornithine was detected in studies culturing CHO-K1 cells in different media (Mohmad-Saberi et al. 2013). From these reports it may be assumed that NH_3 detoxification via urea cycle enzymes may have been present in the CHO clones used in this study. Induction of metabolic acidosis led to a decrease in rat plasma pH, plasma HCO_3^- concentrations and liver urea concentrations. Based on the obtained data, the authors suggested a relation between metabolic acidosis and inhibited NH_3 detoxification via the urea cycle (Molinas et al. 2015). To investigate a relation between urea cycle, external NH_3 and extracellular pH, perfusion studies of rat livers were carried out. Experiments revealed carbonic anhydrase-dependent urea synthesis in experiments with livers perfused with ammonium chloride (NH_4Cl). Low external pH decreased carbonic anhydrase activity leading to lowered enzymatic HCO_3^- generation and decreased urea synthesis (Häussinger and Gerok 1985). Since high NH_3 levels in SSC*Na conditions studied in this work might be related to metabolic acidosis, a relation of carbonic anhydrase-dependent urea synthesis might be hypothesized. Further, several human carbonic anhydrase isoforms were shown to be inhibited by sulfate (Innocenti et al. 2005), thus higher sulfate levels as observed in SSC*Na conditions in this study might have negatively impacted the enzymes´ activity. Impacts on carbonic anhydrase activity either by pH and/or sulfate might have negatively influenced urea cycle activity and NH_3 detoxification in toxic SSC*Na conditions studied in this work.

To investigate the participation of the urea cycle in NH_3 detoxification, one might evaluate intracellular and extracellular concentrations of ornithine, citrulline and urea as important molecules of the urea cycle accompanied by intracellular and extracellular NH_3 quantification in the state-of-the-art fed-batch process with all three clones. Next, one might follow these parameters in 15 mM and 20 mM SSC*Na compared with control to see possible differences in urea cycle activity when using L-cysteine or the L-cysteine derivative. This might be accompanied by the measurement of extracellular online pH measurement. Further, one might study the expression levels of urea cycle enzymes e.g. carbamoyl phosphate synthetase and ornithine transcarbamylase in the three tested clones after a fixed number of pre-passages to evaluate basal levels of enzyme expression. This might be also carried out for carbonic anhydrase. Next, one might follow the expression of the aforementioned enzymes in 15 mM and 20 mM SSC*Na compared with control to see possible differences in expression over time when using L-cysteine or the L-cysteine derivative. One might further evaluate the activities of the aforementioned enzymes in 15 mM and 20 mM SSC*Na compared with control. The reaction rate of hydration of CO_2 by carbonic anhydrase may be measured with a spectrophotometer. Measurements of the color change of the indicator phenol red may be followed continuously in Tris buffer at 25°C when CO_2 is constantly bubbled through the solution (Datta and Shepard 1959). Carbamoyl phosphate synthetase activity may be followed based on the chemical conversion of carbamoyl phosphate to hydroxyurea by hydroxylamine. The absorption of the resulting chromophore may be detected at 458 nm (Pierson 1980).

Since extracellular NH_3 levels were higher in SSC*Na conditions compared with control, an inhibition of the urea cycle might not be excluded. The accumulating NH_3 might have then been transported from the cell into the culture broth. The pH-dependent NH_4^+ equilibrium in aqueous solution is described as $NH_4^+ \leftrightarrow NH_3$ (aq) + H^+ (Emerson et al. 1975). At physiological pH, NH_4^+ ions are largely predominant compared with NH_3. NH_3 diffusion over the cell membrane is mainly carried out when NH_3 is present in the form of NH_3 but transporters for NH_4^+ import are also known (Martinelle and Häggström 1993) e.g. proton ATPases as reviewed (Ludewig et al. 2001). To investigate the extracellular pH in the presence of cells and NH_3, a murine myeloma cell line was exposed to NH_3 in phosphate buffer saline. Addition of NH_3 to cells resulted in a sharp decrease in extracellular pH followed by a slow increase in extracellular pH. The authors suggested a relation of NH_3, NH_4^+, protons, and extracellular pH as follows: After addition of NH_3 to cells, NH_3, NH_4^+ and protons were present. Although NH_4^+ is predominantly present at physiological pH, it may be assumed that the small amount of NH_3 may diffuse into the cells thereby leaving protons in the broth causing an acidification of the broth as suggested by the authors.

The followed increase in extracellular pH was assumed to rely on NH_4^+ import via transporters and parallel diffusion of NH_3 from the cell into the broth (Martinelle and Häggström 1993). These observations were similar to the observations made in fed-batch with clone 2 using toxic 20 mM SSC*Na. In fed-batch with toxic 20 mM SSC*Na, two extracellular pH drops were observed each followed by an increase in extracellular pH between days 5 and 7. It is noteworthy that after addition of neutral pH feed containing 20 mM SSC*Na on day 5 the first extracellular pH drop was observed. Extracellular pH increased on day 6 and decreased again between days 6 and 7, in a period where no feed was added. It might not be excluded that a connection relying on small levels of NH_3 diffusion and NH_4^+ transport might be present in fed-batch cultured cells in the presence of 20 mM SSC*Na leading to two pH drops intermitted with phases of (slight) increases and stabilization in pH. Further, a relation of proton extrusion and parallel NH_3 excretion was studied in isolated rat kidneys being exposed to HCl initiating thereby a chronic metabolic acidosis. This study revealed an increased expression of apical NH_3 transporter Rh C glycoprotein (Rhcg) (Seshadri et al. 2006). A connection of increased NH_3 transporter expression levels in response to extracellular acidosis, NH_3 diffusion and NH_4^+ transport and decreased urea cycle activity might not be excluded in toxic SSC*Na conditions in fed-batch and batch mode using different clones.

To investigate the participation of Rhcg in NH_3 transport, one might evaluate the expression levels of Rhcg in the three tested clones after a fixed number of pre-passages to evaluate basal levels of transporter expression. Next, one might follow expression of Rhcg in 15 mM and 20 mM SSC*Na compared with control to see possible differences in expression differences when using L-cysteine, the L-cysteine derivative or different L-cysteine derivative concentrations. Further, one might decrease Rhcg expression by the use of siRNA in all three clones to test if disturbed NH_3 transport may impact NH_3 concentration, extracellular pH and growth of the clones in control, 15 mM and 20 mM SSC*Na. Further, one might measure intracellular and extracellular NH_4^+ levels by photometric methods (as described in the material and methods part of this work) while extracellular NH_3 may be followed in bioreactors by NH_3 sensitive electrodes over time in fed-batch processes using 15 mM and 20 mM SSC*Na compared with control.

6.5.4. Rescue options

Spiking with sodium carbonate to toxic 20 mM SSC*Na resulted in rescued growth compared with 20 mM SSC*Na alone. Addition of increased sodium L-glutamate or Cu (II) sulfate concentrations compared with the basal feed formulation to toxic SSC fed-batch cultures resulted in rescued growth of clone 2 cells compared with 20 mM SSC*Na alone. In all rescue options, the extracellular pH increased with sodium carbonate spiking being the most effective method in increasing extracellular

pH amongst the tested options. Importantly, sodium carbonate spiking revealed lowest extracellular NH_3 concentrations amongst the tested rescue option comparable with control.

The addition of sodium carbonate to toxic SSC fed-batch cultures of clone 2 revealed rescued growth and it might be assumed that carbonate gave rise to bicarbonate. A relation of increased HCO_3^- concentrations and stimulated urea cycle activity might exist. In acute respiratory acidosis, decreased arterial blood pH, increased arterial blood pCO_2 and increased blood HCO_3^- levels were observed in rats (Unwin et al. 1997). In respiratory acidosis, carbonic anhydrase-independent urea synthesis was shown to be predominant being dependent on CO_2 and HCO_3^- supply. Increasing the external CO_2 supply increased this type of urea synthesis (Häussinger and Gerok 1985). From these data it may be assumed that addition of carbonate led to HCO_3^- production which stimulated carbonic anhydrase-independent urea synthesis thereby generating lower detectable extracellular NH_3 concentrations. To do so, HCO_3^- needed to be taken up by the cells via transporters. The HCO_3^- flux was decreased when extracellular pH was decreased as studied in tumor cell lines (Hulikova et al. 2011).The activity of the Cl^-/HCO_3^- transporter being responsible for HCO_3^- uptake was observed to decrease when external pH decreased (Boyer and Tannock 1992). Based on these data it may be assumed that cells took up HCO_3^- thereby stimulating carbonic anhydrase independent urea cycle activity. Due to stabilized extracellular pH, HCO_3^- uptake may be postulated in the sodium carbonate rescue option with 20 mM SSC*Na presented in this study.

To investigate the participation of the Cl^-/HCO_3^- transporter in pH regulation, one might determine the expression of this transporter in the three tested clones after a fixed number of pre-passages to evaluate basal levels of enzyme expression. Next, one might follow expression of Rhcg in 15 mM and 20 mM SSC*Na compared with control to see possible differences in expression variations when using L-cysteine, the L-cysteine derivative or different L-cysteine derivative concentrations. Further, one might decrease Cl^-/HCO_3^- transporter expression by the use of siRNA in all three clones to test if disturbed HCO_3^- ion transport may impact extracellular pH and growth of the clones in control, 15 mM and 20 mM SSC*Na. Accompanied, one might evaluate the expression of carbonic anhydrase in the three tested clones after a fixed number of pre-passages to evaluate basal levels of enzyme expression. Next, one might follow carbonic anhydrase expression in 15 mM and 20 mM SSC*Na compared with control to see possible differences in expression differences when using L-cysteine, the L-cysteine derivative or different L-cysteine derivative concentrations. Further, one may evaluate impacts of decreased Cl^-/HCO_3^- transporter expression on carbonic anhydrase activity for possible assistant pH regulation mechanisms in control, 15 mM and 20 mM SSC*Na.

The addition of increased sodium L-glutamate levels to toxic 20 mM SSC*Na fed-batch cultures led to prolonged growth and increased, stabilized culture pH being accompanied by increased NH_3 levels as observed with 20 mM SSC*Na alone. As suggested by Martinelle and Häggström, interconnection of mitochondrial, cytosolic and external pH exists relying on the connection of NH_4^+, NH_3 and protons in mitochondria, cytosol and extracellular space (Martinelle and Häggström 1993). When sodium L-glutamate is added and metabolized into NH_3 e.g. by glutamate dehydrogenase as reviewed (Spanaki and Plaitakis 2012), the mitochondrial and cytosolic pH will turn acidic as observed in cortical astrocytes from mice perfused with L-glutamate (Azarias et al. 2011). Due to the hypothesis of Martinelle and Häggström, mitochondrial produced NH_3 will diffuse into the cytosol leaving protons behind. In the cytosol, NH_3 concentration increases. NH_3 may further diffuse to the outside of the cell leaving again protons behind as described above. In the form of NH_4^+, it may be again taken up by the cells via transporters thereby shifting extracellular NH_3 / NH_4^+, equilibrium to NH_4^+ production and thereby increasing the external pH as shown in figure 50 (Martinelle and Häggström 1993).

Addition of Cu (II) sulfate to cultures may have led to increased CuSOD activity as shown in *Podospora anserina* (Borghouts et al. 2002). This might have helped to scavenge superoxide radicals. Since it was shown that superoxide radicals may decrease intracellular pH in human amnion cells (Ikebuchi et al. 1991), it might not be excluded that activation of SOD caused stimulated superoxide scavenging thereby possibly leading to increased intracellular pH. It is assumed that sodium L-glutamate and Cu (II) sulfate impact pH regulation in the cell.

To investigate the role of sodium L- glutamate as a rescue option in toxic SSC condition in fed-batch with clone 2, one may follow intracellular and extracellular L-glutamate concentrations via UPLC analytics. Accompanied, one may measure intracellular pH via BCECF and extracellular pH via online measurement using pH sensors over time in control, 15 mM SSC*Na, 20 mM SSC*Na and 20 mM SSC*Na with additionally supplemented glutamate. By this, a relation between L-glutamate concentration and pH may be studied intracellularly and extracellularly.

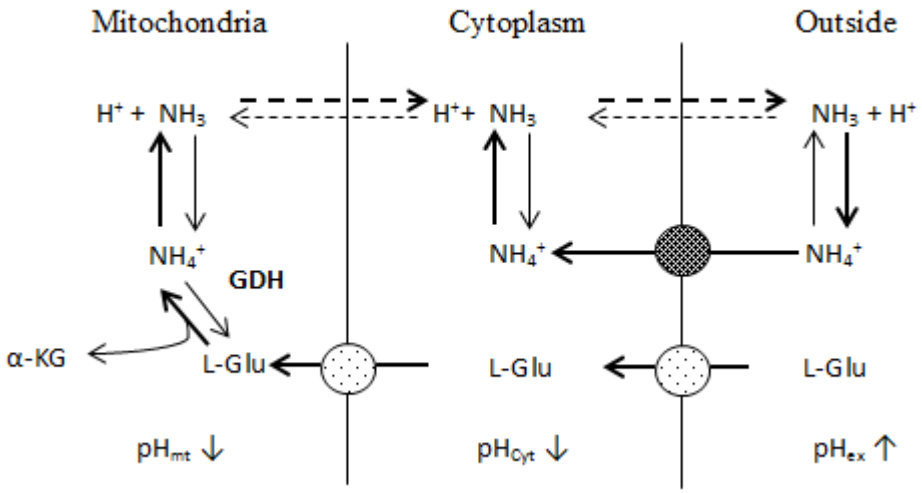

Figure 50: Schematic representation of the hypothesized rescue mechanism of increased sodium L-glutamate feeding in toxic SSC*Na condition in fed-batch using clone 2.

GDH: glutamate dehydrogenase, Glu: glutamate, α-KG: α-ketoglutarate, pH_{mt}: mitochondrial pH, pH_{Cyt}: cytosolic pH, pH_{ex}: extracellular pH (modified from Martinelle and Häggström, 1993)

To investigate the role of copper sulfate, one might quantify intracellular superoxide radical formation by the use of dihydroethidium in control, 15 mM SSC*Na, 20 mM SSC*Na and 20 mM SSC*Na with additionally supplemented Cu (II) sulfate. In parallel, one may follow intracellular SOD-1 and SOD-2 activity in these conditions to investigate if additional Cu (II) sulfate may increase SOD activity in rescued 20 mM SSC*Na. Accompanied, one may measure intracellular pH via BCECF and extracellular pH via online measurement using pH sensors in control, 15 mM SSC*Na, 20 mM SSC*Na and 20 mM SSC*Na with additionally supplemented Cu (II) sulfate.

7. Conclusion

In this work, it was shown for the first time that SSC*Na was used as a L-cysteine derivative in cell culture. The L-cysteine derivative SSC*Na was successfully integrated in a chemically defined, complex, highly concentrated neutral pH feed together with the L-tyrosine derivative PTyr2Na^{+}. This strategy successfully led to the development of a single-feed comprising all nutrients in one neutral pH feed applicable in CHO suspension fed-batch cultures.

In this study, it was demonstrated that the single feed comprising SSC*Na was stable in chemically defined, complex, highly concentrated neutral pH over three months at 4°C in the absence of light. Further, it was shown that SSC*Na might replace L-cysteine in batch mode with CHO suspension clone 1 indicating the use of SSC*Na as a L-cysteine source. In fed-batch experiments with clone 2, the single feed containing 15 mM SSC*Na elicited significantly prolonged growth, significantly increased extracellular NH_3 concentrations and significantly increased titers in spin tubes and bioreactors compared with the standard two-feed strategy. Further, mAbs produced from 15 mM SSC*Na showed no change in cQAs compared with the antibody produced from standard fed-batch process. The use of SSC*Na as a L-cysteine source was shown to rely on the formation of GSH- SSC mixed disulfides. The positive effect of 15 mM SSC*Na on cell culture performance was correlated to the molecules´ anti-oxidant potential represented by increased total intracellular glutathione pools, increased SOD-1 and SOD-2 concentrations and decreased intracellular ROS levels. Toxic effects of SSC*Na on cell growth were observed to be dependent on SSC*Na concentration, cultivation mode and the used clone. As such, reproduced cell death of clone 2 was observed in batch experiments using SSC*Na instead of L-cysteine. Further, clone 3 did not grow in batch mode using SSC*Na instead of L-cysteine. In fed batch experiments, growth of clone 3 was inhibited with 15 mM SSC*Na compared with the standard process. Fed-batch cultures with 20 mM SSC*Na showed reproducible rapid cell death between days 7 and 10 with clone 2 compared with the standard process. The detrimental effects of 20 mM SSC*Na in fed-batch experiments with the high producing clone 2 were correlated to a drastic extracellular pH drop between days 7 and 10. Toxic effects of SSC*Na in fed-batch clone 2 cultures were compensated by the supplementation of sodium carbonate, increased sodium L- glutamate or Cu (II) sulfate concentrations.

The developed neutral pH single feed comprising the L-cysteine derivative was shown to avoid the observed pH peaks resulting from feedings in the standard fed-batch and simplified fed-batch cultivation. Since SSC*Na application was shown to be clone, cultivation mode and concentration dependent, the use of SSC*Na in tailored CDM is suggested. The mentioned rescue options in toxic SSC*Na concentrations might not be applicable to all CHO suspension clones due to clone specific differences in L-glutamate and Cu sensitivities.

Further tests on the relation of urea cycle, extracellular/ intracellular pH and NH_3 production in toxic SSC*Na conditions will gather further inside into the toxicity of SSC.

8. References

Abbas, Xia, Tranberg, Wigström, Weber, Sandberg: S-sulfo-cysteine is an endogenous amino acid in neonatal rat brain but an unlikely mediator of cysteine neurotoxicity, 2008, Neurochemical Research, Vol. 30, pp. 301-307

Adlersberg: The immunoglobulin hinge (interdomain) region, 1976, La Ricerca in Clinica e in Laboratorio, Vol. 6, pp. 191-205

Ahmed, Saeed, Iqbal, Tahir and Islam: Solvent free synthesis of copper (II) cysteine complexes, 2011, World of Applied Sciences Journal, Vol. 14, pp. 210-214

Alexander, Benson, Faccenda, Pawson, Sharman, Spedding, Peters, Harmar and CGTP Collaborators: The concise guide to pharmacology 2013/14: transporters, 2013, British Journal of Pharmacology, Vol. 170, pp. 1706- 1796

Aoyama and Nakaki: Impaired glutathione synthesis in neurodegeneration, 2013, International Journal of Molecular Sciences, Vol. 14, pp. 21021-21044

Arigony, de Oliveira, Machado, Bordin, Bergter, Prá, Henriques: The influence of micronutrients in cell culture: a reflection on viability and genomic stability, 2013, BioMed Research International 2013

Ash, Igo Jr, Morgan, Grey: Selection of Chinese hamster ovary cells (CHO-K1) with reduced glutamate and aspartate uptake, 1993, Somatic Cell and Molecular Genetics, Vol. 19, pp. 231-243

Atkuri, Mantovani, Herzenberg, Herzenberg: N-acetylcysteine - a safe antidote for cysteine/glutathione deficiency, 2007, Current Opinion in Pharmacology, Vol. 7, pp. 355–359

Azarias, Perreten, Lengacher, Poburko, Demaurex, Magistretti, Chatton: Glutamate transport decreases mitochondrial pH and modulates oxidative metabolism in astrocytes, 2011, The Journal of Neuroscience, Vol. 31, pp. 3550-3559

Bachhawat ,Thakur, Kaur, Zulkifli: Glutathione transporters, 2013, Biochimica et Biophysica Acta, Vol. 1830, pp. 3154–3164

Bannai: Transport of cystine and cysteine in mammalian cells, 1984, Biochimica et Biophysica Acta, Vol. 779, pp. 289-306

Banerjee: Redox outside the box: Linking extracellular redox remodeling with intracellular redox metabolism, 2012, The Journal of Biological Chemistry, Vol. 287, pp. 4397-4402

Baran: Model studies related to vanadium biochemistry: recent advances and perspectives, 2003, Journal of the Brazilian Chemical Society, Vol. 14, pp. 878-888

Bass, Hedegaard, Dillehay, Moffett, Englesberg: The A, ASC, and L systems for the transport of amino acids in Chinese hamster ovary cells (CHO-K1), 1981, The Journal of Biological Chemistry, Vol. 256, pp. 10259-10266

Behrsing and Micheel: Monoklonale Antikörper: Grundlagen und ihre Bedeutung in Diagnostik und Therapie, 2008, Ganten/Ruckpaul (Hrsg.), Grundlagen der Molekularen Medizin, 3. Auflage, Springer-Verlag Berlin Heidelberg, pp. 450-475

Belaidi and Schwarz: Molybdenum cofactor deficiency: metabolic link between taurine and S-sulfocysteine, 2013, Taurine 8, Nutrition and Metabolism, Protective Role, and Role in Reproduction, Development, and Differentiation (Eds.) A. El Idrissi; W.J. L´Amoreaux, pp. 13-19

Bermudez, Páez-Ochoa, Gotor, Romero: Arabidopsis S-sulfocysteine synthase activity is essential for chloroplast function and long-day light-dependent redox control, 2010, Plant Cell, Vol. 22, pp. 403-416

Berthon: The stability constants of metal complexes of amino acids with polar side chains, 1995, Pure and Applied Chemistry, Vol. 67, pp. 1117-1240

Bjelton and Fransson: Availability of cysteine and of L-2-oxo-thiazolidine-4-carboxylic acid as a source of cysteine in intravenous nutrition, 1990, Journal of parenteral and enteral nutrition, Vol. 14, pp. 177-182

Boniello, Mayr, Bolivar, Nidetzky: Dual-lifetime referencing (DLR): a powerful method for on-line measurement of internal pH in carrier-bound immobilized biocatalysts, 2012, BMC Biotechnology, Vol. 12, pp. 11

Borghouts, Scheckhuber, Werner, Osiewacz: Respiration, copper availability and SOD activity in *P. anserina* strains with different lifespan, 2002, Biogerontology, Vol. 3, pp. 143-153

Boyer and Tannock: Regulation of intracellular pH in tumor cell lines: Influence of microenvironmental conditions, 1992, Cancer Research, Vol. 52, pp. 4441-4447

Bridges and Patel: Pharmacology of glutamate transport in the CNS: Substrates and inhibitors of excitatory amino acid transporters (EAATs) and the glutamate/cystine exchanger system x_c^-, 2009, Topics in Medicinal Chemistry, Vol. 4, pp. 187-222

Brunner, Frank, Appl, Schöffl, Pfaller, Gstraunthaler: Serum-free cell culture: The serum-free media interactive online database, 2010, Alternatives to Animal Experimentation, Vol. 27, pp. 53-62

Burroni and Ceccarini: The Effect of alkaline pH on the cell growth of six different mammalian cells in tissue culture, 1984, Experimental Cell Research, Vol. 150, 505-508

Cacciactore, Cornacchia,Pinnen, Mollica, Di Stefano: Prodrug approach for increasing cellular glutathione levels, 2010, Molecules, Vol. 15, pp. 1242-1264

Camire: Chinese hamster overy cells for the production of recombinant glycoproteins, 2000, Art to Science, Vol. 19, pp. 150-151

Chaderjian, Chin, Harris, Etcheverry: Effect of copper sulfate on performance of a serum-free CHO cell culture process and the level of free thiol in the recombinant antibody expressed, 2005, Biotechnology Progress, Vol. 21, pp. 550-553

Chakravarthi and Bulleid: Glutathione is required to regulate the formation of native disulfide bonds within proteins entering the secretory pathway, 2004, The Journal of Biological Chemistry, Vol. 279, pp. 39872–39879

Chan and Carter: Therapeutic antibodies for autoimmunity and inflammation, 2010, Nature Reviews Immunology, Vol. 10, pp. 301-316

Chen and Swanson: The glutamate transporters EAAT2 and EAAT3 mediate cysteine uptake in cortical neuron cultures, 2003, Journal of Neurochemistry, Vol. 84, pp. 1332–1339

Chong, Thng, Hiu, Lee, Yong Chan, Ho: LC-MS-based metabolic characterization of high monoclonal antibody-producing Chinese hamster ovary cells, 2012, Biotechnology and Bioengineering, Vol. 109, pp. 3103-3111

Christensen, Liang, Archer: A distinct Na+-requiring transport system for alanine, serine, cysteine, and similar amino acids, 1967, The Journal of Biological Chemistry, Vol. 242, pp. 5237-5246

Clincke, Guedon, Yen, Ogier, Roitel, Goergen: Effect of surfactant pluronic F-68 on CHO cell growth, metabolism, production, and glycosylation of human recombinant IFN-γ in mild operating conditions, 2011, Biotechnology Progress, Vol. 27, pp. 181-190

Clincke, Mölleryd, Zhang: Very high density of CHO cells in perfusion by ATF or TFF in WAVE bioreactor™. Part I. Effect of the cell density on the process, 2013, Biotechnology Progress, Vol. 29, pp. 754-767

Costa, Rodrigues, Henriques, Azeredo, Oliviera: Guidelines to cell engineering for monoclonal antibody production, 2010, European Journal of Pharmaceutics and Biopharmaceutics, Vol. 74, pp. 127-138

Cromwell, Hilario, Jacobson: Protein aggregation and bioprocessing, 2006, The AAPS Journal, Vol. 8, pp. 572-579

Croset, Delafosse, Gaudry, Arod, Glez, Losberger, Begue, Krstanovic, Robert, Vilbois, Chevalet, Antonsson: Differences in the glycosylation of recombinant proteins expressed in HEK and CHO cells, 2012, Journal of Biotechnology, Vol. 161, pp. 336-348

Cuozzo and Kaiser: Competition between glutathione and protein thiols for disulphide-bond formation, 1999, Nature Cell Biology, Vol. 1, pp. 130-135

Datta and Shepard: Carbonic Anhydrase: a Spectrophotometric Assay, 1959, Archives of Biochemistry and Biophysics, Vol. 79, pp. 136-145

D`Autréaux and Toledano: ROS as signalling molecules: mechanisms that generate specificity in ROS homeostasis, 2007, Nature reviews molecular cell biology, Vol. 8, pp. 813-824

deZengotita, Kimura, Miller: Effects of CO_2 and osmolality on hybridoma cells: growth, metabolism and monoclonal antibody production, 1998, Cytotechnology, Vol. 28, pp. 213-227

Dhillon, Nagasawa, Yamada: Microbial process for L-cysteine production, 1987, Enzyme and Microbial Technology, Vol. 9, pp. 277-280

Dilger and Baker: Excess dietary L-cysteine causes lethal metabolic acidosis in chicks, 2008, The Journal of Nutrition, Vol. 138, pp. 1628–1633

Dimski: Ammonia metabolism and the urea cycle: Function and clinical implications, 1994, Journal of Veterinary Internal Medicine, Vol. 8, pp. 73- 78

Distler: Zur Chemie der Buntesalze, 1967, Angewandte Chemie, Vol. 79, pp. 520-529

Doverskog, Han, Häggström: Cystine/cysteine metabolism in cultured Sf9 cells: influence of cell physiology on biosynthesis, amino acid uptake and growth, 1998, Cytotechnology, Vol. 26, pp. 91-102

Drake, De La Rosa, Stipanuk: Metabolism of cysteine in rat hepatocytes. Evidence for cvsteinesulphinate-independent pathwavs, 1987, Biochemical Journal, Vol. 244, pp. 279-286

Dunlop, Fear, Griffiths: Glutamate uptake into synaptic vesicles - inhibition by sulphur amino acids, 1991, NeuroReport, Vol. 2, pp. 377-379

Dwivedi and Arnold: Chemistry of Thiamine Degradation in Food Products and Model Systems: A Review, 1973, Journal of Agricultural and Food Chemistry, Vol. 21, pp. 54-60

Elisaf, Tsatsoulis, Katopodis, Siamopoulos: Acid-base and electrolyte disturbances in patients with diabetic ketoacidosis, 1996, Diabetes Research and Clinical Practice, Vol. 34, pp. 23-27

Emerson, Russo, Lund, Thurston: Aqueous ammonia equilibrium calculations: Effect of pH and temperature, 1975, Journal of the Fisheries Research Board of Canada, Vol. 32, pp. 2379-238

Eon-Duval, Broly, Gleixner: Quality attributes of recombinant therapeutic proteins: An assessment of impact on safety and efficacy as part of a quality by design development approach, 2012, Biotechnology Progress, Vol. 28, pp. 608-622

Eriksson and Eriksson: Synthesis and characterization of the L-cysteine-glutathione mixed disulfide, 1967, Acta Chemica Scandinavia, Vol. 21, pp. 1304-1312

Feeney, Carvalhal, Yu, Chan, Michels, Wang, Shen, Ressl, Dusel, Laird: Eliminating tyrosine sequence variants in CHO cell lines producing recombinant monoclonal antibodies, 2013, Biotechnology and Bioengineering, Vol. 110, pp. 1087-1097

Fenech: Folate (vitamin B9) and vitamin B12 and their function in the maintenance of nuclear and mitochondrial genome integrity, 2012, Mutation Research/Fundamental and Molecular Mechanisms of Mutagenesis, Vol. 733, pp. 21-33

Fernandez, Carrascal, Rousaud, Abían, Zorzano, Palacín, Chillarón: rBAT-b^{0+} AT heterodimer is the main apical reabsorption system for cystine in the kidney, 2002, American Journal of Physiology. Renal Physiology, Vol. 283, pp. F540-F548

Franchi-Gazzola, Gazzola, Dall'Asta, Guidotti: The transport of alanine, serine, and cysteine in cultured human fibroblasts, 1982, The Journal of Biological Chemistry, Vol. 16, pp. 9582-9587

Gallogy and Mieyal: Mechanisms of reversible protein glutathionylation in redox signaling and oxidative stress, 2007, Current Opinion in Pharmacology, Vol. 7, pp. 381-391

Gan and Wells: Purification and properties of thioltransferase, 1986, The Journal of Biological Chemistry, Vol. 261, pp. 996-1001

Garcia, Goldstein, Pathak, Anderson, Brown: Molecular characterization of a membrane transporter for lactate, pyruvate, and other monocarboxylates: Implications for the cori cycle, 1994, Cell, Vol. 76, pp. 865-873

Garnier, Voyer, Tom, Perret, Jardin, Kamen: Dissolved carbon dioxide accumulation in a large scale and high density production of TGFβ receptor with baculovirus infected *Sf-9* cells, 1996, Cytotechnology, Vol. 22, pp. 53-63

Gevondyan, Volynskaia, Gevondyan: Four free cysteine residues found in human IgG1 of healthy donors, 2006, Biochemistry (Moscow), Vol. 71, pp. 279-284

Ghaderi, Zhang, Hurtado-Ziola, Varki: Production platforms for biotherapeutic glycoproteins. Occurrence, impact, and challenges of non-human sialylation, 2012, Biotechnology and Genetic Engineering Reviews, Vol. 28, pp. 147-176

Gigout, Buschmann, Jolicoeur: The fate of pluronic F-68 in chondrocytes and CHO cells, 2008, Biotechnology and Bioengineering, Vol. 100, pp. 975-987

Giustarini, Milzani, Dalle-Donne, Tsikas, Rossi : N-Acetylcysteine ethyl ester (NACET): A novel lipophilic cell-permeable cysteine derivative with an unusual pharmacokinetic feature and remarkable antioxidant potential, 2012, Biochemical Pharmacology, Vol. 84, pp. 1522-1533

Gladyshev, Liu, Novoselov, Krysan, Sun, Kryukov, Kryukov, Lou: Identification and characterization of a new mammalian glutaredoxin (thioltransferase), Grx2, 2001, The Journal of Biological Chemistry, Vol. 276, pp. 30374–30380

Glazenburg, Jekel-Halsema, Scholtens, Baars, Mulder: Effects of variation in the dietary supply of cysteine and methionine on liver concentration of glutathione and "active sulfate" (PAPS) and serum levels of sulfate, cystine, methionine and taurine: Relation to the metabolism of acetaminophen, 1983, The Journal of Nutrition, Vol. 113, pp. 1363- 1373

Gomes, Fernandes, Lima: Fluorescence probes used for detection of reactive oxygen species, 2005, Journal of Biochemical and Biophysical Methods, Vol. 65, pp. 45-80

Gotor and Romero: S-sulfocysteine synthase function in sensing chloroplast redox status, 2013, Plant Signaling and Behavior, Vol. 8, pp. e23313-1 - e23313-3

Grattagliano, Wieland, Schranz, Lauterburg: Disposition of glutathione monoethyl ester in the rat: Glutathione ester is a slow release form of extracellular glutathione, 1995, The Journal of Pharmacology and Experimental Therapeutics, Vol. 272, pp. 484-488

Gray, Chen, Howarth, Inlow, Maiorella: CO_2 in large-scale and high-density CHO cell perfusion culture, 1996, Cytotechnology, Vol. 22, pp. 65-78

Griffiths, Grieve, Dunlop, Damgaard, Fosmark, Schousboe: Inhibition by excitatory sulphur amino acids of the high-affinity L-glutamate transporter in synaptosomes and in primary cultures of cortical astrocytes and cerebellar neurons, 1989, Neurochemical Research, Vol. 14, pp. 333-343

Grinberg, Fibach, Amer, Atlas: N-acetylcysteine amide, a novel cell-permeating thiol, restores cellular glutathione and protects human red blood cells from oxidative stress, 2005, Free Radical Biology & Medicine, Vol. 38, pp. 136-145

Gronemeyer, Ditz, Strube: Trends in upstream and downstream process development for antibody manufacturing, 2014, Bioengineering, Vol. 1, pp. 188-212

Gu, Wen, Weinreb, Sun, Zhang, Foley, Kshirsagar, Evans, Mi, Meier, Pepinsky: Characterization of trisulfide modification in antibodies, 2010, Analytical Biochemistry, Vol. 400, pp. 89-98

Güzeloğlu, Yalçin, Pekin: The determination of stability constants of N-acetyl-L-cysteine chrome, nickel, cobalt and iron complexes by potentiometric method, 1998, Journal of Organometallic Chemistry, Vol. 568, pp. 143-147

Hajela: Structure and function of Fc receptors, 1991, Biochemical Education, Vol. 19, pp. 50-57

Halestrap and Price: The proton-linked monocarboxylate transporter (MCT) family : structure, function and regulation, 1999, Biochemical Journal, Vol. 343, pp. 281-299

Halliwell: Reactive species and antioxidants. Redox biology as a fundamental theme of aerobic life, 2006, Plant Physiology, Vol. 141, pp. 312-322

Hara, Yonezawa, Sakaue, Ando, Kotani, Kitamura, Kitamura, Ueda, Stephens, Jackson, Waterfield, Kasuga: 1-Phosphatidylinositol 3-kinase activity is required for insulin stimulated glucose transport but not for RAS activation in CHO cells, 1994, Proceedings of the National Academy of Sciences of the United States of America, Vol. 91, pp. 7415-7419

Harman, Mottley, Mason: Free radical metabolites of L-cysteine oxidation, 1984, The Journal of Biological Chemistry, Vol. 259, pp. 5606-5611

Hatakeyama, Lee, Chon, Hayashi, Mizoguchi: Purification and some properties of rabbit liver cytosol thioltransferase, 1985, Biochemical Journal, Vol. 97, pp. 893-897

Häussinger and Gerok: Hepatic urea synthesis and pH regulation. Role of CO_2, HCO_3^-, pH and the activity of carbonic anhydrase, 1985, European Journal of Biochemistry, Vol. 152, pp. 381 -386

Havre, O'Reilly, McCormick, Brash: Transformed and tumor-derived human cells exhibit preferential sensitivity to the thiol antioxidants, N-Acetyl cysteine and penicillamine, 2002, Cancer Research, Vol. 62, pp. 1443-1449

Hayes, Cosgrave, Struwe, Wormald, Davey, Jefferis, Rudd: Glycosylation and Fc receptors, 2014, M. Daëron and F. Nimmerjahn (eds.), Fc Receptors, Current Topics, in Microbiology and Immunology 382

Hayes, Wießner, Rauen, McBean: Transport of L-[^{14}C]cystine and L-[^{14}C]cysteine by subtypes of high affinity glutamate transporters over-expressed in HEK cells, 2005, Neurochemistry International, Vol. 46, pp. 585-594

Hecklau, Pering, Seibel, Schnellbaecher, Wehsling, Eichhorn, von Hagen, Zimmer: S-Sulfocysteine simplifies fed-batch processes and increases the CHO specific productivity via anti-oxidant activity, 2016, Journal of biotechnology, Vol. 218, pp. 53-63

Hediger, Romero, Peng, Rolfs, Takanaga, Bruford: The ABCs of solute carriers: physiological, pathological and therapeutic implications of human membrane transport proteins, 2004, European Journal of Physiology, Vol. 447, pp. 465-468

Himi, Ikeda, Yasuhara, Nishida, Morita: Role of neuronal glutamate transporter in the cysteine uptake and intracellular glutathione levels in cultured cortical neurons, 2003, Journal of Neural Transmission, Vol. 110, pp. 1337-1348

Hinderlich, Weidemann, Yardeni, Horstkorte, Huizing: UDP-GlcNAc 2-epimerase/ManNAc kinase (GNE), a master regulator of sialic acid synthesis, 2015, Topics in Current Chemistry, Vol. 366, pp. 97-137

Holmgren: Thioredoxin catalyzes the reduction of insulin disulfides by dithiothreitol and dihydrolipoamide, 1979, The Journal of Biological Chemistry, Vol. 254, pp. 9627-9632

Hossler, Khattak, Li: Optimal and consistent protein glycosylation in mammalian cell culture, 2009, Glycobiology, Vol. 19, pp. 936-949

Hossler, McDermott, Racicot, Fann: Improvement of mammalian cell culture performance through surfactant enabled concentrated feed media, 2013, Biotechnology Progress, Vol. 29, pp. 1023-1033

Hsiao, Walter, Anderson, Hamilton: Enzymatic production of amino acids, 1988, Biotechnology and Genetic Engeneering Reviews, Vol. 6, pp. 179-219

Huang, Hu, Rustandi, Chang, Yusuf-Makagiansar, Ryll: Maximizing productivity of CHO cell-based fed-batch culture using chemically defined media conditions and typical manufacturing equipment, 2010, Biotechnology Progress, Vol. 26, pp. 1400-1410

Huckabee: Abnormal resting blood lactate. II. Lactic acidosis, 1961, American Journal of Medicine, Vol. 30, pp. 840-848

Hulikova, Vaughan-Jones, Swietach: Dual role of CO_2/HCO_3^- buffer in the regulation of intracellular pH of three-dimensional tumor growths, 2011, The Journal of Biological Chemistry, Vol. 286, pp. 13815-13826

Hundal and Taylor: Amino acid transceptors: gate keepers of nutrient exchange and regulators of nutrient signaling, 2009, American Journal of Physiology. Endocrinology and Metabolism, Vol. 296, pp. E603-E613

Igo and Ash: New mutations and phenotypes associated with glutamate and aspartate transport in chinese hamster ovary (CHO-K1) cells, 1996, Somatic Cell and Molecular Genetics, Vol. 22, pp. 87-103

Ikebuchi, Masumoto, Tasaka, Koike, Kasahara, Miyake, Tanizawa: Superoxide anion increases intracellular pH, Intracellular free calcium, and arachidonate release in human amnion cells, 1991, The Journal of Biological Chemistry, Vol. 266, pp. 13233-13237

Imai-Nishiya, Mori, Inoue, Wakitani, Iida, Shitara, Satoh: Double knockdown of α1,6-fucosyltransferase (FUT8) and GDP-mannose 4,6-dehydratase (GMD) in antibody-producing cells: a new strategy for generating fully non-fucosylated therapeutic antibodies with enhanced ADCC, 2007, BMC Biotechnology, Vol. 7, p. 84

Innocenti, Vullo, Scozzafava, Supuran: Carbonic anhydrase inhibitors. Inhibition of isozymes I, II, IV,V, and IX with anions isosteric and isoelectronic with sulfate, nitrate, and carbonate, 2005, Bioorganic & Medicinal Chemistry Letters, Vol. 15, pp. 567-571

Isaev, Stelmashook, Lukin, Freyer, Mergenthaler, Zorov: Acidosis-induced zinc-dependent death of cultured cerebellar granule neurons, 2010, Cellular and Molecular Neurobiology, Vol. 30, pp. 877-883

Issels, Nagele, Eckert, Wilmanns: Promotion of cystineuptake and ist utilization for glutathione biosynthesis induced by cysteamine and N-acetylcysteine, 1988, Biochemical Pharmacology, Vol. 37, pp. 881-888

Jacob, Giles, Giles, Sies: Schwefel und Selen: Bedeutung der Oxidationsstufe für Struktur und Funktion von Proteinen, 2003, Angewandte Chemie, Vol. 115, pp. 4890-4907

Janáky, Varga, Hermann, Saransaari, Oja: Mechanisms of L-cysteine neurotoxicity, 2000, Neurochemical Research, Vol. 25, pp. 1397-1405

Jayapal, Wlaschin, Hu, Yap: Recombinant protein therapeutics from CHO cells - 20 years and counting, 2007, Chemical Engineering Progress, Vol. 103, pp. 40-47

Jayme and Smith: Media formulation options and manufacturing process controls to safeguard against introduction of animal origin contaminants in animal cell culture, 2000, Cytotechnology, Vol. 33, pp. 27-36

Jayme, Watanabe, Shimada: Basal medium development for serum-free culture: a historical perspective, 1997, Cytotechnology, Vol. 23, pp. 95-101

Jerums and Yang: Optimization of cell culture media, 2005, BioProcess International, Vol. 3, pp. 38-44

Jiang, Song, Bergelson, Arroll, Parekh, May, Chung, Strouse, Mire-Sluis, Schenerman: Advances in the assessment and control of the effector functions of therapeutic antibodies, 2011, Nature Reviews Drug Discovery, Vol. 10, pp. 101-110

Jones, Castillo, Levine: Advances in the development of therapeutic monoclonal antibodies, 2007, BioPharm International, Vol. 20, pp. 96-114

Jordan, Voisard, Berthoud, Tercier, Kleuser, Baer, Broly: Cell culture medium improvement by rigorous shuffling of components using media blending, 2013, Cytotechnology, Vol. 65, pp. 31-40

Kågedal, Källberg, Sörbo: Possible involvement of glutathione in the detoxification of sulfite, 1986, Biochemical and Biophysical Research Communications, Vol. 136, pp. 1036-1041

Kamel and Halperin: Acid-base problems in diabetic ketoacidosis, 2015, The New England Journal of Medicine, Vol. 372, pp. 546-554

Kamoun: Endogenous production of hydrogen sulfide in mammals, 2004, Amino Acids, Vol. 26, pp. 243-254

Kanai: Family of neutral and acidic amino acid transporters: molecular biology, physiology and medical implications, 1997, Current Opinion in Cell Biology, Vol. 9, pp. 565-572

Kanai and Hediger: The glutamate/neutral amino acid transporter family SLC1: molecular, physiological and pharmacological aspects, 2004, European Journal of Physiology, Vol. 447, pp. 469-479

Kanai, Clémençon, Simonin, Leuenberger, Lochner, Weisstanner, Hediger: The SLC1 high-affinity glutamate and neutral amino acid transporter family, 2013, Molecular Aspects of Medicine, Vol. 34, pp. 108-120

Kao and Puck: Genetics of somatic mammalian cells, VII. Induction and isolation of nutritional mutants in chinese hamster cells, 1968, Proceedings of the National Academy of Sciences, Vol. 60, pp. 1275-1281

Katoh, Tresguerres, Lee, Kaneko, Aida, Goss: Cloning of rainbow trout SLC26A1: involvement in renal sulfate secretion, 2006, American Journal of Physiology. Regulatory, Integrative and Comparative Physiology, Vol. 290, pp. R1468-R1478

Khetan, Huang, Dolnikova, Pederson, Wen,Yusuf-Makagiansar, Chen, Ryll : Control of misincorporation of serine for asparagine during antibody production using CHO cells, 2010, Biotechnology and Bioengineering, Vol. 107, pp. 116-123

Kilberg, Christensen, Handlogten: Cysteine as a system-specific substrate for transport system ASC in rat hepatocytes, 1979, Biochemical and Biophysical Research Communications, Vol. 88, pp. 744-751

Kim and Eberwine: Mammalian cell transfection: the present and the future, 2010, Analytical and Bioanalytical Chemistry, Vol. 397, pp. 3173-3178

Kim and Kim: Glycosylation variant analysis of recombinant human tissue plasminogen activator produced in urea-cycle-enzyme-expressing chinese hamster ovary (CHO) cell line, 2006, Journal of Bioscience and Bioengineering, Vol. 102, pp. 447-451

Kim and Lee: Differences in optimal pH and temperature for cell growth and antibody production between two chinese hamster ovary clones derived from the same parental clone, 2007, Journal of Microbiology and Biotechnology, Vol. 17, pp. 712-720

Kishishita, Katayama, Kodaira, Takagi, Matsuda, Okamoto, Takuma, Hirashima, Aoyagi: Optimization of chemically defined feed media for monoclonal antibody production in Chinese hamster ovary cells, 2015, Journal of Bioscience and Bioengineering, Vol. 120, pp. 78-84

Kojer and Riemer: Balancing oxidative protein folding: The influences of reducing pathways on disulfide bond formation, 2014, Biochimica et Biophysica Acta, Vol. 1844, pp. 1383-1390

Kruglikova-L´vova: A new vitamin preparation, thiamine propyl disulfide and other disulfide derivatives of thiamine, 1970, Pharmaceutical Chemistry Journal, Vol. 4, pp. 657-658

Kshirsagar, McElearney, Gilbert, Sinacore, Ryll: Controlling trisulfide modification in recombinant monoclonal antibody produced in fed-batch cell culture, 2012, Biotechnology and Bioengineering, Vol. 109, p. 2523-2532

Lan, Lan, Chan, Hsieh, Chang, Jeng : The effects of extracellular citric acid acidosis on the viability, cellular adhesion capacity and protein synthesis of cultured human gingival fibroblasts, 1999, Australian Dental Journal, Vol. 44, pp. 123-130

Landaas and Jakobs: The occurrence of 2-hydroxyisovaleric acid in patients with lactic acidosis and ketoacidosis, 1977, Clinica Chimica Acta, Vol. 78, pp. 489-493

Lappi and Ruddock: Reexamination of the role of interplay between glutathione and protein disulfide isomerase, 2011, Journal of Molecular Biology, Vol. 409, pp. 238-249

Lauterburg, Corcoran, Mitchell: Mechanism of action of N-acetylcysteine in the protection against the hepatotoxicity of acetaminophen in rats in vivo, 1983, Journal of Clinical Investigation, Vol. 71, pp. 980-991

Leichter and Joslyn: Kinetics of thiamin cleavage by sulphite, 1969, Biochemical Journal, Vol. 113, pp. 611-615

Lewerenz, Klein, Methner: Cooperative action of glutamate transporters and cystine/glutamate antiporter system X_c^- protects from oxidative glutamate toxicity, 2006, Journal of Neurochemistry, Vol. 98, pp. 916-925

Lewis, Liu, Li, Nagarajan, Yerganian, O'Brien, Bordbar, Roth, Rosenbloom, Bian,Xie, Chen, Li, Baycin-Hizal, Latif, Forster, Betenbaugh, Famili, Xu, Wang, Palsson: Genomic landscapes of chinese hamster ovary cell lines as revealed by the Cricetulus griseus draft genome, 2013, Nature Biotechnology, Vol. 31, pp. 759-765

Lill: Function and biogenesis of iron–sulphur proteins, 2009, Nature Review Insight, Vol. 460, pp. 831-838

Lin, Vera, Chaganti, Golde: Human monocarboxylate transporter 2 (MCT2) is a high affinity pyruvate transporter, 1998, The Journal of Biological Chemistry, Vol. 273, pp. 28959-28965

Lipman, Jackson, Trudel, Weis-Garcia: Monoclonal versus polyclonal antibodies: Distinguishing characteristics, applications, and information resources, 2005, The Institute of Laboratory Animal Resources Journal, Vol. 46, pp. 258-268

Liu: Antibody glycosylation and its impact on the pharmacokinetics and pharmacodynamics of monoclonal antibodies and Fc-fusion proteins, 2015, Journal of Pharmaceutical Sciences, Vol. 104, pp. 1866-1884

Liu and May: Disulfide bond structures of IgG molecules, 2012, mAbs, Vol. 4, pp. 17-23

Liu, Chen, Zhang-van Enk, Plant, Dillon, Flynn: Human IgG2 antibody disulfide rearrangement *in vivo*, 2008, The Journal of Biological Chemistry, Vol. 283, pp. 29266-29272

Lo Conte and Carroll: The chemistry of thiol oxidation and detection, 2012, Oxidative stress and redox regulation. Jakob, U. Ed.; Springer: New York 2012, Chapter 1,

Lo, Wang, Gout: The x_c^- cystine/glutamate antiporter: A potential target for therapy of cancer and other diseases, 2008, Journal of Cellular Physiology, Vol. 215, pp. 593-602

Long and Halliwell: Oxidation and generation of hydrogen peroxide by thiol compounds in commonly used cell culture media, 2001, Biochemical and Biophysical Research Communications, Vol. 286, pp. 991-994

Longmore and Schachter: Product-identification and substrate-specificity studies of the GDP-L-fucose: 2-acetamido-2-deoxy-β-D-glucoside (Fuc → Asn-linked GlcNAc) 6-α-L-fucosyl transferase in a Golgi-rich fraction from porcine liver, 1982, Carbohydrate Research, Vol. 100, pp. 365-392

Lu, Toh, Burnett, Li, Hudson, Amanullah, Li: Automated dynamic fed-batch process and media optimization for high productivity cell culture process development, 2013, Biotechnology and Bioengineering, Vol. 110, pp. 191-205

Ludewig, von Wirén, Rentsch, Frommer: Rhesus factors and ammonium: a function in efflux?, 2001, Genome Biology, Vol. 2, pp. 1010.1–1010.5

Lundblad: The Modification of cystine, 2014, Chemical Reagents for Protein Modification, Fourth Edition, CRC Press, pp. 339-376

Ma, Ellett, Okediadi, Hermes, McCormick, Casnocha: A single nutrient feed supports both chemically defined NS0 and CHO fed-batch processes: Improved productivity and lactate metabolism, 2009, Biotechnology Progress, Vol. 25, pp. 1353-1363

Magagnin, Bertran, Werner, Markovich, Biber, Palacin, Murer: Poly(A)$^+$RNA from rabbit intestinal mucosa induces $b^{0,+}$ and y^+ amino acid transport activities in Xenopus laevis oocytes, 1992, The Journal of Biological Chemistry, Vol. 267, pp. 15384-15390

Mailloux, Seifert, Bouillaud, Aguer, Collins, Harper: Glutathionylation acts as a control switch for uncoupling proteins UCP2 and UCP3, 2011, The Journal of Biological Chemistry, Vol. 286, pp. 21865-21875

Malo and Fliegel: Physiological role and regulatio of the Na^+/H^+ exchanger, 2006, Canadian Journal of Physiology and Pharmacology, Vol. 84, pp. 1081-1095

Mannarino, Vilela, Brasil, Aranha, Moradas-Ferreira, Pereira, Costa, Eleutherio: Requirement of glutathione for Sod1 activation during lifespan extension, 2011, Yeast, Vol. 28, pp. 19-25

Mari, Morales, Colell, García-Ruiz, Fernández-Checa: Mitochondrial glutathione, a key survival antioxidant, 2009, Antioxidants and Redox Signaling, Vol. 11, pp. 2685-2700

Markovich: Physiological roles of mammalian sulfate transporters NaS1 and Sat1, 2011, Archivum Immunologiae et Therapiae Experimentalis, Vol. 59, pp. 113-116

Marliss, Aoki, Toews, Felig, Connon, Kyner, Huckabee, Cahill: Amino Acid metabolism in lactic acidosis, 1972, The American Journal of Medicine, Vol. 52, pp. 474-481

Martens, Offermanns, Scherberich: Einfache Synthese von racemischem Cystein, 1981, Angewandte Chemie, Vol. 93, pp. 680-683

Martinelle and Häggström: Mechanisms of ammonia and ammonium ion toxicity in animal cells: Transport across cell membranes, 1993, Journal of Biotechnology, Vol. 30, pp. 339-350

Mathai, Missner, Kügler, Saparov, Zeidel, Lee, Pohl: No facilitator required for membrane transport of hydrogen sulfide, 2009, Proceedings of the National Academy of Sciences, Vol. 106, pp. 16633-16638

McAtee, Tempelton and Young: Role of chinese hamster ovary central carbon metabolism in controlling the quality of secreted biotherapeutic proteins, 2014, Pharmaceutical Bioprocessing, Vol. 2, pp. 63-74

McCord and Fridovich: Superoxide Dismutase. An enzymic function for erythrocuprein (hemocuprein), 1969, The Journal of Biological Chemistry, Vol. 244, pp. 6049-6055

McCoy, Costa, Morris: Factors that determine stability of highly concentrated chemically defined production media, 2015, Biotechnology Progress, Vol. 31, pp. 493-502

McKinney, Dilwith, Belfort: Optimizing antibody production in batch hybridoma cell culture, 1995, Journal of Biotechnology, Vol. 40, pp. 31-48

Meister: Glutathione Metabolism and its selective modification, 1988, The Journal of Biological Chemistry, Vol. 263, pp. 17205-17208

Metzler and Snell: Deamination of serine. I. Catalytic deamination of serine and cysteine by pyridoxal and metal salts, 1952, The Journal of Biological Chemistry, Vol. 198, pp. 353-361

Mimura, Sondermann, Ghirlando, Lund, Young, Goodall, Jefferis: Role of oligosaccharide residues of IgG1-Fc in FcRIIb binding, 2001, The Journal of Biological Chemistry, Vol. 276, pp. 45539-45547

Módis, Coletta, Erdélyi, Papapetropoulos, Szabo: Intramitochondrial hydrogen sulfide production by 3-mercaptopyruvate sulfurtransferase maintains mitochondrial electron flow and supports cellular bioenergetics, 2013, The Official Journal of the Federation of American Societies for Experimental Biology, Vol. 27, pp. 601-611

Mohan and Lee: Effect of inducible co-overexpression of protein disulfide isomerase and endoplasmic reticulum oxidoreductase on the specific antibody productivity of recombinant Chinese hamster ovary cells, 2010, Biotechnology and Bioengineering, Vol. 107, pp. 337-346

Mohan, Park, Chung, Lee: Effect of doxycycline-regulated protein disulfide isomerase expression on the specific productivity of recombinant CHO cells: Thrombopoietin and antibody, 2007, Biotechnology and Bioengineering, Vol. 98, pp. 611-615

Mohmad-Saberi, Hashim, Mel, Amid, Ahmad-Raus, Packeer-Mohamed: Metabolomics profiling of extracellular metabolites in CHO-K1 cells cultured in different types of growth media, 2013, Cytotechnology, Vol. 65, pp. 577-586

Molinas, Soria, Marrone, Danielli, Trumper, Marinelli: Acidosis-induced downregulation of hepatocyte mitochondrial aquaporin-8 and ureagenesis from ammonia, 2015, Biochemistry and Cell Biology, Vol. 93, pp. 417-420

Molteni, Fassio, Ciriolo, Filomeni, Pasqualetto, Fagioli, Sitia: Glutathione limits Ero1-dependent oxidation in the endoplasmic reticulum, 2004, The Journal of Biological Chemistry, Vol. 279, pp. 32667-32673

Mooney, Leuendorf, Hendrickson, Hellmann: Vitamin B6: A long known compound of surprising complexity, 2009, Molecules, Vol. 14, pp. 329-351

Moore, Chen, Karki, Lazar: Engineered Fc variant antibodies with enhanced ability to recruit complement and mediate effector functions, 2010, mAbs, Vol. 2, pp. 181-189

Munday, Munday, Winterbourn: Inhibition of copper-catalyzed cysteine oxidation by nanomolar concentrations of iron salts, 2004, Free Radical Biology and Medicine, Vol. 36, pp. 757-764

Mustafa, Sikka, Gazi, Steppan, Jung, Bhunia, Barodka, Gazi, Barrow, Wang, Amzel, Berkowitz, Snyder: Hydrogen sulfide as endothelium-derived hyperpolarizing factor sulfhydrates potassium channels, 2011, Circulation Research, Vol. 109, pp. 1259-1268

Nagasawa, Goon, Muldoon, Zera: 2-Substituted thiazolidine-4(R)-carboxylic acids as prodrugs of L-cysteine.Protection of Mice against Acetaminophen Hepatotoxicity, 1984, Journal of Medicinal Chemistry, Vol. 27, pp. 591-596

Nakamori, Kobayashi, Kobayashi, Takagi: Overproduction of L-cysteine and L-cystine by *Escherichia coli* strains with a genetically altered serine acetyltransferase, 1998, Applied and Environmental Microbiology, Vol. 64, pp. 1607-1611

Nakanishi, Akabane, Nanami, Kiyobayashi, Moriguchi, Hasuike, Otaki, Miyagawa, Itahana, Izumi: Comparison of cytotoxicity of cysteine and homocysteine for renal epithelial cells, 2005, Nephron Experimental Nephrology, Vol. 100, pp. e11-e20

Nakatani, Ohtsu, Nonaka, Wiriyathanawudhiwong, Morigasaki, Takagi: Enhancement of thioredoxin/glutaredoxin-mediated L-cysteine synthesis from S-sulfocysteine increases L-cysteine production in *Escherichia coli*, 2012, Microbial Cell Factories, Vol. 11, p. 9

Nath and Salahudeen: Autoxidation of cysteine generates hydrogen peroxide: cytotoxicity and attenuation by pyruvate, 1993, American Journal of Physiology, Vol. 264, pp. F306-F314

Nazhat, Golding, Johnson, Jones: Destruction of vitamin B12 by reaction with ascorbate: The role of hydrogen peroxide and the oxidation state of cobalt, 1989, Journal of Inorganic Biochemistry, Vol. 36, pp. 75-81

Nielsen, Baer, Müller, Gregersen, Mønster, Rasmussen, Weilguny, Tolstrup: Single-batch production of recombinant human polyclonal antibodies, 2010, Molecular Biotechnology, Vol. 45, pp. 257-266

Nimmerjahn and Ravetch: Fcγ receptors: Old friends and new family members, 2006, Immunity, Vol. 24, pp. 19-28

Nishiuch, Sasaki, Nakayasu, Oikawa: Cytotoxicity of cysteine in culture media, 1976, In Vitro, Vol. 12, pp. 635-638

Noda, Iwakiri, Fujimoto, Rhoads, Aw: Exogenous cysteine and cystine promote cell proliferation in CaCo-2 cells, 2002, Cell Proliferation, Vol. 35, pp. 117-129

Olney, Misra, De Gubareff: Cysteine-S-sulfate: Brain damaging metabolite in sulfite oxidase deficiency, 1975, Journal of Neuropathology and Experimental Neurology, Vol. 34, pp. 167-177

Önnerfjord, Heathfield,Heinegård: Identification of tyrosine sulfation in extracellular leucine-rich repeat proteins using mass spectrometry, 2004, The Journal of Biological Chemistry, Vol. 279, pp. 26-33

Orellana, Marcellin, Schulz, Nouwens, Gray, Nielsen: High-antibody-producing Chinese hamster ovary cells up-regulate intracellular protein transport and glutathione synthesis, 2015, Journal of Proteome Research, Vol. 14, pp. 609-618

Oz, Chen, Nagasawa: Comparative efficacies of 2 cysteine prodrugs and a glutathione delivery agent in a colitis model, 2007, Translational Research, Vol. 150, pp. 122-129

Ozturk, Riley, Palsson: Effects of ammonia and lactate on hybridoam growth, metabolism, and antibody production, 1991, Biotechnology and Bioengineering, Vol. 39, pp. 418-431

Padawer, Ling, Bai: Case study: An accelerated 8-day monoclonal antibody production process based on high seeding densities, 2013, Biotechnology Progress, Vol. 29, pp. 829-832

Padlan: Anatomy of the antibody molecule, 1994, Molecular Immunology, Vol. 31, pp. 169-217

Palamara, Brandi, Rossi, Millo, Benatti, Nencioni, Iuvara, Garaci, Magnani: New synthetic glutathione derivatives with increased antiviral activities, 2004, Antiviral Chemistry and Chemotherapy, Vol. 15, pp. 77-85

Patro, Adhikari, Mukherjee, Chattopadhyay: Possible role of hydroxyl radicals in the oxidative degradation of folic acid, 2005, Bioorganic and Medicinal Chemistry Letters, Vol. 15, pp. 67-71

Paul, Graff-Meyer, Stahlberg, Lauer, Rufer, Beck, Briguet, Schnaible, Buckel, Boeckle: Structure and function of purified monoclonal antibody dimers induced by different stress conditions, 2012, Pharmaceutical Research, Vol. 29, pp. 2047-2059

Paulsen and Carroll: Cysteine-mediated redox signaling: Chemistry, biology, and tools for discovery, 2012, Chemical Reviews, Vol. 113, pp. 4633-4679

Pecci, Montefoschi, Musci, Cavallini: Novel findings on the copper catalysed oxidation of cysteine, 1997, Amino Acids, Vol. 13, pp. 355-367

Pelis, Edwards, Kunigelis, Claiborne, Renfro: Stimulation of renal sulfate secretion by metabolic acidosis requiresNa^+/H^+ exchange induction and carbonic anhydrase, 2005, American Journal of Physiology. Renal Physiology, Vol. 289, pp. F208-F216

Pierson: A rapid colorimetric assay for carbamyl phosphate synthetase I, 1980, Journal of Biochemical and Biophysical Methods, Vol.3, pp. 31-37

Pineda, Wagner, Bröer, Stehberger, Kaltenbach, Gelpí, Martín de Río, Zorzano, Palacín, Lang, Bröer: Cystinuria-specific rBAT(R365W) mutation reveals two translocation pathways in the amino acid transporter rBAT-$b0^{,+}$AT, 2004, Biochemical Journal, Vol. 377, pp. 665-674

Piste: Cysteine - Master Antioxidant, 2013, International Journal of Pharmaceutical, Chemical and Biological Sciences, Vol. 3, pp. 143-149

Pouysségur, Sardet, Franchi, L`Allemain, Paris: A specific mutation abolishing Na^+/H^+ antiport activity in hamster fibroblasts precludes growth at neutral and acidic pH, 1984, Proceedings of the National Academy of Sciences, Vol. 81, pp. 4833-4837

Price, Uras, Banks, Ercal: A novel antioxidant N-acetylcysteine amide prevents gp120- and Tat-induced oxidative stress in brain endothelial cells, 2006, Experimental Neurology, Vol. 201, pp. 193-202

Puppo and Halliwell: Formation of hydroxyl radicals from hydrogen peroxide in the presence of iron, 1988, Biochemical Journal, Vol. 249, pp. 185-190

Qian, Khattak, Xing: Cell culture and gene transcription effects of copper sulfate on Chinese hamster ovary cells, 2011, Biotechnology Progress, Vol. 27, pp. 1190-1194

Qu, Lee, Bian, Low, Wong: Hydrogen sulfide: Neurochemistry and neurobiology, 2008, Vol. Neurochemistry International, Vol. 52, pp. 155-165

Rader and Langer: Biopharmaceutical manufacturing: Historical and future trends in titers, yields, and efficiency in commercial-scale Bioprocessing, 2014, BioProcessing Journal, Vol. 13, pp. 47-54

Raghavan and Bjorkman: Fc receptors and their interactions with immunoglobulins, 1996, Annual Review of Cell and Development Biology, Vol. 12, pp. 181-220

Raju: Glycosylation variations with expression systems and their impact on biological activity of therapeutic immunoglobulins, 2003, BioProcess International, Vol. 1, pp. 44-54

Raju: Terminal sugars of Fc glycans influence antibody effector functions of IgGs, 2008, Current Opinion in Immunology, Vol. 20, pp. 471-478

Raju and Jordan: Galactosylation variations in marketed therapeutic antibodies, 2012, mAbs, Vol. 4, pp. 385-391

Ralph, Hitchman, Millington, Walsh (a): The electrochemistry of L-cystine and L-cysteine. Part 1: Thermodynamic and kinetic studies, 1994, Journal of Electroanalytical Chemistry, Vol. 375, pp. 1-15

Ralph, Hitchman, Millington, Walsh (b): The electrochemistry of L-cystine and L-cysteine. Part 2: Electrosynthesis of L-cysteine at solid electrodes, 1994, Journal of Electroanalytical Chemistry, Vol. 375, pp. 17-27

Read, Bewick, Graves, MacPherson, Salah, Theriault, Wyand: The kinetics and mechanism of the oxidation of S-methyl-L-cysteine, L-cystine and L-cysteine by potassium ferrate, 2000, Inorganica Chimica Acta, Vol. 303, pp. 244-255

Regino and Richardson: Bicarbonate-catalyzed hydrogen peroxide oxidation of cysteine and related thiols, 2007, Inorganica Chimica Acta, Vol. 360, pp. 3971-3977

Ribeiro, Pinto, Lima, Volpato, Cabral, de Sousa: Chemical stability study of vitamins thiamine, riboflavin, pyridoxine and ascorbic acid in parenteral nutrition for neonatal use, 2011, Nutrition Journal, Vol. 10, p.9

Rigo, Corazza, di Paolo, Rossetto, Ugolini, Scarpa: Interaction of copper with cysteine: stability of cuprous complexes and catalytic role of cupric ions in anaerobic thiol oxidation, 2004, Journal of Inorganic Biochemistry, Vol. 98, pp. 1495-1501

Roberts, Nagasawa, Zera, Fricke, Goon: Prodrugs of L-cysteine as protective agents against acetaminophen-induced hepatotoxicity. 2-(polyhydroxyalky1)-and 2-(polyacetoxyalkyl) thiazolidine-4(R)-carboxylic acids, 1987, Journal of Medicinal Chemistry, Vol. 30, pp. 1891-1896

Robinson and Pasternak: The isolation of S-sulphoglutathione from the small intestine of the rat, 1964, Biochemical Journal, Vol. 93, pp. 487-492

Salahudeen, Clark, Nath: Hydrogen peroxide-induced renal injury. A protective role for pyruvate in vitro and in vivo, 1991, Journal of Clinical Investigation, Vol. 88, pp. 1886-1893

Salek, Costagliola, Lehmann: Protein tyrosine-O-sulfation analysis by exhaustive product ion scanning with minimum collision offset in a NanoESI Q-TOF tandem mass spectrometer, 2004, Analytical Chemistry, Vol. 76, pp. 5136- 5142

Samuni, Goldstein, Dean, Berk: The chemistry and biological activities of N-acetylcysteine, 2013, Biochimica et Biophysica Acta, Vol. 1830, pp. 4117–4129

Sauer, Burky, Wesson, Sternard, Qu: A high-yielding, generic fed-batch cell culture process for production of recombinant antibodies, 2000, Biotechnology and Bioengineering, Vol. 67, pp. 585-597

Schubert: Reactions of semimercaptals with amino compounds, 1937, The Journal of Biological Chemistry, Vol. 121, pp. 539-548

Schumpp and Schlaeger: Growth study of lactate and ammonia double-resistant clones of HL-60 cells, 1992, Cytotechnology, Vol. 8, pp. 39-44

Schwartzman, Blair, Segal: A common renal transport system for lysine, ornithine, arginine and cysteine, 1966, Biochemical and Biophysical Research Communications, Vol. 23, pp. 220-226

Searle and Willson: Stimulation of microsomal lipid peroxidation by iron and cysteine. Characterization and the role of free radicals, 1983, Biochemical Journal, Vol. 212, pp. 549-554

Seegan, Smith, Schumaker: Changes in quaternary structure of IgG upon reduction of the interheavy-chain disulfide bond, 1979, Proceedings of the National Academy of Sciences, Vol. 76, pp. 907-911

Segal and Crawhall: Characteristics of cystine and cysteine transport in rat kidney cortex slices, 1968, Proceedings of the National Academy of Sciences of the United States of America, Vol. 59, pp. 231-237

Segawa, Fukasawa, Miyamoto, Takeda, Endou, Kanai: Identification and functional characterization of a Na^+-independent neutral amino acid transporter with broad substrate selectivity, 1999, The Journal of Biological Chemistry, Vol. 274, pp. 19745-19751

Selvarasu, Ho, Chong, Wong, Yusufi, Lee, Yap, Lee: Combined in silico modeling and metabolomics analysis to characterize fed-batch CHO cell culture, 2012, Biotechnology and Bioengineering, Vol. 109, pp. 1415-1429

Seshadri, Klein, Kozlowski, Sands, Kim, Han, Handlogten, Verlander, Weiner: Renal expression of the ammonia transporters, Rhbg and Rhcg, in response to chronic metabolic acidosis, 2006, American Journal of Physiology. Renal Physiology, Vol. 290, pp. F397-F408

Shade and Anthony: Antibody glycosylation and inflammation, 2013, Antibodies, Vol. 2, pp. 392-414

Shane: Folate and vitamin B12 metabolism: Overview and interaction with riboflavin, vitamin B6, and polymorphisms, 2008, Food and Nutrition Bulletin, Vol. 29, pp. S5-S16

Shanker, Allen, Mutkus, Aschner: The uptake of cysteine in cultured primary astrocytes and neurons, 2001, Brain Research, Vol. 902, pp. 156-163

Sheu, Zhu, Fung: Direct observation of trapping and release of nitric oxide by glutathione and cysteine with electron paramagnetic resonance spectroscopy, 2000, Biophysical Journal, Vol. 78, pp. 1216-1226

Shields, Lai, Keck, O'Connell, Hong, Meng, Weikert, Presta: Lack of fucose on human IgG1 N-Linked oligosaccharide improves binding to human Fc RIII and antibody-dependent cellular toxicity, 2002, The Journal of Biological Chemistry, Vol. 277, pp. 26733-26740

Shindo and Brown: Infrared spectra of complexes of L-cysteine and related compounds with zinc(II), cadmium(II), mercury(II), and lead(II), 1965, Journal of the American Chemical Society, Vol. 87, pp. 1904-1909

Shotwell and Oxender: The regulation of neutral amino acid transport by amino acid availability in animal cells, 1983, Trends in Biochemical Sciences, Vol. 8, pp. 314-316

Shotwell, Jayme, Kilberg, Oxender: Neutral amino acid transport systems in Chinese hamster ovary cells, 1981, The Journal of Biological Chemistry, Vol. 256, pp. 5422-5427

Sloan and Mager: Cloning and functional expression of a human Na^+ andCl^--dependent neutral and cationic amino acid transporter B^{0+}, 1999, The Journal of Biological Chemistry, Vol. 274, pp. 23740-23745

Soghier and Brion: Cysteine, cystine or N-acetylcysteine supplementation in parenterally fed neonates (Review), Cochrane Database of Systematic Reviews, pp. 1-13

Sörbo: On the metabolism of thiosulfate esters, 1958, Acta Chemica Scandinavia, Vol. 12, pp. 1990-1996

Spanaki and Plaitakis: The role of glutamate dehydrogenase in mammalian ammonia metabolism, 2012, Neurotoxicity Research, Vol. 21, pp. 117–127

Stelmashuk, Belyaeva, Isaev: Effect of acidosis, oxidative stress, and glutamate toxicity on the survival of mature and immature cultured cerebellar granule cells, 2007, Neurochemical Journal, Vol. 1, pp. 66-69

Stipanuk and Ueki: Dealing with methionine/homocysteine sulfur: Cysteine metabolism to taurine and inorganic sulfur, 2011, Journal of Inherited Metabolic Disease, Vol. 34, pp. 17-32

Stojanovich and Ihle: Role of beta-hydroxybutyric acid in diabetic ketoacidosis: A review, 2011, The Canadian Veterinary Journal, Vol. 52, pp. 426-430

Stracke, Emrich, Rueger, Schlothauer, Kling, Knaupp, Hertenberger, Wolfert, Spick, Lau, Drabner, Reiff, Koll, Papadimitriou: A novel approach to investigate the effect of methionine oxidation on pharmacokinetic properties of therapeutic antibodies, 2014, mAbs, Vol. 6, pp. 1229-1242

Sunitha, Hemshekhar, Thushara, Santhosh, Yariswamy, Kemparaju, Girish: N-Acetylcysteine amide: a derivative to fulfi ll the promises of N-Acetylcysteine, 2013, Free Radical Research, Vol. 47, pp. 357-367

Swan: Thiols, disulphides, and thiosulphates: Some new reactions and possibilities in peptide and protein chemistry, 1957, Nature, Vol. 180, pp. 643-645

Tabuchi, Sugiyama, Tanaka, Tainaka: Overexpression of taurine transporter in Chinese hamster ovary cells can enhance cell viability and product yield, while promoting glutamine consumption, 2010, Biotechnology and Bioengineering, Vol. 107, pp. 998-1003

Takada and Bannai: Transport of cystine in isolated rat hepatocytes in primary culture, 1984, The Journal of Biological Chemistry, Vol. 259, pp. 2441-2445

Tamarappoo, McDonald, Kilberg: Expressed human hippocampal ASCT1 amino acid transporter exhibits a pH-dependent change in substrate specificity, 1996, Biochimica et Biophysica Acta, Vol. 1279, pp. 131 - 136

Taylor, Yan, Wang: The iron (III) -catalyzed oxidation of cysteine by molecular oxygen in the aqueous phase. An example of a two-thirds-order reaction, 1966, JournaI of the American Chemical Society, Vol. 88, pp. 1663-1667

Templeton, Dean, Reddy, Young: Peak antibody production is associated with increased oxidative metabolism in an industrially relevant fed-batch CHO cell culture, 2013, Biotechnology and Bioengineering, Vol. 110, pp. 2013-2024

Togawa, Kato, Nagai, Imanari: Determination of S-sulfocysteine and S-sulfoglutathione in plasma and red blood cells by high performance liquid chromatography, 1988, Analytical Sciences, Vol. 4, pp. 101-104

Tous, Wie, Feng, Bilbulian, Bowen, Smith, Strouse, McGeehan, Casas-Finet, Schenerman: Characterization of a novel modification to monoclonal antibodies: Thioether cross-link of heavy and light chains, 2005, Analytical Chemistry, Vol. 77, pp. 2675-2682

Ubuka, Yuasa, Kinuta, Akagi: Production of S-sulfocysteine from so-called cystine disulfoxide in the presence of aspartate aminotransferase, 1979, Physiological Chemistry and Physics, Vol. 11, pp. 353-357

Unwin, Stidwell, Taylor, Capasso: The effects of respiratory alkalosis and acidosis on net bicarbonate flux along the rat loop of Henle in vivo, 1997, American Journal of Physiology, Vol. 273, pp. F698–F705

Utsunomiya-Tate, Endou, Kanai: Cloning and functional characterization of a system ASC-like Na^+-dependent neutral amino acid transporter, 1996, The Journal of Biological Chemistry, Vol. 271, pp. 14883–14890

van der Valk, Brunner, De Smet, Fex Svenningsen, Honegger, Knudsen, Lindl, Noraberg, Price, Scarino, Gstraunthaler: Optimization of chemically defined cell culture media – Replacing fetal bovine serum in mammalian in vitro methods, 2010, Toxicology in Vitro, Vol. 24, pp. 1053-1063

Verrey: System L: heteromeric exchangers of large, neutral amino acids involved in directional transport, 2003, European Journal of Physiology, Vol. 445, pp. 529-533

Wada, Awano, Haisa, Takagi, Nakamori: Purification, characterization and identification of cysteine desulfhydrase of *Corynebacterium glutamicum*, and its relationship to cysteine production, 2002, FEMS Microbiology Letters, Vol. 217, pp. 103-107

Wada and Takagi: Metabolic pathways and biotechnological production of L-cysteine, 2006, Applied Microbiology and Biotechnology, Vol. 73, pp. 48-54

Wagner, Buettner, Burns: Vitamin E slows the rate of free radical-mediated lipid peroxidation in cells, 1996, Archives of Biochemistry and Biophysics, Vol. 334, pp. 261-267

Wainer: Mitochondrial oxidation of cysteine, 1966, Biochimica et Biophysica Acta, Vol. 141, pp. 466-472

Waley: Acidic peptides of the lens. 5. S-sulphoglutathione, 1959, Biochemical Journal, Vol. 71, pp. 132-137

Walsh: Post-translational modifications of protein biopharmaceuticals, 2010, Drug Discovery Today, Vol. 15, pp. 773-780

Walsh and Jefferis: Post-translational modifications in the context of therapeutic proteins, 2006, Nature Biotechnology, Vol. 24, pp. 1241-1252

Wang, Singh, Zeng, King, Nema: Antibody structure, instability, and formulation, 2006, Journal of Pharmaceutical Sciences, Vol. 96, pp. 1-26

Wang, Wang, Balthasar: Monoclonal antibody pharmacokinetics and pharmacodynamics, 2007, Clinical Pharmacology and Therapeutics, Vol. 84, pp. 548-558

Wang, Tamba, Kimata, Sakamoto, Bannai, Sato: Expression of the activity of cystine/glutamate exchange transporter, system x_c^- , by xCT and rBAT, 2013, Biochemical and Biophysical Research Communications, Vol. 305, pp. 611-618

Watts, Torres-Salazar, Divito, Amara: Cysteine transport through excitatory amino acid transporter 3 (EAAT3), 2014, PLoS ONE, Vol. 9, pp. 1-12

Wen, Vecchi, Gu, Su, Dolnikova, Huang, Foley, Garber, Pederson, Meier: Discovery and investigation of misincorporation of serine at asparagine positions in recombinant proteins expressed in Chinese hamster ovary cells, 2009, The Journal of Biological Chemistry, Vol. 284, pp. 32686-32694

Whitford: Supplementation of animal cell culture media, 2005, BioProcess International, Vol. 3, pp. 28-36

Whitford: Fed-batch mammalian cell culture in bioproduction, 2006, BioProcess International, Vol. 4, pp. 30-40

Williams, Waterman, Keresztesy, Buchman: Studies of crystalline vitamin B1. III. Cleavage of vitamin with sulfite, 1935, Journal of the American Chemical Society, Vol. 57, pp. 536-537

Winter and Ueda: Glutamate uptake system in the presynaptic vesicle: Glutamic acid analogs as inhibitors and alternate substrates, 1993, Neurochemical Research, Vol. 18, pp. 79-85

Wlodek and Rommelspacher: 2-Methyl-thiazolidine-2,4-dicarboxylic acid as prodrug of L-cysteine. Protection against paracetamol hepatotoxicity in mice, 1997, Fundamental and Clinical Pharmacology, Vol. 11, pp. 454-459

Wlodek, Rommelspacher, Susilo, Radomski, Höfle: Thiazolidine derivatives as source of free L-cysteine in rat tissue, 1993, Biochemical Pharmacology, Vol. 46, pp. 1917-1928

Wörn and Plückthun: An intrinsically stable antibody scFv fragment can tolerate the loss of both disulfide bonds and fold correctly, 1998, FEBS Letters, Vol. 427, pp. 357-361

Wright, Tao, Kabat, Morrison: Antibody variable region glycosylation: position effects on antigen binding and carbohydrate structure, 1991, The EMBO Journal, Vol. 10, pp. 2717-2723

Wurm: Production of recombinant protein therapeutics in cultivated mammalian cells, 2004, Nature Biotechnology, Vol. 22, pp. 1393-1398

Wurm: CHO quasispecies-Implications for manufacturing processes, 2013, Processes, Vol. 1, pp. 296-311

Xie and Wang: Integrated approaches to the design of media and feeding strategies for fed-batch cultures of animal cells, 1997, Trends in Biotechnology, Vol. 15, pp. 109-113

Yang and Wells: Catalytic Mechanism of Thioltransferase, 1991, The Journal of Biological Chemistry, Vol. 266, pp. 12766-12771

Yang and Xiong: Culture conditions and types of growth media for mammalian cells, 2012, Biomedical Tissue Culture, Dr. Luca Ceccherini-Nelli (Ed.), InTech Open Access Publisher, pp. 3-18

Yang, Wang, Chen, Hou, Hung, Mao: Tyrosine sulfation as a protein post-translational modification, 2015, Molecules, Vol. 20, pp. 2138-2164

Yoshiba-Suzuki, Sagara, Bannai, Makino: The dynamics of cysteine, glutathione and their disulphides in astrocyte culture medium, 2011, The Journal of Biological Chemistry, Vol. 150, pp. 95-102

Yu, Hoffhines, Moore, Leary: Determination of the sites of tyrosine O-sulfation in peptides and proteins, 2007, Nature Methods, Vol. 4, pp. 583-588

Zampagni, Wright, Cascella, D'Adamio, Casamenti, Evangelisti, Cardona, Goti, Nacmias, Sorbi, Liguri, Cecchi: Novel S-acyl glutathione derivatives prevent amyloid oxidative stress and cholinergic dysfunction in Alzheimer disease models, 2012, Free Radical Biology and Medicine, Vol. 52, pp. 1362-1371

Zauner, Selman, Bondt, Rombouts, Blank, Deelder, Wuhrer: Glycoproteomic analysis of antibodies, 2013, Molecular and Cellular Proteomics, Vol. 12, pp. 856-865

Zerangue and Kavanaugh: Interaction of L-cysteine with a human excitatory amino acid transporter, 1996, Journal of Physiology, Vol. 493, pp. 419-423

Zhang, Zhang, Hewitt, Tran, Gao, Qiu, Tejada, Gazzano-Santoro, Kao: Identification and characterization of buried unpaired cysteines in a recombinant monoclonal IgG1 antibody, 2012, Analytical Chemistry, Vol. 84, pp. 7112−7123

Zhang, Schenauer, McCarter, Flynn: IgG thioether bond formation *in vivo*, 2013, The Journal of Biological Chemistry, Vol. 288, pp. 16371-16382

Zhao, Zhang, Lu, Wang: The vasorelaxant effect of H_2S as a novel endogenous gaseous K_{ATP} channel opener, 2001, The EMBO Journal, Vol. 20, pp. 6008-6016

Zhou, Coles, Kartha, Nash, Mishra, Lund, Cloyd: Intravenous administration of stable-labeled N-acetylcysteine demonstrates an indirect mechanism for boosting glutathione and Improving redox status, 2015, Journal of Pharmaceutical Sciences, Vol. 104, pp. 2619-2626

Zimmer, Mueller, Wehsling, Schnellbaecher, von Hagen: Improvement and simplification of fed-batch bioprocesses with a highly soluble phosphotyrosine sodium salt, 2014, Journal of Biotechnology, Vol. 186, pp. 110-118

Zmijewski, Banerjee, Bae, Friggeri, Lazarowski, Abraham: Exposure to hydrogen peroxide induces oxidation and activation of AMP-activated protein kinase, 2010, The Journal of Biological Chemistry, Vol. 285, pp. 33154-33164

Zoltewicz, Kauffman, Uray: A mechanism for sulphite ion reacting with vitamin B1 and its analogues, 1984, Food Chemistry, Vol. 15, pp. 75-91

9. Appendix

9.1. Abbreviations and chemical formulas

Abbreviation/ chemical formula	Meaning
2-AB	2-amino benzamide
ADCC	Antibody-dependent cellular cytotoxicity
ADCP	Antibody-dependent cellular phagocytosis
AMPK	5′-adenosine monophosphate-activated protein kinase
ASC	Alanine-serine-cysteine transporter
Asn	Asparagine
AST	Aspartate aminotransferase
ATP	Adenosine triphosphate
AUC	Area under the curve
BCECF	2',7'-bis(2-carboxyethyl)-5,6-carboxyfluorescein
carboxy-H_2DCFDA	6-carboxy-2',7'-dichlorodihydrofluorescein diacetate
CBS	Cystathionine β-synthase
CD	Cluster of differentiation
CDC	Complement-dependent cytotoxicity
CDM	Chemically defined media
cDNA	Complementary deoxyribonucleic acid
CDO	Cysteine dioxygenase
CDR	Complementary determining regions
CDS	Cystine disulfoxide
CE	Capillary electrophoresis
c_H	Constant domain of the heavy chain
CHO	Chinese hamster ovary cells
CHO-ori	original Chinese hamster ovary cell line
CHO-Sc	Chinese hamster ovary suspension commercial
CHO-So	Chinese hamster ovary suspension original cells
cIEF	Capillary isoelectric focusing
cIVC	Corrected integral viable cell concentration
c_L	Constant domain of the light chain
C/mL	Cells per milliliter

CMP-NeuAc	Cytidine 5´-monophospho-N-acetylneuraminic acid
CO_2	Carbon dioxide
CoA	Acetyl coenzyme A
cQAs	Critical quality attributes
CSE	Cystathionine γ-lyase
Cu	Copper
CysD	Cysteine desulfhydrase
CysHCl*H_2O	L-cysteine hydrochloride monohydrate
DHFR	Dihydrofolate reductase
DMEM	Dulbeccos minimal essential medium
DNA	Deoxyribonucleic acid
DO	Dissolved oxygen
DoE	Design of experiment
DP	Dipeptidase
EAAT	Excitatory amino acid transporter
ER	Endoplasmatic reticulum
ESI	Electrospray ionization
Fab	Fragment antigen binding
Fc	Fragment crystallisable
FcRn	Neonatal Fc receptor
FcγR	Fragment crystallisable gamma receptors
Fe	Iron
Fuc	Fucose
FUT8	Fucosyltransferase 8
Gal	Galactose
GAPDH	Glycerinaldehyde -3- phosphate-dehydrogenase
gDNA	Genomic deoxyribonucleic acid
GDP	Guanosine diphosphate
GLAST	Glutamate-aspartate transporter
GlcNAc	N-acetylglucosamines
GLT	Glutamate transporter
γ-GluCys	γ-glutamylcysteine
GMD	Guanosine diphosphate-mannose 4,6-dehydratase
GNE	Uridine diphosphate-N-acetylglucosamine 2-epimerase

GnTIII	β-(1,4)-N-acetylglucosaminyltransferase III
GRX	Glutaredoxin
GS	Glutamine synthetase
GS-Cys	mixed disulfide of L-cysteine and glutathione
GSH	Glutathione (reduced)
GSSG	Glutathione, oxidized
$GS\text{-}SO_3$	Sulfoglutathione
GT	γ-glutamyltranspeptidase
H_2O_2	Hydrogen peroxide
H_2S	Hydrogen sulfide
HC	Heavy chain
HCl	Hydrogen chloride
HCO_3^-	Bicarbonate
HCy	Homocysteine
HEK	Human ebryonic kidney cells
IAM	Iodoacetamide
IC	Ion chromatography
ICP-HR-MS	Inductively coupled plasma high resolution mass spectrometry
ICP-MS	Inductively coupled plasma mass spectrometry
Ig	Immunoglobulins
IgG	Immunoglobulin G
α-KG	α-ketoglutarate
LAT	L-type amino acid transporter
LC	Light chain
LC-HRMS	Liquid chromatography-high resolution mass spectrometry
LC-MS	Liquid chromatography – mass spectrometry
LDH	Lactate dehydrogenase
M	Molar or mol/L
mAb	Monoclonal antibody
Man	Mannose
ManNAc	N-acetylmannosamine
MCT	Monocarboxylate transporter
MEM	Minimal essential medium

Met	Methionine
µM	Micromolar or µmol/L
mM	Millimolar or mmol/L
mRNA	Messenger ribonucleic acid
MS	Mass spectrometry
MSX	Methionine sulfoximine
MTX	Methotrexate
NAC	N-acetyl-L-cysteine
NACA	N-acetylcysteine amide
NACET	N-acetylcysteine ethyl ester
NAD	Nicotinamide adenine dinucleotide
NADH	Nicotinamide adenine dinucleotide (reduced form of NAD+)
NADP	Nicotinamide adenine dinucleotide phosphate
NADPH	Nicotinamide adenine dinucleotide phosphate (reduced form of NADP+)
NANA	N-acetylneuraminic acid
NaOH	Sodium hydroxide
NGNA	N-glycolylneuraminic acid
NH_3	Ammonia
NH_4^+	Ammonium
NK	Natural killer
nM	Nanomolar or nmol/L
NMR	Nuclear magnetic resonance
NO	Nitric oxide
OH^-	Hydroxyl ions
OTC	L-2-oxothiazolidine-4-carboxylic acid
pAb	Polyclonal antibodies
PAPS	3´-phosphoadenosine-5´-phosphosulfate
PBS	Phosphate buffered saline
pCO2	Partial pressure of carbon dioxide
Phe	Phenylalanine
pI	Isoelectric point
PK	Pharmacokinetics

PLP	Pyridoxal phosphate
ppm	Parts per million
PTM	Posstranslational modification
PTyr2Na$^+$	Phosphotyrosine disodium salt
PVDF	Polyvinylidene difluoride
RibCys	D-ribose-L-cysteine
ROS	Reactive oxygen species
RPMI	Roswell Park Memorial Institute
RS	Reactive species
RT-PCR	Real-Time polymerase chain reaction
SEM	Standard error of the mean
Sf	*Spodoptera frugiperda*
SLC	Solute carrier
SOD	Superoxide dismutase
SSC	S-Sulfocysteine
SSC*Na	S-sulfocyteine monosodium salt
SV40	Simian virus 40
TCA	Tricarboxylic acid cycle
TFB-TBOA	(3S)-3-[[3-[[4-(trifluoromethyl)benzoyl]amino]phenyl]methoxy]-L-aspartic acid
THF	Tetrahydrofolate
Tris	Tris(hydroxymethyl)aminomethane
TRX	Thioredoxin
TT	Thioltransferase
Tyr	Tyrosine
UCP3	uncoupling protein 3
UCPH 101	2-amino-5,6,7,8-tetrahydro-4-(4-methoxyphenyl)-7-(naphthalen-1-yl)-5-oxo-4H-chromene-3-carbonitrile
UDP-GlcNAc	Uridine diphosphate N-acetylglucosamine
UHPLC	Ultra high performance liquid chromatography
UHPLC-MS/MS	Ultra-high pressure liquid chromatography-mass spectrometry-mass spectrometry
UPLC	Ultra performance liquid chromatography
UV	Ultraviolet

VCD	Viable cell concentrations
v_H	Variable domain of the heavy chain
v_L	Variable domain of the light chain

9.2. List of figures

Figure 1: Cell culture workflow for protein production. 9

Figure 2: Cell culture and protein production in batch (discontinuous) process mode. 10

Figure 3: Cell culture and protein production in continuous process mode. 11

Figure 4: Cell culture and protein production in perfusion mode as a special case of continuous culture. 11

Figure 5: Cell culture and protein production in fed-batch mode. 12

Figure 6: The bicarbonate (HCO_3^-) /carbon dioxide (CO_2) buffer system. 16

Figure 7: Structure of an IgG1 molecule. 21

Figure 8: Schematic representation of three main effector functions mediated by Fc part of antibodies 23

Figure 9: Schematic representation of N-glycan positioned at Asn297 in the C_{H2} domain (Fc part) of an IgG. 26

Figure 10: Chemical reaction mechanism of DL-cysteine hydrochloride monohydrate. 33

Figure 11: Enzymatic L-cysteine production catalysed by cysteine desulfhydrylase (EC 4.4.1.1). 33

Figure 12: Enzymatic L-cysteine production catalysed by L-ATC acid hydrolase and L-NCC amidohydrolase. 34

Figure 13: Enzymes serine acetyltransferase (SAT) and cysteine desulfhydrase in *corynebacterium glutamicum* as genetic manipulation options. 35

Figure 14: Structures of L-cysteine and L-cystine. 36

Figure 15: Titration reactions for pKa determination of L-cysteine. 36

Figure 16: Reactions of L-cysteine with iron ions and reactions of L-cysteine and L-cystine with ferrate ions. 38

Figure 17: Schematic function of selected import L-cysteine and L-cystine transporters. 47

Figure 18: Intracellular L-cysteine anabolism. 48

Figure 19 : Intracellular catabolic pathways of L-cysteine. 52

Figure 20: Structure of N-acetyl-L-cysteine (NAC) 55

Figure 21: 2-substituted thiazolidine-4(R)-carboxylic acids as a prodrug for L-cysteine release. 58

Figure 22: Structure of S-sulfocysteine (SSC) 59

Figure 23: Cell free production of S-sulfocysteine from cystine disulfoxide. 60

Figure 24: Cell free production of S-sulfocysteine from S-glutathione. 60

Figure 25: In vitro reaction of S-Sulfocysteine with reduced glutathione into L-cysteine, oxidized glutathione and inorganic sulfite for thioltransferase activity determination 61

Figure 26: Structure of reduced L-glutathione (GSH) 62

Figure 27: Formula for the calculation of the specific productivity (l pg/(cell.day)) at Merck 69
Figure 28: Formula for the calculation of the corrected integral viable cell concentration (cIVC) (mio.V.day/mL) at Merck 69
Figure 29: Formula for the calculation of purity (w %) using data obtained from NMR spectra measurements at Merck.....78
Figure 30: Schematic representation of the workflow in the L-cysteine derivative screening process. 86
Figure 31: Stability study of SSC*Na in concentrated, chemically defined neutral pH feed after three months at 4°C protected from light. 96
Figure 32: L-cysteine replacement by dose response of SSC*Na-A in L-cysteine deficient medium using spin tube batch processes with clone 1. 103
Figure 33: Spin tube fed-batch process with neutral pH feed containing SSC*Na-A using CHO suspension clone 2.....109
Figure 34: Bioreactor fed-batch experiment with neutral pH feed containing SSC*Na-A using CHO suspension clone 2.....112
Figure 35: Impact of SSC*Na-containing feed on key quality attributes charge variant distribution, N-glycosylation pattern and peptide mapping. 116
Figure 36: Cell lysate spiking with SSC*Na alone and pre-treatment of cell lysates with IAM followed by SSC*Na spiking. 118
Figure 37: Cell-free interaction studies of SSC*Na and GSH at different pH alone and together. 121
Figure 38: Fate of SSC in presence of GSH and after spiking with cell lysate. 123
Figure 39: Anti-oxidative properties of two SSC*Na batches in fed-batch cell cultures. 126
Figure 40: Microarray studies of transcript levels of different enzymes in fed-batch cultures using 15 mM SSC*Na compared with control. 127
Figure 41: Antioxidative properties of SSC*Na on enzymatic expression levels and enzyme protein levels. 128
Figure 42: Spin tube fed-batch experiment with neutral pH feed containing 20 mM SSC*Na-B using CHO suspension clone 3. 131
Figure 43: Spin tube fed-batch experiment with neutral pH feed containing 20 mM of different SSC*Na batches using CHO suspension clone 2. 136
Figure 44: NH_3 concentrations from spin tube fed-batch experiment with neutral pH feed containing 20 mM SSC*Na using CHO suspension clone 2. 138
Figure 45: L-cysteine replacement by 1.5 mM SSC*Na-B in L-cysteine deficient medium in spin tube batch processes using CHO suspension clones 2 and 3. 144

Figure 46: Expression levels of five high affinity glutamate transporters (SLC1a2, SLC1a3, SLC1a6 and SLC7a11) in CHO suspension clones 2 and 3. 146
Figure 47: Evaluation of L-glutamate transporter inhibition of cells grown in L-cysteine depleted medium supplemented with 1.5 mM SSC*Na in batch test using clone 2. 148
Figure 48: Spin tube batch and fed-batch experiments with neutral pH feed containing different SSC*Na-B concentrations using CHO suspension clone 2. 150
Figure 49: Rescue options of spin tube fed-batch experiments with neutral pH feed containing theoretically 20 mM SSC*Na-B using CHO suspension clone 2. 153
Figure 50: Schematic representation of the hypothesized rescue mechanism of increased sodium L-glutamate feeding in toxic SSC*Na condition in fed-batch using clone 2.....170

9.3. List of tables

Table 1: Summary of literature-based L-cysteine transport systems 42

Table 2: Summary of literature-based L-cystine transport systems 46

Table 3: Gradient parameters of UHPLC for amino acid and SSC quantification 82

Table 4: Summary of physico- chemical tests (solubility and stability in concentrated, neutral pH feed) and short term batch cultures in L-cysteine replacement strategy using clone 1 with 11 chemically modified L-cysteine derivatives. 87

Table 5: Maximum solubility of SSC*Na in water and concentrated, neutral pH feed. 92

Table 6: Different SSC*Na batches synthesized from different methods showing purities and all contaminations coming from syntheses. 100

Table 7: Purity, corrected molecular weight, theoretical and real SSC*Na concentrations of different externally and internally synthesized SSC*Na batches. 132

Table 8: Externally and internally synthesized and tested SSC*Na research batches showing impurities coming from synthesis method (copper, sulfate, L-cystine, thiosulfate), real applied SSC*Na concentrations and observations from small scale fed-batch processes using the theoretical concentration of 20 mM. 141

9.4. Curriculum vitae

Background

Secondary school	09/1996 - 07/2005
Graduation: Highschool diploma	
Studies of food chemistry (state examination) at MLU Halle (Saale)	10/2005 - 09/2006
Early termination	
Studies of biotechnology (B. Sc.) at FH Jena university of applied sciences	10/2006 - 09/2007
Early termination	
Studies of biotechnology (B. Sc.) at HS Anhalt university of applied sciences	10/2007 - 11/2009
Graduation: Bachelor of Science (B. Sc.)	
Internship at L'école nationale supérieure d'agronomie et des industries alimentaires (ENSAIA) in Nancy, France	01/2010 - 06/2010
Studies of biotechnology (M. Sc.) at HS Anhalt university of applied sciences	10/2010 - 12/2012
Graduation: Master of Science (M. Sc.)	
Doctoral program at TU Darmstadt in collaboration with Merck	01/2013 - 10/2016

City, Date

Bad Vilbel, 08.07.2016

Signature

9.5. Acknowledgement

Numerous people have contributed to the successful completion of this work and have generously given time, advice, valuable information and encouragement.

I am grateful to Prof. Dr. Kolmar at TU Darmstadt for the supervision of this work and for the opportunity to be an external PhD student in his team. Further, I would like to thank Prof. Dr. Eckl at University Salzburg for accompanying and co-supervising this project. Moreover, I am grateful for the co-supervision of this work by Prof. Dr. Neumann at TU Darmstadt.

Many people at Merck KGaA have supported me throughout these studies and I am thankful for all your support. I am grateful to Prof. Dr. Dipl.-Ing. von Hagen for his co-supervision and the fruitful discussions. Further, I am truly indebted to Dr. Aline Zimmer for all her valuable information, patience, motivation and exchange. Without her, this work has not been possible and I am aware of her fundamental contributions, ideas and advice making this thesis realizable. A “thank you” is not able to precisely describe my gratitude.

Further, I would like to thank the lab team for all your support and encouragement by helping me with measurements and experiments, helpful discussions, corrections and for always being willing to listen: Sascha, Jenny, Maria, Yasmin, Linda, Janike, Ronja, and Alisa. Many warm thanks go out to the physico-chemical team: Andrew, Anke, Julia, Sabrina, Janin, Anna Lena, Marie Sophie and Markus for sharing their physicochemical knowledge and experiences with me. Also, many thanks for your hospitality in your lab. Further, I am truly indebted for the help and mental support of my collegue Caro who was always there for me even if she was working in a different lab. Thank you for your unconditional support. Also, people from other departments at Merck gave valuable information and assisted me with measurements and questions-and-answers-sessions and I am grateful for your support: Angela and their colleagues, Jens and Thomas. Further, a huge thank you goes to Sylvia and her colleagues as well as to Mrs. Wenzel for measuring some metabolites presented in this study.

Some collegues became friends and I appreciated the time in the lab(s), getting to know you all, sharing ups and downs. I am glad for the nice lunch sessions and for the moments apart from work.

I am truly grateful for the support of my family throughout this journey. You were always there and willing to listen.Words cannot express my gratitude for all the love and support. Moreover, my deep gratitude goes out to you Sebastian and his family. You were always there for me. This is for you.

10. Affirmations

Caroline Hecklau
Zur schönen Aussicht 20c
61118 Bad Vilbel

08.07.2016

Erklärung

Ich erkläre hiermit, dass ich meine Dissertation selbstständig und nur mit den angegebenen Hilfsmitteln angefertigt habe.

Unterschrift

Caroline Hecklau
Zur schönen Aussicht 20c
61118 Bad Vilbel

08.07.2016

Erklärung

Ich erkläre hiermit, noch keinen Promotionsversuch unternommen zu haben.

Unterschrift